Spatial and Temporal Variability of Hydraulic Response in Fractured, Low Permeability Sediments

by

Scott Richard Fidler

A thesis
presented to the University of Waterloo
in fulfillment of the
thesis requirement for the degree of
Doctor of Philosophy
in
Earth Sciences

Waterloo, Ontario, Canada, 1997

National Library of Canada
Acquisitions and Bibliographic Services
395 Wellington Street
Ottawa ON K1A 0N4
Canada

Bibliothèque nationale du Canada
Acquisitions et services bibliographiques
395, rue Wellington
Ottawa ON K1A 0N4
Canada

Your file Votre référence

Our file Notre référence

0-612-30608-9

Canada

The University of Waterloo requires the signatures of all persons using or photocopying this thesis. Please sign below, and give address and date.

ABSTRACT

The relative importance of fractures and other macropores in clay-rich glacial deposits depends on the temporal and spatial scales being considered. Hydraulic conductivity of such materials generally depends on the scale at which the measurement is made, as a result of the localised high conductivity associated with the macropores. Small scale measurements tend to be highly variable, whereas tests conducted at a sufficiently large scale yield a relatively constant value for hydraulic conductivity, since they encompass a representative portion of the macropore network. Tests which involve rapidly varying hydraulic conditions will mainly influence the macropore network, since rapid changes in pressure can propagate quickly through these high conductivity, low storage features, while the pressure in the low conductivity, high storage matrix remains unchanged or changes very slowly. On the other hand, if sufficiently slow pressure changes are applied to the system, very little pressure disequilibrium will develop between the macropores and the matrix.

In this thesis, field and modelling studies are employed to investigate particular aspects of the spatial and temporal scale dependence of hydraulic behaviour in naturally fractured clay-rich glacial deposits. The overall objective of the thesis is to develop appropriate field methods, and conceptual models for their interpretation, for measuring parameters which control hydraulic behaviour in heavily fractured, near surface clays. Some of these parameters, such as bulk vertical hydraulic conductivity, have been very rarely measured in this type of material. Similarly, the methods used in this thesis to interpret transient hydraulic tests have not commonly been used for tests in fractured clays.

Two field experiments were conducted at locations separated by approximately 1 km, at a site in the St. Clair Clay Plain in south-western Ontario. At this site, glacio-lacustrine clay is present from the surface to a depth of approximately 40m. The upper 2-4m of the clay are

heavily fractured and pervasively weathered. Below the zone of pervasive weathering the clay is unweathered except in the vicinity of fractures, which are visible to a depth of 6m. Hydraulic testing and mapping of fractures and other macropore features was carried out in the upper weathered zone at the two experimental sites.

The results of the mapping provide the context and important parameters for the interpretation of the hydraulic tests, and also indicate the potential variability in fracture patterns between two nearby sites within the same clay plain. Although surface observations at the sites did not reveal any features that suggest they are atypical of the clay plain in general, two very different fracture patterns were observed in the weathered near-surface clay at the two sites considered. Mapping of preferential flow paths was carried out at one of the two sites by infiltrating a dye and then mapping its distribution in the subsurface. At this site, it was found that loosely infilled, primarily vertical, cylindrical cavities were major conduits for fluid flow. Open root holes, often located along fracture faces, were also identified as important conduits for fluid flow. Dye staining did not indicate distributed flow throughout the plane of major fractures in any instances.

Hydraulic testing was carried out at the two sites using an experimental arrangement in which a pond was maintained at the surface, overlying several flat-lying sand-filled induced fractures. This arrangement was used to conduct a variety of transient and steady state hydraulic tests, which were monitored using a network of electronic strain gauge pressure transducers. At both sites, the pond and induced fractures were several metres in diameter, and thus influence a relatively large volume of the fractured clay, in proportion to the volume that would be tested with single-well tests.

Steady state conditions during pumping tests in which water was pumped from the induced fractures allow the calculation of vertical hydraulic conductivity and its variation with

depth, and also indirectly allow horizontal hydraulic conductivity to be estimated. At the first site, it was found that vertical hydraulic conductivity does not change with depth in the weathered clay, whereas vertical hydraulic conductivity decreased by an order of magnitude over the depth of the weathered zone at the second site. It was also found that the ratio of bulk horizontal hydraulic conductivity to bulk vertical hydraulic conductivity was much lower at the second site than at the first site.

The use of induced fractures to conduct pumping tests made it possible to observe differences in behaviour between the fracture network and the clay matrix during transient hydraulic tests. The results of pumping tests conducted at the first site indicates that disequilibrium between fractures and the clay matrix can persist for several hours. Thus in general, interpretation of scenarios in which hydraulic conditions vary on the time scale of hours or less will require models which account for the interaction between the fractures and the clay. Such models can reproduce certain aspects of behaviour, such as the rapid transmission of pressure through fractures and the concurrent slow changes in pressure in the clay matrix, which can not be described using equivalent porous medium models. A discrete fracture model was used to interpret the transient hydraulic field tests. The values obtained for parameters such as bulk hydraulic conductivity and specific storage of the clay are consistent with values measured independently in other tests.

ACKNOWLEDGEMENTS

Trudging about a clay plain in south western Ontario in the middle of winter is not exactly what I had in mind 4 years ago as I planned to leave Australia to commence my studies at Waterloo. For someone who had not even seen snow until the age of 22, the idea of actually doing field work while it was -20 degrees outside was incomprehensible. However, there were to be many aspects of my stay in Waterloo which I had not expected - some of them pleasantly surprising, and some of them not. Throughout it all, my supervisor Dr. David Rudolph has been unfailingly enthusiastic and supportive. On a technical level, his judgement and intuition have proved invaluable. I would also like to thank the other members of my committee, Dr. Garth van der Kamp, Dr. John Cherry and Dr. Ed Sudicky for their encouragement and ideas.

In the field, I was assisted on many occasions, by many people. The assistance of Dr. Larry Murdoch and Dr. Bill Slack from the University of Cincinnati/FRx Ltd. in creating the induced fractures that made most of this work possible is gratefully acknowledged. Paul Johnson made it possible to implement some of my more crazy ideas, by translating them into slightly more orthodox ideas that probably worked a lot better. His carpentry skills also allowed me to stay relatively warm and dry in my greenhouse while it was -20 degrees outside, and to be the only student in the department with a sun tan throughout the year. Rick Gibson spent many a long day with me driving to the site and back, and helped sort out lots of small details with things like plumbing, while I was off doing something else. In the field mapping exercises, which involved sitting in a hole in the ground for days at a time, scraping clay in search of fractures, I was cheerfully assisted by Rick Gibson, Steve Markesic, Suzanne O'Hara, Brigid Burke, and Paul Johnson. I would also like to thank Knut Erik Klint for his help and suggestions with the mapping. Glen Kirkpatrick, Tina Jung, Beth Parker and Diane Grady also assisted with other aspects of the field work. Back at Waterloo, Rob McLaren spent quite a few hours with me, helping to sort out why the computer wasn't doing what I wanted it to.

Sometimes it was my fault, sometimes it was the computer, but Rob always sorted out the problem quickly when he most likely had more important matters to deal with.

I would like to thank Laidlaw Environmental Services for providing equipment and access to their facility, and for not evicting me from my first experimental site until I had collected enough data. Funding for this research was provided by an NSERC operating grant to Dr. David Rudolph, the Waterloo Centre for Groundwater Research, the University Consortium Solvents-in-Groundwater Research Program at the University of Waterloo, and in kind support from FRx Ltd. I was supported throughout by a generous scholarship from Golder Associates.

Most importantly, I must thank my wife Dominique for her love and support throughout the past 4 years. While I got the excitement and intellectual stimulation of doing a PhD, she got to put her life and career on hold for 4 years. Her strength and positive attitude have been astounding.

TABLE OF CONTENTS

LIST OF TABLES

LIST OF FIGURES

CHAPTER 1

INTRODUCTION

BACKGROUND

Clay-rich deposits of glacial origin were deposited at or near the surface over large areas of northern North America, Great Britain and Scandinavia during late Pleistocene time. These deposits often overlie aquifers of sand, gravel or bedrock, and provide them with some degree of protection from contamination due to surface activities (Cherry, 1989). Near the surface, such deposits are extensively weathered, typically to a depth of several metres. The total thickness of such deposits is commonly several tens of metres, and in such cases, substantial thicknesses of unweathered clay underlie the surficial weathered clay. Macropores such as fractures and abandoned root holes are commonly observed in the weathered clay near the surface (for example, Williams and Farvolden, 1967; Hendry, 1982; Ruland et. al., 1991). Although they are more common and generally much more closely spaced in near surface weathered deposits, fractures have also been observed or inferred from hydraulic and solute transport evidence in deeper, unweathered clay at various locations in North America by Keller et. al. (1986), Rudolph et. al. (1991), and Pach (1994).

Close to the surface, fractures are often formed by shrinkage of the clay as it dries due to evapotranspiration. The process of wetting and drying of near surface soils is a cyclic process governed by seasonal variations in precipitation, evaporation and plant growth, and thus desiccation cracking extends almost to the depth of seasonal moisture change (Morris et. al., 1992). Near surface fractures can also be formed by freeze-thaw processes (Graham and Au, 1985). Morris et. al. (1992) suggest that fractures which extend beyond the depth of current seasonal moisture variations were formed during sustained warmer and drier climatic conditions in the past. Fractures at all depths can also be caused by stresses which result from tectonic activity or over-riding glaciers (Klint, 1996).

Issues of flow and solute migration in clayey deposits can generally be classified as relating to relatively uniform downward flow and transport to confined aquifers, or to more spatially and temporally variable flow and transport in shallow flow systems which occur in upper weathered and fractured horizons (Cherry, 1989). Due to the low hydraulic conductivity of intact clay, recharge and vertical migration of solutes to underlying aquifers through thick, clay-rich deposits will be limited if a substantial thickness of unfractured clay is present at depth. In many instances, solute migration in unfractured clay-rich glacial deposits is controlled by matrix diffusion (for example, Desaulniers, 1986; and Remenda, 1993), and consequently Pleistocene age water, identified by very negative $\delta^{18}O$ values, remains at depth in these deposits.

In contrast, the presence of an interconnected network of fractures in near surface weathered clays imparts an overall hydraulic conductivity which is much higher than that of the intact material, and allows active flow systems to develop. The presence of fractures and other macropores can increase hydraulic conductivity by up to 4 orders of magnitude above the hydraulic conductivity of the clay material itself (Keller et. al., 1986; and McKay et. al., 1993a) and can lead to rates of solute migration that are well in excess of the low, diffusion controlled rates that would be expected for an unfractured clay (Balfour, 1991; and McKay et. al. 1993b). Ruland et. al. (1991) observed tritium at depths of up to 12m, and seasonal hydraulic head fluctuations in excess of 0.5m at depths of up to 11.5m, at a number of sites in the St. Clair Clay Plain in south-western Ontario. In this area, the clay is heavily fractured and pervasively weathered to a depth of 2-4m, and a fractures are visible to a maximum depth of 6m. In the same area, Adomait (1991) and Harris (1994) observed increases in hydraulic head of up to 1m in shallow piezometers immediately following rainfall events, followed by a gradual decrease over a period of days.

The relative importance of fractures and other macropores depends on the temporal and spatial scales being considered. For example, hydraulic conductivity of such materials generally depends on the scale at which the measurement is made, as a result of the localised high conductivity associated with the macropores (Bradbury and Muldoon, 1990; Jones et. al., 1992; McKay et. al., 1993). In some instances small scale measurements will be directly influenced by the high local conductivity of macropores in the vicinity of the measurement location, whereas in other instances there will be no macropores in the immediate vicinity of the measurement location and a low hydraulic conductivity will result. In contrast, tests conducted at a sufficiently large scale encompass a representative portion of the macropore network, and thus a relatively constant value of hydraulic conductivity will be measured regardless of the particular location of the measurement device, assuming spatial homogeneity of the macropore network.

Since fractures in these types of deposits are in many cases predominantly vertical (Hendry, 1982; Morris et. al., 1992; McKay and Fredericia, 1995), larger scale measurements of hydraulic conductivity could demonstrate anisotropy, since networks of predominantly vertical fractures would tend to enhance conductivity in a vertical direction more than in a horizontal direction. However, in the majority of cases, hydraulic conductivity measurements have been derived from tests in which the imposed gradient is predominantly horizontal. Anisotropy of hydraulic conductivity and changes in large scale hydraulic conductivity with depth are both factors which will have an important influence on solute transport, seasonal and shorter term hydraulic head fluctuations, and recharge in the near-surface weathered zone. However, very little information is available in the literature regarding these two aspects of hydraulic conductivity for clay-rich glacial deposits.

Differences in behaviour will also occur at different temporal scales. For example, due to the difference in conductivity between the macropores and the clay matrix, rapid changes in pressure which are applied to the system can propagate quickly through the macropores, while the pressure in the matrix remains unchanged or changes very slowly. On the other hand, if sufficiently slow pressure changes are applied to the system, very little pressure disequilibrium will develop between the macropores and the matrix. If pressure disequilibrium exists between the fracture and the matrix, fluid will flow from one to the other. Similar differences in behaviour would be observed for solute transport scenarios in which large and small advective velocities in the fractures apply.

It might also be expected that transient hydraulic response and solute transport behaviour would be affected by the macropore geometry, since the contact area between the clay and these features will have a controlling influence on how quickly water and solutes can be exchanged between the two. In the case of planar features such as fractures, the contact area between the macropore and the matrix is relatively large, whereas in the case of linear features such as root holes, the contact area is relatively small.

Thus, although the spatial scale of a particular problem may be such that it encompasses a representative portion of the macropore network, it may not be possible to adequately describe transient behaviour using a single-continuum model, which does not allow for transient disequilibrium and consequently fluid or solute transfer between the low conductivity matrix and the macropores. In these instances, it will be necessary to describe the behaviour of the system using a model which allows for disequilibrium between the macropores and the matrix, and which accounts for the transfer of fluid or solute between the two.

Interpretation of hydraulic tests or tracer tests in fractured clays using models other than conventional, single continuum type models requires the geometry of the real fracture network

to be represented in the model using a simplified, surrogate network. Information on the actual fracture network which is to be represented in the models can be derived from direct observations of the fracture network through coring and excavation (for example, McKay et. al., 1993a, and Hinsby et. al., 1996). However, the manner in which field observations of fracture patterns should be translated into surrogate fracture networks for mathematical models requires some consideration. Guidance is required on the parameters which much be measured in the field so as to allow valid idealisation of the real fracture network with a simplified network.

Discrete fracture models and dual continuum models, which can account for fluid and solute transfer between the fractures and the matrix, have been used fairly widely to interpret examples of solute transport in fractured clays (for example, by Rudolph et. al., 1991; McKay et. al., 1993b; and Hinsby et. al., 1996), but it does not appear that they have been widely used to interpret transient hydraulic tests in these types of materials. The potential inability of single continuum models to adequately describe transient hydraulic phenomena in fractured clays is significant, since hydraulic parameters for these types of materials are often derived using tests which impose transient hydraulic conditions. While it may be possible in some situations to use single continuum models to derive parameters such as hydraulic conductivity and specific storage which adequately describe the results of particular transient hydraulic tests, it is likely that these parameters are specific to the spatial and temporal scales considered, since interactions between the macropores and the low conductivity matrix are not accounted for. If this is the case, the parameters derived from the continuum models will not be useful for predicting the behaviour of the system under different conditions, particularly for different temporal and spatial scales.

RESEARCH GOAL AND SCOPE

In this thesis, field and modelling studies are employed to investigate particular aspects of the spatial and temporal scale dependence of hydraulic behaviour in naturally fractured clay-rich glacial deposits. The overall objective of the thesis is to develop appropriate field methods, and conceptual models for their interpretation, for measuring parameters which control hydraulic behaviour in heavily fractured, near surface clays. Some of these parameters, such as bulk vertical hydraulic conductivity, have been very rarely measured in this type of material. Similarly, the methods used in this thesis to interpret transient hydraulic tests have not commonly been used for tests in fractured clays.

Specific objectives of this thesis are:

- to develop a method to measure bulk vertical hydraulic conductivity, and its variation with depth in the near-surface highly fractured zone of clay-rich deposits;
- to demonstrate the relationships between monitoring-well scale measurements and larger scale measurements of hydraulic conductivity in these types of materials, to gain an understanding of the features which control hydraulic conductivity at each scale;
- to measure and evaluate differences in response between the fractures and clay matrix in transient hydraulic tests;
- to determine whether a discrete fracture model can be used to interpret the results of transient hydraulic tests to give results which are consistent with other methods of testing;
- to assess various fracture mapping techniques, and their applicability for deriving parameters to be used in generating simplified surrogates of the real fracture network; and
- to examine the influence of macropore geometry on transient hydraulic response and solute transport.

ORGANISATION OF THESIS

Two field experiments were conducted at locations separated by approximately 1 km, at a site in the St. Clair Clay Plain in south-western Ontario. At this site, glacio-lacustrine clay is present from the surface to a depth of approximately 40m. The upper 2-4m of the clay are heavily fractured and pervasively weathered. Below the zone of pervasive weathering the clay is unweathered except in the vicinity of fractures, which are visible to a depth of 6m. Several studies of flow and solute transport have previously been conducted in the weathered zone in the St. Clair Clay Plain, by Rodvang (1987), D'Astous et. al. (1988), Balfour (1991), Ruland et. al. (1991), McKay et. al. (1993a and b), and Harris (1994). These studies provided a basis for the experimental design, and provided a basis for comparison for some of the results of this study.

This thesis contains 6 chapters, 4 of which (Chapters 2-5) have been written as independent papers for eventual submission to peer review journals. Chapter 2 discusses the results of mapping of the distribution of fractures and other macropores at the locations of the two experiments. At one of the sites, observations of preferential flow pathways through the fracture and macropore network were made using a dye tracer. The observations in this chapter provide the context and important parameters for the interpretation on hydraulic tests in Chapters 3 and 5. In a broader context, various mapping techniques for deriving fracture network parameters are considered in this chapter, and conclusions are drawn on appropriate mapping techniques and important parameters that should be measured in mapping exercises.

An experimental design used to measure values of bulk vertical hydraulic conductivity, and the manner in which it varies with depth, is described in Chapter 3. The design was also used to derive estimates of the degree of hydraulic conductivity anisotropy at a bulk scale. The measured values of bulk scale hydraulic conductivity for the two experimental sites are

reported in Chapter 3. The relationship of these values to previous smaller scale measurements of hydraulic conductivity at the same site, and previous measurements of bulk scale horizontal hydraulic conductivity are also discussed.

The results of transient hydraulic tests are described and interpreted in Chapter 4. The experimental design which was used in Chapter 3 to measure bulk vertical hydraulic conductivity in steady state tests was again employed for the transient tests. The design allows hydraulic head transients in the fractures and in the matrix to be independently measured. The results of the tests are interpreted using a discrete fracture numerical model.

In Chapter 5, the influence of macropore geometry on transient hydraulic response and on solute transport are investigated using a numerical model. The differences between macropores with a large surface area such as fractures, and macropores with a low surface area such as root holes are investigated. Furthermore, since root holes are often found to be preferentially located along fracture faces (Bouma and Dekker, 1977; Ruland et. al., 1991; McKay and Fredericia, 1995), interaction between these types of macropores is also investigated in Chapter 5.

The conclusions of Chapters 2 - 5 are summarised in Chapter 6.

REFERENCES

Adomait, M., Hydraulic responses in fractured clay, M.Sc. project, University of Waterloo, Waterloo, Ontario, Canada, 1991.

Balfour, D. J., Evaluation of lateral solute migration in surficial weathered clayey till, M.Sc. project, University of Waterloo, Waterloo, Ontario, Canada, 1991.

Bouma, J. and L.W. Dekker, A case study on infiltration into dry clay soil 1. Morphological observations, *Geoderma*, 20, 27-40, 1978.

Bradbury, K.R. and M. Muldoon, Hydraulic conductivity determination in unlithified glacial and fluvial materials, *Ground Water and Vadose-Zone Monitoring*, ASTM STP 1053, D.M. Nielson and A.I. Johnston, eds, American Society for Testing and Materials, Philadelphia, 138-151, 1990.

Cherry, J.A., Hydrogeologic contaminant behaviour in fractured and unfractured clayey deposits in Canada, Proceedings of the International Symposium on Contaminant Transport in Groundwater, Stuttgart, Germany, 11-20, 1989.

D'Astous, A. Y., W.W. Ruland, J.R.G. Bruce, J.A. Cherry, and R. W. Gillham, Fracture effects in the shallow groundwater zone in weathered Sarnia-area clay, *Can. Geotech. J.*, 26, 43-56, 1988.

Desaulniers, D.E., Groundwater origin, geochemistry and solute transport in three major glacial clay plains of east central North America, Ph.D. thesis, University of Waterloo, Waterloo, Ontario, Canada, 1986.

Graham, J. and V.C.S. Au, Influence of freeze-thaw and softening effects on stress-strain behaviour of natural plastic clay at low stress, *Can. Geotech. J.*, 22, 69-78, 1985.

Harris, S. M., Characterization of the hydraulic properties of a fractured clay till, M.Sc. Thesis, University of Waterloo, Waterloo, Ontario, Canada, 1994.

Hendry, M.J., Hydraulic conductivity of a glacial till in Alberta, *Groundwater*, 20 (2), 162-169, 1982.

Hinsby, K., L.D. McKay, P. Jorgensen, M. Lenczewski and C.P. Gerba, Fracture aperture measurements and migration of solutes, viruses and immiscible creosote in a column of clay-rich till, *Groundwater*, 34(6), 1065-1075, 1996.

Jones, L., T. Lemar and, C. Tsai, Results of two pumping tests in Wisconsinon Age weathered till in Iowa, *Groundwater*, 30(4), 529-538, 1992.

Keller, C.K., G. van der Kamp, and J.A. Cherry, Fracture permeability and groundwater flow in clayey till near Saskatoon, Saskatchewan, *Can. Geotech. J.*, 23, 229-240, 1986.

Klint, K.E.S., Fractures and depositional features of the St. Joseph Till and the upper part of the Black Shale Till at the Laidlaw site, Lambton County, Ontario, Geological Survey of Denmark and Greenland, Report 1996/9, 1996.

McKay, L. D., J.A. Cherry, and R. W. Gillham, Field experiments in a fractured clay till 1. Hydraulic conductivity and fracture aperture, *Water Resour. Res.*, 29(4), 1149-1162, 1993a.

McKay, L.D., R.W. Gillham, and J.A. Cherry, Field experiments in a fractured clay till 2. Solute and colloid transport, *Water Resour. Res.*, 29(12), 3879-3890, 1993b.

McKay, L.D., and J. Fredericia, Distribution, origin, and hydraulic influence of fractures in a clay-rich glacial deposit, *Can. Geotech. J.*, 32, 957-975, 1995.

Morris, P.H., J. Graham and D.J. Williams, Cracking in drying soils, *Can. Geotech. J.*, 29, 263-277, 1992.

Pach, J.A., Hydraulic and solute transport characteristics of a fractured glacio-lacustrine clay Winnipeg, Manitoba, M.Sc. Thesis, University of Waterloo, Waterloo, Ontario, Canada, 1994.

Remenda, V.H., Origin and migration of natural groundwater tracers in thick clay tills of Saskatchewan and the Lake Aggassiz Clay Plain, Ph.D. thesis, University of Waterloo, Waterloo, Ontario, Canada, 1993.

Ruland, W. W., J.A. Cherry, and S. Feenstra, The depth of fractures and active groundwater flow in a clayey till plain in south-western Ontario, *Groundwater*, 29(3), 405-417, 1991.

Rudolph, D.L., J.A. Cherry and R.N. Farvolden, Groundwater flow and solute transport in fractured lacustrine clay near Mexico City, *Water Resour. Res.*, 27(9), 2187-2201, 1991.

Rodvang, S.J., Geochemistry of the weathered zone of a fractured clayey deposit in southwestern Ontario, M.Sc. thesis, University of Waterloo, Waterloo, Ontario, Canada, 1987.

Williams, R.E. and R.N. Farvolden, The influence of joints on the movement of groundwater through glacial till, *J. of 12Hydrol.*, 5, 163-170, 1967.

CHAPTER 2

MAPPING OF FRACTURES AND OTHER MACROPORE FEATURES IN A WEATHERED CLAY-RICH GLACIAL DEPOSIT

INTRODUCTION

The presence of fractures in the clayey tills which cover large parts of North America, and their influence on hydraulic and solute transport behaviour is now widely recognised (for example, Grisak and Cherry, 1975; Keller et. al., 1986; Jones et. al., 1992; and McKay et. al., 1993a and b). Their presence can increase hydraulic conductivity by up to 4 orders of magnitude above the hydraulic conductivity of the clay material itself (Keller et. al., 1986; and McKay et. al., 1993a), and can lead to rates of solute migration that are well in excess of the low, diffusion controlled rates that would be expected for an unfractured clay (Balfour, 1991; and McKay et. al. 1993b).

Although the effects of fractures are recognised in general terms, methods of interpreting observations of flow and transport phenomena in these materials are still being developed. Interpretation of hydraulic tests or tracer tests in fractured clays using models other than conventional, single continuum type models requires some information on fracture geometry. Since it is not possible to explicitly represent in a model all the fractures in the real system, one approach is to represent the actual fracture network using a surrogate network generated from statistical information on the distributions of fracture orientation, trace length, and the number of fractures within a unit volume (Harrison et. al., 1992; Therrien and Sudicky, 1996). Another possible approach is to represent the fracture network using an idealised network based on a regular, repeating geometry, such as equally spaced parallel fractures (Sudicky and Frind, 1982; Huyakorn et. al., 1983). In either case, information on the actual fracture network which is to be represented in the models can be derived from direct observations of the fracture network through coring and excavation (for example, McKay et. al., 1993a, and Hinsby et. al., 1996). However, in some cases, direct observations of the fracture network are not possible, for example if the fractures are present at considerable depths below the surface, and in such

cases, estimates of parameters such as fracture spacing can be derived indirectly from information such as solute breakthrough (for example, Rudolph et. al., 1991).

Indirect assessments of fracture spacing derived from modelling of solute breakthrough can also be compared to direct observations of the fracture network, in order to assess whether only some of the visible fractures are hydraulically "active". Sidle et. al. (1997) compare values of fracture spacing derived from mapping in an excavation, with values derived by matching solute breakthrough data from a controlled, large-scale, vertical-flow tracer test, and the predictions of the equally spaced, parallel-fracture model of Sudicky and Frind (1982). They conclude that the solute breakthrough data indicate a fracture spacing less than the visible spacing, and therefore that all the visible fractures are "active", and also that localised fractures which were not considered in the fracture mapping must also be "active". McKay et. al. (1993b) similarly matched solute breakthrough data from a controlled, large-scale, horizontal-flow tracer test with the equally spaced, parallel-fracture model of Sudicky and Frind (1982), but constrained the spacing in the model to that derived from fracture mapping in an excavation. The close match obtained between the model and the observed concentrations suggests that the spacing derived from fracture mapping is a reasonable estimate of the spacing of "active" fractures. McKay et al. (1993b) also considered vertical profiles of solute concentration, and the uniformity of the profiles did not indicate the presence of preferential pathways through the fracture network. However, the homogenisation effects of diffusion over the time period of this test may have considerably diminished the concentration differences between pathways through which rapid advection takes place, and pathways in which advective velocities are much lower.

In addition to the variable contributions of different fractures to overall hydraulic conductivity, and the different advective velocities through different fractures for a particular

overall applied gradient, flow will be distributed unevenly throughout the plane of individual fractures as a result of variable apertures within the plane of fractures. The phenomenon of flow "channelling" has been observed experimentally in fractured rock at the field scale and at the laboratory scale (Raven and Gale, 1985; Rasmuson and Neretnieks, 1986), and has been described by numerous models (for example, Rasmuson and Neretnieks, 1986; Brown, 1987; Tsang and Tsang, 1987; Raven et. al., 1988; and Johns and Roberts, 1991). Laboratory scale observations of channelling of immiscible liquids in fractures in large clay columns has been reported by Hinsby et. al. (1996) and O'Hara et. al. (1997). Direct observations of flow "channelling" at the field scale in fractured clays are limited. Using a dye, Bouma and Dekker (1978) observed infiltration patterns in clays with different macropore patterns, and observed flow along narrow bands within the plane of fractures. These observations are, however, complicated by the fact that the dye was infiltrated into a dry soil with originally unsaturated macropores. The rough nature of fracture surfaces in clay has been reported by McKay et. al (1993a), Unger and Mase (1993), and Klint (1996), and the preferential location of root holes on fracture faces has been reported by Bouma and Dekker (1977), Hendry (1982), Ruland et. al. (1991), and Hinsby et. al. (1996) and it is therefore likely that some channelling will occur at the field scale in saturated fractures in clay.

In this chapter, the results of fracture mapping and observations of other macropore features at two sites in a weathered, clayey glacial deposit are presented. Detailed hydraulic testing, which will be discussed in the following chapters, was carried out at these two sites, and one of the primary objectives of the mapping was to obtain information which may assist in the interpretation of the hydraulic tests. The information contained in this chapter, therefore, provides the context and important parameters for the interpretation of the hydraulic test results.

The two sites for which fracture mapping results are presented in this chapter are located in close proximity (within 1 km within the same geological unit) to sites where several previous fracture mapping investigations have been conducted. The results of these previous investigations have been reported by Ruland et. al. (1991), McKay et. al. (1993a), McKay and Fredericia (1995), and Klint (1996), and similar descriptions of the fracture network are reported in all of these studies. From these studies, information on fracture orientation and persistence are available for depths between 2m and 7m below ground surface. These parameters are an important component required to generate statistically equivalent fracture networks for numerical analyses of flow and transport. Although qualitative descriptions of the fractures above a depth of 2m are available from previous studies, very little quantitative information on fracture spacing, orientation and persistence is available. In this chapter distributions of fracture orientations and trace length are obtained for the fracture network between the ground surface and a depth of 2m. In a broader context, various mapping techniques for deriving fracture network parameters are considered in this chapter, and conclusions are drawn on appropriate mapping techniques and important parameters that should be measured in mapping exercises.

This chapter also describes the observed differences between fracture patterns at two apparently similar sites which are located within the same clay plain, and observations of preferential flow paths that were made at the field scale using a dye tracer to assess the importance of flow channelling within fractures and the relative contributions of different features to overall bulk hydraulic conductivity.

FIELD SITE AND PREVIOUS INVESTIGATIONS

Mapping of fractures and other macropore features was carried out at the Laidlaw hazardous waste treatment and disposal facility, located approximately 12 km south-east of

Sarnia, Ontario (see Figure 2.1). This site lies within an extensive clay plain, the Lambton Clay Plain, which forms the northern third of the 5900 km^2 St. Clair Clay Plain (Chapman and Putnam, 1984). Throughout the clay plain, clay-rich Quaternary age tills and glacio-lacustrine sediments extend from within 1m of the ground surface to the bedrock at depths ranging between 25m and 50m, and averaging 40m (Desaulniers, 1986).

For purposes of stratigraphic classification, these tills and glacio-lacustrine sediments have been divided into two units (Fitzgerald et al., 1979). The lower unit, known as the Black Shale Till is generally 30-35m thick and contains numerous black shale clasts. The upper unit, the St. Joseph Till extends generally to the surface, although it is overlain locally by thin deposits of sand and gravel. It is generally 7-13m thick, and is typically a silty clay (25-45% <2μm diameter) with a small fraction (<20%) of sand and gravel (McKay and Fredericia, 1995). This unit is thought to consist of glacio-lacustrine sediments which have been deformed by grounding icebergs and/or internal slumping of weakly consolidated material (Klint, 1996).

The upper 4-6m of the St. Joseph Till are visibly oxidised and fractured. Pervasive chemical weathering extends to a depth of 2-4m, and is marked by a colour change in the clay matrix from brown above to grey below (Ogunbadejo and Quigley, 1973). Below the zone of pervasive oxidation, chemical weathering is only evident in the immediate vicinity of major fractures. Klint (1996) noted that fractures are generally indiscernible at the Laidlaw site below a depth of 6m. Notwithstanding, fractures have been observed at depths in excess of 9m (Adams, 1969), and roots have been observed at depths of up to 9m (Hanna, 1966), in drill cores from other locations in the Lambton Clay Plain. Abandoned root holes are common in the near-surface weathered St. Joseph Till, and are often preferentially located on fracture faces (D'Astous et. al., 1988; Ruland et. al., 1991; Harris, 1994; McKay and Fredericia, 1995; Klint, 1996).

In terms of their geometry, McKay et. al. (1993a) and Klint (1996) classified the fractures in the St. Joseph Till according to a hierarchy of scales. First-order fractures are the dominant fractures which cross-cut all other fractures, and at the Laidlaw site, the first-order fractures are predominantly vertical. Second-order fractures, which are also predominantly vertical, sometimes connect first-order fractures but do not cross them. Vertical and horizontal third-order fractures further divide the clay between the first and second order fractures into roughly cubic peds, which are on the order of 1 cm across. Klint (1996) noted that horizontal third-order fractures often follow thin silt/fine sand laminae. McKay et. al. (1993a) observed that at a depth of 3m, the clay was divided into polygonal columnar blocks by the first-order fractures, and that these blocks were further subdivided by second- and third-order fractures.

Klint (1996) noted a relation between the intensity of first- and second-order fractures and local topography, with fewer fractures extending to shallower depths in relative topographic lows, when compared to relative topographic highs. The local topography is characterised by linear drainage depressions which are separated by several tens of metres to hundreds of metres, and which are up to 0.5m lower in elevation than the high ground between the depressions. He also observed that fractures in relative topographic lows tend to be preferentially oriented in two orthogonal directions, whereas fractures in other areas tend to form higher-order polygonal systems.

Harris (1994) and McKay et al. (1993a) report that the water table at the Laidlaw site varies seasonally between the ground surface and a depth of 1.5m, and it has been observed to respond quickly to individual rainfall events (Adomait, 1991; and Harris, 1994). Ruland et al. (1991), based on measurements at various sites throughout the St. Clair Clay Plain, report that the water table is usually within 2m of the surface, but that piezometers used in their study went dry at depths of up to 4.9m in particularly dry summers. The presence of weathered clay

at depths of up to 4m indicates that the water table was likely lower than at present for a prolonged period of time at some point since the clay was deposited (Soderman and Kim, 1969).

FIELD METHODS

Fracture Mapping

Fracture mapping was carried out at two sites at the Laidlaw facility. Surface observations at both sites did not reveal any characteristics that particularly distinguished them from other locations at the Laidlaw facility, or indeed from other locations throughout the Lambton clay plain. However, the sites were distinguished by the fact that the first site was located on a relative topographic high, and the second site was located in a relative topographic low. The sites were separated by approximately one kilometre. Detailed hydraulic testing was carried out at these two sites prior to excavation for the fracture mapping. The hydraulic testing will be described in Chapters 3 and 4.

At both sites, fracture mapping was carried out on vertical excavation faces and on horizontal faces. Immediately after the excavation was completed, the faces to be mapped were prepared by removing the "smeared" clay with hand tools. On the vertical faces, the surface of first- and second-order fractures was carefully exposed in order to measure their orientation. In all cases, fractures were identified by their tendency to part along a clearly defined surface, and the presence of visible staining or precipitation on that surface.

On the horizontal faces, the exposed fracture pattern was traced onto clear plastic. At the first site, the following information was recorded for each fracture intersecting the vertical excavation faces: position along a horizontal reference line, order (first or second), orientation, trace length, surface precipitation, and the presence or absence of roots on the fracture

surface. At the second site, only fracture orientations were recorded. No attempt was made to count third-order fractures, however their presence or absence in different areas was noted. The presence of any other features such as zones with apparently different clay content, or persistent macropores other than fractures was also noted.

In accordance with the classification scheme used by Klint (1996), first-order fractures were classified as fractures which did not cross-cut any other fractures, and fractures which connected or intersected these fractures were classified as second-order fractures. The distinction between first- and second-order fractures on this basis is illustrated in Figure 2.2, for a fracture pattern which is similar to those observed in the field. This classification is of course somewhat arbitrary, since fractures may intersect out of the plane of the vertical cross-section on which the fractures are mapped, or at a depth greater than that considered in a particular excavation.

At the first site, fractures were first mapped on a horizontal surface at a depth of 0.6m below ground surface, and then on six vertical faces from 0.6m to 2.1m below ground surface. Five of the six vertical faces were close to parallel, and were formed by successively widening the excavation in four stages, as illustrated in Figure 2.3. At each stage, the new vertical face was cleaned and mapped. The sixth face which was mapped (Profile F on Figure 2.3) was perpendicular to the other five, and was fully exposed at the completion of the four stages of excavation. At the second site, fractures were mapped on a single horizontal surface at a depth of 1.5m below ground surface, and on a single vertical face from 1.5m to 3.0m below ground surface (see Figure 2.4).

Dye Infiltration and Mapping

At the second site, preferential flow paths within the clay were investigated using a 0.4 g/l solution of the dye methylene blue ($C_{16}H_{18}ClN_3S$). This dye is absorbed well by the clay, and provides a good colour contrast. Its use for identifying preferential flow paths in clay with macropore features has been reported by Bouma et. al. (1977), Bouma and Dekker (1978), and Bootlink et. al. (1993).

Infiltration of the dye was achieved by inducing a strong downwards gradient with an injection/withdrawal system involving two, sand-filled hydraulically induced fractures at depths of 1.0 m and 2.0 m below the ground surface. The system is illustrated in Figure 2.5. A third induced fracture at a depth of 3.0m below ground surface was not used in the dye infiltration system. The set of three induced fractures was used for the hydraulic testing described in Chapters 3 and 4, and the dye infiltration was carried out at the completion of that testing. The hydraulic testing and dye infiltration experiment were carried out approximately 20m from the fracture mapping area at the second site.

Hydraulic fracturing at the field sites was carried out by FRx Ltd in association with Dr. Larry Murdoch at the University of Cincinnati. The procedure for creating hydraulically induced fractures is described by Murdoch (1995). Briefly, the fractures are created by driving a plugged steel casing to the desired depth, then driving the plug downwards from the base of the casing to form a short uncased section of borehole at the base of the cased section. A horizontal notch is cut in the uncased section of borehole with a high pressure water jet, which acts to initiate the fracture in a horizontal plane when a sand/gel mixture is pumped in under pressure. The driven casing is left in place after fracture injection, and can be used to inject and/or withdraw fluid from the induced fractures.

The geometry of the two induced fractures used in the dye infiltration system was determined by detailed surveying when the site was excavated to map the distribution of dye, and is illustrated in Figure 2.6. The uppermost induced fracture, injected at a depth of 1.0 m, rose relatively sharply towards the surface, and terminated at a depth of 0.4 m at a maximum distance of 1.6m from the injection point. In the area beneath the uppermost induced fracture, the induced fracture which was injected at a depth of 2.0 m was relatively flat lying. This induced fracture was larger than the overlying induced fracture, and coring indicated that it extended to a maximum distance of 2.5m from the injection point.

Prior to the dye injection, the water table was at a depth of 0.5 below the ground surface, and therefore fully saturated conditions were maintained throughout the injection period in the interval between the two induced fractures used for injection and withdrawal. A Marriotte system was used to maintain a constant water level at 0.4m above ground surface in the injection well, and a peristaltic pump was used to maintain a constant water level of 0.6m below ground surface in the withdrawal casing, which is equivalent to a unit vertical gradient between the injection and withdrawal points. Prior to the injection of the dyed water, undyed water was used until the injection and withdrawal flow rates stabilised at steady state values. At steady state, the injection flow rate was approximately 8.4 l/hr, and the withdrawal flow rate was approximately 9.6 l/hr. A total of 375 l of dye solution was injected. At the completion of injection, dye was detectable in the effluent from the withdrawal well, but at a much lower concentration than that of the injection solution.

Two days after the completion of the dye injection, the site was excavated in order to trace the patterns of dye movement. Firstly, the soil was carefully removed by hand from above the upper induced fracture, so that the induced fracture itself and the distribution of dye within it remained intact. The surface of the induced fracture and the areas which were stained

with dye were then surveyed. The distribution of dye was then mapped on four horizontal benches between the injection and withdrawal levels, as shown in Figure 2.6. At each level, the smear caused by the excavation equipment was removed with hand tools, and the locations of dye staining were surveyed. Dye staining patterns were also observed on vertical profiles in two trenches which were excavated to either side of the area in which the mapping was carried out on horizontal benches.

RESULTS AND DISCUSSION

Results of Fracture Mapping at First Site

The nature of weathering and fracturing observed at the first site is consistent with the qualitative descriptions for the same depth interval which are provided by Ruland et. al. (1991), McKay et. al. (1993a), Harris (1994), McKay and Fredericia (1995) and Klint (1996), from studies conducted at other locations at the Laidlaw site. Within the depth interval considered (0.6 m to 2.1m below ground surface), the clay was brown in colour, with orange, red and grey staining throughout. The most persistent fractures (those classified as either first- or second-order) were predominantly vertical, and almost exclusively stained with a light grey precipitate, which is assumed to consist of reduced iron-containing minerals as suggested by McKay and Fredericia (1995). Towards the base of the vertical profiles, a small number of fractures were stained with red and black minerals, which are assumed to be oxidised iron- and manganese-containing minerals. The clay blocks between the first- and second-order fractures were intact in places, and in other places were divided into roughly cubic peds on the order of 1 cm in size by vertical and horizontal third-order fractures. The surfaces of third-order fractures were in many cases unstained, but in some cases were stained with red and black minerals. The light grey staining observed on first- and second-order fractures was not observed on any third-order fractures at this site. Although the fractures could be classified

according to a hierarchy of scales as at other sites, the columnar structure reported by McKay et. al. (1993a) at a depth of 3m was not apparent within the excavation at the first site. The pattern of fracturing observed at the first site can be idealised as shown in Figure 2.7. Roots and root traces were observed on the surface of essentially all first- and second-order fractures.

The map of fracture traces on the horizontal mapping face at a depth of 0.6 m below ground surface is illustrated in Figure 2.8. It can be seen that many of the fracture intersections are perpendicular or close to perpendicular. The most persistent fractures observed on this face were several metres in length. Also illustrated in Figure 2.8 is a large (approximately 3 m x 1 m) pocket of sandy clay. On the vertical profiles, this sandy clay pocket was observed to extend to a depth of approximately 1m below ground surface. On the horizontal mapping plane at a depth of 0.6 m, no fractures were present in this feature, however fractures within the sandy clay were observed at greater depths on the vertical mapping profiles. Grain size analyses on samples taken from this feature indicate a sand content of up to 41%, in contrast to a typical value of less than 20% in other locations. Several smaller pockets (approximately 20 cm in width) of similar material were observed on the vertical profiles. McKay and Fredericia (1995) report observing a 1.5m wide, "isolated lump" of sandy clay between depths of 1.8 m and 3.2 m in an excavation at the Laidlaw site. Klint (1996) observed similar features at depths of up to 6m at the Laidlaw site.

The variations in trace length, dip, and strike for first- and second-order fractures are illustrated in Figure 2.9, for all of the vertical profiles at the first site. The average trace length for first-order fractures is 0.85m, whereas for second-order fractures it is 0.52m. It can be seen from Figure 2.9a that the range of trace lengths for first-order fractures is much larger than for second-order fractures. It can also be seen from Figure 2.9b that the majority of

fractures are within 10° of vertical (62% of first-order fractures and 76% of second-order fractures), and that practically all fractures are within 20° of vertical.

Since observations of fracture strike on a particular profile will be biased against fractures which are almost parallel to the wall, fracture orientation data has been assessed by combining the information from profiles A-E, which are essentially parallel, with the information from profile F, which is perpendicular to those profiles. In combining the information from these two sets of profiles, the orientation data from profile F and the averaged orientation data from profiles A-E have been weighted by the lengths of the profiles. The formula for combining the data from the two sets of profiles, and the combined results are illustrated in Figure 2.9c. In this figure, no distinction has been made between first- and second-order fractures, as it was found that both types of fractures had similar distributions of orientation. Three preferential fracture orientations are evident with strikes of 70°, 110° and 150°, with fractures aligned towards 70° dominating.

The local variability in fracture pattern was assessed by considering the variability in fracture orientations for the five parallel profiles A-E. Fracture strike data from each of these profiles is illustrated separately in Figure 2.10. It can be seen that although there are differences between the profiles, each profile gives a similar indication of the preferential fracture orientations. This indicates that the fracture pattern does not vary substantially within localised areas at the Laidlaw site. However, Klint (pers. comm.) observed that although preferential fracture orientations may be locally uniform, different preferential orientations are observed at different locations at the Laidlaw site.

The preferential fracture orientations derived from fracture mapping on vertical profiles are illustrated in Figure 2.8, in conjunction with the map of fracture traces on a horizontal plane at a depth of 0.6 m below ground surface. The fracture pattern suggested by fracture mapping

on vertical profiles is broadly consistent with the pattern observed in a horizontal plane. This is significant since vertical exposures are more common, and it indicates that it should be possible to assess changing fracture orientations with depth in a single vertical profile, rather than a series of horizontal excavations which would be more time consuming and would cause more disturbance. However, it is not possible to assess the horizontal persistence of fractures in a vertical excavation, and therefore both types of exposures are required to develop a three-dimensional picture of the fracture network.

Results of Mapping at Second Site - General Observations

The most prominent macropore features in the upper 2 m at the second site were not in fact fractures, but were cylindrical cavities which were loosely infilled with "plugs" of soft silty clay material. A clearly visible open annulus of up to several millimetres between the walls of the cavities and the infilling "plugs" was present in most cases, for at least part of the perimeter of the cavities. An example of two such cavities is illustrated in Figure 2.11, and a typical "plug" of infilling material is illustrated in Figure 2.12. These features are not reported in any of the previous studies undertaken at the Laidlaw site, but were observed at both the fracture mapping area and the dye infiltration area at the second site. They were observed to be continuous over vertical distances of up to 1m, and were predominantly vertical, although cavities inclined at up to thirty degrees from the vertical were also observed. The cavities themselves were up to 5 cm in diameter, however a "halo" of soft and moist clay up to 10 cm in diameter was present around the perimeter of most of the cavities. In the majority of cases, the interior of the cavities and the infilling material were coated with a light grey precipitate, similar to the fracture coating commonly found on near-surface first- and second-order fractures at the Laidlaw site. Roots and root traces were present in the majority of the cavities.

The origin of the cavities is not known. It is possible that they could be abandoned root holes of large trees which inhabited the area prior to agricultural development in the 19th century, and that the infilling material is silt and clay sediment that settled in the cavities during localised flooding of the topographic low in which they were observed.

The frequency of the cavities was assessed by counting the number of cavities on the horizontal excavation face at a depth of 1.5 m at the fracture mapping area, and approximately 20 m away at the dye infiltration area, on a horizontal face at a depth of 2.1 m. The locations of cavities in these two areas is shown in Figure 2.13. The frequency of the cavities appears to decrease with depth (5 cavities/m^2 at 2.1m depth, as opposed to 10.5 cavities/m^2 at 1.5m depth), but this could also be natural variability between the two locations at which the frequencies were measured. However, at the fracture mapping area, where a frequency of 10.5 cavities/m^2 was measured at a depth of 1.5 m, none were observed at a depth of 3 m, suggesting that a trend of decreasing frequency with depth is likely.

In addition to the presence of the cavities at the second site, the fracture network at the second site was different in many respects to that observed at the first site. Above a depth of 1.5m, the hierarchy of first-, second- and third-order fractures observed at the first site and at other sites was not evident. The most persistent fractures were randomly oriented, were generally less than 0.3m in length, and terminated at their intersection with other fractures, rather than cross-cutting other fractures. These fractures were almost exclusively coated with a light grey precipitate, which appeared in general to be considerably thicker than fracture coatings of the same precipitate at the first site. In some cases the fracture coating was in the vicinity of 1 mm in thickness. Furthermore, randomly oriented third-order fractures dividing the clay into irregular peds with an average maximum dimension on the order of 1.5 cm were

present throughout above a depth of 1.5 m, and were commonly stained with a light grey precipitate.

Below a depth 1.5 m, the fracture pattern more closely resembled that observed at the first site. Predominantly vertical first-and second-order fractures could be identified, with the most persistent first-order fractures traceable to the maximum depth of the excavation at 3.0 m. Randomly oriented third-order fractures were also present below 1.5 m to a maximum depth of approximately 2.2 m, although they were absent in some areas. Below 1.5 m, third-order fractures were stained with either a light grey precipitate or an orange precipitate, however in the vicinity of cavities they tended to be stained with a light grey precipitate. Root traces were observed down to a depth of 3 m, and were predominantly located along fracture faces.

The geometrical relationship between the cavities and first- and second-order fractures is illustrated in Figure 2.13, at depths of 1.5m and 2.1m below the ground surface. It can be seen that, in general, the cavities are intersected by fractures. Such an arrangement might suggest a causal relationship between the two features, but is not sufficient to establish the particular nature of the relationship. It may suggest that the cavities pre-date the fractures, since such features would be preferential initiation sites for desiccation fractures due to the non-uniform stress conditions in their vicinity. However, if the cavities are in fact abandoned root holes, this could suggest that the roots followed pre-existing fractures, due to the lower resistance to growth along fractures, and the greater ease with which water can be drawn from the fractures into the roots.

In addition to the observed geometrical relationship between fractures and the cavities, it was noted that, in the vicinity of the cavities, the density of root traces on the surfaces of first- and second-order fractures was higher than elsewhere, and that the root traces were in general

wider than elsewhere. It was also noted the cavities were almost exclusively surrounded by a zone of third-order fracturing, in which roots and root traces also appeared to be more highly concentrated than elsewhere.

The differences in fracture patterns between the two sites in this study is possibly due to the presence of the cavities at the second site, and their influence on fracture development. However, the reason why cavities and the type of fracture pattern seen at the second site have not been observed at any other location at the Laidlaw site is not clear. The only notable difference between the sites from surface observations is that the second site is located in a topographic low, whereas the first site is located on a topographic high. However, Klint (pers. comm.) examined vertical profiles in both topographic highs and lows at the Laidlaw site, and did not observe the presence of cavities or qualitatively different fracture patterns in the topographic lows.

Results of Mapping at Second Site - Dye Mapping

The locations at which dye staining was observed at each of the excavation levels are illustrated in Figure 2.14. At a particular excavation level, the boundaries of the area that was cleaned and mapped were not the same as for the area that was mapped on the excavation level above, although there was always an overlap from one level to the next. The boundaries of the areas that were cleaned and mapped at each level are shown in Figure 2.14. Also illustrated is the outline of the observed limit of dye staining in the upper induced fracture, into which the dye was injected. Dye staining was present at all locations within this outline, and was observed to extend to within 10 cm of the ultimate boundaries of the induced fracture.

The majority of the dye staining was associated with the cavities, either as staining in the annulus between the infilling material and the walls of the cavity, or in abandoned root traces

and on fracture faces in the zone third-order fracturing in the immediate vicinity of the cavity. In some cases where dye staining occurred in the annulus between the walls of the cavity and the infilling material, the dye was found over almost the entire inner perimeter of the cavity and over almost the entire surface of the "plugs" of infilling material (see Figure 2.15). In some other cases, the dye was found along reasonably discrete, tortuous pathways along the annulus (see Figure 2.12). A typical example of dye staining in the fractured zone in the vicinity of a cavity is shown in Figure 2.16. It can be seen that the flow path in this region was extremely tortuous, leaving a dendritic pattern of dye staining along the surfaces of third-order fractures and along abandoned root holes. This type of flow pattern was observed only at the fourth excavation level, at a depth of approximately 1.8m.

At each excavation level, dye staining was also observed in isolated, open root holes up to 10 mm in diameter, however not all root holes were stained. These features were most prominent at the first excavation level, and decreased in frequency with depth. On the vertical profiles in the trenches to either side of the dye mapping area (see Figure 2.14), it was observed that these features were commonly located along the surface of major fractures. Dye staining on fracture faces was limited to root traces, and in the case of third-order fractures, to the patterns of staining similar to that shown in Figure 2.16. In no cases was dye staining which indicated distributed flow throughout the plane of a major fracture observed.

A comparison of the locations of dye staining at each excavation level (Figure 2.14) indicates that few of the preferential flow paths indicated by staining can be correlated from one excavation level to the next, and those that can reasonably be correlated are associated with cavities. It can also be seen that staining was not limited to the volume of clay directly beneath the limit of dye staining in the upper induced fracture, which indicates that flow was not limited to vertical pathways.

Controls on Hydraulic Conductivity at the Two Sites

At the second site, mapping of the distribution of dye indicates that for the hydraulic conditions imposed, the majority of the fluid flux took place through isolated, infilled cavities and highly fractured clay in their immediate vicinity. Dye was also observed in isolated, open root holes, but was not observed to be distributed throughout the faces of major fractures. This indicates that at this site, bulk-scale vertical hydraulic conductivity is controlled by the influence of isolated, essentially linear features. It was also observed that although third-order fractures were present throughout above a depth of 1.5m, they tended to be stained only in the vicinity of cavities. This may indicate that these fractures are not generally highly conductive.

No direct observations of preferential flow paths were made at the first site, and therefore it is not possible to make conclusions about which features control bulk hydraulic conductivity. The cavities which were observed at the second site and in which the majority of the dye staining was observed were not present at the first site, nor at any of the other sites investigated by previous researchers. It might therefore be expected that the first- and second-order fractures would make a more significant contribution to the bulk hydraulic conductivity at these sites. However, root holes were observed at the first site and at sites investigated by previous researchers, and these features were also identified as preferential flow paths at the second site. Thus, although fractures would be expected to make a more significant contribution to bulk hydraulic conductivity than at the second site, root holes may still make the largest contribution to bulk vertical hydraulic conductivity.

IMPLICATIONS OF REGIONAL SCALE HETEROGENEITY

The observation that two very different fracture and macropore patterns are present at two locations separated by approximately 1 km within the same clay plain indicates that the assumption of regionally similar fracture patterns, based on factors such as a regionally similar

depositional environment, climate and mineralogy, may be incorrect. The variability of fracture patterns, and of the relative conductivities of fractures and other high conductivity macropore features, will lead to variability in processes such as recharge and contaminant transport in such environments.

The relative contributions of different types of macropores (fractures, root holes and cavities) to bulk hydraulic conductivity will have an important influence on transient hydraulic behaviour and on solute transport. The rate of transient pressure changes in the macropore and the rate of movement of a solute through the macropores will be greatly influenced by the ratio of contact area between the macropore and the surrounding porous medium to the volume of the macropore, due to the controlling influence of this ratio on the process of diffusion of water and solutes away from the macropore. This can be seen, for example, by considering the formulation for solute transport through a discretely fractured porous medium given by Sudicky and Frind (1982). Planar features such as fractures have a much higher contact area to volume ratio than linear features such as root holes and cavities, and therefore will act to more effectively retard the movement of pressure perturbations and solutes.

The relative conductivities of the different types of macropores will also influence the bulk scale anisotropy in hydraulic conductivity. Although a network of predominantly vertical fractures can provide an interconnected pathway for horizontal flow, albeit with a lower hydraulic conductivity than for flow in the vertical direction due to the increased tortuosity of the flow path, a group of predominantly vertical linear features are far less likely to provide laterally interconnected pathways. Thus, in cases where flow is controlled by predominantly vertical linear features such as root holes or the cavities observed at the second site, the bulk scale horizontal hydraulic conductivity will be considerably less than the bulk scale vertical hydraulic conductivity.

The potential variability in fracture and macropore patterns which was observed has important consequences for the degree and type of investigation required for waste disposal facilities in such environments. Based on the differences observed at two sites which were 1 km apart, substantially different solute transport characteristics may apply at different locations within the area of a proposed landfill.

REPRESENTING FRACTURE NETWORKS USING SIMPLIFIED FRACTURE GEOMETRIES

It is common practice to represent real fracture networks such as those described in the foregoing with an idealised fracture network which is based on a regular, repeating pattern such as equally spaced parallel fractures (Sudicky and Frind, 1982; Huyakorn et. al., 1983; Rudolph et. al., 1991; McKay et. al., 1993b) or equally spaced orthogonal fractures (McKay et. al., 1993a; Hinsby et. al., 1996; O'Hara et. al. 1997). When choosing an idealised fracture network to represent a particular real fracture network, it is important to consider how the behaviour of the system is controlled by various aspects of the fracture network geometry. For example, in a system where the fractures are predominantly vertical, the bulk vertical hydraulic conductivity will be controlled in part by the total trace length of fractures per unit area in the horizontal plane. Similarly, the ratio of fracture/clay contact area to volume of unfractured clay will exercise an important control on transient hydraulic response and solute concentrations in the clay matrix, through its effect on diffusion of water and solutes into the matrix. Accordingly, these parameters should be the same for the idealised representation of the fracture network and for the real fracture network.

In the case of vertical fractures only, the trace length per unit area, and the contact area to volume ratio are directly related and can thus both be directly determined from measuring fracture trace lengths on horizontal excavation faces (the contact area to volume ratio is twice

the trace length per unit area). For the remainder of this chapter, these related parameters will both be referred to using the general term fracture intensity. Thus, if measurements of fracture intensity are available from mapping on horizontal exposures, idealised fracture networks can be defined which have the same values of fracture intensity. If the fracture network is idealised as parallel, equally spaced fractures, the required spacing is given by:

$$2B = 1/\text{fracture intensity}.$$

If, on the other hand, the fracture network is idealised as two sets of orthogonal, equally spaced fractures, the required spacing is given by:

$$2B = 2/\text{fracture intensity}.$$

The choice of parallel fractures or two sets of orthogonal fractures to represent the real fracture network will depend on the observed geometry of the real fracture network. If there is a strong tendency for fractures to be oriented in one particular direction, then this would be best represented by an idealised system of parallel fractures. However, if fractures are preferentially oriented in more than one direction, or if they are more randomly oriented, this would be better represented by two orthogonal sets of fractures, or perhaps some higher order geometrical arrangement. However, systems of parallel or orthogonal fractures offer the advantage of mathematical simplicity, and to idealise the fracture network using a more complex but regular geometrical arrangement may be difficult to justify due to the uncertainty in other parameters (a more reasonable approach to representing complex fracture network geometry is to generate statistically equivalent fracture networks from measured distributions of relevant parameters).

It is far more common, however, to map fractures along vertical profiles than on horizontal exposures, and the manner in which fracture intensity can be determined from fracture spacing information on vertical profiles is not immediately obvious. A common

approach is to determine the average fracture spacing, 2B, by dividing the length of the profile by the total number of fractures observed along the profile, and to then represent the fracture network with a set of parallel vertical fractures with the same, equal spacing (for example, McKay et. al. 1993b). For this idealised set of fractures, fracture intensity is given by the inverse of the fracture spacing.

The results of the fracture mapping previously discussed can be used to investigate how the fracture intensity thus determined for the idealised system of fractures compares to that determined from mapping of the fracture network on horizontal faces. Fracture intensities for idealised networks, and the values from which they were derived are summarised in Table 2.1, for each of the six vertical profiles at the first site, and the single vertical profile at the second site. Also given in Table 2.1 are the values of fracture intensity determined from mapping on horizontal faces at both sites. It can be seen that at the first site, fracture intensities for the idealised fracture networks are consistently less than the fracture intensity measured on the horizontal mapping surface, and that the average idealised fracture intensity for all of the vertical profiles is approximately half the measured value. However, at the second site, the fracture intensity for the idealised fracture network is approximately equal to the intensity measured on the horizontal mapping surface. This indicates that, in general, fracture mapping on vertical profiles only can not be used to derive values of fracture intensity since no information is obtained on lateral persistence, and that complimentary measurements on horizontal exposures are therefore required.

CONCLUSIONS

Two very different fracture patterns have been observed in the weathered near-surface clay at two sites in the St Clair Clay Plain. Surface observations at the sites, which were separated by approximately 1km, did not reveal any features that suggest they are atypical of

the clay plain in general, and thus it was not expected a priori that there would be substantial differences between the two sites.

At the first site, the fracture pattern was qualitatively similar to that observed in five previous investigations conducted in the same area. At this site, major fractures (so-called first- and second-order fractures) in the weathered clay are predominantly vertical. The most persistent of these fractures are greater than 1.5 m in length, and tend to cross-cut other less persistent fractures which they intersect. The clay between the first- and second-order fractures is in some areas divided into roughly cubic peds on the order of 1 cm in size by closely spaced vertical and horizontal fractures (so-called third-order fractures). No change in the nature of the fracture pattern was apparent between 0.6 m and 2.5 m below ground surface. The results of fracture mapping at this site provide information of the distributions of fracture orientation and persistence, which are important components of techniques which generate artificial fracture networks for numerical analysis of flow and transport.

At the second site, major fractures in the upper 1.5 m tend to be randomly oriented and generally less persistent than at the first site, terminating in most cases at their intersection with other fractures rather than cross-cutting them. Randomly oriented third-order fractures dividing the clay into irregular peds with an average maximum dimension of 1.5 cm are present throughout to a depth of 1.5 m. Below 1.5 m, the fracture pattern at the second site is qualitatively similar to that observed at the first site.

Another substantial difference between the two sites is the presence at the second site of primarily vertical cylindrical cavities which were loosely infilled with "plugs" of soft silty clay material. The cavities themselves were up to 5 cm in diameter, although a zone of soft and moist clay of up to 10 cm in diameter was present around most of the cavities. The cavities were observed to be continuous for distances of up to 1m. The origin of the cavities is not

known, however it is postulated that they may be abandoned root holes from large trees which were present in the area prior to the commencement of agriculture in the 19th century.

The reasons for differences between the two sites are not certain, however it is likely that the presence of the cavities has had some influence on the development of fractures at the second site. It is not known whether the cavities and (possibly) associated fracture pattern which were observed at the second site are local features, or whether they may occur elsewhere throughout the clay plain. They have not been reported in any of the previous investigations that have been conducted at nearby sites.

Mapping of preferential flow paths at the second site was carried out by infiltrating a dye and then mapping its distribution in the subsurface. It was found that the cavities were major conduits for fluid flow, both through the open annulus between the walls of the cavities and the "plugs" of infilling material, and through highly fractured zones immediately surrounding the cavities. Open root holes, often located along fracture faces, were also identified as important conduits for fluid flow. Dye staining did not indicate distributed flow throughout the plane of major fractures in any instances. Since root holes were observed to be preferentially located along fracture faces at the first site, and at all nearby sites studied in previous investigations, it may be that in the weathered zone throughout the Lambton Clay Plain, root holes make a more significant contribution to bulk vertical hydraulic conductivity than fractures. Dye infiltration studies at other sites are required to confirm this proposition. Although closely spaced, third-order fractures were present throughout in the area of dye infiltration, they were generally only stained in the immediate vicinity of the cavities, which indicates that they are not, in general, highly conductive.

A comparison of fracture mapping on vertical and horizontal faces at the first site indicates that the common practice of determining average fracture spacing from vertical

profiles only, and then idealising the fracture network as equally spaced parallel fractures will not in general produce an idealised network which is equivalent to the actual network in terms of important parameters which control flow and transport. Important information, such as the lateral persistence of fractures, is not obtained from mapping on vertical profiles only, and therefore complimentary mapping on horizontal surfaces is also required.

REFERENCES

Adams, J.I, Effect of groundwater levels on stress history of the St. Clair clay till deposit: Discussion, *Can. Geotech. J.*, 7, 190-193, 1969.

Adomait, M., Hydraulic responses in fractured clay, M.Sc. project, University of Waterloo, Waterloo, Ontario, Canada, 1991.

Brown, S.R., Fluid flow through rock joints: The effect of surface roughness, *J. Geophys. Res.* 92, 1337-1347, 1987.

Balfour, D. J., Evaluation of lateral solute migration in surficial weathered clayey till, M.Sc. project, University of Waterloo, Waterloo, Ontario, Canada, 1991.

Bootlink, H.W.G., R. Hatano and J. Bouma, Measurement and simulation of bypass flow in a structured clay soil: a physio-morphological approach, *J. of Hydrol.*, 148, 149-168, 1993.

Bouma, J., A. Jongerius, O. Boersma, A. Jager and D. Schoonderbeek, The function of different types of macropores during saturated flow through four swelling soil horizons, *Soil Sci. Soc. Am. J.*, 41, 945-950, 1977.

Bouma, J. and L.W. Dekker, A case study on infiltration into dry clay soil 1. Morphological observations, *Geoderma*, 20, 27-40, 1978.

Chapman, L.P. and D.F. Putnam, Physiography of southern Ontario, 3rd. ed., Ontario Geological Survey, Special Vol. 2, 1984.

D'Astous, A. Y., W.W. Ruland, J.R.G. Bruce, J.A. Cherry, and R. W. Gillham, Fracture effects in the shallow groundwater zone in weathered Sarnia-area clay, *Can. Geotech. J.*, 26, 43-56, 1988.

Desaulniers, D.E., Groundwater origin, geochemistry and solute transport in three major glacial clay plains of east central North America, Ph.D. thesis, University of Waterloo, Waterloo, Ontario, Canada, 1986.

Fitzgerald, W.D., E. Janicki, and D.J. Storrinson, Sarnia-Brights Grove area, southern Ontario, Ontario Geological Survey, Preliminary Map P-2222, 1979.

Hanna, T.H., Engineering properties of glacial-lake clays near Sarnia, Ontario, *Ontario Hydro Research Quarterly*, 3rd Quarter, 1-12, 1966.

Harris, S. M., Characterization of the hydraulic properties of a fractured clay till, M.Sc. Thesis, University of Waterloo, Waterloo, Ontario, Canada, 1994.

Harrison, B., E.A. Sudicky and J.A. Cherry, Numerical analysis of solute migration through fractured clayey deposits into underlying aquifers, *Water Resour. Res.*, 28(2), 515-526, 1992.

Hendry, M.J., Hydraulic conductivity of a glacial till in Alberta, *Groundwater*, 20 (2), 162-169, 1982.

Hinsby, K., L.D. McKay, P. Jorgensen, M. Lenczewski and C.P. Gerba, Fracture aperture measurements and migration of solutes, viruses and immiscible creosote in a column of clay-rich till, *Groundwater*, 34(6), 1065-1075, 1996.

Huyakorn, P.S., B.H. Lester and C.R. Faust, Finite element techniques for modeling groundwater flow in fractured aquifers, *Water Resour. Res.*, 19(4), 1019-1035, 1983.

Johns, R.A. and P.V. Roberts, A solute transport model for channelized flow in a fracture, *Water Resour. Res.*, 27(8), 1797-1808, 1991.

Jones, L., T. Lemar and, C. Tsai, Results of two pumping tests in Wisconsinon Age weathered till in Iowa, *Groundwater*, 30(4), 529-538, 1992.

Keller, C.K., G. van der Kamp, and J.A. Cherry, Fracture permeability and groundwater flow in clayey till near Saskatoon, Saskatchewan, *Can. Geotech. J.*, 23, 229-240, 1986.

Klint, K.E.S., Fractures and depositional features of the St. Joseph Till and the upper part of the Black Shale Till at the Laidlaw site, Lambton County, Ontario, Geological Survey of Denmark and Greenland, Report 1996/9, 1996.

McKay, L. D., J.A. Cherry, and R. W. Gillham, Field experiments in a fractured clay till 1. Hydraulic conductivity and fracture aperture, *Water Resour. Res.*, 29(4), 1149-1162, 1993a.

McKay, L.D., R.W. Gillham, and J.A. Cherry, Field experiments in a fractured clay till 2. Solute and colloid transport, *Water Resour. Res.*, 29(12), 3879-3890, 1993b.

McKay, L.D., and J. Fredericia, Distribution, origin, and hydraulic influence of fractures in a clay-rich glacial deposit, *Can. Geotech. J.*, 32, 957-975, 1995.

Ogunbadejo, T.A. and R.M. Quigley, Micro-structural and mineralogical influences on the compaction characteristics of weathered clays from Sarnia, Ontario, University of Western Ontario Soil Mechanics Research Report SM-2-73, 1973.

O'Hara, S.K., B.L. Parker, P.R. Jorgenson and J.A. Cherry, Trichloroethene DNAPL flow and mass distribution in naturally fractured clay: 1. Evidence of aperture variability, Submitted to *Water Resour. Res.*, November 1997.

Rasmuson, A. and I. Neretnieks, Radionuclide transport in fast channels in crystalline rock, *Water Resour. Res.*, 22(8), 1247-1256, 1986.

Raven, K.G. and J.E. Gale, Water flow in a natural rock fracture as a function of stress and sample size, *Int. J. Rock Mech. Min. Sci. and Geomech. Abstr.*, 22(4), 251-261, 1985.

Raven, K.G., K.S. Novakowski and P.A. Lapcevic, Interpretation of field tracer tests of a single fracture using a transient solute storage model, *Water Resour. Res.*, 24(12), 2019-2032, 1988.

Rudolph, D.L., J.A. Cherry and R.N. Farvolden, Groundwater flow and solute transport in fractured lacustrine clay near Mexico City, *Water Resour. Res.*, 27(9), 2187-2201, 1991.

Ruland, W. W., J.A. Cherry, and S. Feenstra, The depth of fractures and active groundwater flow in a clayey till plain in south-western Ontario, *Groundwater*, 29(3), 405-417, 1991.

Sidle, R.C., B. Nilsson, M. Hansen and J. Fredericia. Spatially varying hydraulic and solute transport characteristics of a fractured till determined by field tracer tests, Funen, Denmark. Submitted to *Water Resour. Res.*, 1997.

Soderman, L.G. and Y.D. Kim, Effect of groundwater levels on stress history of the St. Clair clay till deposit, *Can. Geotech. J.*, 7, 173-187, 1969.

Sudicky E.A. and E.O. Frind, Contaminant transport in fractured porous media: Analytical solution for a system of parallel fractures, *Water Resour. Res.*, 18(6), 1634-1642, 1982.

Therrien, R. and E.A. Sudicky, Three-dimensional analysis of variably-saturated flow and solute transport in discretely-fractured porous media, *J. Cont. Hydrology*, 23, 1-44, 1996.

Tsang, Y.W. and C.F. Tsang, Channel model of flow through fractured media, *Water Resour. Res.*, 23(3), 467-479, 1987.

Unger, A.J.A. and C.W. Mase, Numerical study of the hydromechanical behaviour of two rough fracture surfaces in contact, *Water Resour. Res.*, 29(7), 2101-2114, 1993.

Profile	Profile Length L_p (m)	Number of Fractures N_f	Spacing $2B=L_p/N_f$	Fracture Intensity for idealised fracture network $I=1/2B$ (m/m^2)	Fracture Intensity from mapping on horizontal faces (m/m^2)
1'st site Profile A	4	14	0.29	3.44	8.2
1'st site Profile B	3.5	15	0.23	4.35	
1'st site Profile C	4.5	19	0.24	4.17	
1'st site Profile D	5	31	0.16	6.25	
1'st site Profile E	5.5	33	0.17	5.88	
1'st site Profile F	4.3	18	0.24	4.17	
2'nd site	5	33	0.15	6.67	6.9

Table 2.1 - Comparison of fracture intensities from mapping on vertical profiles and mapping on horizontal surfaces

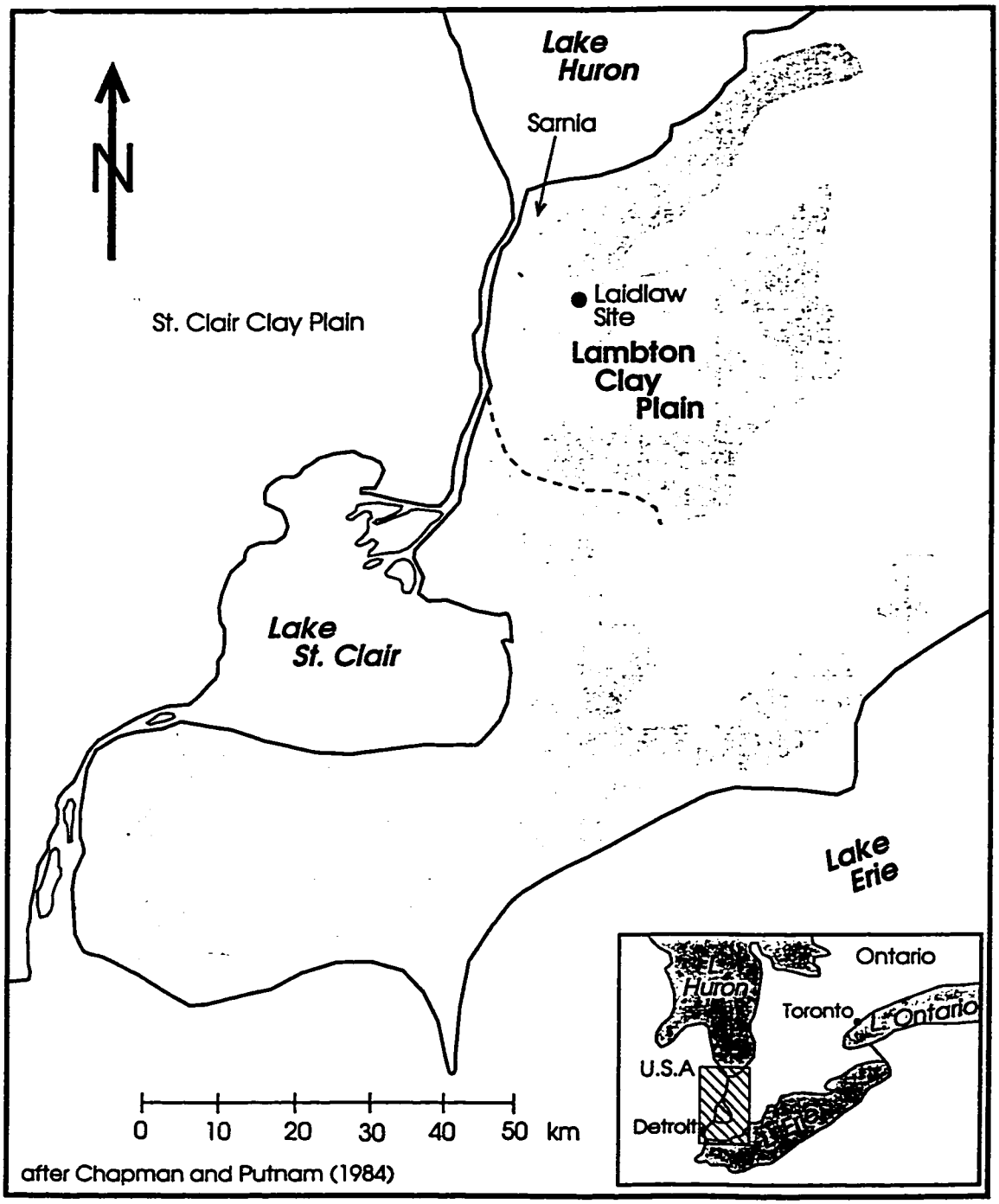

Figure 2.1 - Location of study site

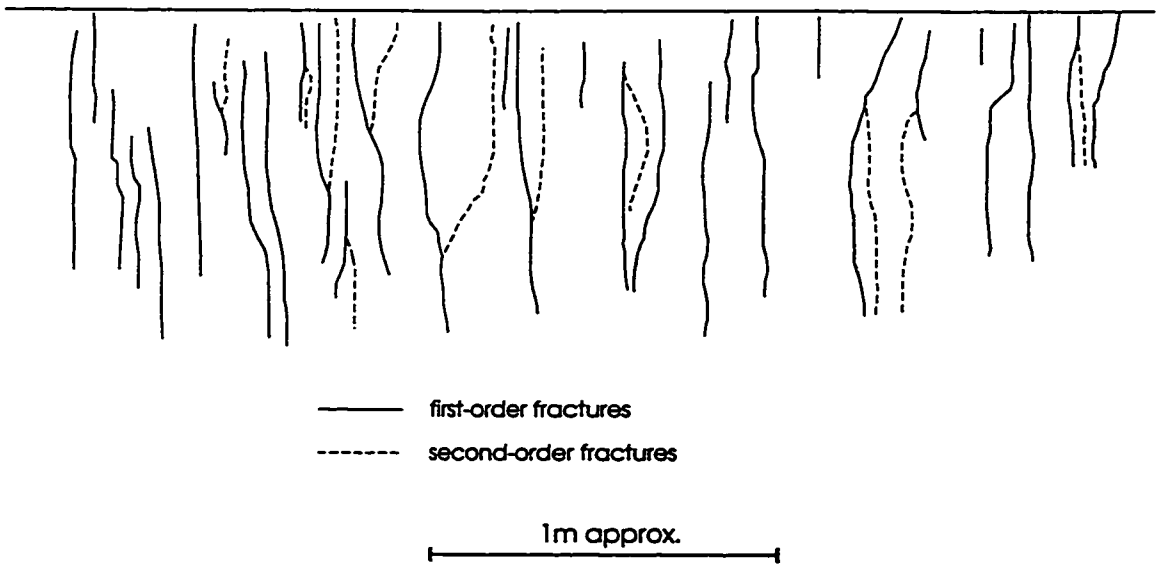

Figure 2.2 - Distinction between first- and second-order fractures for a typical fracture network

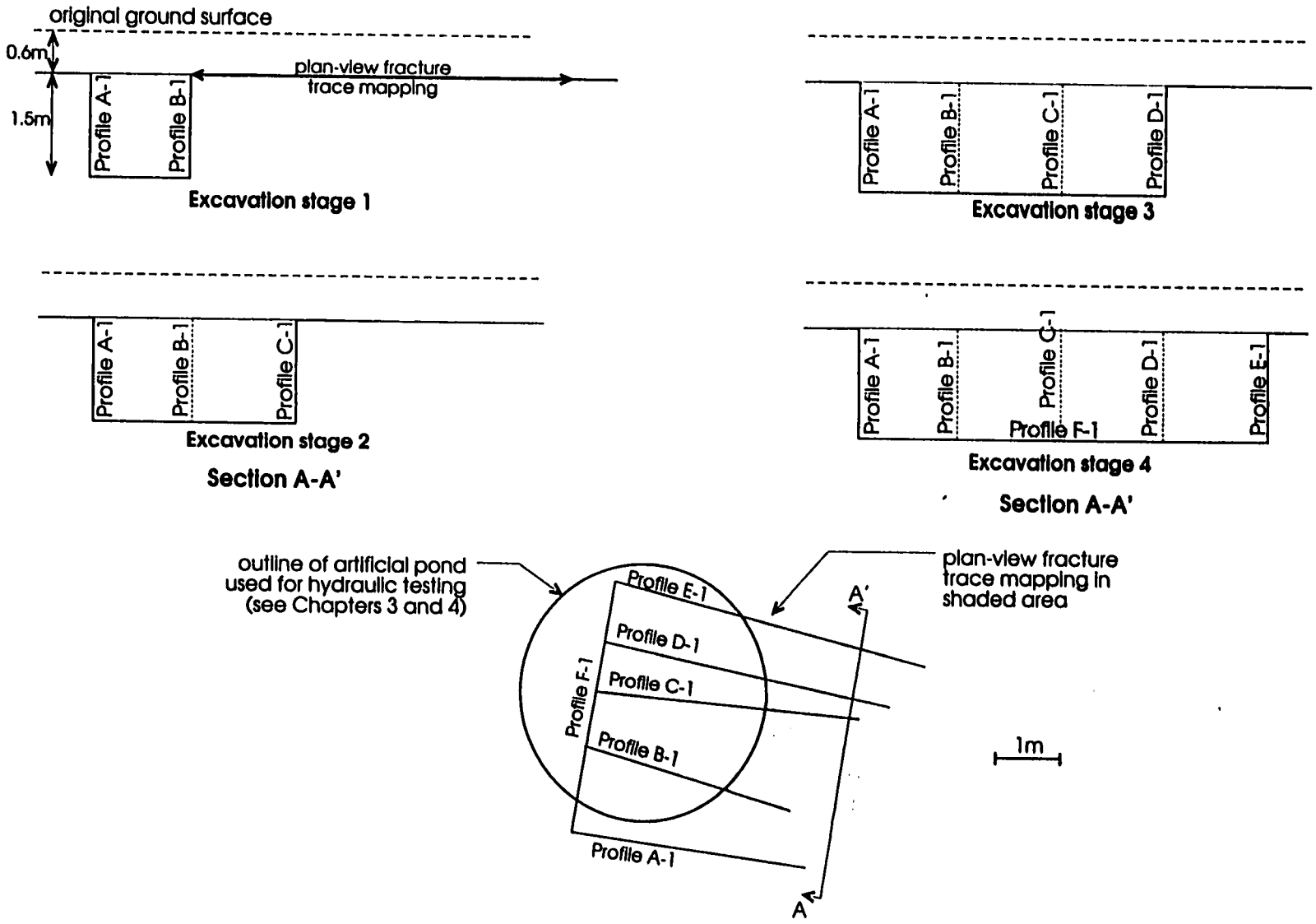

Figure 2.3 - Excavation sequence and profile locations for fracture mapping at first site

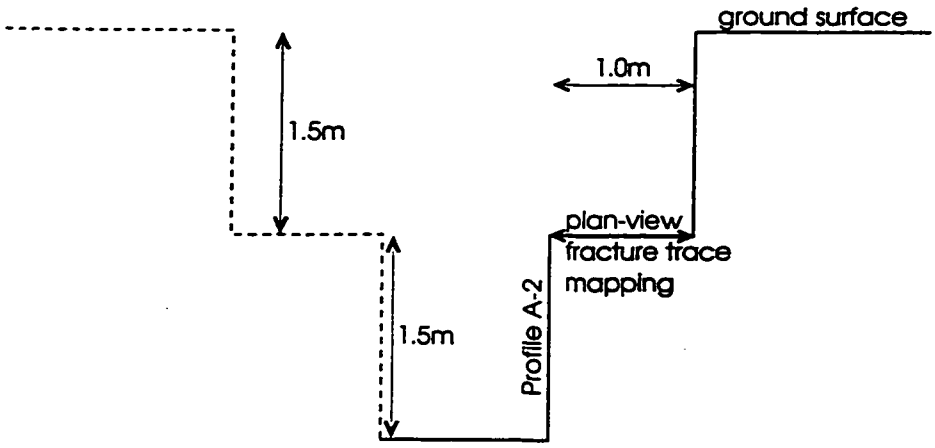

Figure 2.4 - Excavation geometry for fracture mapping at second site

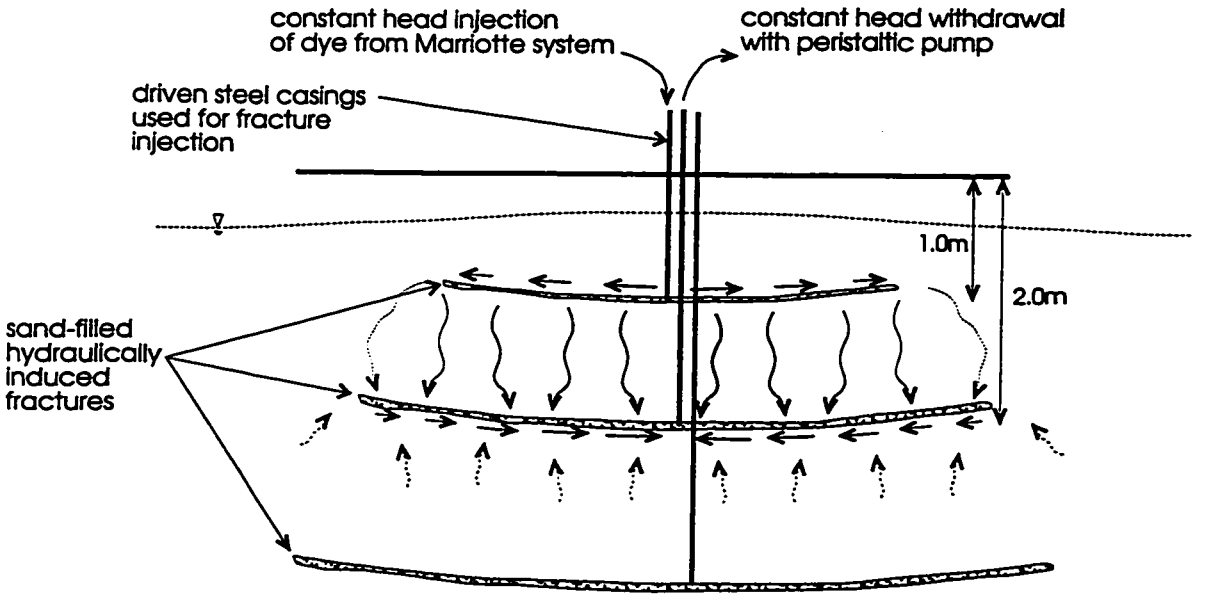

Figure 2.5 - Circulation of dye using two induced fractures

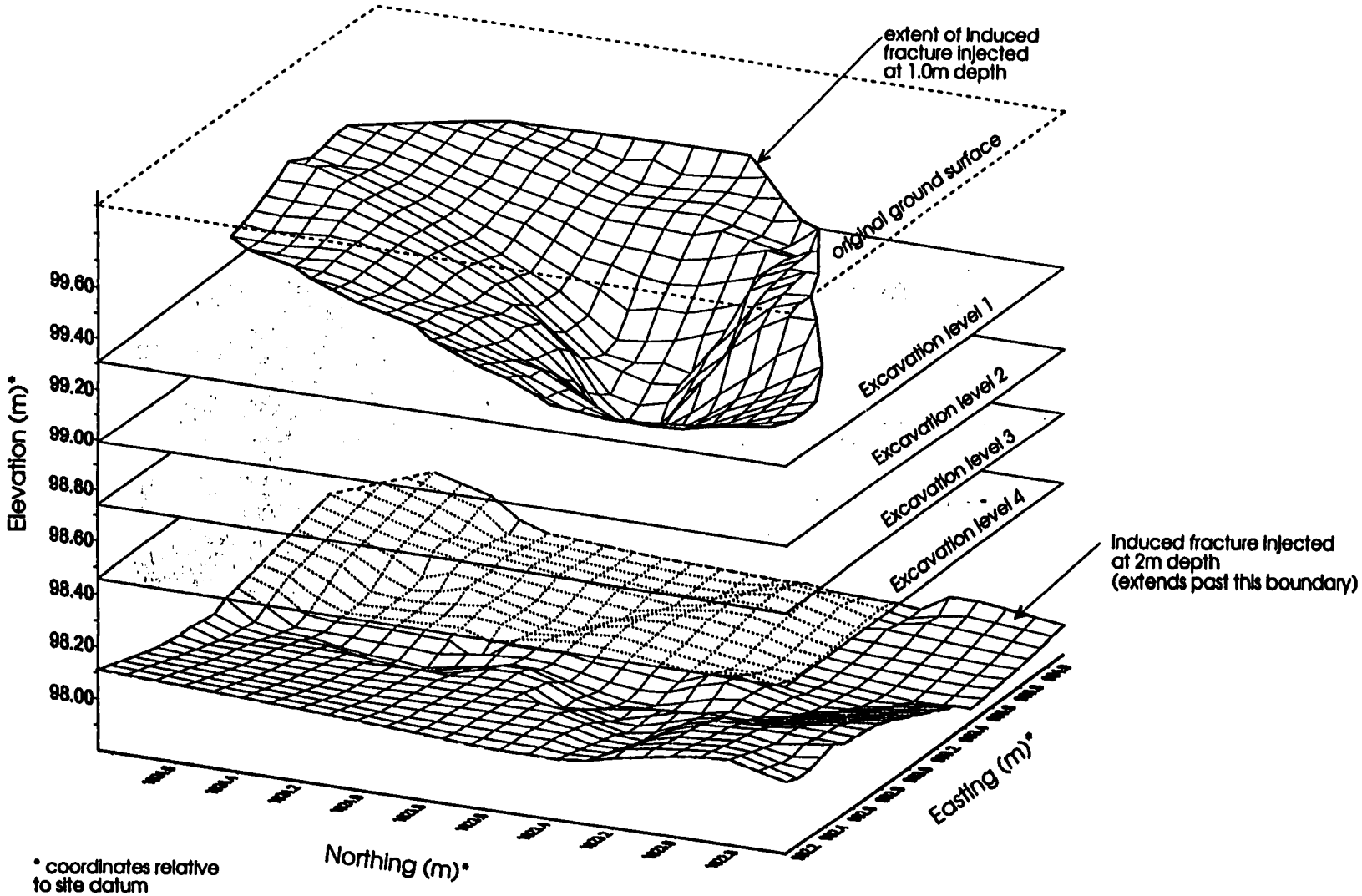

Figure 2.6 - Induced fracture geometry and excavation sequence for dye mapping

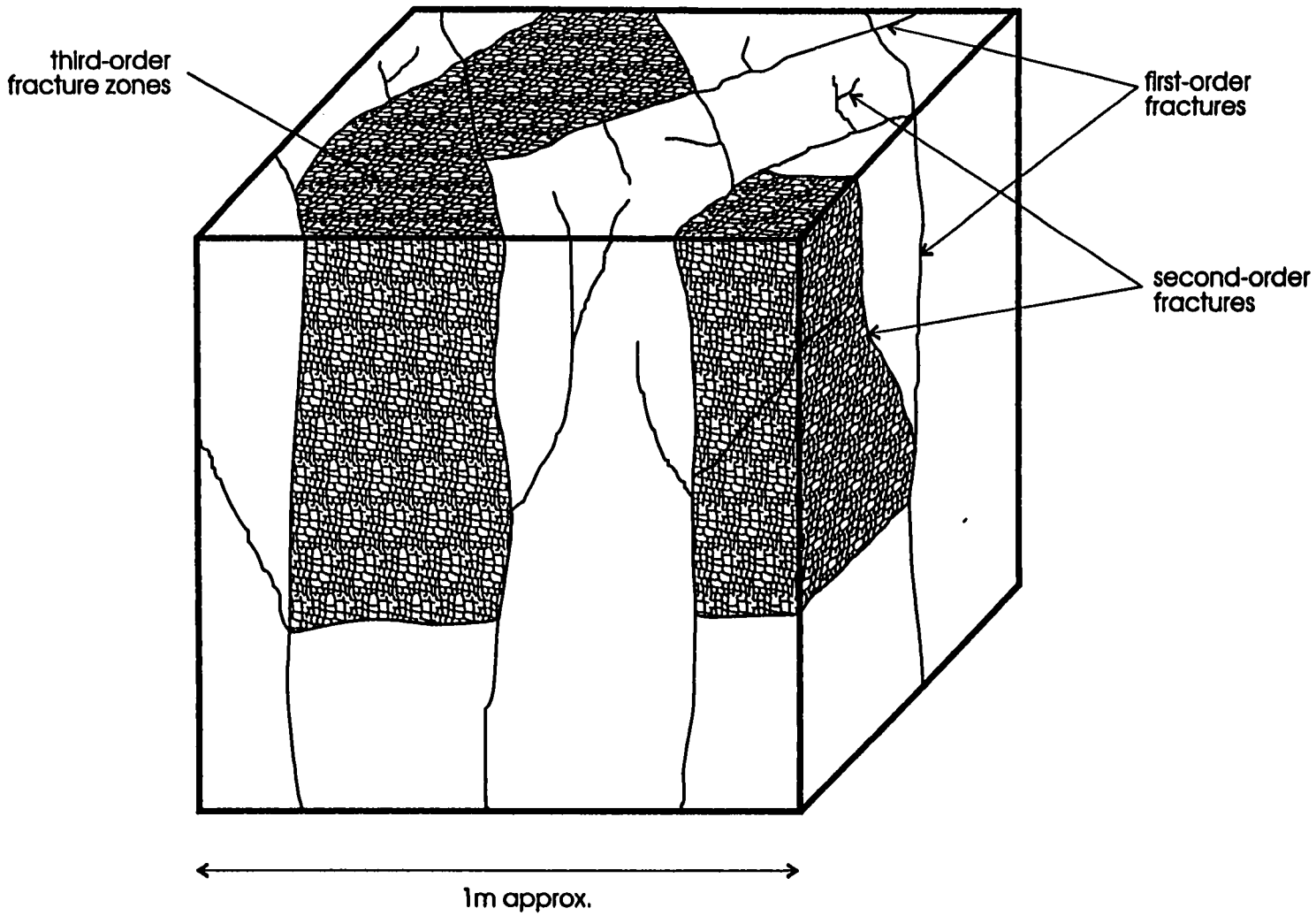

Figure 2.7 - Idealised fracture network geometry at first site

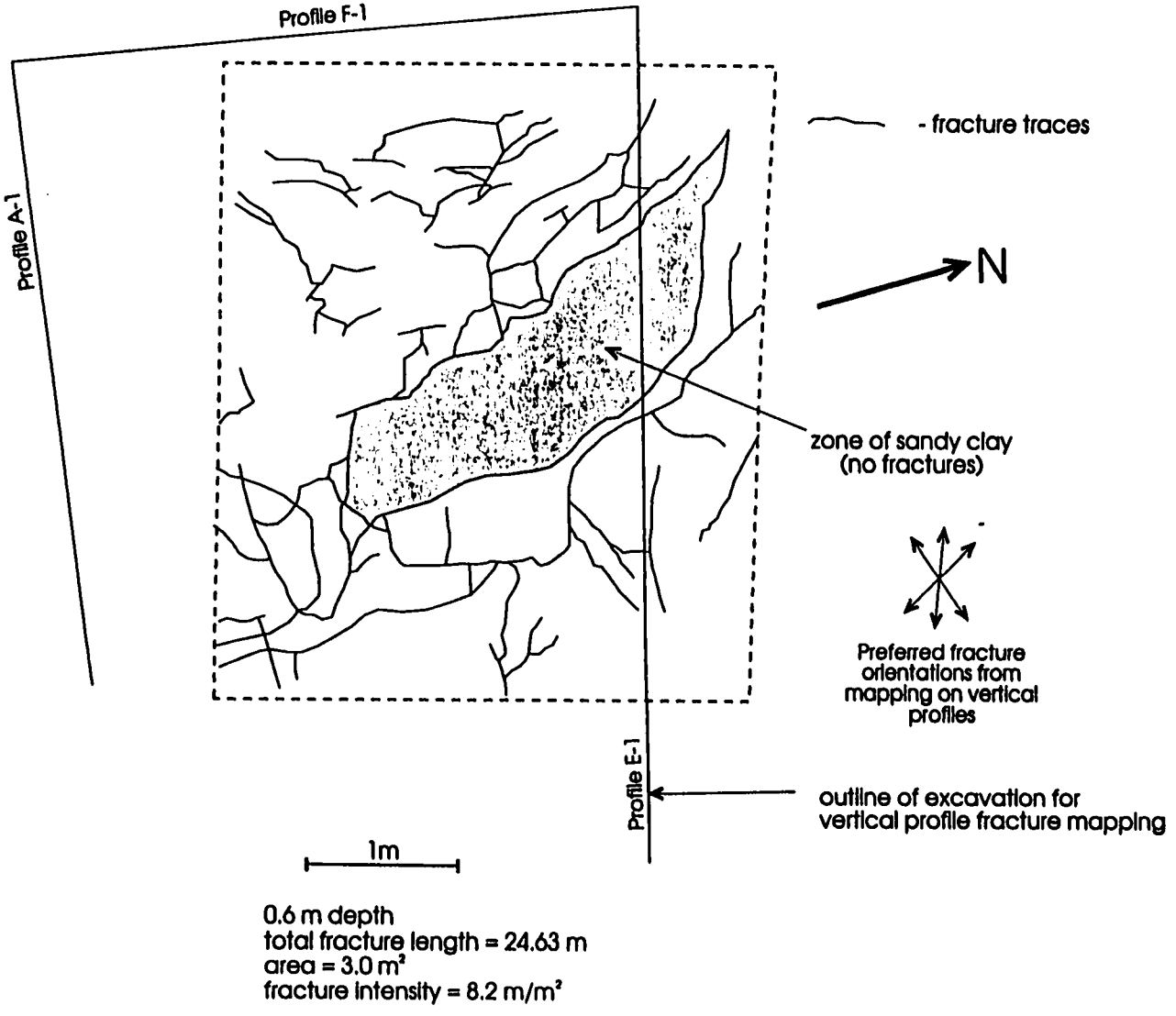

Figure 2.8 - Plan-view fracture traces at first site

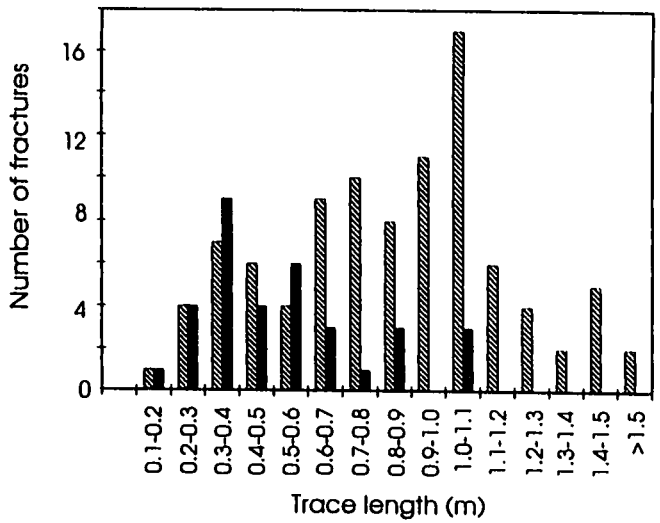

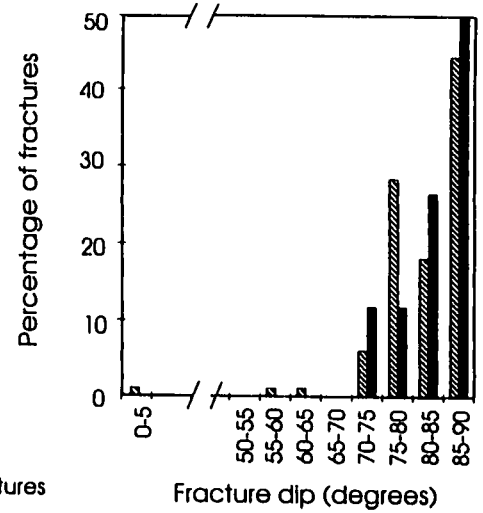

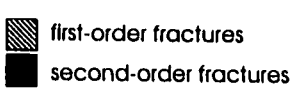

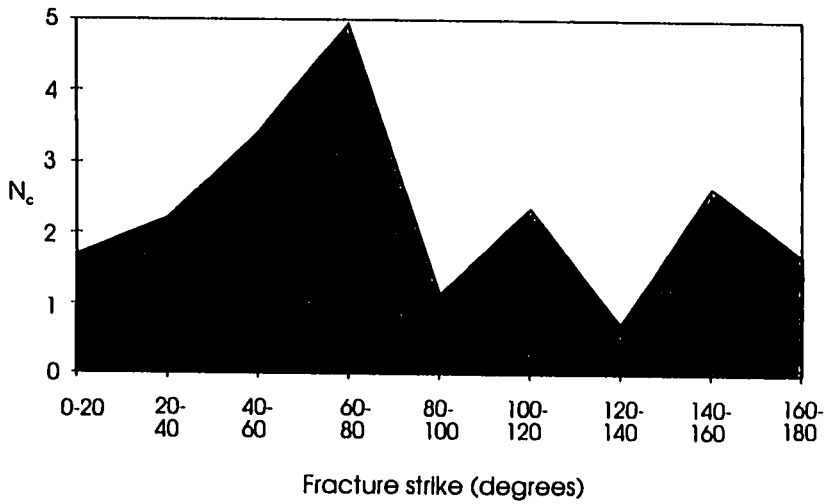

$$N_c = \frac{\left(\frac{\sum_{\alpha=A}^{F} N\alpha_{0\text{-}20} \cdot L\alpha}{\sum_{\alpha=A}^{F} L\alpha} \cdot \frac{\sum_{\alpha=A}^{F} L\alpha}{5} + NF_{0\text{-}20} \cdot LF \right)}{\left(\sum_{\alpha=A}^{F} L\alpha + NF_{0\text{-}20} \cdot LF \right)}$$

$N\alpha_{0\text{-}20}$ = number of fractures with strike between 0° and 20° for profile α (both first- and second-order fractures)

$L\alpha$ = length of profile α

Figure 2.9 - Distributions of trace length, dip and strike for fractures at first site

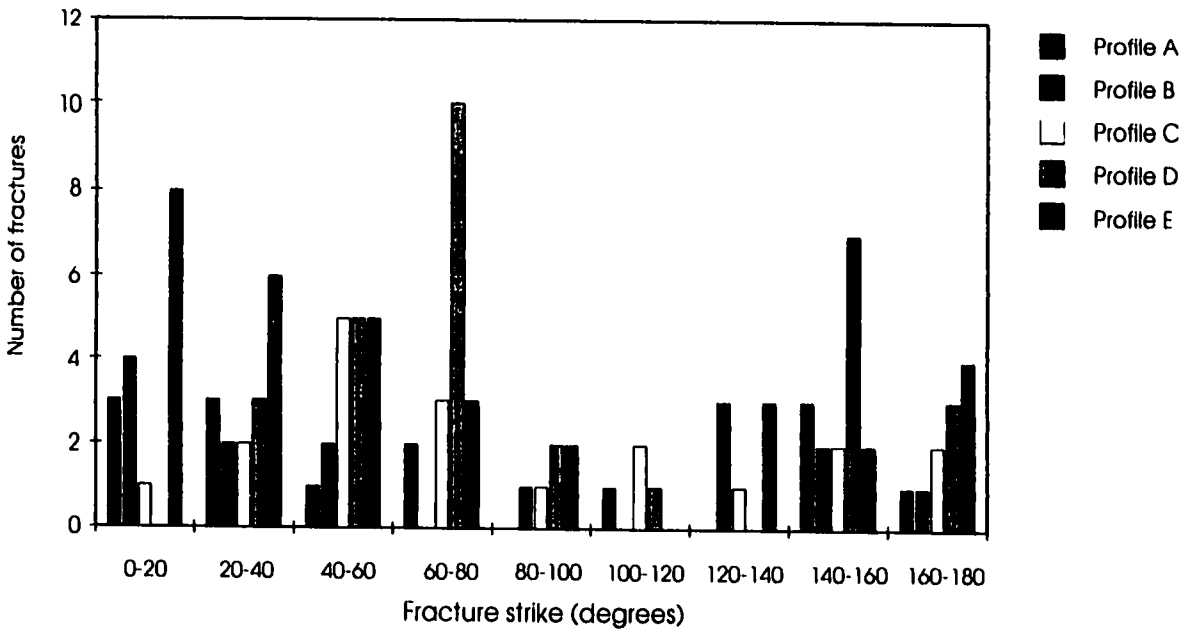

Figure 2.10 - Comparison of fracture orientations for different profiles

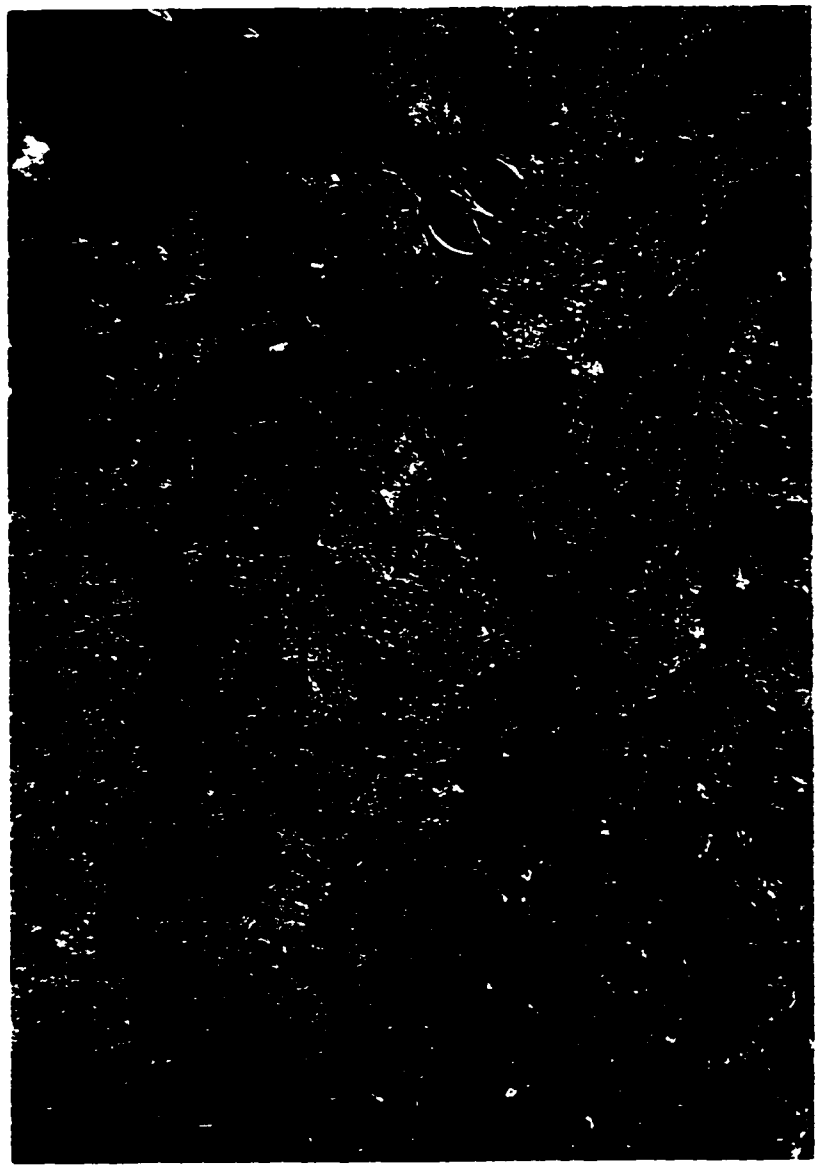

Figure 2.11 - View of typical cavities on vertical excavation face at second site

Figure 2.12 - Typical plug of cavity infilling material

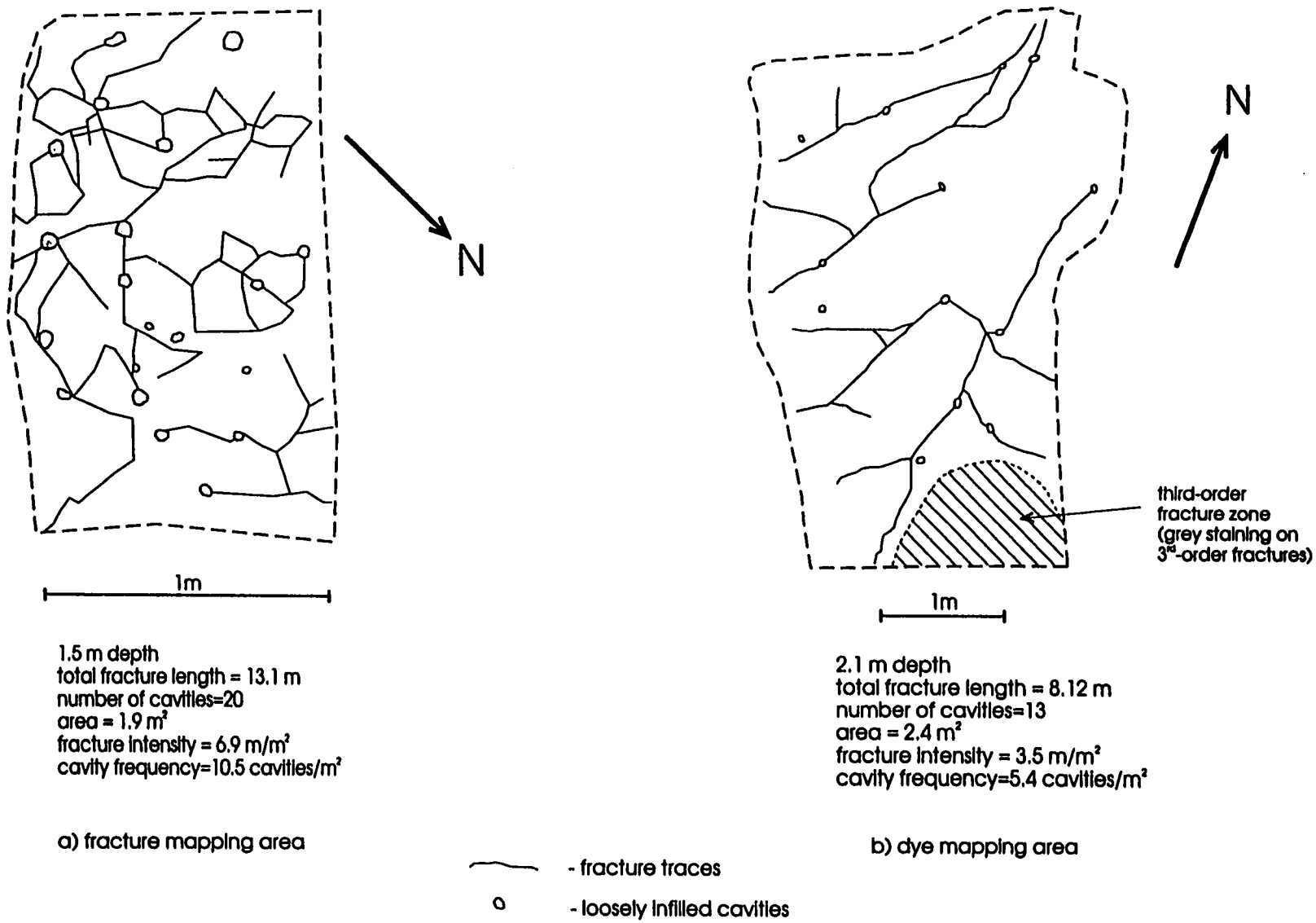

Figure 2.13 - Plan-view fracture traces and positions of cavities at second site

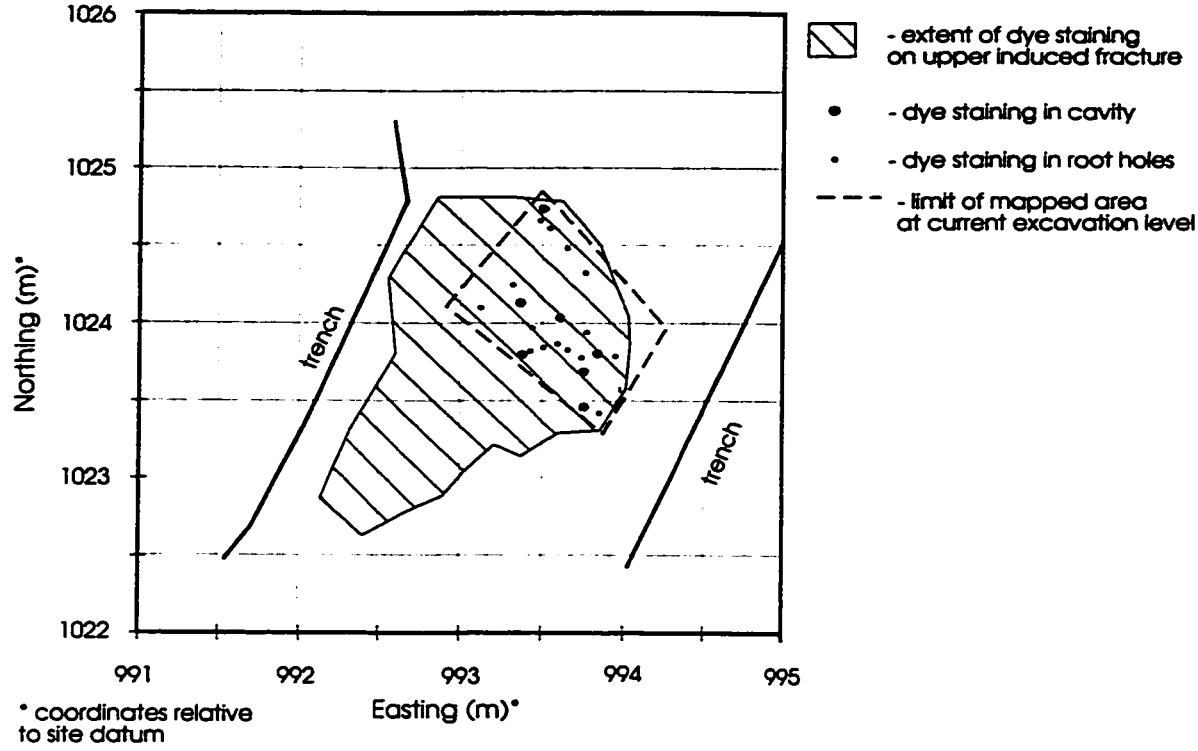

a) Locations of dye staining on first excavation level - 0.7m below ground surface

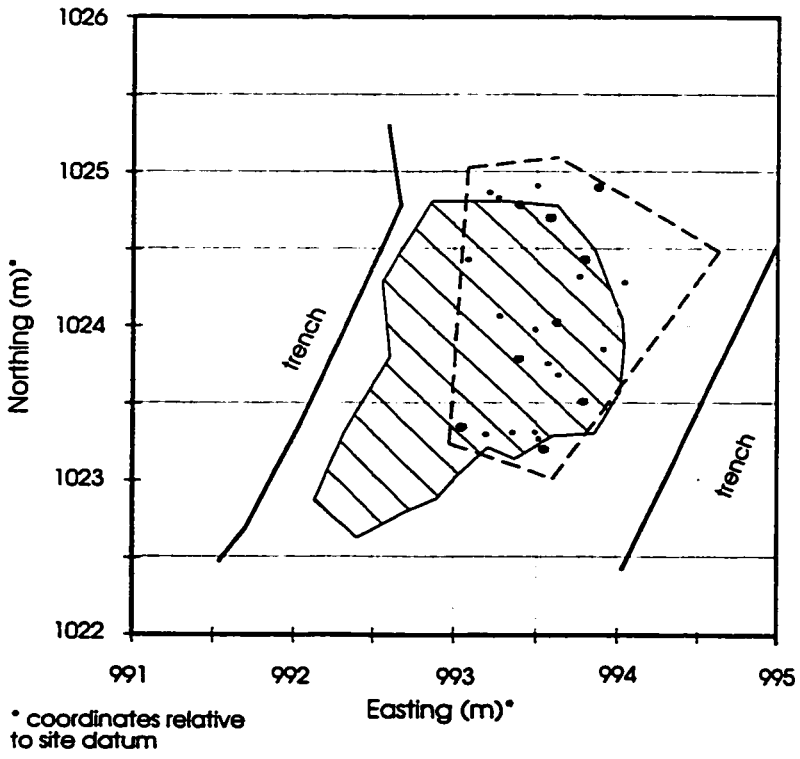

b) Locations of dye staining on second excavation level - 0.9m below ground surface

Figure 2.14 - Dye staining patterns

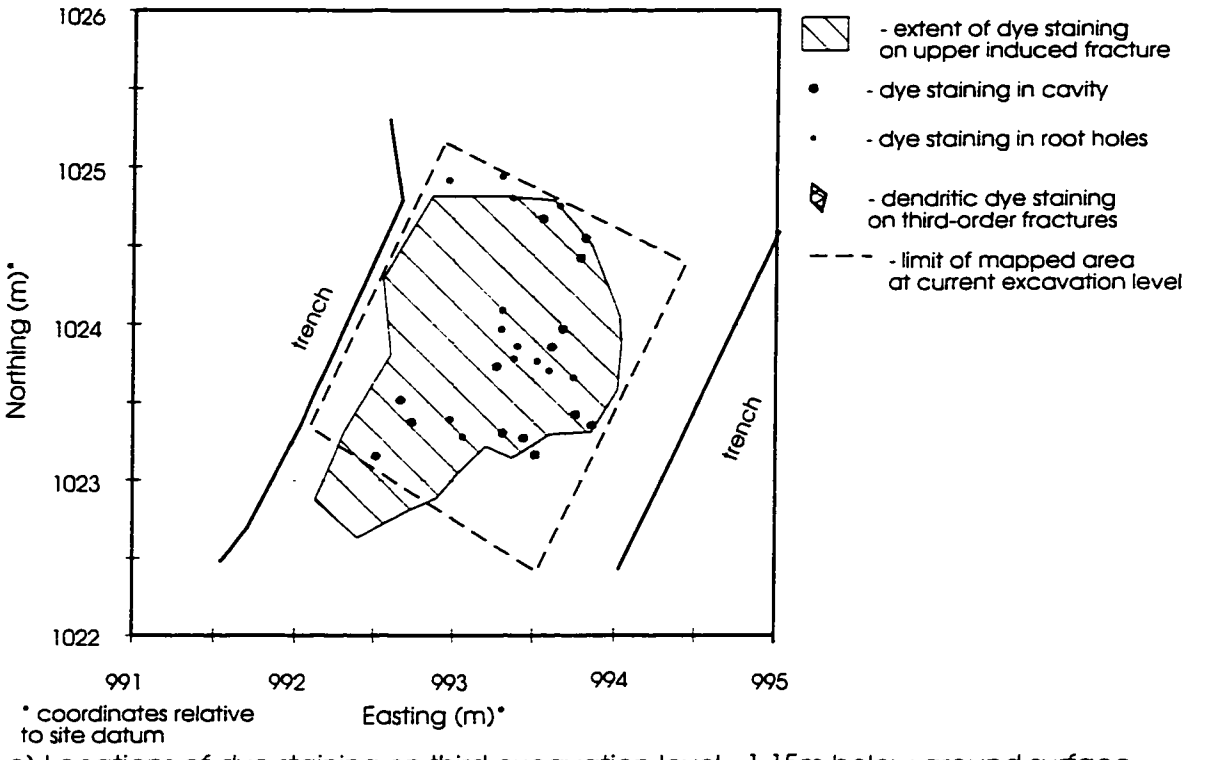

c) Locations of dye staining on third excavation level - 1.15m below ground surface

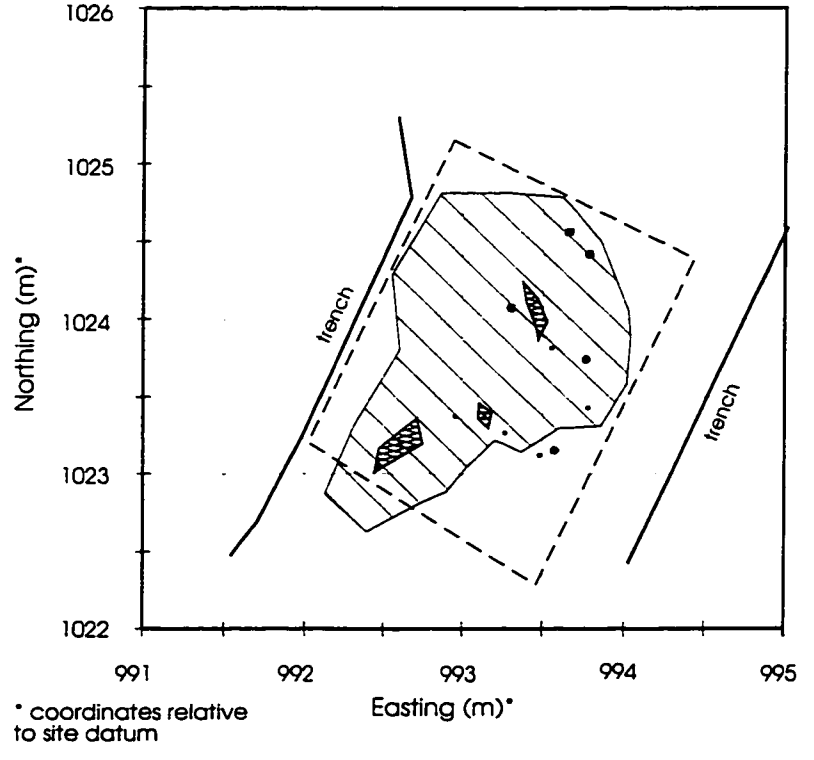

d) Locations of dye staining on fourth excavation level - 1.8m below ground surface

Figure 2.14 (cont) - Dye staining patterns

Figure 2.15 - Dye staining on plugs of infilling material

Figure 2.16 - Dye staining in the third-order fracture zone in the vicinity of a cavity

CHAPTER 3

SCALE DEPENDENCE, ANISOTROPY, AND DEPTH DEPENDENCE OF HYDRAULIC CONDUCTIVITY IN A WEATHERED, CLAY-RICH GLACIAL DEPOSIT

INTRODUCTION

Clay-rich glacial deposits are located at or near the surface over large areas of Canada and the northern United States. Near the surface, such deposits are typically extensively weathered, to a depth of several metres. The total thickness of such deposits is commonly several tens of metres, and in such cases, substantial thicknesses of unweathered clay underlie the surficial weathered clay. Macropores such as fractures and abandoned root holes are commonly found in the weathered clay near the surface, but have also been observed or inferred in deeper unweathered clay (Keller et. al. 1986; Rudolph et. al, 1991; Klint, 1996).

The hydraulic conductivity of these deposits generally depends on the scale at which the measurement is made (Bradbury and Muldoon, 1990; Jones et. al., 1992; McKay et. al., 1993), often as a result of the localised high conductivity associated with macropores. Small scale laboratory measurements on these glacial sediments from different parts of Canada tend to give very low values for hydraulic conductivity (generally in the range $1x10^{-11}$ m/s to $1x10^{-10}$ m/s; Keller et. al., 1986; McKay et. al., 1993a), which are considered to represent the hydraulic conductivity of the intact clay. Intermediate scale measurements of hydraulic conductivity, based on single well response tests in standard monitoring wells, tend to be highly variable in many deposits of this type (Jones et. al., 1992; McKay et. al. 1993a), since at this scale it is possible that some of the instruments used for the measurements will intersect macropore features and others will not. The lowest measured values determined from monitoring well-scale instruments are generally found to be similar in magnitude to the values determined in laboratory tests, whereas the largest values can be several orders of magnitude larger. In addition to the issue of relative proximity to macropores, variability in fracture aperture or root hole diameter is a potential source of variability in monitoring well-based measurements. Some knowledge of the variability of these parameters is important, since it is known that isolated, highly conductive discrete features can have a substantial influence on contaminant

transport rates (Harrison et. al., 1992). It is for this reason that measurements at this scale are important, since unlike large scale tests which tend to average the effects of a large number of macropore features, they can identify the presence of localised high conductivity features if a sufficient number of tests are conducted.

Larger scale measurements of hydraulic conductivity which combine the influence of many discrete high conductivity features should in principle be less variable at a particular site than well-scale measurements. Bear (1993) discusses the application of the concept of Representative Elementary Volumes (REV's) to a fractured porous medium, and concluded that an REV could be established for a network of fractures. The properties of REV's are such that measurements of hydraulic conductivity made at this range of scales will be relatively constant regardless of the particular location of the volume on which the measurement is made. The term bulk hydraulic conductivity is often used in the literature, generally with the implication that the measurement has been made on an REV. However, to establish whether the values that have been measured are in fact representative, numerous measurements are required at the REV scale. In some instances this has been possible (Keller et. al., 1988), however in most cases, it has not been established that the values of bulk hydraulic conductivity which are reported actually apply to an REV. In most instances, this is due to the greater resources and time generally required to conduct large scale experiments from which bulk scale values of hydraulic conductivity can be determined.

McKay et. al. (1993b) report the results of a large scale tracer test conducted in a near surface, fractured, clayey glacio-lacustrine deposit. They concluded that an equivalent porous medium approach could be used to predict the movement of the solute tracer through the weathered and highly fractured clay found at the surface, whereas a discrete fracture approach was required to predict the movement of the tracer through the less fractured, unweathered

clay at a greater depth. It is axiomatic that if an equivalent porous medium approach can be used to predict the movement of a solute at a particular scale, that scale represents an REV, and the groundwater velocity used in the prediction must be derived from an REV scale hydraulic conductivity.

Thus, in the highly weathered zone near the surface of clayey glacial deposits it is important to make measurements of hydraulic conductivity at a scale which is large enough to encompass a Representative Elementary Volume. It is the value of hydraulic conductivity at this scale which will control the long term migration of solutes, the seasonal dynamics of fluctuations of the water table, and as a consequence the amount of recharge which takes place through the underlying unweathered clay. In some cases, such as that reported by Keller et. al. (1988), REV scale measurements can be made with long screen piezometers, however in many cases it is likely that larger instruments will be required. However, in instances where the hydraulic conductivity varies spatially in a systematic manner, such as a variation with depth, there is an upper limit to the size of REV's, and therefore an upper limit on the useful size of measurement devices.

Since fractures in these types of deposits are in many cases predominantly vertical (Hendry, 1982; Morris et. al., 1992; McKay and Fredericia, 1995), larger scale measurements of hydraulic conductivity could demonstrate anisotropy, since networks of predominantly vertical fractures would tend to enhance conductivity in a vertical direction more than in a horizontal direction. Changes in REV scale hydraulic conductivity with depth, and hydraulic conductivity anisotropy at this scale are both factors which will have an important influence on solute transport, seasonal hydraulic fluctuations and recharge. It is these two characteristics in particular for which little information is available in the literature for clay-rich glacial deposits. In the majority of cases, hydraulic conductivity measurements have been derived from tests in

which the imposed gradient is predominantly horizontal. Very few direct measurements of vertical hydraulic conductivity are available. Jones et. al. (1992), McKay et. al. (1993), and Harris (1994) report values for horizontal hydraulic conductivity from tests conducted at the scale of several metres in weathered clay-rich glacial materials. In these tests, uniform horizontal gradients were imposed over vertical intervals of several metres, and thus no information was obtained on the manner in which the horizontal hydraulic conductivity changed with depth. Direct measurements of vertical hydraulic conductivity have been made by Grisak and Cherry (1975) and Keller et. al. (1986) by measuring the response to pumping from an underlying aquifer, and in a similar manner by Keller et. al. (1989) by monitoring the downward propagation of seasonal fluctuations of the water table. Such methods for determining large scale values of vertical hydraulic conductivity have only been applied to deeper, unweathered clay, as it is difficult to apply them in the upper weathered horizon due to the large uncontrolled hydraulic fluctuations which take place. To the author's knowledge, the only other direct measurement of large scale vertical hydraulic conductivity for this type of material was made in an experiment conducted in a fractured glacial till in Denmark, in which horizontal wells were used to induce a vertical gradient (Sidle et. al., 1997).

The first objective of this investigation is to determine from field experimentation whether hydraulic conductivity measured at a large scale decreases with depth for a particular weathered, clayey-glacial deposit, and whether large-scale hydraulic conductivity is anisotropic for this deposit. The second objective is demonstrate the relationships between monitoring-well scale measurements and larger scale measurements for this deposit, to gain an understanding of the features which control hydraulic conductivity at each scale.

The design of a set of experiments to directly measure vertical hydraulic conductivity at a scale of several metres, and its variation with depth in the weathered zone, is described in this

chapter. The technique used relies on the placement of horizontal, sand-filled induced fractures which can then be pumped to induce vertical gradients. Horizontal hydraulic conductivity at a similar scale is also indirectly determined from the experiments.

In this chapter, the term bulk scale hydraulic conductivity is used in a general sense to refer to measurements that have been made at a scale larger than that measured with a monitoring well, and where possible the scale at which the measurements were made is specified. Where this term is used, it is not implied that the measurement has been made at the scale of a Representative Elementary Volume, although this may be the case.

FIELD SITE

Field experiments were carried out at the Laidlaw hazardous waste treatment and disposal facility, located approximately 12km south-east of Sarnia, Ontario (see Figure 3.1). This site lies within an extensive clay plain, the Lambton Clay Plain, which forms the northern third of the 5900 km^2 St. Clair Clay Plain (Chapman and Putnam, 1984). Devonian age shale which dips gently towards the west underlies the clay plain at depths ranging between 25m and 50m, and averaging 40m (Desaulniers, 1986). The upper few metres of the bedrock is fractured, and the bedrock is overlain by intermittent deposits of sand and gravel.

Throughout the clay plain, clay-rich Quaternary age tills and glacio-lacustrine sediments extend from within 1m of the ground surface to the bedrock. For purposes of stratigraphic classification, these tills and glacio-lacustrine sediments have been divided into two units (Fitzgerald et al., 1979). The lower unit, known as the Black Shale till is generally 30-35m thick and contains numerous black shale clasts. The upper unit, the St Joseph Till extends generally to the surface, although it is overlain locally by thin deposits of sand and gravel. It is generally 7-13m thick, and is a silty clay (25-45% <2 μm diameter) with a small fraction (<20%)

of sand and gravel (McKay and Fredericia, 1995). This unit is thought to consist of glacio-lacustrine sediments which have been deformed by grounding icebergs and/or internal slumping of weakly consolidated material (Klint, 1996).

The upper 4-6m of the St. Joseph Till are visibly oxidised and fractured. Pervasive chemical weathering extends to a depth of 2-4m, and is marked by a colour change in the clay matrix from brown above to grey below (Ogunbadejo and Quigley, 1973). The clay-size minerals in the weathered zone are predominantly illite and chlorite (McKay and Fredericia, 1995). Below this zone of pervasive oxidation, chemical weathering is only evident in the immediate vicinity of fractures. Fracture frequency diminishes sharply below a depth of 3-4m, and fractures are generally indiscernible below a depth of 6m (Klint, 1996). Notwithstanding, fractures have been observed in drill cores at depths in excess of 9m (Adams, 1969), and roots have been observed at depths of up to 9m (Hanna, 1966).

Harris (1994) and McKay et al. (1993a) report that the water table at the Laidlaw site varies seasonally between the ground surface and a depth of 1.5m, and it has been observed to respond quickly to individual rainfall events (Adomait, 1991; and Harris, 1994). Ruland et al. (1991), based on measurements at various sites throughout the St. Clair Clay Plain, report that the water table is usually within 2m of the surface, but that piezometers used in their study went dry at depths of up to 4.9m in particularly dry summers. They also observed tritium at depths of up to 12m, and seasonal hydraulic head fluctuations in excess of 0.5m at depths of up to 11.5m. The presence of weathered clay at depths of up to 4m indicates that the water table was likely lower than at present for a prolonged period of time at some point since the clay was deposited (Soderman and Kim, 1969).

The hydrogeology of the Laidlaw site is reasonably well understood, as a result of numerous previous studies. Hydraulic conductivity measurements at the Laidlaw site have

The hydrogeology of the Laidlaw site is reasonably well understood, as a result of numerous previous studies. Hydraulic conductivity measurements at the Laidlaw site have been made by Harris (1994), McKay et. al. (1993), Balfour (1991), Ruland et. al. (1991), D'Astous et. al. (1989), and Desaulniers (1986). This work provides useful data and background information to complement the measurements which have been made in the current study.

FIELD METHODS

General Experimental Design

The experimental design that was used to make large-scale measurements of vertical hydraulic conductivity in the weathered zone relied on the placement of thin, relatively continuous, sub-horizontal layers of conductive material in the subsurface. This was achieved by hydraulically inducing fractures, and by using a sand proppant in the induced fractures to maintain them as relatively conductive pathways over the duration of the experiment.

Hydraulic fracturing at the field sites was carried out by FRx Ltd in association with Dr. Larry Murdoch at the University of Cincinnati. The procedure for creating hydraulically induced fractures is described by Murdoch (1995). Briefly, the fractures are created by driving a plugged steel casing to the desired depth, then driving the plug downwards from the base of the casing to form a short uncased section of borehole at the base of the cased section. A horizontal notch is cut in the uncased section of borehole with a high pressure water jet, which acts to initiate the fracture in a horizontal plane when a sand/gel mixture is pumped in under pressure. The gel breaks down over a period of hours following the fracture injection, due to enzymatic action.

The geometry of the induced fractures was determined by coring at the time of installation of instruments for monitoring hydraulic testing, and by mapping in excavations after completion of the hydraulic testing. In general the fractures were disc shaped and rose gently towards the surface from the point of injection, to their extremities at a distance of several metres from the injection point.

Such sand filled hydraulically induced fractures provide the opportunity to impose changes in hydraulic head which influence a large volume of the surrounding medium, and since they are horizontal they also allow the imposition of hydraulic gradients which are vertical or close to vertical.

Since the focus of the study is the upper few metres of the weathered zone where substantial hydraulic activity occurs, there was the potential that the results of any hydraulic testing carried out in this zone could be affected by transient fluctuations in the water table, even for relatively short duration tests. Furthermore, it was possible that during periods of low water table at the end of the summer the zone of interest could become unsaturated (or at least the fractures and/or root holes in the zone of interest could become unsaturated), thus complicating the assessment of the saturated hydraulic conductivity. In order to avoid these problems, ponded water at a constant level was maintained over the area to be tested. The experimental set-up, including the induced fractures and the artificial pond, is illustrated schematically in Figure 3.2a. An additional benefit of the pond is that it provides a source of water for longer term hydraulic tests which induce downward flow and which would thus normally cause a lowering of the water table.

Water pressure in the area beneath the pond was measured using a network of electronic strain gauge pressure transducers (Adara Systems 10 PSIG transducers), which were connected to a datalogger (Campbell Scientific CR-10 datalogger). The pressure

transducers and other instruments were installed in vertical holes which were cored using a direct push continuous coring method described by Einarson (1995). Some of the transducers were located within short (approximately 10 cm) sand packs at the base of boreholes which terminated at a depth midway between induced fractures, and other transducers were located within a short sand pack located at the depth where the borehole intersected an induced fracture (see Figure 3.2a). Hydraulic head in the induced fractures was also measured using 1/2" I.D. PVC piezometers which were similarly screened in a short sand pack located at the depth where the borehole intersected an induced fracture. This arrangement for piezometers and transducers is illustrated in Figure 3.2b. The induced fractures were readily identified in the cores since they were filled with sand, and it was thus a relatively simple procedure to locate the instruments and sand packs as illustrated. In addition to the transducers and 1/2" PVC piezometers, hydraulic head in the induced fractures was measured in the steel casings which were originally used for fracture injection and left in place after injection (see Figure 3.2a).

As indicated on Figure 3.2b, the pressure transducers were not vented to the atmosphere, and thus to convert pressure measurements obtained from the transducers to hydraulic head values which could be directly compared to the water levels measured in piezometers and the water level in the pond, it was necessary to measure atmospheric pressure at the surface and subtract this value from the values measured in the subsurface. Atmospheric pressure was measured using a thermally isolated transducer of the same design as the transducers used to measure water pressure.

The open boreholes in which the transducers and piezometers were installed were sealed with a thick bentonite slurry above the sand pack (see Figure 3.2b) to eliminate direct vertical hydraulic connection in the boreholes. Since the bentonite remained saturated beneath

the pond, it is unlikely that it would have undergone shrinkage and thus created an open annulus around the perimeter of the boreholes.

The water level in the pond was maintained at a constant level by means of a large Marriotte system which comprised two 450 litre tanks (see Figure 3.3). The tanks were continuously weighed using an electronic scale which was constructed using a temperature compensated stainless steel "S" type load cell to support approximately half the weight of the tanks. The load cell output was calibrated to give cumulative outflow from the tanks by successively adding known volumes of water to the tanks and noting the changes in load cell output.

Details of the Two Experimental Installations

The experimental design described in the foregoing and illustrated in Figures 3.2 and 3.3 was installed at two separate locations on the Laidlaw property. Results from both sites are presented and discussed in this chapter. Specific details of the two installations are illustrated in Figures 3.4 and 3.5 for the first and second sites respectively, and are discussed in the following.

At the first site, three hydraulically induced fractures were created at depths of 1.8m, 2.2m and 2.6m below the ground surface. These depths refer to the depth below surface of the point where the fracture is initiated and the sand injected, however as previously noted, the fractures rise towards the surface as they propagate away from this point. Coring and mapping in an excavation indicated that at this site, the induced fractures were relatively horizontal features in the area beneath the pond. Cores to a maximum depth of 3.8m were taken at this site, and it was found that the clay was pervasively weathered down to this depth. The depth of the transition from weathered clay to unweathered clay was not determined.

At this site the topsoil was removed down to a depth of 0.4m prior to installation of instruments and construction of the pond. A pond of 4m diameter was used at this site, which was smaller than the extent of the induced fractures. A total of 15 pressure transducers were installed, with an emphasis on obtaining pressure distributions in the middle induced fracture, and at the mid-point of the vertical interval between this fracture and the upper induced fracture. An attempt was made to place the transducers so as to obtain a reasonable spatial distribution at each of these levels. The locations and depths of the 15 transducers are illustrated in Figure 3.4. Piezometers to measure hydraulic head in the induced fractures were not installed at this site. Background fluctuations in the water table away from the influence of the pond were monitored by measuring the depth to water in open casings which were used to inject other induced fractures at varying distances from the pond.

At the second site (Figure 3.5), three hydraulically induced fractures were created at depths of 1.0, 2.0m and 3.0m below the ground surface. Coring indicated that at the pond perimeter, the induced fractures had risen to minimum depths below ground surface of approximately 0.25m, 1.8m and 2.85m respectively. Thus the two deepest induced fractures at this site were relatively horizontal features in the area beneath the pond, whereas the uppermost induced fracture changed elevation significantly over this area. Examination of cores taken from this site indicated that the transition from weathered clay to unweathered clay was at approximately 2.5m below the ground surface in the area beneath the pond.

A pond of 3m diameter was installed at this site, and the uppermost induced fracture extended to or just beyond the pond perimeter, whereas the deeper two fractures extended several metres beyond the pond perimeter in all directions. A total of 21 pressure transducers were installed at this site, with an emphasis on obtaining vertical profiles of hydraulic head. The transducers were thus installed in 3 "nests", in each of which 7 transducers and 3 1/2" I.D.

piezometers were installed in separate boreholes within a 0.5m by 0.5m area. The transducers were all located within the intervals between induced fractures, and hydraulic head measurements in the induced fractures themselves were made in the piezometers. Details of the depths and locations of transducers and piezometers are illustrated in Figure 3.5. At this site, no pressure transducers were installed at the levels of the induced fractures, however pressure transducers were suspended below inflated packers in the large diameter steel casings for selected hydraulic tests, in order to measure the transient changes in hydraulic head in the induced fractures. Pressure changes in the area outside the pond were monitored in three pressure transducers which were located radially outwards from each "nest", at a distance of 5m from the centre of the pond (Transducers AWT, BWT and CWT in Figure 3.5). These transducers were sealed in uncased boreholes, in sand packs which extended from 1.5m to 2.5m below ground surface. Background fluctuations in the water table away from the influence of the pond were also monitored by measuring the depth to water in open casings which were used to inject other induced fractures at varying distances from the pond.

Types of Hydraulic Tests Conducted with Pond/Induced Fracture Installations

Constant head pumping tests were carried out with the artificial pond and induced fracture installations shown in Figures 3.4 and 3.5, by pumping at a constant head from the large diameter steel casings originally used for fracture injection. A constant head in the casing was maintained using a peristaltic pump, which continued to draw a mixture of air and water after the water level in the casing had been drawn down to the level of the intake tubing. The flow rate from the pumped induced fracture was measured by diverting the pump outflow to a large tank which was continuously weighed using an electronic scale constructed using a temperature compensated stainless steel "S" type load cell to support approximately half the weight of the tank. The pumping and flow measurement system is illustrated in Figure 3.6. The load cell output was calibrated to give cumulative flow to the tanks by successively adding

known volumes of water to the tanks and noting the changes in load cell output. The increased flow rate from the pond was also monitored using the weighed Marriotte system previously described.

The pressure transients caused by pumping were monitored in the network of pressure transducers, and the pumping was continued until the output from the transducers indicated that steady state had been reached. At steady state, additional measurements of hydraulic head in the induced fractures beneath the pond were made in the 1/2 " I.D. piezometers and in the steel casings which were originally used for fracture injection. Throughout the duration of the pumping tests, the fluctuations in the background water level away from the pond were monitored. A total of 5 tests of this type were carried out, one in each of the induced fractures at the second site, and one in each of the lower two induced fractures at the first site.

IDEALISED BEHAVIOUR OF SYSTEM DURING LARGE SCALE COMBINED INFILTRATION AND PUMPING TESTS

The concepts used to understand the dynamics of multi-aquifer/aquitard systems (Hantush and Jacob, 1955; Neuman and Witherspoon, 1969; Frind, 1979) are useful in conceptualising the behaviour of the combined pond and induced fracture installations during the constant head pumping tests. As a result of the large conductivity contrast between the induced fractures and the surrounding clay, water should flow approximately vertically in the clay units towards the induced fracture which is pumped, and then radially towards the casing through the induced fracture. Since the storage in the induced fracture is minimal, essentially all of the pumped water is supplied by leakage from the clay above and below the induced fracture except for a short period immediately after the start of the test. In the initial stages of the test, a substantial proportion of the vertical leakage into the induced fracture may be derived by release of water from storage in the clay, but as the test approaches steady state,

water is derived primarily from downward recharge from the pond. Since the clay is not intact but is penetrated by predominantly vertical fractures and root holes which represent high conductivity, low storage pathways, water released from storage in the clay matrix blocks will tend to migrate laterally to the naturally conductive macropores, and then downwards to the pumped induced fracture. The other induced fractures which are not pumped do not provide a source of additional water since their storage is negligible, however they will act to dissipate any radial gradients that may be induced at early time in the clay in the vicinity of the pumping point, and thus tend to promote primarily vertical gradients through the clay. Similarly, the storage represented by the compressibility of the macropores is negligible.

The idealised behaviour of the system during pumping tests is illustrated in Figure 3.7, in terms of changes in hydraulic head, and in terms of the infiltration rate from the pond and the flow rate from the pumped induced fracture. The distributions of hydraulic head illustrated in Figure 3.7 represent the changes in head which would be imposed by pumping, in the vertical macropores and in the clay matrix. Hydraulic head in the pumped induced fracture and macropores will approach an almost constant distribution quickly after commencement of the tests due to the low storage in these elements, and will then continue to change slowly as water is released to these features from storage in the clay itself. Hydraulic head in the blocks of clay will change more slowly, depending on the relative proximity of macropores.

At the commencement of pumping, the flow rate from the pumped induced fracture will be high, due to the initially high rate of release of water from storage in the clay. Water is initially released very quickly from storage in the clay due to steep hydraulic head gradients at the interfaces between the clay and macropores. As the head gradient between the macropores and the clay matrix blocks decreases and the head distribution in the system approaches a steady state, the flow rate from the pumped induced fracture will decrease

towards a steady state value that is primarily dictated by the overall vertical hydraulic conductivity of the fractured block of clay between the induced fracture and the pond, and the difference in head between the pond and the pump intake.

Similarly, the infiltration rate from the pond will increase from the background value which existed prior to the commencement of pumping and which is governed by the difference in head between the pond and the background water table, to a steady state value. However, in general, the flow rate from the pumped induced fracture will not equal the infiltration rate from the pond even at steady state, for a variety of reasons. For example, if the induced fracture does not extend significantly past the perimeter of the pond, some of the lateral flow outwards from the pond may not be captured by the pumping. Furthermore, some water will be derived from upward flow to the pumped fracture, and although the storage capacity of the underlying clay is limited, laterally inwards flow to the clay beneath the pumped fracture could supply an ongoing source of water.

RESULTS AND DISCUSSION

Determination of Vertical Hydraulic Conductivity from Steady State Conditions During Pumping Tests

As noted above, the infiltration rate from the pond will not in general equal the flow from the pumped induced fracture, as a result of lateral flow outward from the pond or inward to the induced fracture. Similarly, the profiles of hydraulic head beneath the pond will be affected by the interaction between the imposed conditions (that is, the constant head over the area of the pond, and the constant head at the withdrawal point in the pumped induced fracture), and the surrounding uncontrolled hydrologic regime. It is proposed, however, that it is possible to assess hydraulic conductivity in a relatively uncomplicated manner by considering the changes to flow rate and hydraulic head which are superimposed on the pre-existing conditions by the

pumping. The conceptual model which is thus used to calculate hydraulic conductivity is illustrated in Figure 3.8.

Hydraulic conductivity is essentially calculated by applying Darcy's Law to a vertical block of clay extending downwards from the pond to the induced fracture. It is assumed that the increase in flow rate associated with the pumping is accommodated by vertically downwards flow within the block of clay outlined by the perimeter of the pond, and that the applied vertical head gradient is uniform at any position across the width of the pond. In Figure 3.8 the head change imposed by the pumping is shown as changing linearly between the pond and the pumped induced fracture, which would correspond to the case of uniform hydraulic conductivity with depth. It is envisaged that changes in hydraulic conductivity with depth would be reflected in the profile of head change with depth, and that hydraulic conductivity over a given vertical increment can be determined using the same Darcy-type calculation and the slope of the head change profile over that increment.

In order to investigate the types of steady state responses to be expected with the given system geometry and various hydraulic conductivity patterns, and in order to test the applicability of the conceptual model illustrated in Figure 3.8, an idealised version of the system was modelled using a numerical simulator. The approach that was adopted for the simulations was to calculate the steady state flow rates and head distributions for cases with and without pumping, and then to use the approach described in Figure 3.8 with these calculated values to check the correspondence between the hydraulic conductivity thus determined, and that specified in the model definition. The numerical model FRAC3DVS (Therrien et. al., 1995) was used for the simulations. This model can be used to simulate three dimensional transient and steady state groundwater flow in discretely fractured porous formations, using various solution

techniques. The capabilities of the simulator and the solution techniques employed are described by Therrien and Sudicky (1996).

The general model geometry and boundary conditions which were considered are illustrated in Figure 3.9. The size of the model domain was reduced by making use of symmetry conditions, and thus only one quarter of the pond and of the induced fractures needed to be considered. The induced fractures were included in the model as discrete planar features located at representative distances below the pond, and were assigned values of transmissivity which are considered to be representative of sand-filled induced fractures. In Chapter 4, values of transmissivity for induced fractures in the range 8.3×10^{-6} m^2/s to 11.2×10^{-6} m^2/s are calculated, based on the results of recovery tests in wells directly connected to induced fractures. The conclusions of the current modelling investigation are not sensitive to the exact value of the transmissivity of the induced fractures, but do rely on these features being much more conductive than the surrounding material.

A constant head boundary condition was applied over the area of the pond, and a no-flow boundary condition was applied over the remainder of the upper horizontal boundary. A constant head boundary condition of a magnitude lower than that applied over the pond was applied on those vertical boundaries which were not symmetry boundaries, to represent the distant water table level. It was found that the conclusions of the current modelling investigation were not sensitive to the distance from the pond to the lateral boundaries, nor to the absolute value of the head difference between the pond and these boundaries. The lower horizontal boundary was specified as a no-flow boundary. A constant head boundary node was specified directly beneath the centre of the pond, at the level of the deepest induced fracture, in order to simulate the constant head pumping tests carried out in the field experiments.

Various distributions of hydraulic conductivity for the clay beneath the pond were considered in the modelling. The simplest case considered was that of a homogeneous, isotropic material throughout the entire domain, followed by the case of a layer of material of greater (isotropic) hydraulic conductivity at the surface. The location of the boundary between the upper, more conductive material and the lower, less conductive material is illustrated in Figure 3.9. In addition, the case of layered, anisotropic media was also considered.

The results of the simulations are summarised in Table 3.1, and in Figure 3.10. It can be seen from the results given in Table 3.1 that the conceptual model illustrated in Figure 3.8 should allow the calculation of vertical conductivity to within considerably less than an order of magnitude, provided sufficiently accurate measurements of flow rate and of hydraulic head are available. Furthermore, it can be seen from Figure 3.10 that hydraulic conductivity contrasts of one order of magnitude are readily apparent from the hydraulic head profiles beneath the pond, and from the results given in Table 3.1 it can be seen that hydraulic conductivity can also be calculated relatively accurately in such cases where it varies with depth. Anisotropy was found to have no significant effect on the accuracy of the calculated vertical hydraulic conductivity, as might be expected since the imposed hydraulic gradient is very close to vertical throughout the area beneath the pond.

The approach illustrated in Figure 3.8 was therefore used to determine values of vertical hydraulic conductivity from the pond infiltration rates and hydraulic head distributions which were measured during the pumping tests. The data which were used to calculate hydraulic conductivity in this manner are illustrated in Figures 3.11 and 3.12 for the first experimental installation, and in Figures 3.13 and 3.14 for the second experimental installation. It can be seen from these figures that in most cases, the changes in hydraulic gradient and infiltration rate that were caused by the pumping were easily distinguishable with the measurement

devices that were used. The infiltration rate measured using the Marriotte system fluctuated within a relatively narrow range even under conditions of apparently constant hydraulic head, however it is considered that the changes in infiltration rate that are noted in Figures 3.12 and 3.14 represent the actual change to within less than 20%. For the pumping test conducted in the induced fracture at a depth of 3m at the second experimental installation, only a marginal increase in infiltration rate was observed, and the fluctuation of the measured rate was of a comparable magnitude to the increase (Figure 3.14c). The values of hydraulic conductivity that were determined from this test may thus be subject to a greater error than those calculated from other tests, however the error in hydraulic conductivity should be less than an order of magnitude. From Figures 3.11 and 3.13, it can be seen that for a particular set of hydraulic conditions, the head change profiles were relatively insensitive to the locations beneath the ponds where they were measured.

The values of vertical hydraulic conductivity which were thus determined are illustrated in Figure 3.15 and Figure 3.16 for the first and second experimental installations respectively, and are tabulated in Table 3.2. It can be seen that within the weathered zone at the first site, there is not a marked decrease in hydraulic conductivity with depth. Although direct measurements of hydraulic conductivity are available only down to the depth of the deepest induced fracture (2.6m), the profiles of hydraulic head illustrated in Figure 3.11 suggest that the vertical hydraulic conductivity at this site does not decrease substantially between the ground surface and a depth of almost 4m. At the second site, the hydraulic conductivity decreases by an order of magnitude from a depth of 0.5m to the base of the weathered zone at a depth of 2.5m, and then appears to decrease rapidly by another order of magnitude below the interface between the weathered and unweathered materials.

Determination of Hydraulic Conductivity Anisotropy from Pond Infiltration Rates

In the previous section, vertical hydraulic conductivity distributions were determined from the increase in pond infiltration rate when an enhanced vertical hydraulic gradient was superimposed on the background conditions by pumping from the underlying induced fractures. Under natural infiltration conditions with no pumping from the induced fractures, the hydraulic conductivity of the clay beneath the pond can also be assessed from the total infiltration rate, and the head difference between the pond and the water table. Under such conditions, flow from the pond is three dimensional in nature, and thus will be affected if the hydraulic conductivity of the clay is anisotropic rather than isotropic at the scale being considered.

The expected steady state flow rate from the pond for a given set of conditions can be assessed using the three dimensional flow simulator discussed above. The geometry and boundary conditions of the model are the same as illustrated in Figure 3.9, except that a constant head node was not specified to represent pumping from the induced fracture. Simulations indicated that the infiltration rate was influenced moderately by the distance between the pond perimeter and the lateral constant head boundaries at the edge of the model domain, with a decrease in the calculated rate with increased distance to the boundaries. The distance to the lateral domain boundaries selected for the simulations was chosen as the distance to a point at which field measurements of the water table depth indicated no influence of the pond. The depth to the water table was specified as the value measured at this point.

The approach that was taken was to initially specify a layered, isotropic hydraulic conductivity distribution, for which the hydraulic conductivity values in all spatial dimensions were set equal to the values of vertical hydraulic conductivity measured in the pumping tests.

The steady state infiltration rates calculated in these simulations were 5-10 times greater than the values measured in the field.

One possible explanation for the apparent discrepancy between the results of the pumping tests and the results derived from natural infiltration conditions is that hydraulic conductivity is anisotropic at the scale being considered. Accordingly, simulations were carried out with layered, anisotropic hydraulic conductivity distributions, for which the values of vertical hydraulic conductivity for each layer were derived from the pumping tests, and the values of horizontal hydraulic conductivity (in both horizontal directions) were a constant proportion of the values in the vertical direction. From these simulations, it was determined that at the first experimental installation, an anisotropy ratio of K_h/K_v=1/7 to 1/5 yielded an infiltration rate equal to that which was measured, whereas at the second site, an anisotropy ratio of K_h/K_v=1/40 to 1/35 was required. The profiles of horizontal hydraulic conductivity which are inferred by these anisotropy ratios are plotted in Figure 3.17, with the profiles of vertical hydraulic conductivity which were used to derive them. The simulations showed very little sensitivity to changes in the anisotropy ratio for the deeper, unweathered clay, and thus the anisotropy ratios of 1/7 to 1/5 for the first site and 1/40 to 1/35 for the second site are considered to apply only to the weathered clay.

The reason for different anisotropy ratios for the two sites is likely related to differences in the nature of macroporosity within the weathered zone at the two sites. At the second site, a dye tracer experiment indicated that flow beneath the pond took place predominantly through large infilled vertical and sub-vertical cavities up to 5 cm in diameter (see Chapter 2). These features are thought to be infilled, abandoned root holes, and were not observed at the first experimental installation. Although a network of predominantly vertical fractures can provide an interconnected pathway for horizontal flow, albeit with a lower hydraulic conductivity than for

flow in the vertical direction due to the increased tortuosity of the flow path, a group of predominantly vertical linear features are far less likely to provide laterally interconnected pathways. Thus, in cases where flow is controlled by predominantly vertical linear features such as root holes or the cavities observed at the second site, the bulk scale horizontal hydraulic conductivity will be considerably less than the bulk scale vertical hydraulic conductivity.

Comparison of Values of Hydraulic Conductivity Measured at Different Scales

McKay et. al (1993a) and Harris (1994) both report the results of studies carried out at the Laidlaw site in which measurements of hydraulic conductivity have been made at various scales. Useful comparisons can be drawn between the results of these previous studies and the results of the current study. The general nature of the fracture pattern at the first site used for the current study (described in Chapter 2 on the basis of fracture mapping in excavations) was similar to that described by McKay et. al. (1993a) and by Harris (1994) at the sites used for those studies. The site used by Harris (1994) was in fact located in a topographically similar setting only 25m from the first experimental installation, and is therefore expected to have a very similar fracture pattern. On this basis, it is considered reasonable to compare the values of bulk scale hydraulic conductivity determined at the first site in this study with the values of hydraulic conductivity determined at various scales by McKay et. al. (1993a) and Harris (1994).

Details of the types of tests and the scales of tests conducted by McKay et. al. (1993) and Harris (1994) are provided in Table 3.3. Values of hydraulic conductivity which were measured by McKay et. al. (1993a) and Harris (1994) using piezometers between the ground surface and a depth of 5m are illustrated in Figure 3.18. Hydraulic conductivity for intact samples of the clay has been measured in the laboratory by McKay et. al. (1993a), Harris

(1994) and Padusenko (1997), and an average value has also been plotted on Figure 3.18. Since the values of conductivity measured using piezometers are almost exclusively greater than the value measured for intact samples of clay, the values measured using piezometers are apparently influenced by relatively more conductive features such as fractures or root holes.

The values of hydraulic conductivity measured by McKay et. al. (1993a) using piezometers vary over up to 3 orders of magnitude at any given depth. The variability in measured conductivity at this scale could be due to variability in the conductivity of fractures and root holes which are intercepted by piezometers, or due to the degree of connectivity of these features to other fractures and root holes. It is also possible that some piezometers could have been placed in isolation from any fractures and thus would have measured the conductivity of the unfractured clay in their vicinity. Harris (1994) used piezometer screens which were much larger than those used by McKay et. al (1993a), and installed the piezometers in angled boreholes to increase the probability of intersecting vertical fractures. Although Harris (1994) measured far fewer values of hydraulic conductivity, it would appear that his results show less variability at any given depth than those of McKay et. al. (1993a), and that the values he measured for hydraulic conductivity are towards the upper end of the range of values measured by McKay et. al. (1993a). This suggests that the responses in the larger-scale slug tests conducted by Harris (1994) were controlled by more widely spaced, consistently higher conductivity features that were less often intercepted by the smaller piezometers used by McKay et. al. (1993a).

Also shown on Figure 3.18 are the values of bulk scale horizontal hydraulic conductivity that were measured by McKay et. al. (1993a) and Harris (1994), and the depth intervals over which these values were averaged. Practically the same value was measured in both studies

(that is, $2x10^{-7}$ m/s), and it can be seen from Figure 3.18 that these values are approximately equal to the largest of the highly variable values measured using piezometers. The profile with depth of bulk scale vertical hydraulic conductivity that was measured at the first site in this study is also illustrated in Figure 3.18, as is the profile of bulk scale horizontal hydraulic conductivity which was inferred from pond flow rates. The profile of bulk scale horizontal hydraulic conductivity is consistent with the depth averaged values measured by McKay et. al. (1993a) and Harris (1994), and is again larger than almost all of the piezometer scale measurements.

A similar relationship between well-scale and large-scale measurements of hydraulic conductivity can be noted in the results reported by Jones et. al. (1992) for a weathered clayey till in Iowa, and by Hanor (1993) for a marine clay with several fractured paleo-weathering horizons in Louisiana. This indicates that such a relationship between well-scale and large-scale measurements of hydraulic conductivity (the upper limit of highly variable values derived from small scale measurements approximately equal to the large-scale value) is not a feature unique to the Laidlaw site.

Since the values of bulk hydraulic conductivity should reflect the aggregate influence of numerous pathways of various conductivity within the volume for which the bulk value is representative, small scale measurements which locally sample the various pathways might be expected to yield values which are both higher and lower than the bulk value. McKay et. al. (1993a) suggest that the bulk hydraulic conductivity should be given by the arithmetic average of the smaller scale measurements. The arithmetic average of the slug test results shown in Figure 3.18 is $5x10^{-8}$ m/s, which is approximately four times less than the measured bulk horizontal hydraulic conductivity.

To clarify the relationships between values derived from small-scale measurements and large-scale measurements in fractured clayey materials, well-scale response tests and large scale constant gradient tests were simulated using the numerical simulator FRAC3DVS (Therrien et. al., 1995) for a 2m x 2m x 2m block of fractured clay. The model geometry used in these simulations is illustrated in Figure 3.19.

The fracture network geometry illustrated in Figure 3.19 is intended to represent an analogue of the fracture network at the Laidlaw site. From fracture mapping conducted by previous researchers (Ruland et. al., 1991; Harris, 1994; McKay and Fredericia, 1995; and Klint, 1996) and as part of the current study, it can be concluded (see Chapter 2) that the fractures at the Laidlaw site are commonly distributed according to a hierarchy of scales as illustrated in Figure 3.20. First-order fractures persist over several metres both vertically and horizontally, and are intersected by less persistent second-order fractures. In the weathered zone, some of the blocks of clay which are bounded by first and/or second-order fractures are divided by third-order fractures into irregular peds which have a diameter on the order of 1 cm, but this is not consistently the case.

In the simulations, fracture apertures between 35 μm and 55 μm were randomly assigned to the 2 dimensional discrete fracture elements which represented first and second-order fractures. The third-order fracture zones were modelled as zones of equivalent porous medium, since a well placed in these regions would intercept many third-order fractures. A value of hydraulic conductivity of 1×10^{-8} m/s was assigned to the third-order fracture zones, which was 2 orders of magnitude greater than that which was specified for the unfractured clay matrix blocks. Although this value has been somewhat arbitrarily chosen, it was found that the response of the wells placed in the first and second-order fracture planes and the overall bulk hydraulic conductivity of the block were not very sensitive to the value of hydraulic conductivity

assigned to the third-order fracture zones. All first and second-order fractures and third-order fracture zones were specified as vertically continuous throughout the entire height of the block.

Large scale constant gradient tests were simulated by specifying different constant head boundary conditions on two opposing faces of the block, and no-flow boundaries on the other faces. Values of bulk hydraulic conductivity in each horizontal direction were determined from the applied overall gradient in these simulations, and the calculated total flux through the block. The values of bulk horizontal hydraulic conductivity thus determined were 7.1×10^{-8} m/s in the x-direction, and 1.1×10^{-7} m/s in the y-direction.

Single-well response tests were simulated using the one dimensional well elements provided in FRAC3DVS. Various well locations relative to the fracture network were considered, as illustrated in Figure 3.19. At each of these locations, the well-screen was defined over a vertical interval of 0.3m, with the mid-point of the well-screen located at the mid-height of the block. For these models, constant head boundaries were specified on all model boundaries, to represent the background water table. The calculated transient response at the well nodes due to an applied perturbation was converted to a value of hydraulic conductivity using the Hvorslev (1951) method, since this method is commonly used to interpret this type of test in these types of materials (Keller et. al., 1986; Ruland et. al, 1991; McKay et. al., 1993a). In all cases, the calculated responses plotted very close to a straight line when plotted as the log of normalised head as a function of time.

The results of the simulations are summarised in Table 3.4. It can be seen that the highest values of well-scale hydraulic conductivity are calculated from the responses of wells placed in the plane of first-order fractures, and are in the range of 1.5 to 4.5 times higher than the values of bulk horizontal hydraulic conductivity for the block. Intermediate values in the range of 0.13 to 0.49 times the values of bulk horizontal conductivity are calculated from the

responses of wells placed in the plane of second-order fractures and in the third-order fracture zones. A hydraulic conductivity of 1.8×10^{-10} m/s is calculated for the response of Well L, which was located in the clay matrix 5 cm from a first-order fracture. Since a value of 1×10^{-10} m/s was specified for the clay matrix, this indicates that the response of piezometers placed in the unfractured clay matrix will not be affected even by fractures in very close proximity to the well.

Thus, for the conditions considered in the simulations, the value of bulk hydraulic conductivity is found to be towards the upper end of a several orders of magnitude range of values that are calculated from the response of wells placed at various locations in relation to the fracture network. The fact that at the Laidlaw site almost no values of hydraulic conductivity higher than the bulk value were measured using piezometers, could indicate that there are laterally persistent high-conductivity features which contribute to bulk hydraulic conductivity but which have not been intercepted by the piezometers. These features would most likely be relatively widely spaced, so that the probability of intercepting them with a piezometer would be low. It could similarly indicate that the installation of piezometers causes disturbance to the surrounding material which tends to decrease hydraulic conductivity in their vicinity.

Conceptual Model for Bulk Scale Hydraulic Conductivity Distribution at the Laidlaw Site

Based on a consideration of the results of this study and studies previously conducted at the Laidlaw site, a new conceptual model can be proposed for the manner in which bulk scale hydraulic conductivity varies with depth and with direction of measurement in the near surface at this site. The measurements on which this conceptual model is based were all derived from tests for which the horizontal dimensions of the areas influenced by the tests were in the range

of 3m to 6m. Thus, for the proposed conceptual model, bulk hydraulic conductivity refers to conductivity at that approximate scale.

Fracture patterns vary across the site, and therefore specific details regarding the distribution of hydraulic conductivity, such as the absolute magnitudes of hydraulic conductivity, may also vary. For the tests conducted at the second experimental site considered in this study, flow took place predominantly through infilled abandoned root holes (see Chapter 2), and as a result the distribution of hydraulic conductivity with depth and degree of anisotropy are markedly different to that observed at the first experimental site. These features were not observed at the first experimental site, where the fracture pattern was similar to that described by McKay et. al. (1993) and Harris (1994) at the sites used for those studies. It is worth noting that the values of bulk scale horizontal hydraulic conductivity for the weathered zone fall within a very limited range for these three sites at which fractures rather than cavities appear to control flow.

The proposed conceptual model is illustrated in Figure 3.21. It is proposed that bulk scale hydraulic conductivity does not decrease with depth in the weathered zone at locations where flow is controlled by the network of first and second order fractures, whereas at locations where flow is controlled by infilled abandoned root holes it decreases by approximately an order of magnitude over the weathered zone. In both cases, a relatively abrupt decrease in bulk scale hydraulic conductivity of 1 to 2 orders of magnitude is proposed at the interface between weathered and unweathered clay. At the bulk scale the clay is anisotropic, with a much larger ratio of horizontal to vertical hydraulic conductivity in cases where flow is controlled by fractures.

The possible reasons for a decrease in hydraulic conductivity at the interface between the weathered clay and the unweathered clay are a decrease in fracture frequency, or a

decrease in fracture hydraulic aperture. Results of various fracture mapping exercises (Ruland et. al., 1991; Harris, 1994; McKay and Fredericia, 1995; and Klint, 1996) do not indicate an abrupt change in the frequency of first and second order fractures (which control bulk scale hydraulic conductivity), and the proposed conceptual model thus implies a decrease in fracture hydraulic aperture at this interface. An abrupt decrease in fracture aperture at the interface between the weathered clay and unweathered clay is supported by the results of a solute tracer test conducted by McKay et. al. (1993b).

CONCLUSIONS

The experimental arrangement described in this paper, in which a pond is maintained at the surface overlying several flat-lying sand filled induced fractures, provides a mechanism for measuring vertical hydraulic conductivity and its variation with depth in near surface weathered clay, and also indirectly allows horizontal hydraulic conductivity to be estimated. The method which has been proposed in this paper for calculating vertical hydraulic conductivity, based on the increase in pond infiltration rate and changes in hydraulic head which are caused by pumping from an induced fracture, appears to be relatively robust.

Using this technique at the Laidlaw site, it was found that vertical hydraulic conductivity does not change with depth in the weathered clay at one location where fractures are thought to control flow; whereas vertical hydraulic conductivity decreases by an order of magnitude over the depth of the weathered zone at another location where infilled abandoned root holes are thought to control flow. An abrupt decrease in hydraulic conductivity was observed at the interface between the weathered clay and the unweathered clay, which is interpreted to indicate an abrupt decrease in fracture hydraulic aperture.

At these two locations, the apparently low infiltration rates from the ponds at times when vertical gradients were not applied by pumping indicate that the hydraulic conductivity is anisotropic at the bulk scale.

A comparison of the values of hydraulic conductivity measured at different scales at the Laidlaw site indicates that at larger scales, hydraulic conductivity is controlled by the influence of a network of widely spaced, laterally persistent, interconnected fractures which have not been intercepted by the numerous small-scale single well response tests that have previously been carried out at the site.

Large scale measurements of horizontal hydraulic conductivity have now been made at three locations at the Laidlaw site, from experiments for which the horizontal dimensions of the affected areas were in the range 3m to 6m. The values determined from these three locations fall within a very narrow range ($2x10^{-7}$ m/s to $3x10^{-7}$ m/s), which indicates that measurements made at this scale sample a representative portion of the controlling fracture network.

While these generalisations regarding hydraulic conductivity at this site are certainly of local interest, it is of wider interest to assess whether such generalisations are appropriate for other deposits of clayey till, since differences in clay mineralogy, stress history and climate could have a substantial influence on the development of fractures. Furthermore, it has been seen that even locally, changes in vegetation and consequent changes in root hole development can have a significant influence on hydraulic conductivity. Unfortunately, such a comprehensive examination of hydraulic conductivity at different scales, at different depths, and in different directions is not common, and until such information is available for other deposits it will not be possible to assess whether these generalisations can be widely applied.

REFERENCES

Adams, J.I., Effect of groundwater levels on stress history of the St. Clair clay till deposit: Discussion, *Can. Geotech. J.*, 7, 190-193, 1969.

Balfour, D. J., Evaluation of lateral solute migration in surficial weathered clayey till, M.Sc. project, University of Waterloo, Waterloo, Ontario, Canada, 1991.

Bear, J, Modeling flow and contaminant transport in fractured rocks, In: *Flow and contaminant transport in fractured rock*, J. Bear, C-F Tsang, and G. de Marsily, eds. Academic Press, San Diego, 1993.

Bradbury, K.R. and M. Muldoon, Hydraulic conductivity determination in unlithified glacial and fluvial materials, *Ground Water and Vadose-Zone Monitoring*, ASTM STP 1053, D.M. Nielson and A.I. Johnston, eds, American Society for Testing and Materials, Philadelphia, 138-151, 1990.

Chapman, L.P. and D.F. Putnam, Physiography of southern Ontario, 3rd. ed., Special Vol. 2, Ontario Geological Survey, 1984.

D'Astous, A. Y., W.W. Ruland, J.R.G. Bruce, J.A. Cherry, and R. W. Gillham, Fracture effects in the shallow groundwater zone in weathered Sarnia-area clay, *Can. Geotech. J.*, 26, 43-56, 1988.

Desaulniers, D.E., Groundwater origin, geochemistry and solute transport in three major glacial clay plains of east central North America, Ph.D. thesis, University of Waterloo, Waterloo, Ontario, Canada, 1986.

Einarson, M.D., Enviro-core - A new direct push technology for collecting continuous soil cores, 9th National Outdoor Action Conference, Las Vegas, 1995.

Fitzgerald, W.D., E. Janicki, and D.J. Storrinson, Sarnia-Brights Grove area, southern Ontario, Ontario Geological Survey, Preliminary Map P-2222, 1979.

Frind, E. O., Exact aquitard response functions for multiple aquifer mechanics, *Adv. Water Resour.*, 2, 77-82, 1979.

Grisak, G.E. and J.A. Cherry, Hydrologic characteristics and response of fractured till and clay confining a shallow aquifer, *Can. Geotech. J.*, 12, 23-43, 1975.

Hanna, T.H., Engineering properties of glacial-lake clays near Sarnia, Ontario, Ontario Hydro Research Quarterly, 3rd Quarter, 1-12, 1966.

Hanor, J.S, Effective hydraulic conductivity of fractured clay beds at a hazardous waste landfill, Louisiana Gulf Coast, *Water Resour. Res.*, 29(11), 3691-3698, 1993.

Hantush, M. S., and C. E. Jacob, Non-steady radial flow in an infinite leaky aquifer, *Eos Trans. AGU*, 36(1), 95-100, 1955.

Harris, S. M., Characterization of the hydraulic properties of a fractured clay till, M.Sc. Thesis, University of Waterloo, Waterloo, Ontario, Canada, 1994.

Harrison, B., E.A. Sudicky, and J.A. Cherry, Numerical analysis of solute migration through fractured clayey deposits into underlying aquifers, *Water Resour. Res.*, 28(2), 515-530, 1992.

Hendry, M.J., Hydraulic conductivity of a glacial till in Alberta, *Groundwater*, 20 (2), 162-169, 1982.

Husain, M.M., Origin and persistence of Pleistocene and Holocene water in a regional clayey aquitard and underlying aquifer in part of south-western Ontario, Ph.D. thesis, University of Waterloo, Waterloo, Ontario, Canada, 1996.

Hvorslev, M.J, Time lag and soil permeability in ground-water observations, Waterways Exp. Sta. Bull. 36, U.S. Army Corps of Engineers, Vicksburg, Miss., 1951.

Jones, L., T. Lemar and, C. Tsai, Results of two pumping tests in Wisconsinon Age weathered till in Iowa, *Groundwater*, 30(4), 529-538, 1992.

Keller, C.K., G. van der Kamp, and J.A. Cherry, Fracture permeability and groundwater flow in clayey till near Saskatoon, Saskatchewan, *Can. Geotech. J.*, 23, 229-240, 1986.

Keller, C.K., G. van der Kamp, and J.A. Cherry, Hydrogeology of two Saskatchewan tills, I. Fractures, bulk permeability, and spatial variability of downward flow, *Journal of Hydrology*, 101, 97-121, 1988.

Keller, C.K., G. van der Kamp, and J.A. Cherry, A multiscale study of the permeability of a thick clayey till, *Water Resour. Res.*, 25(11), 2299-2317, 1989.

Klint, K.E.S., Fractures and depositional features of the St. Joseph Till and the upper part of the Black Shale Till at the Laidlaw site, Lambton County, Ontario, Geological Survey of Denmark and Greenland, Report 1996/9, 1996.

McKay, L. D., J.A. Cherry, and R. W. Gillham, Field experiments in a fractured clay till 1. Hydraulic conductivity and fracture aperture, *Water Resour. Res.*, 29(4), 1149-1162, 1993a.

McKay, L.D., R.W. Gillham, and J.A. Cherry, Field experiments in a fractured clay till 2. Solute and colloid transport, *Water Resour. Res.*, 29(12), 3879-3890, 1993b.

McKay, L.D., and J. Fredericia, Distribution, origin, and hydraulic influence of fractures in a clay-rich glacial deposit, *Can. Geotech. J.*, 32, 957-975, 1995.

Morris, P.H., J. Graham and D.J. Williams, Cracking in drying soils, *Can. Geotech. J.*, 29, 263-277, 1992.

Murdoch, L, Forms of hydraulic fractures created during a field test in overconsolidated glacial drift, *Quart. J. Eng. Geol.*, 28, 23-35, 1995.

Neuman, S. P., and P. A. Witherspoon, Theory of flow in a confined two-aquifer system, *Water Resour. Res.*, 5(4), 817-829, 1969.

Ogunbadejo, T.A. and R.M. Quigley, Micro-structural and mineralogical influences on the compaction characteristics of weathered clays from Sarnia, Ontario, University of Western Ontario Soil Mechanics Research Report SM-2-73, 1973.

Padusenko, G., The influence of scale on hydraulic conductivity measurements, B.Sc. Thesis, University of Waterloo, Waterloo, Ontario, Canada, 1997.

Rudolph, D.L., J.A. Cherry and R.N. Farvolden, Groundwater flow and solute transport in fractured lacustrine clay near Mexico City, *Water Resour. Res.*, 27(9), 2187-2201, 1991.

Ruland, W. W., J.A. Cherry, and S. Feenstra, The depth of fractures and active groundwater flow in a clayey till plain in south-western Ontario, *Groundwater*, 29(3), 405-417, 1991.

Sidle, R.C., B. Nilsson, M. Hansen and J. Fredericia, Spatially varying hydraulic and solute transport characteristics of a fractured till determined by field tracer tests, Funen, Denmark, Submitted to *Water Resour. Res.*, 1997.

Therrien, R., E.A. Sudicky and R.G. McLaren, Users guide for NP - A preprocessor for FRAC3DVS: An efficient simulator for three-dimensional, saturated-unsaturated groundwater flow and chain-decay solute transport in porous or discretely fractured porous formations, University of Waterloo, 1995.

Therrien, R. and E.A. Sudicky, Three-dimensional analysis of variably-saturated flow and solute transport in discretely-fractured porous media, *J. Cont. Hydrology*, 23, 1-44, 1996.

Case	Specified Hydraulic Conductivity Distribution (refer to Figure 3.9 for positions of layers)	Calculated Vertical Hydraulic Conductivity
A-homogeneous, isotropic	$K=K_{1v}=K_{2v}=K_{1h}=K_{2h}=1x10^{-6}$	$K=2.4x10^{-6}$
B - layered, isotropic	$K_1=K_{1v}=K_{1h}=1x10^{-6}$ $K_2=K_{2v}=K_{2h}=1x10^{-7}$	$K_{1v}=1.6x10^{-6}$ $K_{2v}=1.0x10^{-7}$
C - layered, anisotropic	$K_{1v}=10K_{1h}=1x10^{-6}$ $K_{2v}=10K_{2h}=1x10^{-7}$	$K_{1v}=1.3x10^{-6}$ $K_{2v}=1.3x10^{-7}$

Table 3.1 - Comparison of hydraulic conductivity specified in model, and hydraulic conductivity calculated using Darcy-type calculation

NE Quadrant of Pond		NW Quadrant of Pond	
Depth Interval (m)	K_{bulk} (m/s)	Depth Interval (m)	K_{bulk} (m/s)
0.4-1.33	$1.9x10^{-6}$ - $2.0x10^{-6}$	0.4-1.39	$1.8x10^{-6}$ - $2.0x10^{-6}$
1.33-2.02	$1.3x10^{-6}$ - $2.5x10^{-6}$	1.39-1.87	$9.0x10^{-7}$ - $2.3x10^{-6}$
2.02-2.3	$1.5x10^{-6}$ - $2.2x10^{-6}$	1.87-2.09	$1.5x10^{-6}$ - $2.4x10^{-6}$

Table 3.2a - Values of bulk vertical hydraulic conductivity determined from pumping tests - first experimental installation

Nest A		Nest B		Nest C	
Depth Interval (m)	K_{bulk} (m/s)	Depth Interval (m)	K_{bulk} (m/s)	Depth Interval (m)	K_{bulk} (m/s)
0.0-0.36	$1.3x10^{-6}$ - $1.7x10^{-6}$	0.0-0.43	$1.3x10^{-6}$ - $1.5x10^{-6}$	0.0-0.74	$1.5x10^{-6}$ - $2.0x10^{-6}$
0.36-1.35	$4.1x10^{-6}$	0.43-0.96	$2.5x10^{-5}$	0.92-1.85	$8.3x10^{-7}$
1.35-1.58	$1.5x10^{-6}$	0.96-1.43	$2.8x10^{-6}$	2.23-2.63	$1.8x10^{-7}$
1.58-1.98	$5.2x10^{-7}$	1.43-2.30	$9.5x10^{-7}$	2.63-2.94	$2.5x10^{-8}$
2.11-2.41	$3.1x10^{-7}$	2.70-3.10	$2.5x10^{-8}$		
2.41-2.94	$4.1x10^{-8}$				

Table 3.2b - Values of bulk vertical hydraulic conductivity determined from pumping tests - second experimental installation

Previous Study	Type of bulk scale test	Direction of bulk scale test	Plan-view dimensions of bulk scale test	Depth interval of bulk scale test	Piezometer dimensions
McKay et. al. (1993)	constant gradient trench-to trench flow test	horizontal	7mx4.2m 7mx6.2m	0.5-5.5m	length:0.2m diam.:0.02m
Harris (1994)	single well pumping test	horizontal	4m radius from pumping well	2-5m	length:0.7-1.6m diam.:0.08m (piezometers angled at up to 50° from vert.)
Current study	combined infiltration and pumping test	vertical and horizontal	1st site:4m diam. 2nd site:3m diam.	1st site: 0.4-3.8m 2nd site: 0.0-3.0m	no single well tests

Table 3.3 - Details of scale and types of tests in various studies at the Laidlaw site

Well location	Position in Network	K_{well} (m/s)	K_{well}/K_{bulkx}, K_{well}/K_{bulky}*
A	1st order fracture	1.6×10^{-7}	2.3, 1.5
B	1st order fracture	3.2×10^{-7}	4.5, 2.9
C	1st order fracture	2.7×10^{-7}	3.8, 2.5
D	1st order fracture	2.0×10^{-7}	2.8, 1.8
E	1st order fracture	2.4×10^{-7}	3.4, 2.2
F	2nd order fracture	2.7×10^{-8}	0.38, 0.25
G	2nd order fracture	1.9×10^{-8}	0.27, 0.17
H	2nd order fracture	3.5×10^{-8}	0.49, 0.32
I	2nd order fracture	3.5×10^{-8}	0.49, 0.32
J	3rd order fracture zone	1.4×10^{-8}	0.20, 0.13
K	3rd order fracture zone	1.7×10^{-8}	0.24, 0.15
L	unfractured matrix	1.8×10^{-10}	0.003, 0.002

* $K_{bulkx}=7.1\times10^{-8}$ m/s, $K_{bulky}=1.1\times10^{-7}$ m/s

Table 3.4 - Values of hydraulic conductivity calculated from simulated well responses at various locations in fracture network

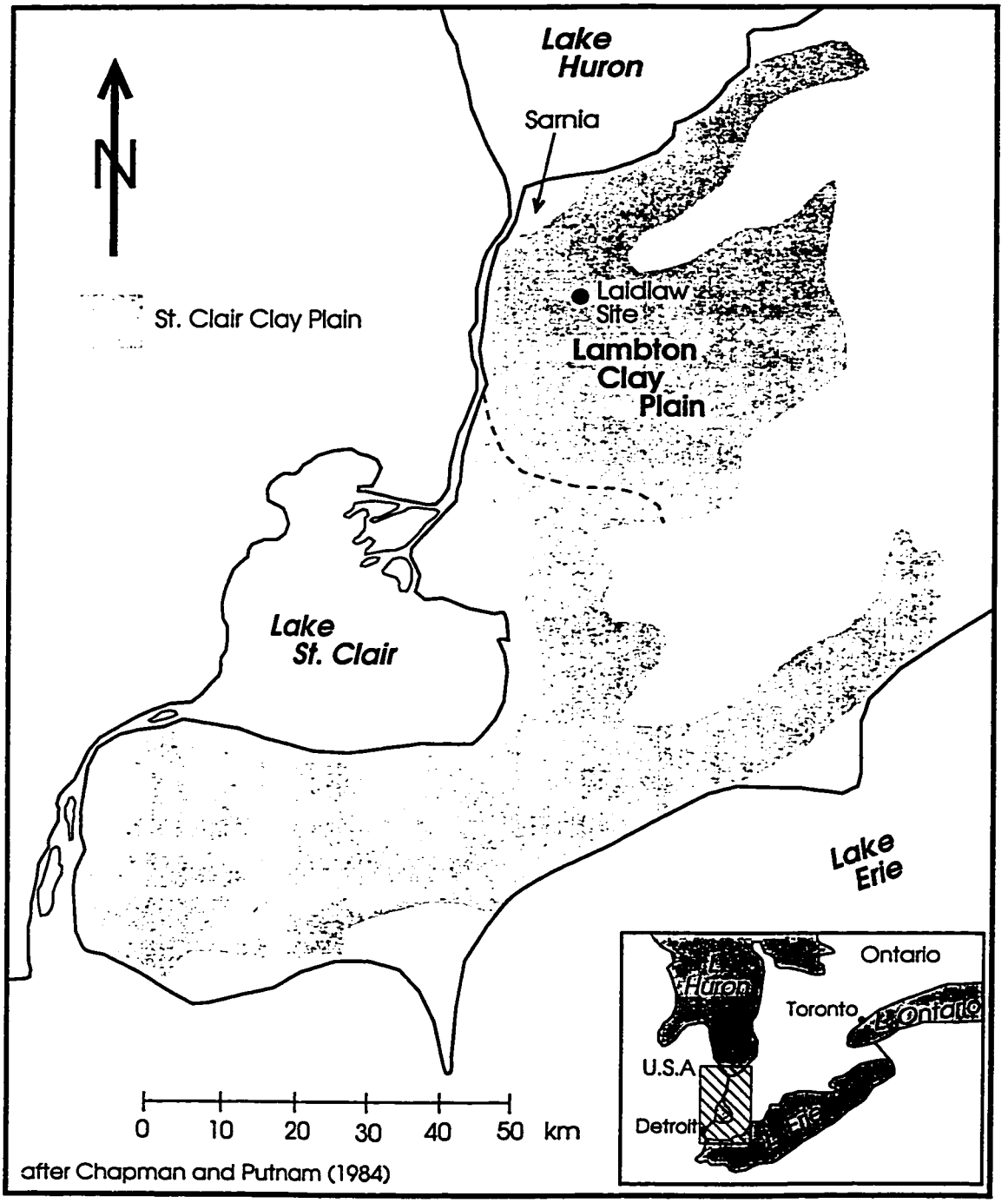

Figure 3.1 - Location of study site

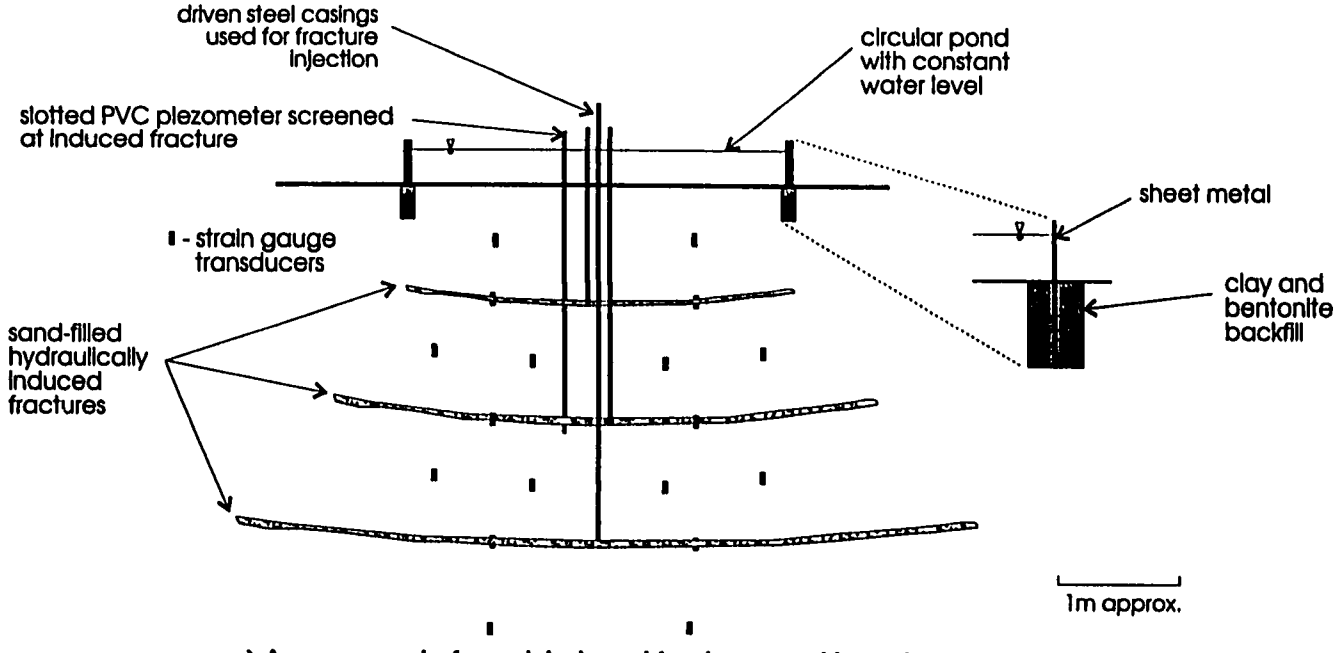

a) Arrangement of pond, induced fractures, and transducers

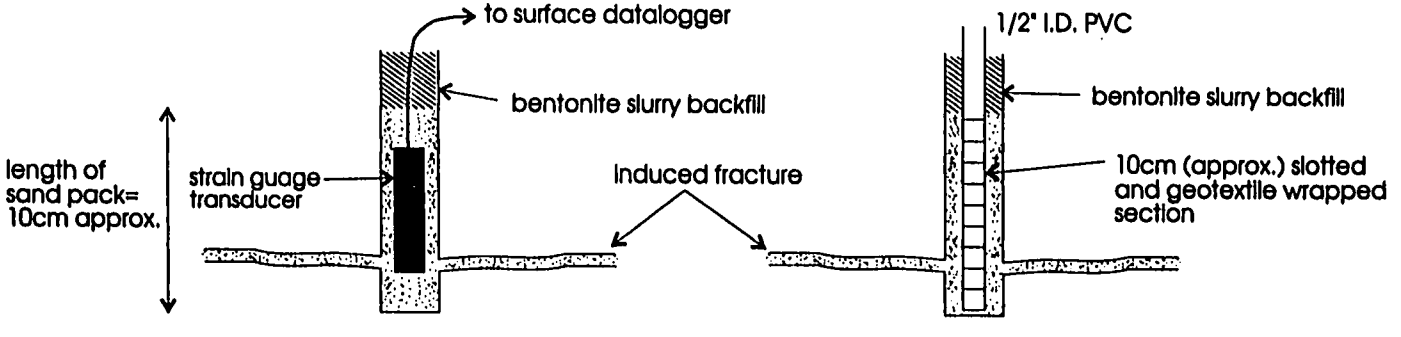

b) Detail of transducer and well placement at the level of an induced fracture

Figure 3.2 - Idealised schematic of experimental setup for large scale combined infiltration and pumping tests

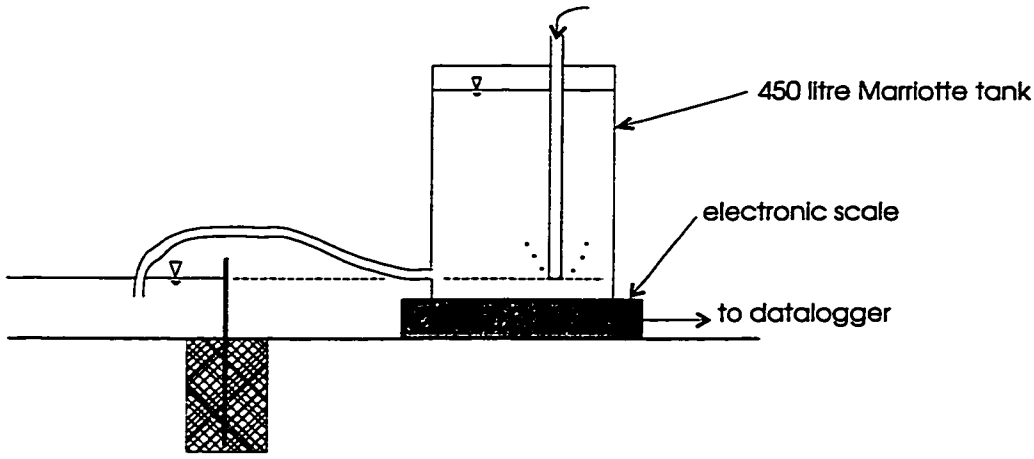

Figure 3.3 - Marriotte system for maintaining pond level and measuring infiltration rate

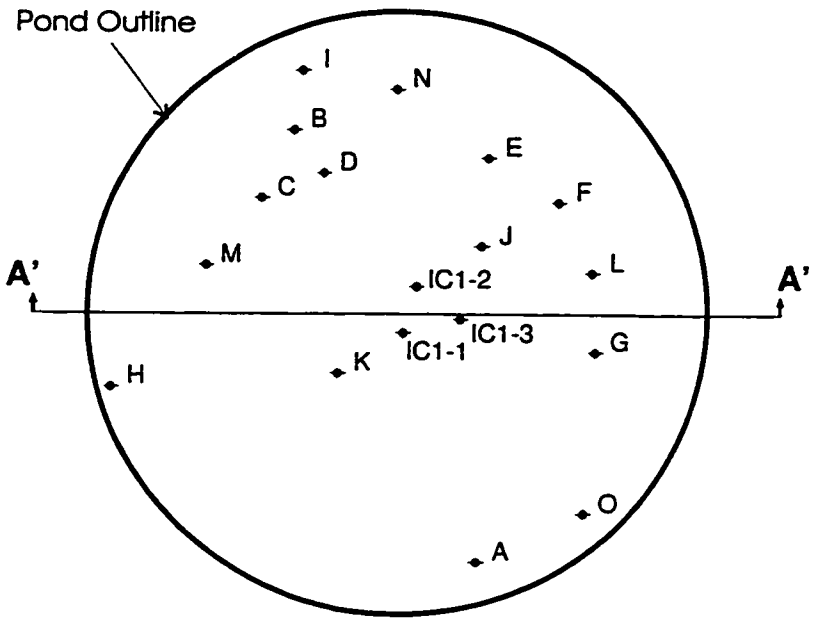

Transducer Location	Depth below pond bottom (m)
A	1.29
B	1.35
C	1.83
D	1.98
E	2.04
F	2.04
G	1.98
H	1.98
I	2.05
J	2.26
K	2.20
L	2.65
M	2.32
N	3.37
O	3.76

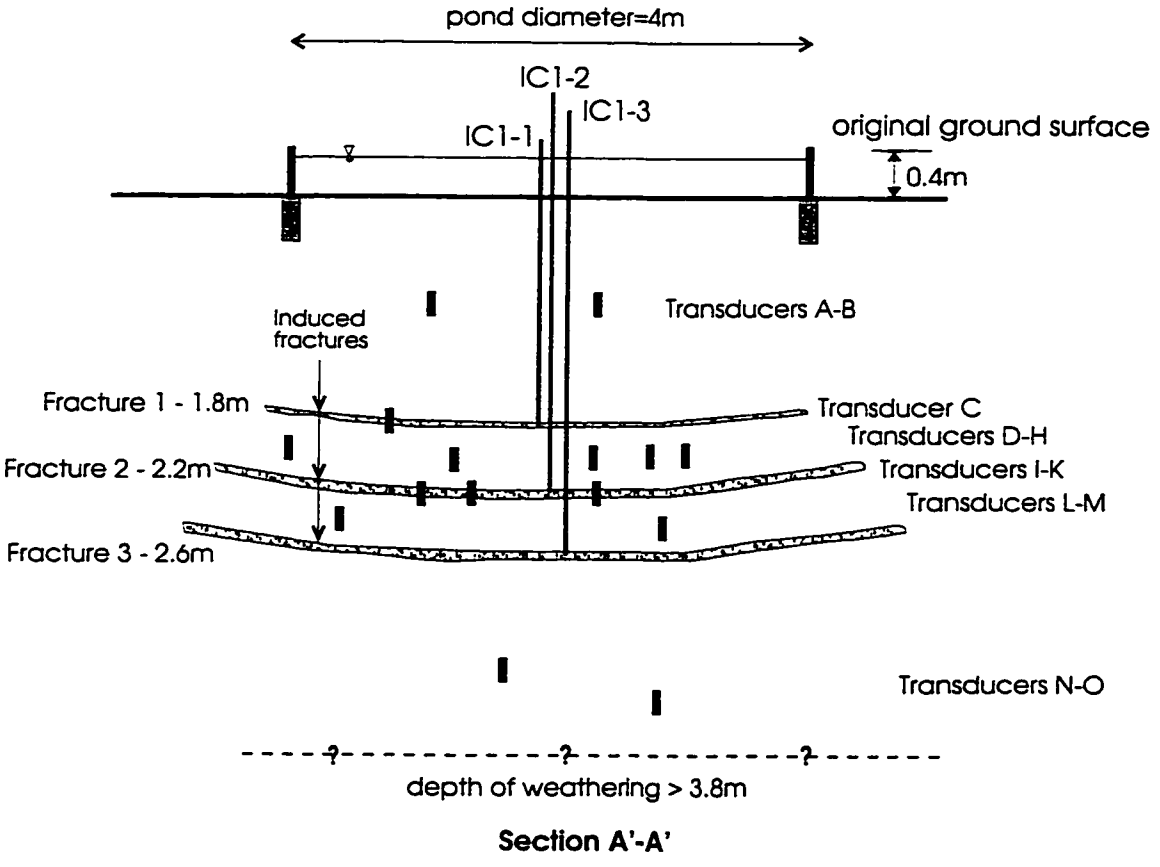

Section A'-A'

Figure 3.4 - Details of instrumentation for second experiment

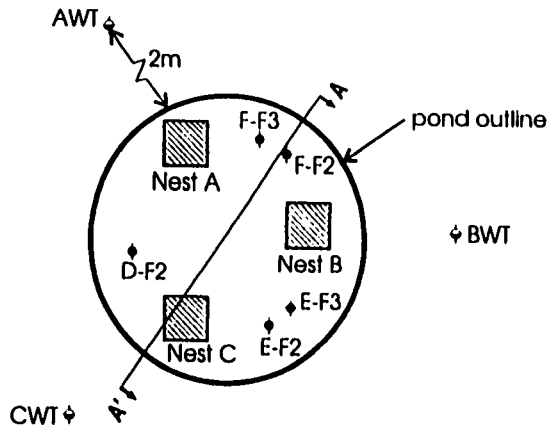

Nest A		Nest B		Nest C		Other wells	
Location	Depth below pond bottom (m)	Location	Depth below pond bottom (m)	Location	Depth below pond bottom (m)	Location	Depth below pond bottom (m)
A-1	-0.33	B-1	-0.28	C-1	-0.28	D-F2	-1.99
A-F1	-0.36	B-F1	-0.47	C-F1	-0.74	E-F2	-1.88
A-2	-1.35	B-2	-0.96	C-2	-0.92	E-F3	-2.99
A-3	-1.58	B-3	-1.43	C-3	-1.44	F-F2	-1.77
A-F2	-1.98	B-4	-2.30	C-F2	-1.846	F-F3	-2.88
A-4	-2.11	B-5	-2.70	C-4	-2.23		
A-5	-2.41	B-F3	-3.10	C-5	-2.63		
A-F3	-2.94	B-6	-3.42	C-F3	-2.94		
A-6	-3.18	B-7	-4.93	C-6	-3.25		
A-7	-4.93			C-7	-4.93		

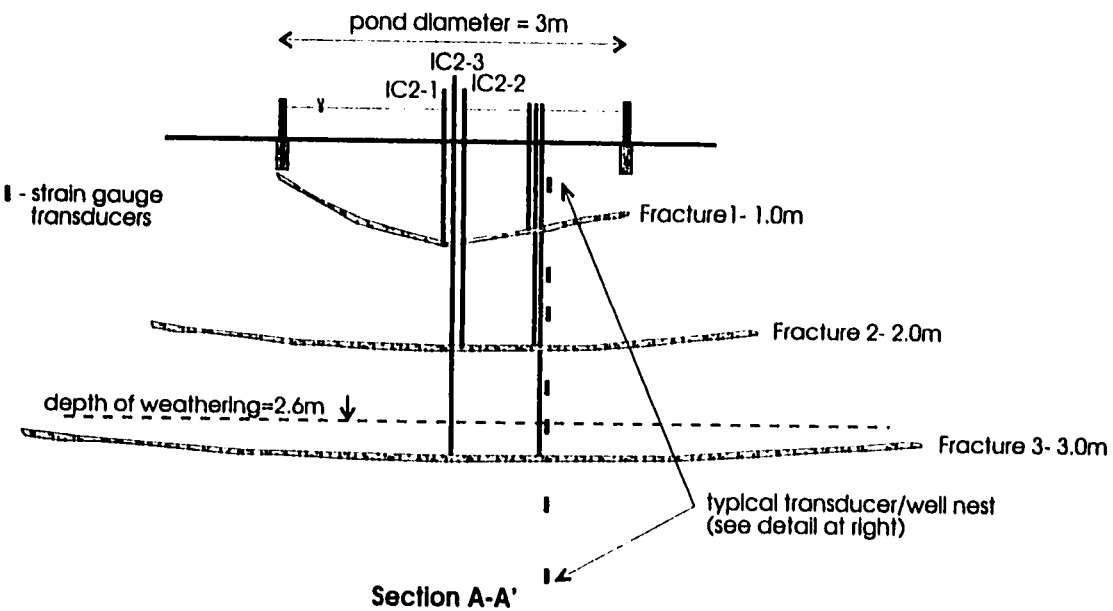

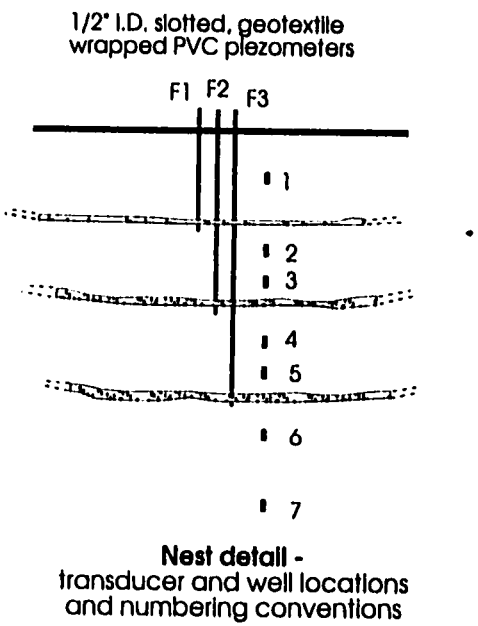

Figure 3.5 - Details of instrumentation for second experiment

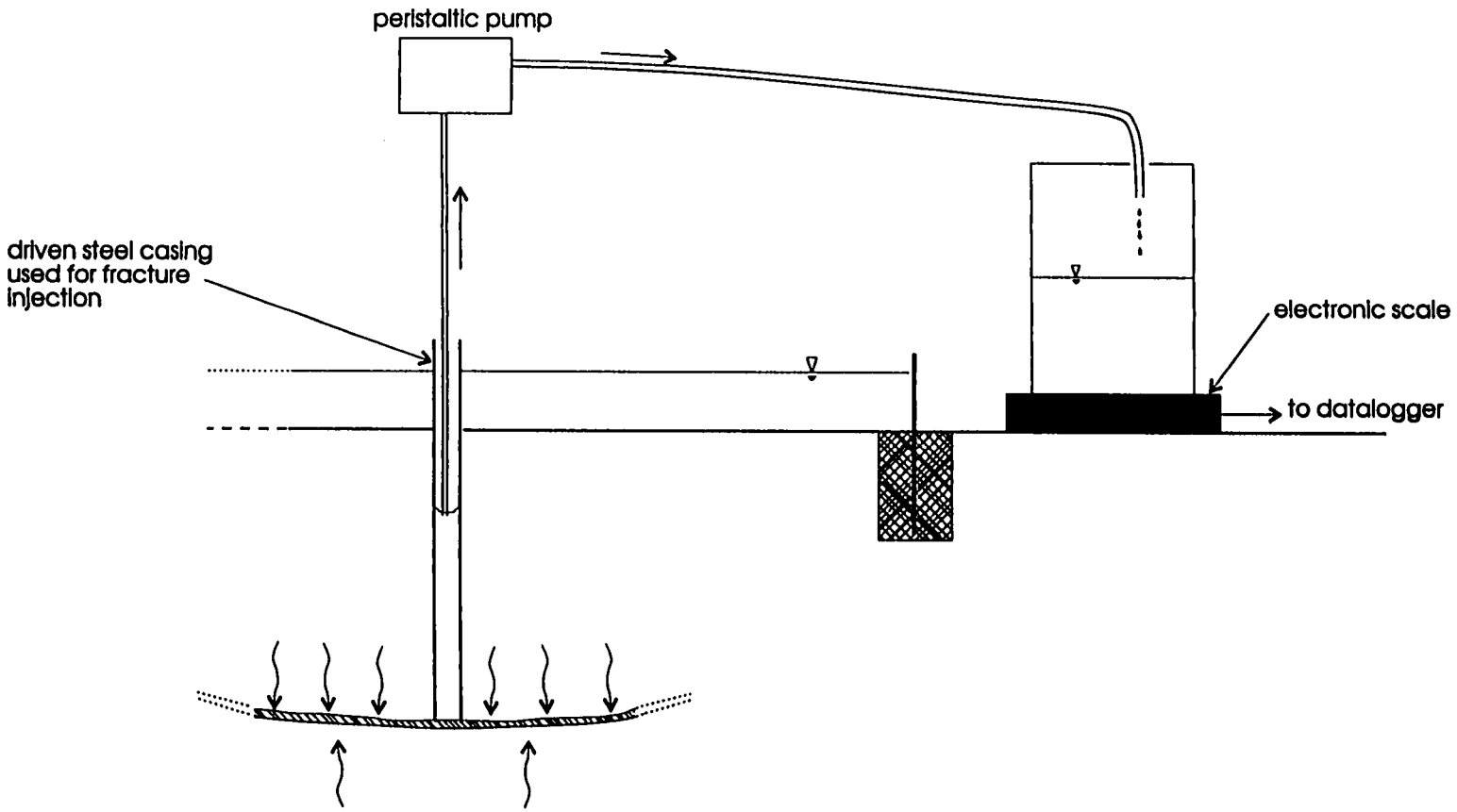

Figure 3.6 - Constant head pumping from fracture well and measurement of pumping rate

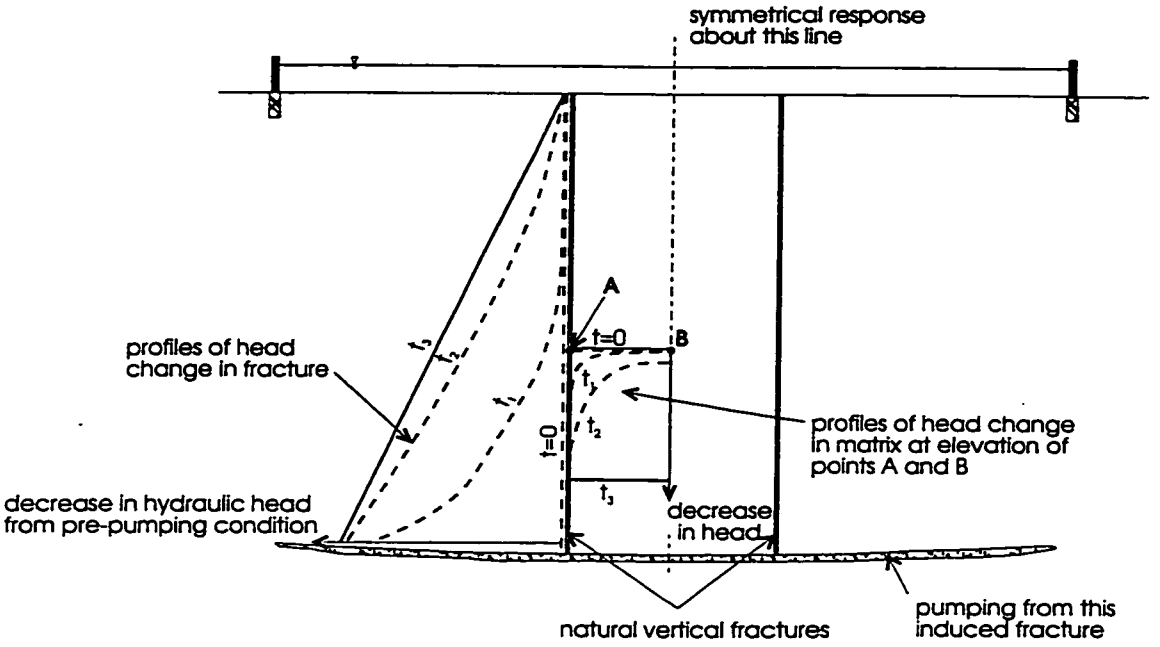

a) Changes in hydraulic head along vertical fractures and through matrix as pumping test proceeds t1<t2<t3

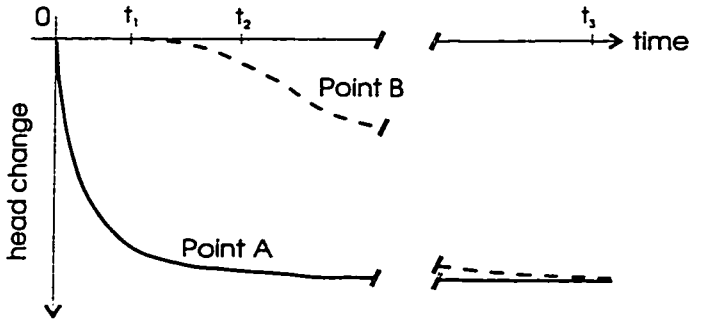

b) Changes in hydraulic head at Points A and B as pumping test proceeds

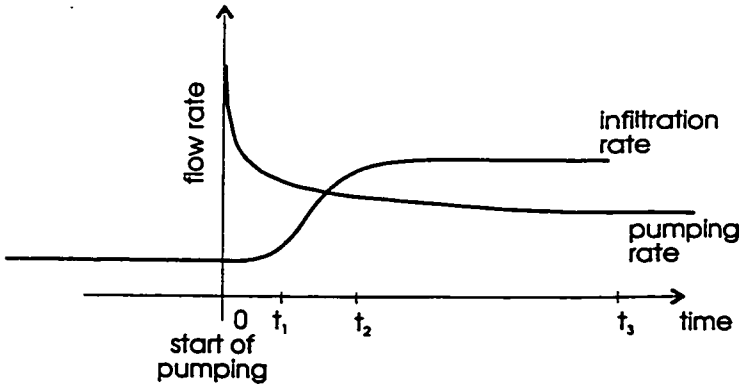

c) Changes in infiltration rate and pumping rate as pumping test proceeds

Figure 3.7 - Idealised behaviour during constant head pumping tests

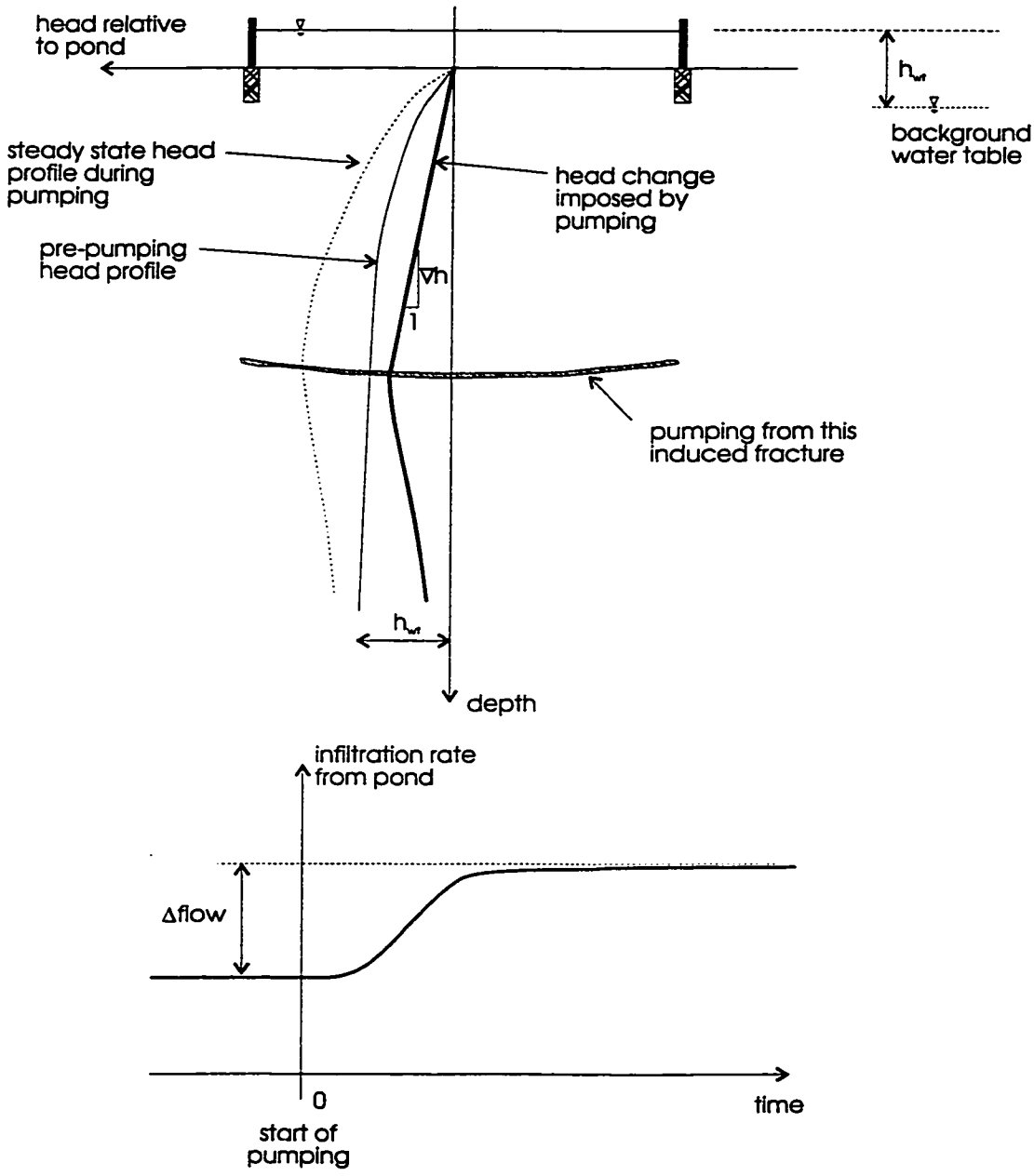

$$K = \frac{\Delta flow/pond\ area}{\nabla h}$$

Figure 3.8 - Conceptual model for calculating hydraulic conductivity from steady state conditions during pumping tests

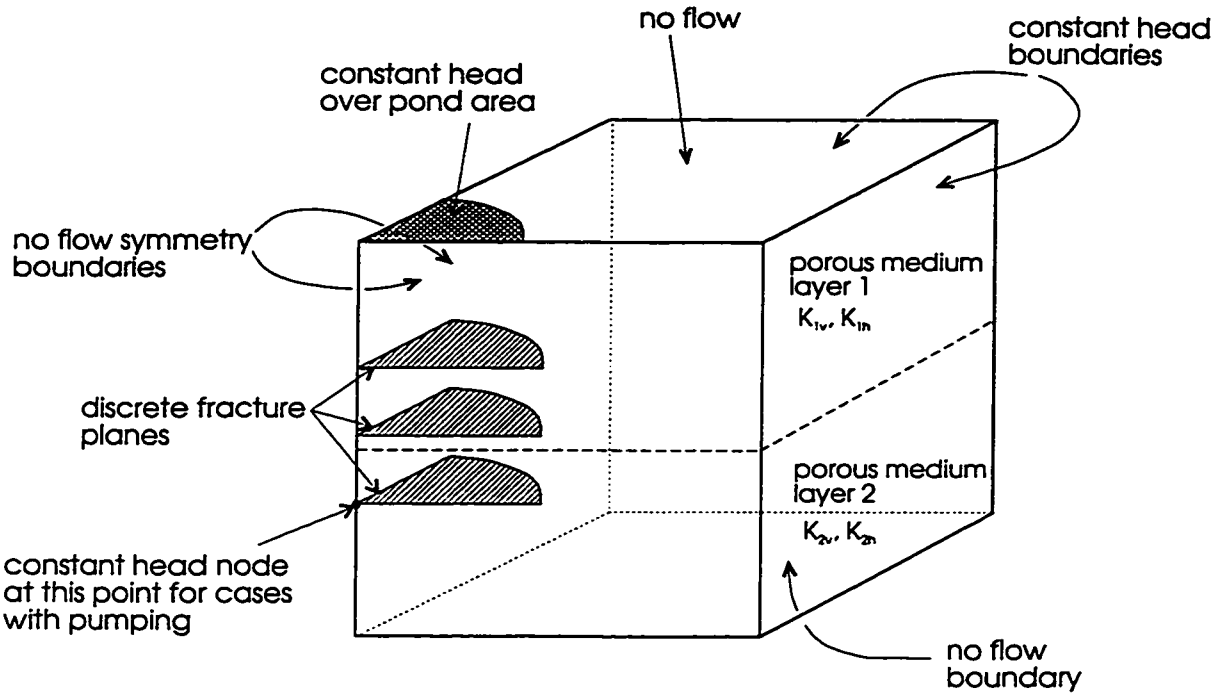

Figure 3.9 - Model geometry used to evaluate proposed method for calculation of hydraulic conductivity

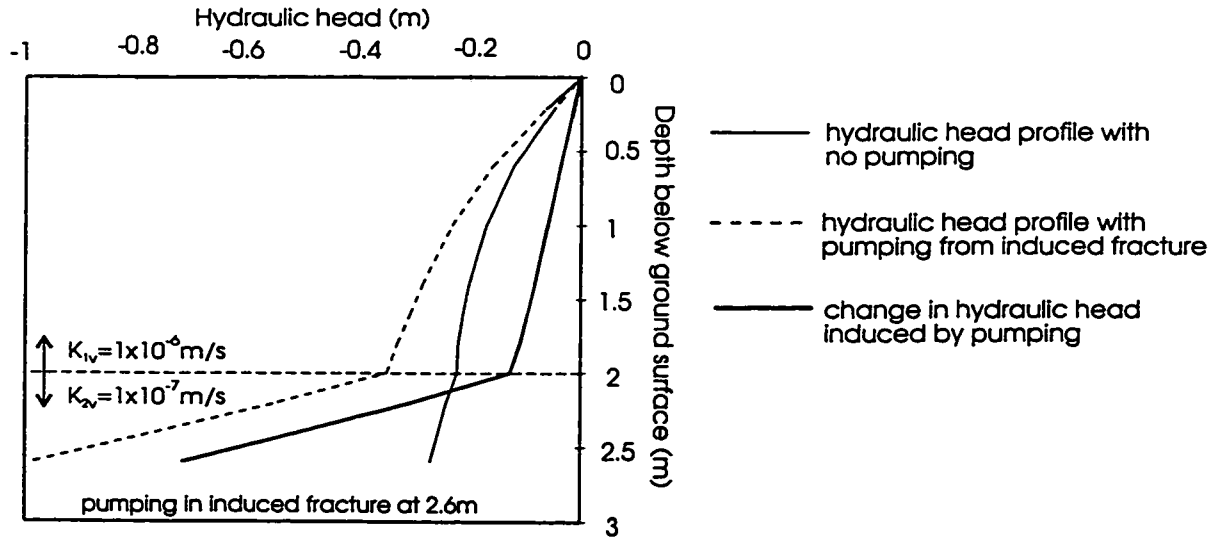

Figure 3.10 - Simulated hydraulic head distributions for the case of layered hydraulic conductivity

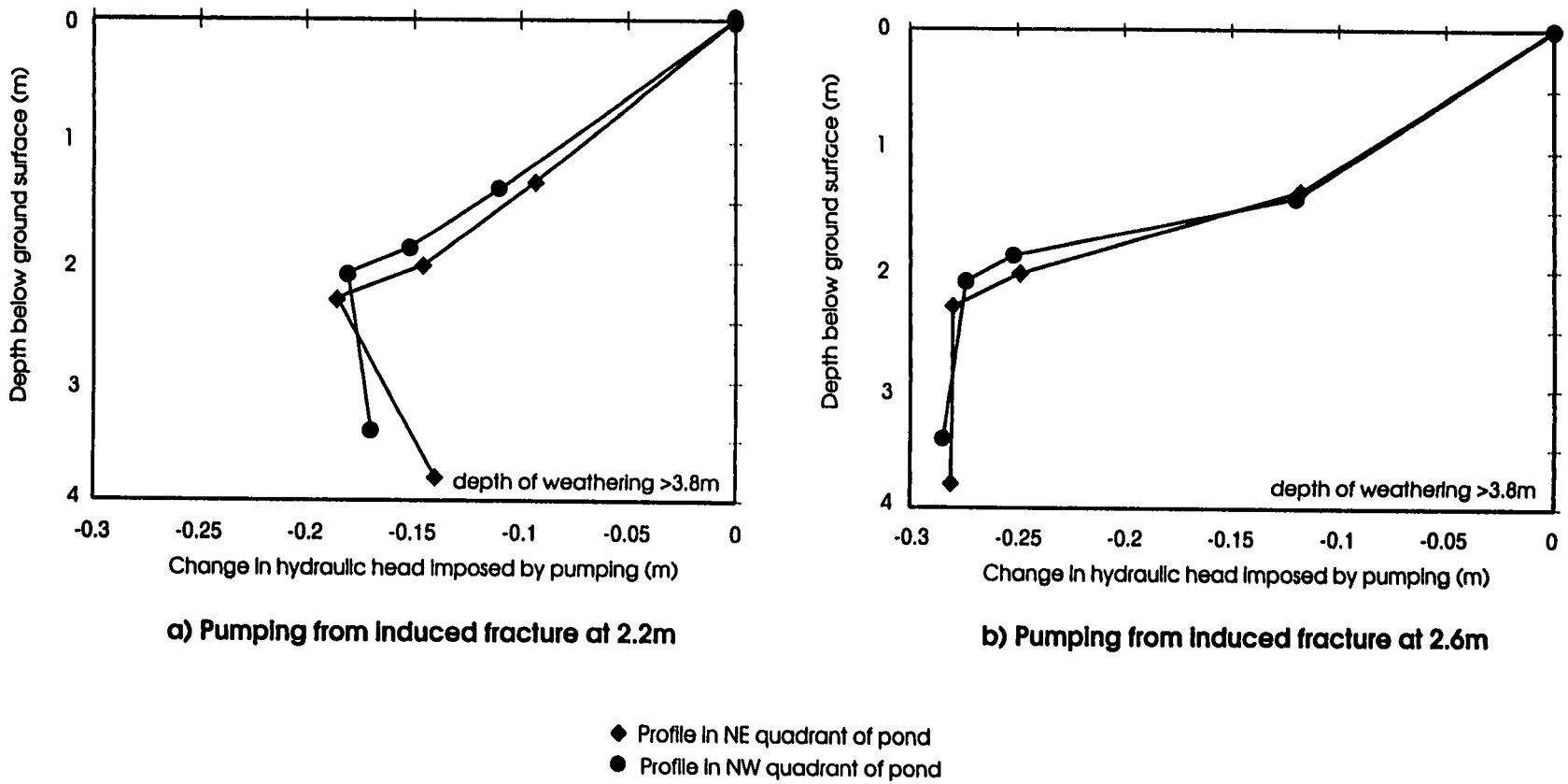

Figure 3.11 - Profiles of change in hydraulic head beneath pond Pumping tests at first experimental installation

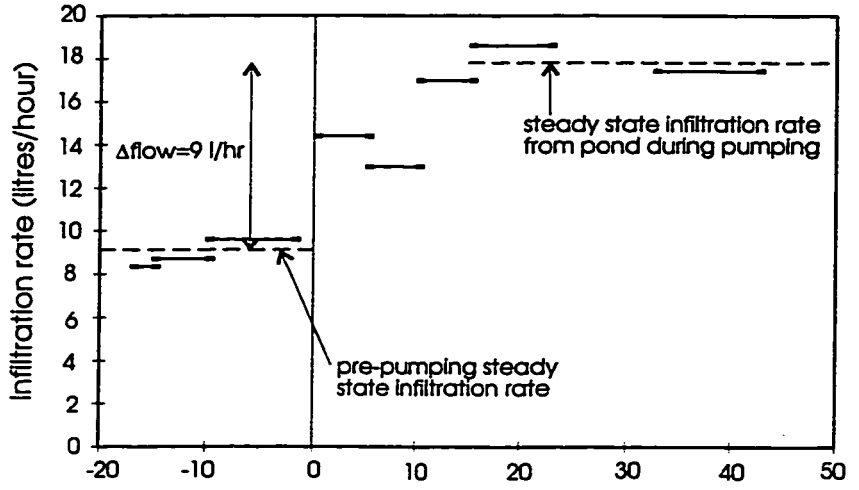

a) Pumping from induced fracture at 2.2m depth

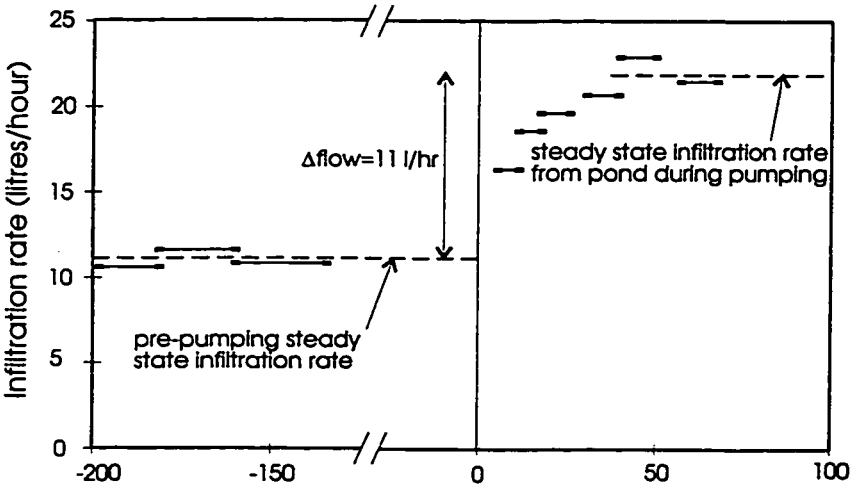

b) Pumping from induced fracture at 2.6m depth

Figure 3.12 - Temporal variations in infiltration rates from the pond for pumping tests at first experimental installation

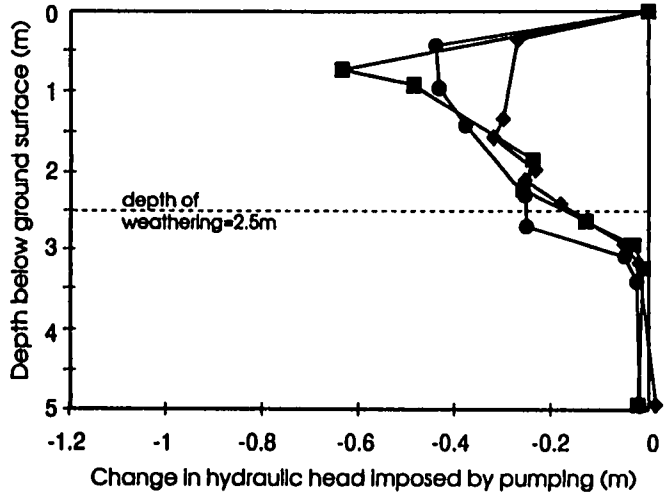

a) Pumping from induced fracture at 1.0m depth

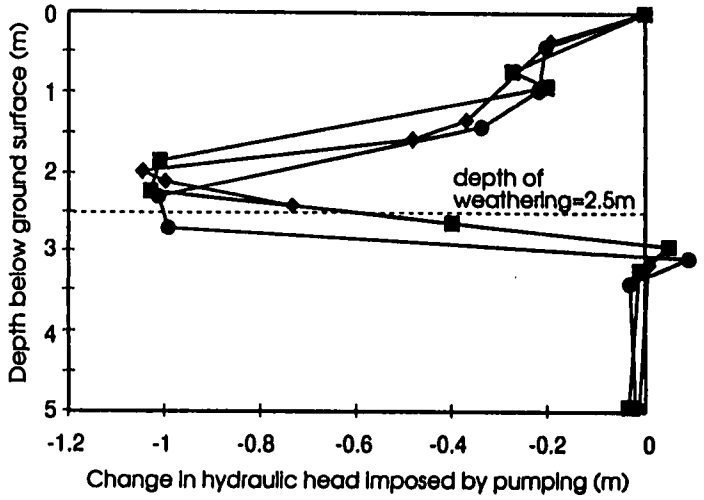

b) Pumping from induced fracture at 2.0m depth

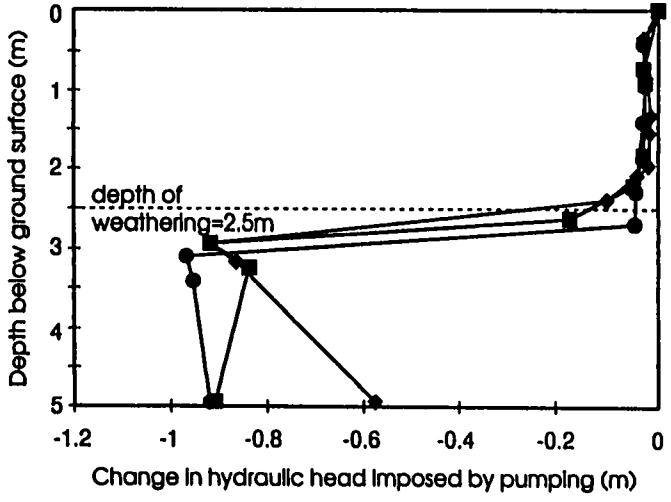

c) Pumping from induced fracture at 3.0m depth

◆ Profile at Nest A
■ Profile at Nest C
● Profile at Nest B

Figure 3.13 - Profiles of change in hydraulic head beneath pond
Pumping tests at second experimental installation

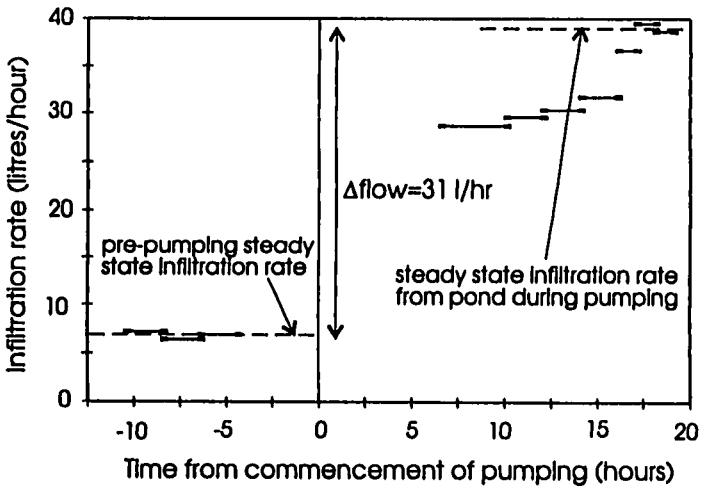

a) Pumping from induced fracture at 1.0m depth

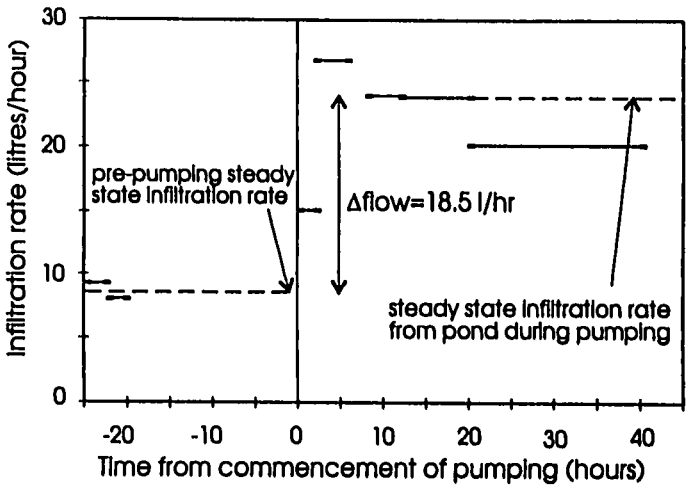

b) Pumping from induced fracture at 2.0m depth

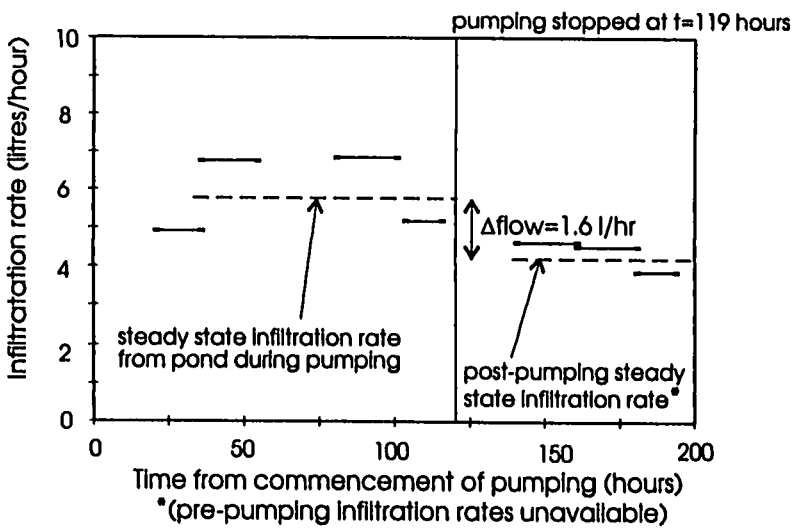

c) Pumping from induced fracture at 3.0m depth

Figure 3.14 - Temporal variations in infiltration rates from the pond for pumping tests at second experimental installation

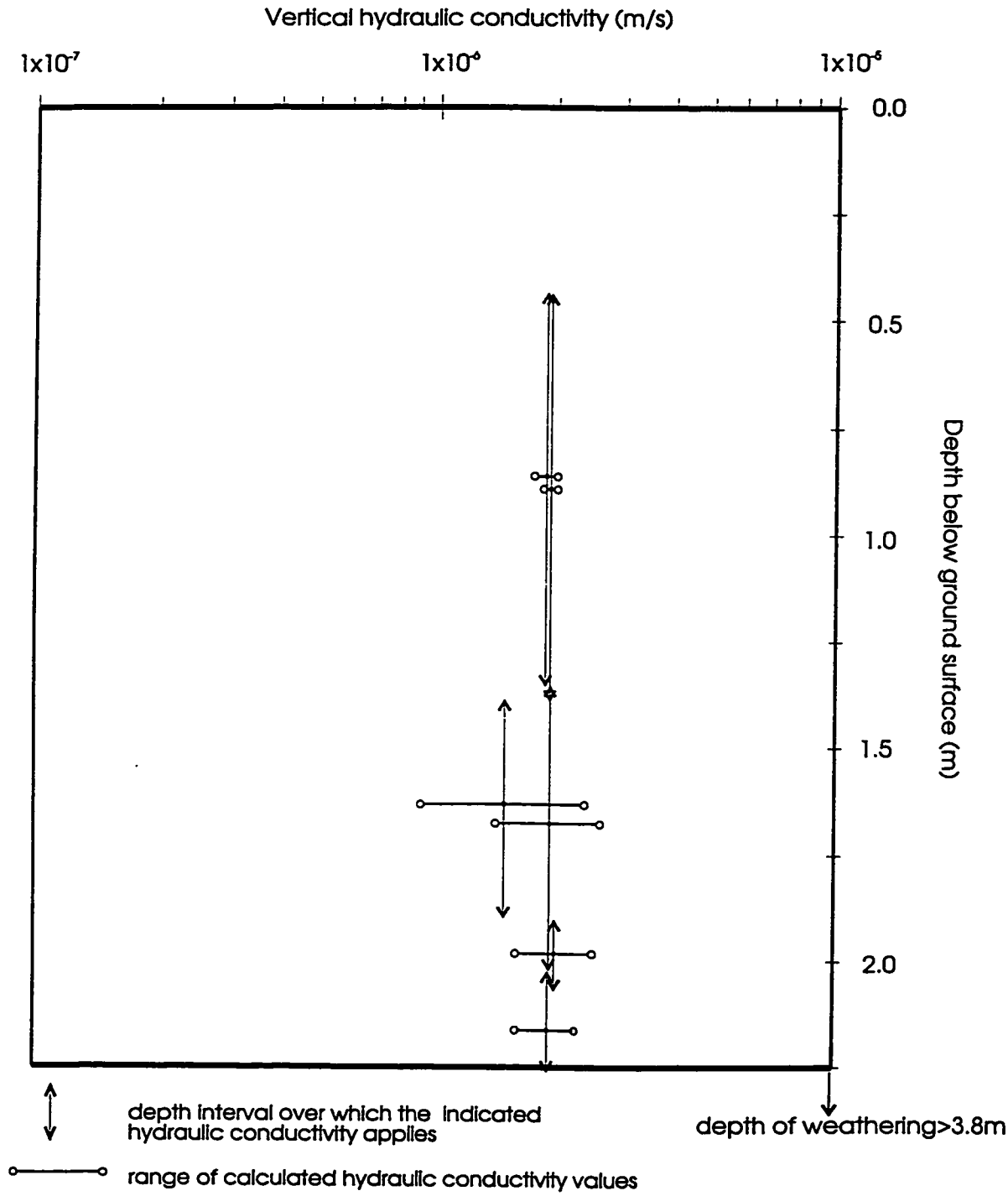

Figure 3.15 - Variation of vertical hydraulic conductivity with depth First experimental installation

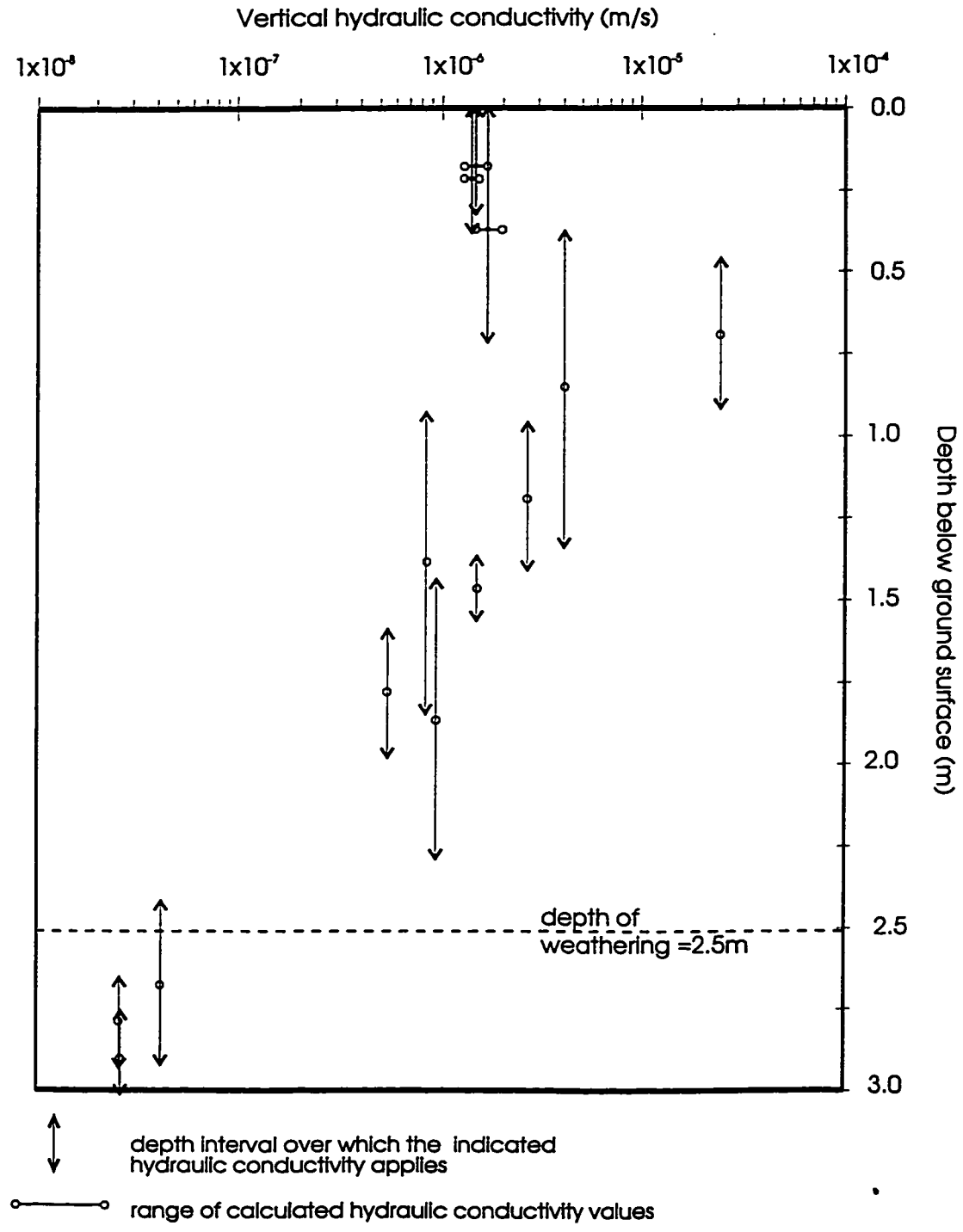

Figure 3.16 - Variation of vertical hydraulic conductivity with depth Second Experimental Installation

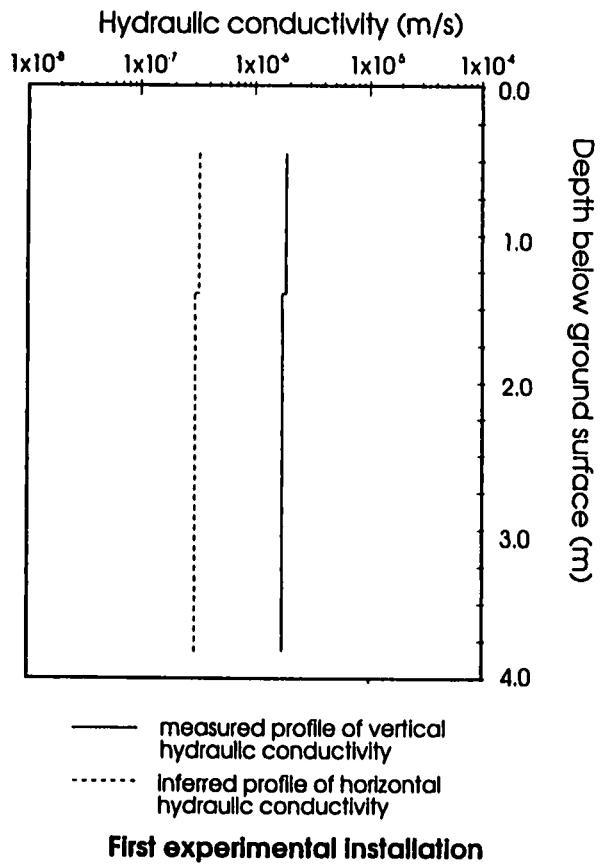

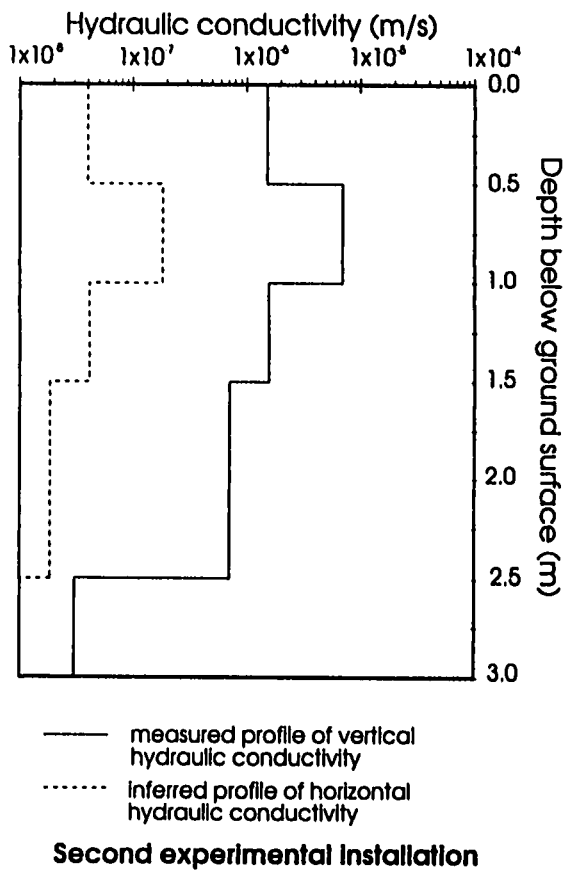

Figure 3.17 - Profiles of vertical and horizontal hydraulic conductivity at first and second experimental installations

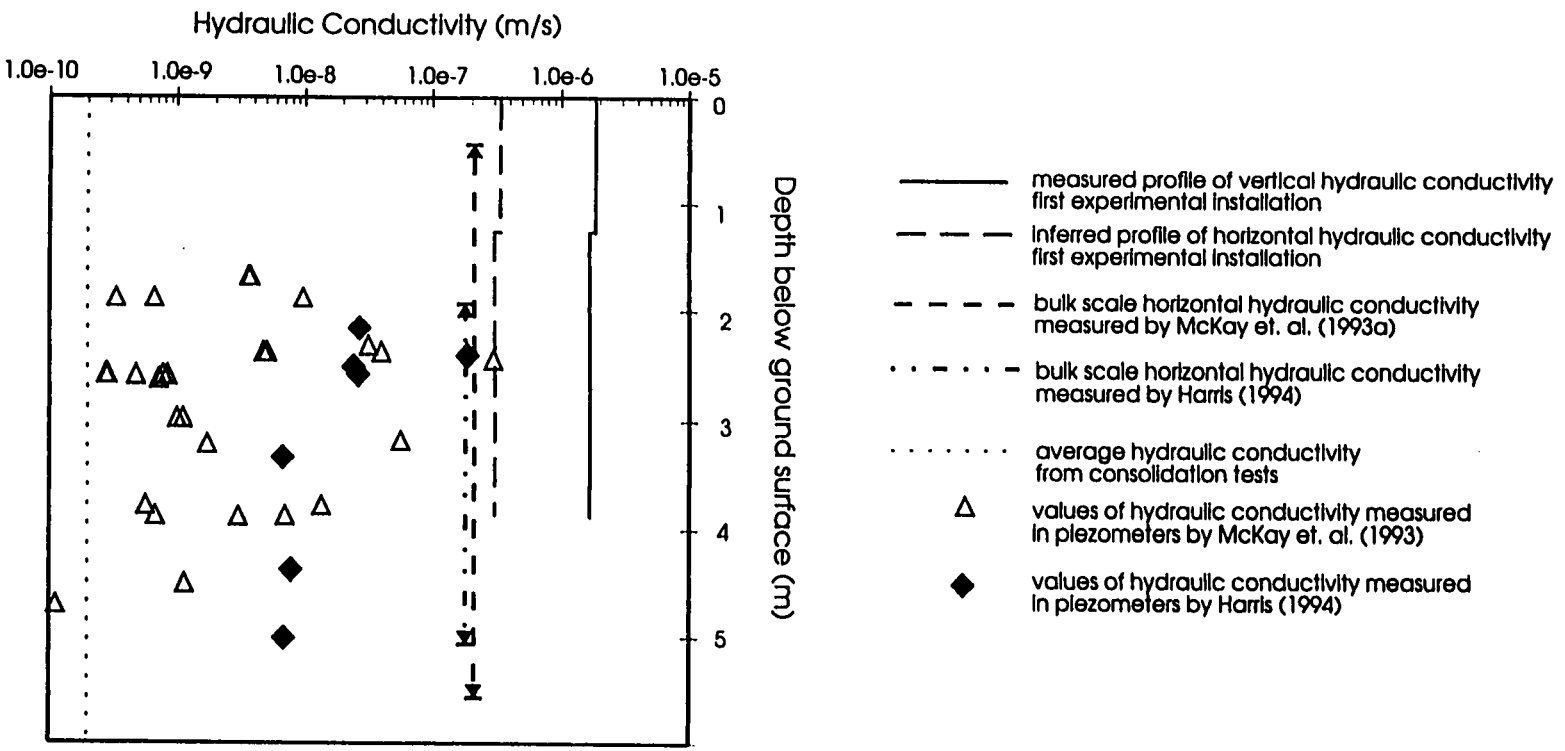

Figure 3.18 - Results of hydraulic conductivity measurements at various scales (see Table 3.3 for scales of various tests)

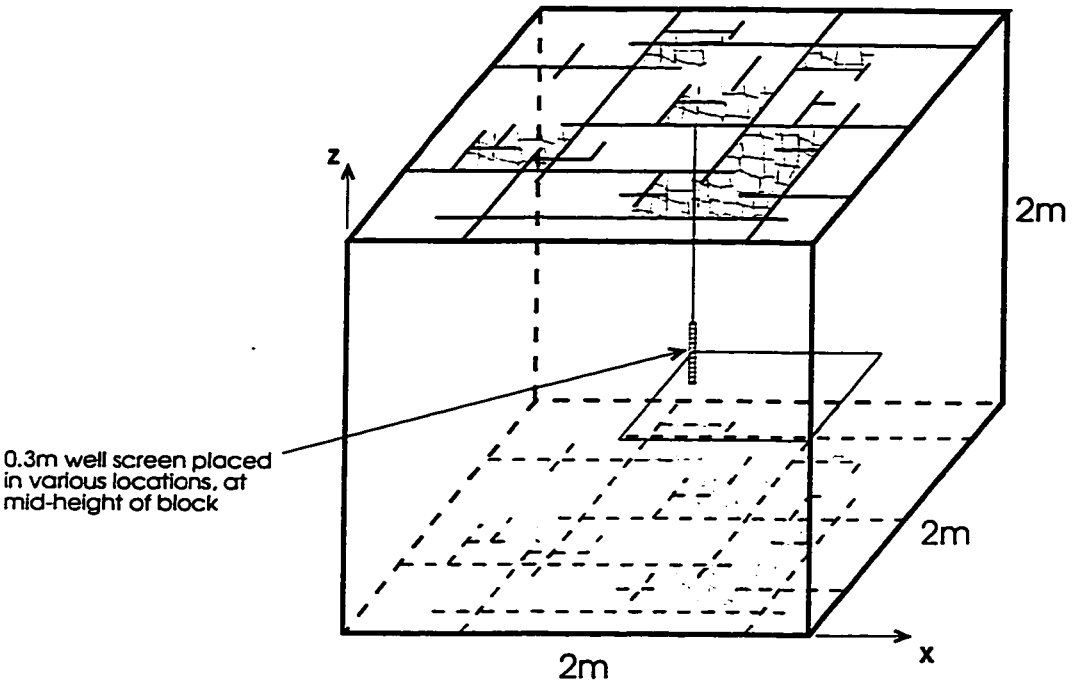

a) Model geometry

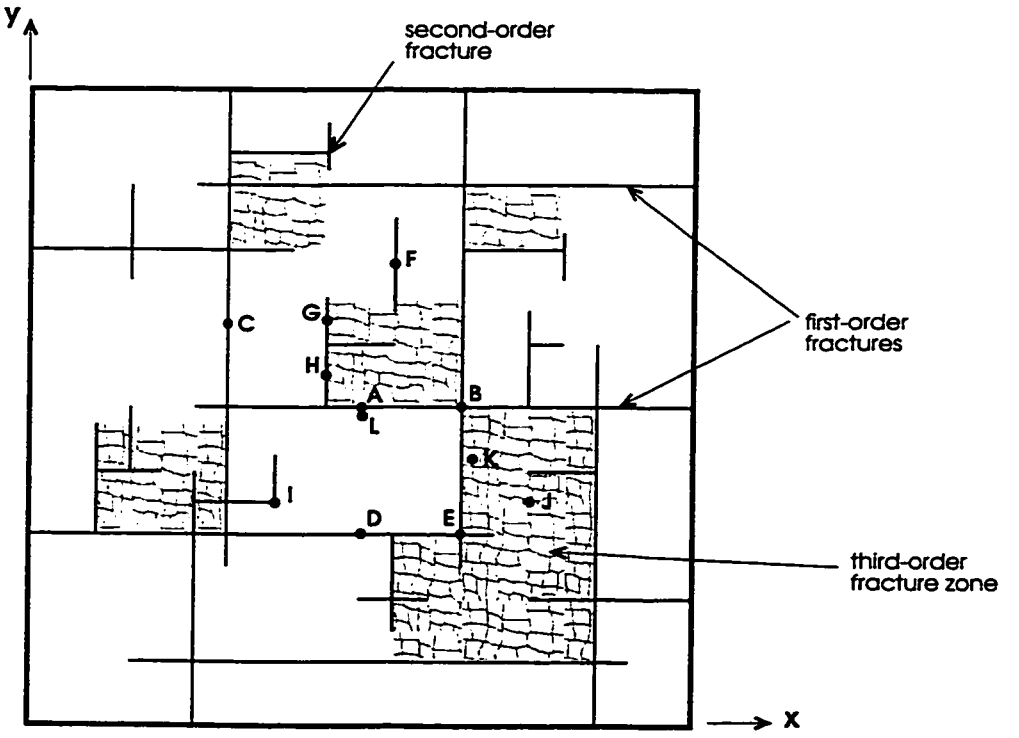

b) Fracture network and locations of wells

Figure 3.19 - Details of model used to assess the relationships between well-scale measurements and large scale measurements of hydraulic conductivity

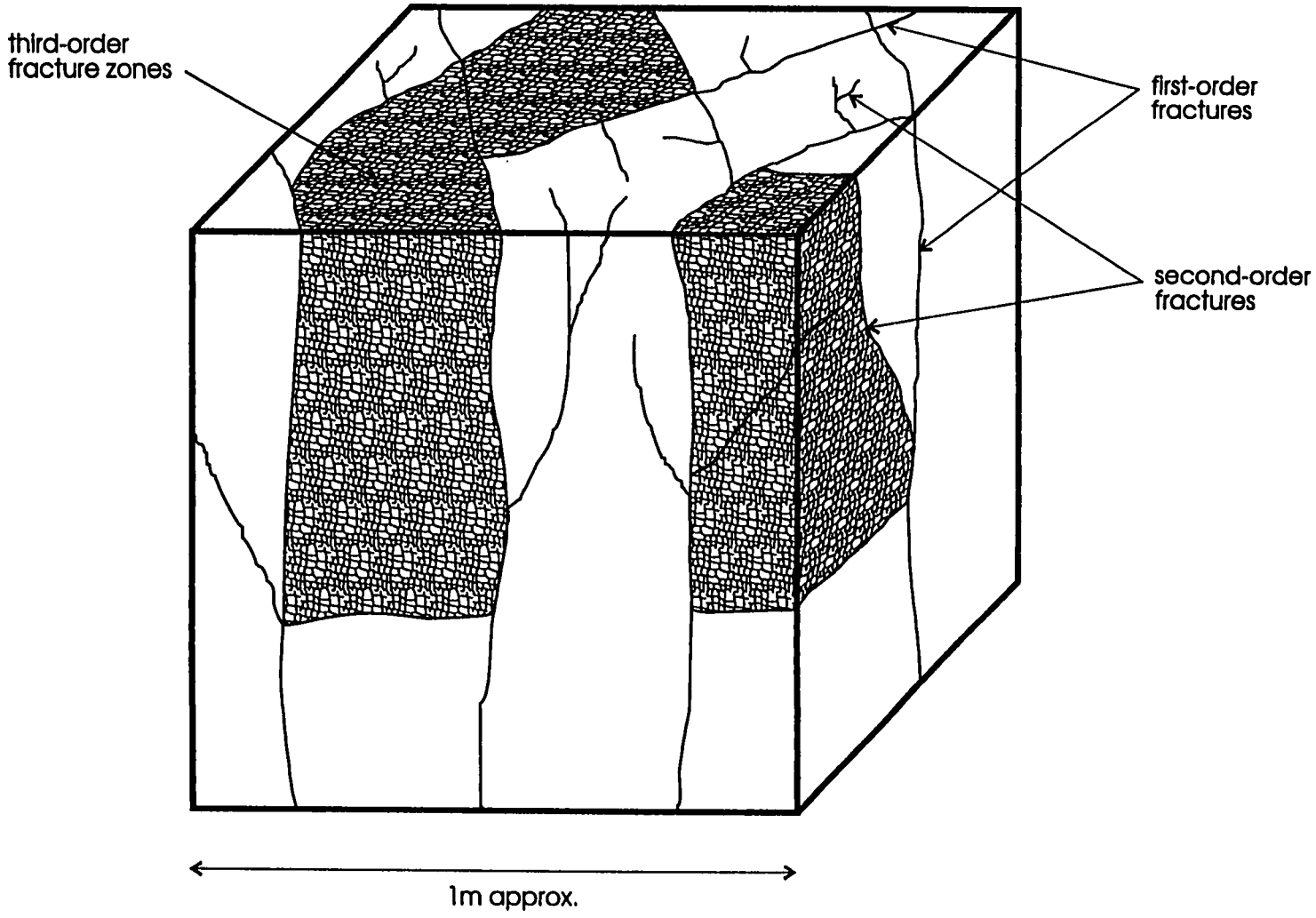

Figure 3.20 - Idealised fracture network geometry at the Laidlaw site

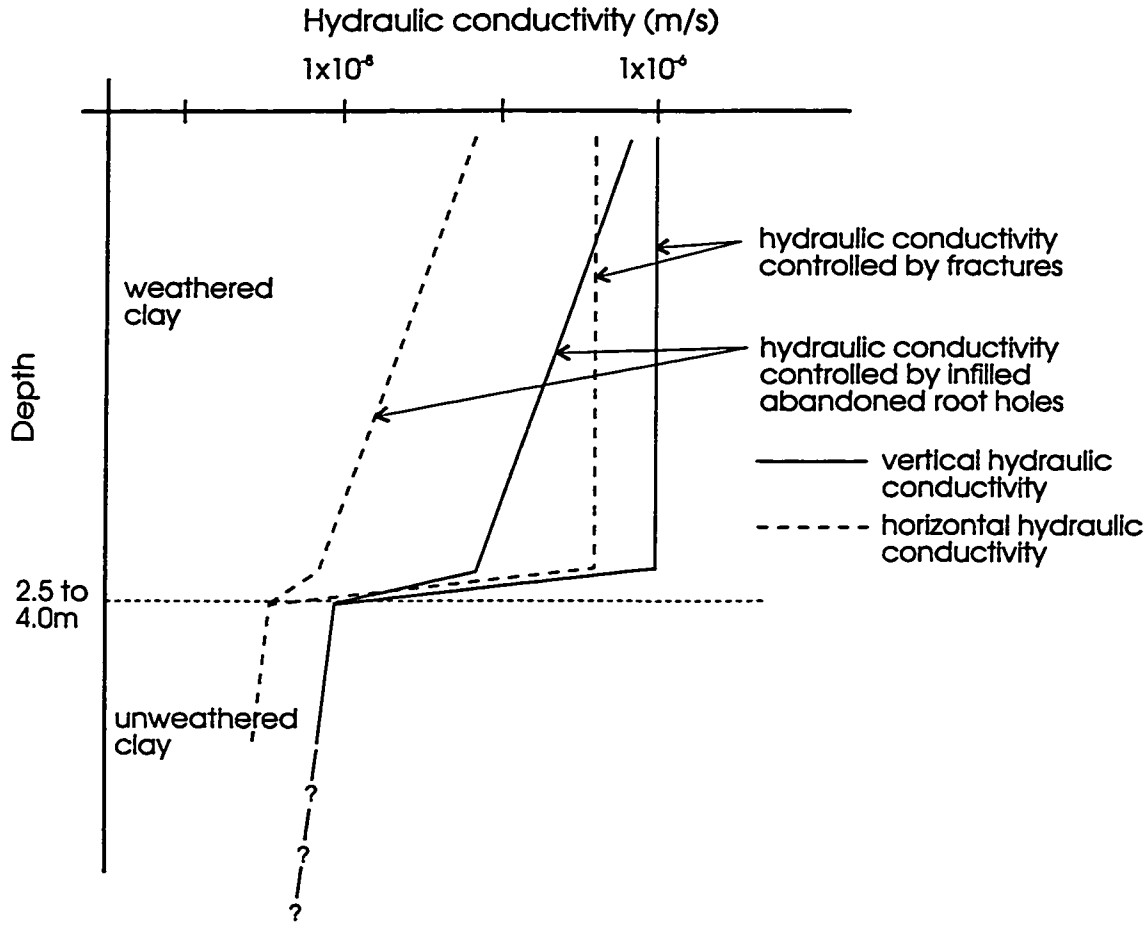

Figure 3.21 - Proposed conceptual model for bulk scale hydraulic conductivity at the Laidlaw Site

CHAPTER 4

FIELD OBSERVATIONS AND MODELLING OF THE TRANSIENT HYDRAULIC RESPONSE OF A FRACTURED CLAY

INTRODUCTION

Near-surface clays commonly contain features such as fractures and root holes, often referred to as macropores, which can affect the way in which water moves through such soils. The relative importance of these features depends on the temporal and spatial scales being considered. For example, the hydraulic conductivity of such materials generally depends on the scale at which the measurement is made, as a result of the localised high conductivity associated with these macropores (Bradbury and Muldoon, 1990; Jones et. al., 1992; McKay et. al., 1993; Chapter 2). In some instances small scale measurements will be directly influenced by the high local conductivity of macropores in the vicinity of the measurement location, whereas in other instances there will be no macropores in the immediate vicinity of the measurement location and a low hydraulic conductivity will result. In contrast, tests conducted at a sufficiently large scale encompass a representative portion of the macropore network, and thus a relatively constant value of hydraulic conductivity will be measured regardless of the particular location of the measurement device, assuming spatial homogeneity of the macropore network.

However, the presence of macropores in clayey soils causes them to display temporally dependent behaviour as well as spatially dependent behaviour. Due to the difference in conductivity between the macropores and the clay matrix, rapid changes in pressure which are applied to the system can propagate quickly through the macropores, while the pressure in the matrix remains unchanged or changes very slowly. On the other hand, if sufficiently slow pressure changes are applied to the system, very little pressure disequilibrium will develop between the macropores and the matrix.

Thus, although the spatial scale of a particular problem may be such that it encompasses a representative portion of the macropore network, it may not be possible to adequately

describe the behaviour of the system using a single-continuum model, which does not allow for transient disequilibrium and consequent fluid transfer between the low conductivity matrix and the macropores. In these instances, it will be necessary to describe the behaviour of the system using a model which allows for disequilibrium between the macropores and the matrix, and which accounts for the transfer of fluid between the two. The types of models which include descriptions of these aspects of behaviour are dual continuum models, and models which include the macropores as discrete features.

The development of dual continuum models has been described extensively in the literature, both for conditions of saturated flow (Barenblatt et. al., 1960; Warren and Root, 1963; Duguid and Lee, 1977; Huyakorn et. al., 1983), and unsaturated flow (Beven and Germann, 1981; Gerke and van Genuchten, 1993). In such models, various simplified descriptions of the transfer of fluid between the macropores and the low conductivity matrix are used, which are based on regular geometries for the matrix blocks such as slabs or spheres. The use of a dual continuum model implies the existence of a Representative Elementary Volume (REV) for the combined matrix/macropore system, and the quantities such as hydraulic head which are calculated using such models are REV averages. Beven and Germann (1981) suggest that an REV for typical macropore networks could be on the order of cubic metres to tens of cubic metres, and that therefore the dual continuum approach could be applied to problems at the scale of a hillslope or catchment.

With models which include the macropores as discrete features, it is possible to consider the conditions in the vicinity of a single macropore. However, it is also possible to consider the interaction between the macropore network and the low conductivity matrix on a larger scale. It is not possible to explicitly define the location of each macropore in a natural system, however, such models can be used with various idealised versions of natural macropore

networks which is sometimes equivalent to reducing the geometry of the matrix blocks to regular geometries such as rectangular prisms and cubes. Furthermore, irregular macropore networks can be defined, based on a statistical description of the natural network. Models with discrete macropores can therefore be used to examine behaviour at a scale which is larger than that of a single macropore, but smaller than that of an REV for the macropore network (that is, the scale referred to as "the near field" by Bear, 1993). Huyakorn et. al. (1983) described the numerical formulation for a discrete fracture transient flow model, and gave an example of its application to the problem of a single fracture in rock intercepting a pumping well. Barker and Black (1983) describe an analytical solution for a slug test carried out in an aquifer with uniform fracturing, which allows for transient exchange of fluid between the fractures and low conductivity matrix blocks. Other examples of discrete fracture transient flow models exist in the literature (for example Berkowitz et. al., 1988; and Therrien and Sudicky, 1996), but it does not appear that they have been widely used to interpret or predict transient hydraulic conditions in clays with macropore features.

The characteristics of clayey soils with macropores, such as hydraulic conductivity, are often derived from the interpretation of tests which impose transient hydraulic conditions. Single-well response tests are most commonly used, however the results of several pumping tests conducted in near surface fractured clays have also been recently reported (Jones et. al. 1992 and Harris, 1994). The spatial scale of these tests is such that they would affect a sub-REV portion of a typical macropore network, however, such tests are almost exclusively interpreted using single continuum models. While it may be possible to use single continuum models to derive parameters such as hydraulic conductivity and specific storage which adequately describe the results of particular transient hydraulic tests, it is likely that these parameters are specific to the spatial and temporal scales considered, since interactions between the macropores and the low conductivity matrix are not accounted for. If this is the

case, the parameters derived from the continuum models will not be useful for predicting the behaviour of the system under different conditions, particularly over longer time periods and at larger scales.

The objectives of this chapter are to describe and evaluate the differences in response between the fractures and clay matrix in transient hydraulic tests in a near-surface weathered and fractured clay, and to determine whether a discrete fracture model based on the parallel plate approximation for fractures can be used to interpret the results of the tests to give results which are consistent with other methods of testing, particularly long-term, constant-gradient measurements of hydraulic conductivity.

The tests were conducted using sub-horizontal, sand-filled induced fractures that were artificially emplaced in a weathered and highly fractured clay-rich sediment. The emplaced fractures were several metres in diameter, and had a high transmissivity relative to the material in which they were placed. These features made it possible to apply transient hydraulic conditions which influenced a relatively large portion of the fracture network, in relation to that which could be influenced with a single-well test. Furthermore, since the induced fractures provide a direct connection to the fracture network, it was possible to identify differences in response between the fractures and the clay matrix with a network of pressure transducers that were placed in the induced fractures and in the clay itself. The results of long-term, constant-gradient tests conducted using the same experimental configuration were described in Chapter 3, and are compared in this chapter to the results of the transient tests.

FIELD SITE

Field experiments were carried out at the Laidlaw hazardous waste treatment and disposal facility, located approximately 12 km south-east of Sarnia, Ontario (see Figure 4.1).

This site lies within an extensive clay plain, the Lambton Clay Plain, which forms the northern third of the 5900 km^2 St. Clair Clay Plain (Chapman and Putnam, 1984). Throughout the clay plain, clay-rich Quaternary age tills and glacio-lacustrine sediments extend from within 1m of the ground surface to the bedrock at depths ranging between 25m and 50m, and averaging 40m (Desaulniers, 1986).

For purposes of stratigraphic classification, these tills and glacio-lacustrine sediments have been divided into two units (Fitzgerald et al., 1979). The lower unit, known as the Black Shale Till is generally 30-35m thick and contains numerous black shale clasts. The upper unit, the St. Joseph Till, extends generally to the surface, although it is overlain locally by thin deposits of sand and gravel. It is generally 7-13m thick, and is a silty clay (25-45% <2 μm diameter) with a small fraction (<20%) of sand and gravel (McKay and Fredericia, 1995). This unit is thought to consist of glacio-lacustrine sediments which have been deformed by grounding icebergs and/or internal slumping of weakly consolidated material (Klint, 1996).

The upper 4-6m of the St. Joseph Till are visibly oxidised and fractured. Pervasive chemical weathering extends to a depth of 2-4m, and is marked by a colour change in the clay matrix from brown above to grey below (Ogunbadejo and Quigley, 1973). The clay-size minerals in the weathered zone are predominantly illite and chlorite (McKay and Fredericia, 1995). The fractures in the upper, pervasively weathered clay are often preferentially oriented in two orthogonal directions (McKay et. al., 1993; Klint, 1996), and root holes are often preferentially located on fracture faces (D'Astous et. al., 1988; Ruland et. al., 1991; Harris, 1994, McKay and Fredericia, 1995; Klint, 1996).

Below the zone of pervasive oxidation, chemical weathering is only evident in the immediate vicinity of fractures. Fracture frequency diminishes sharply below a depth of 3-4m,

and fractures are generally indiscernible below a depth of 6m (Klint, 1996). Notwithstanding, fractures have been observed in drill cores at depths in excess of 9m (Adams, 1969), and roots have been observed at depths of up to 9m (Hanna, 1966).

Harris (1994) and McKay et al. (1993a) report that the water table at the Laidlaw site varies seasonally between the ground surface and a depth of 1.5m, and it has been observed to respond quickly to individual rainfall events (Adomait, 1991; and Harris, 1994). Ruland et al. (1991), based on measurements at various sites throughout the St. Clair Clay Plain, report that the water table is usually within 2m of the surface, but that piezometers used in their study went dry at depths of up to 4.9m in particularly dry summers. They also observed tritium at depths of up to 12m, and seasonal hydraulic head fluctuations in excess of 0.5m at depths of up to 11.5m. The presence of weathered clay at depths of up to 4m indicates that the water table was likely lower than at present for a prolonged period of time at some point since the clay was deposited (Soderman and Kim, 1969).

FIELD METHODS

Experimental Design

The experimental design that was used to conduct transient hydraulic tests in the weathered zone relied on the placement of thin, relatively continuous, sub-horizontal layers of conductive material in the subsurface, over areas of several square metres. The relatively simple geometry of these features and their high transmissivity relative to the surrounding material, combined with a controlled hydraulic boundary condition which was maintained at the ground surface over the area above them, enabled the generation of near-vertical hydraulic gradients. This simplified configuration for the flow field was desired to simplify the interpretation of the transient hydraulic tests.

The thin, conductive layers were produced by hydraulically inducing fractures, and by using a sand proppant in the induced fractures to maintain them as relatively conductive pathways over the duration of the experiment. Hydraulic fracturing at the field sites was carried out by FRx Ltd in association with Dr. Larry Murdoch at the University of Cincinnati. The procedure for creating hydraulically induced fractures is described by Murdoch (1995). Briefly, the fractures are created by driving a plugged steel casing to the desired depth, then driving the plug downwards from the base of the casing to form a short uncased section of borehole at the base of the cased section. A horizontal notch is cut in the uncased section of borehole with a high pressure water jet, which acts to initiate the fracture in a horizontal plane when a sand/gel mixture is pumped in under pressure.

The controlled boundary condition at the surface was maintained by ponding water at a constant level on the ground surface above the induced fractures. The pond was constructed by sealing a continuous length of sheet metal in a narrow, circular trench with bentonite and clay. The water level in the pond was maintained at a constant level by means of a large Marriotte system which comprised two 450 litre tanks (see Figure 3.3). The tanks were continuously weighed using an electronic scale which was constructed using a temperature compensated stainless steel "S" type load cell to support approximately half the weight of the tanks. The load cell output was calibrated to give cumulative outflow from the tanks by successively adding known volumes of water to the tanks and noting the changes in load cell output. Other benefits of the pond, apart from the application of a constant boundary condition, are that it supplied a source of water for the vertical gradient tests, thereby avoiding difficulties in interpretation associated with desaturation of the fractured clay, and that it acted to damp the effects of transient fluctuations in the water table.

The experimental set-up, including the induced fractures and the artificial pond, is illustrated in Figure 4.2. Three induced fractures were created at the site, at depths of 1.8m, 2.2m and 2.6m below ground surface. These depths refer to the depth below surface of the point where the fracture is initiated and the gel/proppant mixture injected. Coring and mapping in an excavation indicated that the induced fractures rose gently towards the surface from the point of injection to their extremities at distances of approximately 4m from the injection point. A pond of 4.0m diameter was constructed, centred above the approximate centre of the induced fractures, and somewhat smaller in diameter than the induced fractures. The topsoil was removed down to a depth of 0.4m prior to construction of the pond.

Water pressure in the area beneath the pond was measured using a network of 15 electronic strain gauge pressure transducers (Adara Systems 10 PSIG transducers), which were connected to a datalogger (Campbell Scientific CR-10 datalogger). The locations of the pressure transducers is illustrated in Figure 4.2. The locations of the pressure transducers were chosen with an emphasis on obtaining pressure distributions in the middle induced fracture, and at the mid-point of the vertical interval between this fracture and the upper induced fracture. The pressure transducers were installed in vertical holes which were cored using a direct push continuous coring method described by Einarson (1995). It is believed that this coring technique causes minimal smearing or disturbance to the clay immediately surrounding the boreholes. Some of the transducers were located within short (approximately 10cm) sand packs at the base of boreholes which terminated at a depth midway between induced fractures, and other transducers were located within a short sand pack located at the depth where the borehole intersected an induced fracture (see Figure 4.3). The induced fractures were readily identified in the cores since they were filled with sand, and it was thus a relatively simple procedure to locate the instruments and sand packs as illustrated.

The pressure transducers were not vented to the atmosphere, and thus to remove pressure transients resulting from atmospheric pressure transients rather than imposed hydraulic conditions, it was necessary to measure atmospheric pressure at the surface and subtract this value from the values measured in the subsurface. Atmospheric pressure was measured using a thermally isolated transducer of the same design as the transducers used to measure water pressure.

The open boreholes in which the transducers and piezometers were installed were sealed with a thick bentonite slurry above the sand pack (see Figure 4.3) to eliminate direct vertical hydraulic connection in the boreholes and well-bore storage effects. Since the bentonite remained saturated beneath the pond, it is unlikely that it would have undergone shrinkage and thus created an open annulus around the perimeter of the boreholes. Inflatable packers were used to seal the open casings which were originally used for fracture injection, in order to minimise the effects of well-bore storage on the transient response (Novakowski, 1989). In some instances, a transducer was suspended below the packer to provide an additional measurement of the transient response in the induced fractures. This arrangement is illustrated in Figure 4.4.

Types of Hydraulic Tests Conducted with Pond and Induced Fracture Installations

Two types of hydraulic testing were conducted with the pond and induced fracture installation illustrated in Figure 4.2: slug tests and constant head tests. Slug tests were conducted in the casings originally used for fracture injection, using the procedure illustrated in Figure 4.5. A pressure transducer of the same design as those installed in the sediment itself was suspended below an inflatable packer and lowered into the casing to below the static water level. The packer was then inflated, and water added to the casing above the packer.

The test was commenced by deflating the packer. Deflation of the packer occurred very rapidly, and thus an effectively instantaneous increase in hydraulic head was applied. In addition to the response in the casing to which the perturbation was applied, the transient responses at other locations in the affected induced fracture were monitored using pressure transducers. Since these transducers were not installed in open wells, the transient response of the system at these points was not affected by observation well storage (Novakowski, 1989). The casings intersecting fractures other than the one being tested were sealed with inflatable packers.

Constant head pumping tests were carried out with the artificial pond and induced fracture installation shown in Figure 4.2, by pumping at a constant head from the casings originally used for fracture injection. A constant head in the selected casing was maintained using a peristaltic pump, which continued to draw a mixture of air and water after the water level in the casing had been drawn down to the level of the intake tubing (see Figure 4.6). The pressure transients caused by pumping were monitored in the network of pressure transducers, and the pumping was continued until the output from the transducers indicated that steady state had been reached. Throughout the duration of the pumping tests, the fluctuations in the background water level away from the pond were monitored in the open casings of other induced fractures, and in a 0.08 m diameter open well screened from 2 m to 5 m below the ground surface.

At the conclusion of hydraulic testing, fractures in the area beneath the pond were mapped on six vertical profiles, and on one horizontal surface. Fracture orientations, trace lengths and spacing were measured on the vertical profiles. Fracture intensity, defined as the total trace length of vertical fractures intersecting a unit area of a horizontal plane, was

measured on the horizontal exposure. The results of this exercise are discussed fully in Chapter 2.

BEHAVIOUR OF SYSTEM DURING SLUG TESTS IN INDUCED FRACTURES - MODELLING INVESTIGATIONS

The response of the system during slug tests conducted in induced fractures will be controlled largely by the interchange of water between the induced fracture and the surrounding formation. As the water level drops in the casing, water flows outwards into the induced fracture and from there into the surrounding material. Since the induced fracture is of limited size and its storage capacity is thus relatively low, the total fluid flux outwards from the induced fracture, integrated over its surface area, will at all times be almost equal to the flux into the induced fracture from the casing. In principle, the response in the casing should depend on both the transmissivity of the induced fracture (which represents its ability to transmit water outwards from the casing), and on the hydraulic conductivity and storage properties of the surrounding material (which represents its ability to remove water from the induced fracture). At points in the induced fracture which are at some distance from the casing, the response will also depend on these properties. A faster and less damped response should be observed away from the injection point for induced fractures with higher transmissivity, and a slower and more damped response should be observed if the surrounding material is more conductive or has a higher specific storage.

Modelling investigations were conducted to test the sensitivity of the response in the casing and at a point in the induced fracture, to factors such as the transmissivity of the induced fracture and the conductivity and storage of the surrounding material. The model geometry considered in these simulations is illustrated in Figure 4.7. The model domain is 4m by 4m in plan, and 5m in height. An induced fracture, idealised as a 2.5m radius circular

feature, was placed at the mid-height of the model domain. Two-dimensional discrete fracture elements were used to represent the induced fracture in the model. Symmetry conditions were utilised to reduce the size of the model, and accordingly two of the vertical model boundaries were specified as no-flow boundaries (see Figure 4.7). The other two vertical boundaries and the upper model boundary were specified as constant head boundaries with zero head, to simulate the static background condition (see Figure 4.7). The lower model boundary was specified as a no-flow boundary. The initial condition for the model was specified as zero head at all nodes, except for the node at the centre of the induced fracture which was assigned a unit head as an initial condition, to represent the instantaneous head change applied at this point in the slug tests.

The use of a circular feature to represent the induced fracture and symmetry conditions to reduced the size of the model implies that real induced fractures, which are generally geometrically non-symmetric and have varying thickness (Murdoch, 1995), can be idealised as circular features which have radially symmetric transmissivity in their plane. The potential effects of a decrease in transmissivity with distance from the initiation point were, however, investigated in the modelling.

The material surrounding the induced fracture was modelled as a discretely fractured porous medium rather than as an equivalent porous medium, in order to explicitly allow for the transient exchange of water between the fractures and the clay matrix that could take place over the relatively short period of the slug tests. The fracture network was idealised as two orthogonal sets of vertical fractures, for which various values of spacing and aperture were considered.

Simulations were performed using the numerical model FRAC3DVS (Therrien et. al., 1995), which can simulate three dimensional transient groundwater flow in discretely fractured

porous media using the finite element technique. The numerical formulation of the model and its capabilities are described in Therrien and Sudicky (1996). Briefly, the model simultaneously solves the transient groundwater flow equations for the fractures and the porous matrix blocks. Continuity of hydraulic head is assumed at the interface between the fracture and the matrix. Darcy's Law is assumed to hold for the fractures and for the matrix. Fracture "conductivities" are calculated from specified fracture apertures using the cubic law (Snow, 1969), and a value of specific storage for the fracture elements can be independently assigned. Fracture aperture and specific storage for a particular fracture are assumed to be constant throughout its plane. Fracture "conductivity" is assumed not to be dependent on hydraulic head.

Since the casings in which the slug tests were performed were entirely unscreened and water flowed out the base of the casing and then directly into the induced fracture, they essentially represented a point source which was neither a constant head nor a constant flow rate source. Therefore, to represent the influence of the casing in the model, an adaptation of the one-dimensional well elements described by Sudicky et. al. (1995) for zero screen length was used. The details of the adaptation of FRAC3DVS for zero screen length are described in Appendix A. Since the screen length is zero, the only contribution to the matrix equations resulting from the finite element discretisation is a lumped storage contribution for the node which is located at the base of the casing. The effect of the zero-length well element is such that, for a given change in head at this node in the model (which corresponds to the same decrease in water level in the casing), the correct volume of water enters the domain (that is, the cross-sectional area of the casing multiplied by the change in water level).

Simulations were performed with various values of transmissivity for the induced fracture; aperture and spacing of the natural vertical fractures; and hydraulic conductivity and specific storage of the clay matrix blocks. The sensitivity to changes in these parameters was

considered in terms of the response at two locations, labelled A and B in Figure 4.7. Point A is located at the centre of the induced fracture, at the point where it is intersected by the casing, and point B is located on the induced fracture at a distance from point A equal to half the induced fracture radius.

Values of aperture in the range of 35 μm to 60μm and values of spacing in the range of 0.125m to 0.5m were considered in the modelling. The specific storage of the fractures was specified as the compressibility of water. For the idealised fracture network geometry illustrated in Figure 4.7, bulk vertical hydraulic conductivity can be calculated using the equation given in Figure 4.7, for various combinations of aperture and spacing. The combinations of aperture and spacing that were considered in the modelling correspond to values of bulk vertical hydraulic conductivity in the range of 5.5×10^{-7}m/s to 2.8×10^{-6} m/s, which is similar to the range of values calculated in Chapter 3 from constant head pumping tests. Values of matrix specific storage in the range 0.25×10^{-3} m^{-1} to 2.5×10^{-3} m^{-1} were considered in the modelling, which is similar to the range of values for weathered clay from the Laidlaw site which has been measured using oedometers by McKay et. al. (1993), Harris (1994) and Padusenko (1997). Values of matrix hydraulic conductivity in the range 1×10^{-10} m/s to 5×10^{-10} m/s were considered in the modelling. Burke (1997) examined the results of 55 previously published laboratory scale measurements of hydraulic conductivity for samples of intact clay from the St. Clair clay plain, and found that these values represented the 95% confidence interval for hydraulic conductivity.

The majority of the analyses were conducted with constant values of transmissivity for all the discrete fracture elements representing the induced fracture. For these analyses, values in the range 8.8×10^{-6} m^2/s to 101.6×10^{-6} m^2/s were considered. In the following section, values towards the lower end of this range were found to provide good matches to observed field

behaviour. One analysis was conducted in which a transmissivity of $10x10^{-6}$ m^2/s was specified for the fracture elements within a radius of 1m of the centre of the induced fracture, reducing to $5x10^{-6}$ m^2/s for elements between 1m and 2m from the centre of the induced fracture, and finally to $1x10^{-6}$ m^2/s for elements between 2m and 2.5m from the centre of the induced fracture.

The modelling results indicate that, for the range of parameters considered, the calculated responses at points A and B were essentially the same for different combinations of fracture hydraulic aperture and spacing that gave a particular value of bulk vertical hydraulic conductivity for the surrounding material. The calculated responses at these points are illustrated in Figure 4.8 for the cases of orthogonal, equally spaced sets of fractures with spacings of 0.125m, 0.25m and 0.5m; and for the case of orthogonal sets of fractures with a spacing of 0.125m in one direction and 0.5m in the other direction. For all these cases, uniform fracture apertures were chosen to give an overall bulk vertical hydraulic conductivity of $8.3x10^{-7}$ m/s, and all other parameters were kept constant. It can be seen that the response is essentially the same in all cases, and it would be expected that a similar finding would apply to other, more geometrically complex fracture networks that have the same bulk vertical hydraulic conductivity. The relatively minor difference in response for systems with different fracture geometries but the same bulk hydraulic conductivity indicates that in general, the use of simple fracture geometries in models which predict transient hydraulic behaviour should not impose unrealistic constraints on the model behaviour.

The sensitivity of the results to bulk vertical hydraulic conductivity, matrix specific storage, and transmissivity of the induced fracture, are illustrated in Figure 4.9. It can be noted that the response at point A is influenced very little by the bulk hydraulic conductivity or specific storage of the surrounding material, whereas it is very sensitive to changes in the

transmissivity of the induced fracture (the results shown in Figure 4.9 are for constant transmissivity). In contrast, the response at point B is affected by changes in the bulk hydraulic conductivity and specific storage of the surrounding material, as well as changes in the transmissivity of the induced fracture. Changes in bulk hydraulic conductivity primarily affect the magnitude of the response at point B, whereas changes in specific storage affect the magnitude and the timing of the response at point B.

Although the results are not presented in Figure 4.9, it was observed that the results were unaltered by variations in the value of matrix hydraulic conductivity within the relatively narrow range of values considered ($1x10^{-10}$ m/s to $5x10^{-10}$ m/s). It might be generally expected that the response of the system would be controlled by both matrix hydraulic conductivity and matrix specific storage. Barker and Black (1983) investigated the influence of matrix hydraulic conductivity on slug test response in fracture aquifers, and found that for the two extremes of an impermeable matrix and an infinitely permeable matrix, the maximum difference in response in the well was approximately 40%. Over wide ranges of matrix hydraulic conductivity (greater than three orders of magnitude), the response in the well was indistinguishable.

The influence of a decrease in transmissivity of the induced fracture with distance from the injection point is illustrated in Figure 4.10 (the distribution of transmissivity is also illustrated in Figure 4.10). In this figure, the response of the system with decreasing transmissivity is compared to the closely matching response of a system with constant transmissivity. It can be seen that if a constant transmissivity model is used to represent an induced fracture in which transmissivity actually decreases with distance from the injection point, the calculated transmissivity will be approximately equal to the value in the vicinity of the casing, and the calculated bulk hydraulic conductivity will be an underestimate of the true value. The calculated matrix specific storage should, however, reflect the true value.

In summary, the response of the system, in terms of the transient head changes in the casing and at an observation point in the induced fracture, is sensitive to the values of transmissivity of the induced fracture, the bulk vertical hydraulic conductivity of the surrounding material, and the specific storage of the clay matrix blocks. Furthermore, the effects caused by changes in each of the three parameters are reasonably unique. For example, the response in the casing is basically determined only by the value of transmissivity for the induced fracture in its vicinity. Once this value has been determined by matching the model response to the field measured response, values of matrix specific storage and bulk vertical hydraulic conductivity can be determined.

INTERPRETATION OF SLUG TESTS IN INDUCED FRACTURES - FIELD RESULTS

Slug tests were performed in the upper and middle induced fractures of the field installation. For the test performed in the upper induced fracture, the response was measured with a transducer in the casing to which the perturbation was applied (IC1-1 in Figure 4.2), and with Transducer C which was placed 1.3m from the casing in the upper induced fracture. For the test performed in the middle induced fracture, the response was measured with a transducer in the casing to which the perturbation was applied (IC1-2 in Figure 4.2), and with Transducers J and K placed in the middle induced fracture, 0.8m and 0.5m from the casing respectively.

Each of these tests was simulated using a model similar to that illustrated in Figure 4.7, in order to determine the values of induced-fracture transmissivity (T_f), matrix specific storage (S_m), and bulk hydraulic conductivity (K_{bulkv}) which gave the closest match between the computed responses and observed responses at the various monitoring locations. A matrix

hydraulic conductivity (K_m) of 2.5×10^{-10} m/s was used in the simulations. Potential decreases in T_f with distance from the injection point were not considered in the modelling.

Attempts to simulate the tests using a model which represented the clay as an equivalent porous medium rather than as a discretely fractured medium were unable to adequately match the features of the observed responses. Furthermore, the closest matches that could be obtained with an equivalent porous medium model required the use of a value for specific storage on the order of 1×10^{-1} m^{-1}, in combination with a bulk hydraulic conductivity on the order of 1×10^{-6}m/s. This value of bulk hydraulic conductivity is similar to the value measured from steady state conditions during pumping tests (see Chapter 3), but the value of specific storage is approximately 25 times larger than the upper end of the range of values which has been measured for clay from the Laidlaw site. Values of specific storage for weathered clay from the Laidlaw site have been measured using oedometers by McKay et. al. (1993), Harris (1994) and Padusenko (1997), and values in the range 3.6×10^{-4} to 3.9×10^{-3} m^{-1} are reported. Equivalent porous medium models require a much larger than reasonable value of specific storage to approximate the response of the system at locations other than the injection point, since the large surface area for fluid exchange between fractures and clay which exists in the real system is not explicitly represented in such models. The ability of equivalent porous medium models to yield reasonable values of hydraulic conductivity, but erroneous values of specific storage for a fractured porous medium, was also observed by Barker and Black (1983). Using an analytical solution for slug tests in fractured aquifers, Barker and Black (1983) determined that aquifer transmissivity could be estimated to within a factor of 3 using an equivalent porous medium model, but that the value of specific storage derived from such models could be in error by a factor ranging from 10^{-6} to 10^{5}.

For the test conducted in the middle induced fracture, it was found that with constant values for T_f, S_m, and K_{bulkv} throughout the model domain, it was not possible to simultaneously match the responses measured with Transducers J and K at two different distances from the casing. In reality, these parameters will vary spatially, and it is for this reason that a model with constant material properties throughout fails to represent the response at a number of spatially distributed locations. However, rather than attempt to arbitrarily assign distributions of these parameters throughout the model domain, the approach that was taken was to independently match the response at each of these locations using models which had different but constant values of T_f, S_m, and K_{bulkv} throughout. This provides a picture of the possible ranges of these parameters within the area tested, but since the response was monitored at only two locations there is far too little information available to attempt to assign spatial distributions for them. It is envisaged that the values determined for these parameters will in each case represent an average of their values for the material between the casing and the monitoring location.

The simulation results and observed field responses are compared in Figure 4.11 for both slug tests. Close matches between the observed responses and the computed responses were obtained for both tests. The values of the parameters T_f, S_m, and K_{bulkv} from which the simulation results were derived are shown in Figure 4.11.

A value for specific storage of 0.25×10^{-3} m^{-1} was required to match the response at Transducer C for the test in the upper induced fracture. For the test conducted in the middle induced fracture, a specific storage value of 0.75×10^{-3} m^{-1} was required to match the response at Transducer K, whereas a value of 2.5×10^{-3} m^{-1} was required to match the response at Transducer J. This range of values is similar to the range of values obtained from laboratory consolidation tests on the Laidlaw clay (McKay et. al., 1993; Harris, 1994; and Padusenko,

1997). Pockets of material with a much higher percentage of sand were observed in the area beneath the pond (see Chapter 2), and the calculated variability in specific storage is possibly a reflection of this type of variability in the natural material.

For the test conducted in the upper induced fracture, a bulk vertical hydraulic conductivity of 1.2×10^{-6} m/s was required to match the response at Transducer C. For the test conducted in the middle induced fracture, a bulk vertical hydraulic conductivity of 1.2×10^{-6} m/s was required to match the response at Transducer K, whereas a value of 5.0×10^{-6} m/s was required to match the response at Transducer J. Since possible decreases in T_f with distance from the injection point were not considered, the calculated values of hydraulic conductivity may be underestimates of the actual values. However, for the depth interval in which these tests were carried out, the values of bulk vertical hydraulic conductivity determined from steady-state conditions during pumping tests were in the range of 9.0×10^{-7} m/s to 2.5×10^{-6} m/s (Chapter 3), which is similar to the range of values determined from the slug tests.

A value of 9.8×10^{-6} m^2/s was obtained for the fracture transmissivity of the upper induced fracture. A range of 8.3×10^{-6} m^2/s to 11.2×10^{-6} m^2/s was obtained for the middle induced fracture. This indicates that fracture transmissivity does not vary greatly for fractures induced at different depths, and that transmissivity varies relatively little throughout the plane of the middle induced fracture (although it should be remembered that in this case, measurements were made on only two areas of the induced fracture which were relatively close to the fracture injection point).

BEHAVIOUR OF SYSTEM DURING CONSTANT HEAD PUMPING TESTS - MODELLING INVESTIGATIONS

During the constant head pumping tests, hydraulic head in the induced fractures and in the natural vertical fractures will approach an almost constant distribution soon after commencement of the tests due to the low storage in these elements, and will then continue to change slowly as water is released to these features from storage in the clay itself. Hydraulic head in the blocks of clay will change more slowly, depending on the relative proximity of fractures. This conceptual model of the system behaviour during pumping tests is illustrated in Figure 4.12.

The temporal variations in hydraulic head distribution beneath the pond during constant head pumping tests were investigated using the numerical model FRAC3DVS (Therrien et. al., 1995). The model geometry employed for this simulation was similar to that used to model the slug tests (see Figure 4.7), with some changes to the boundary conditions. The upper boundary was specified as a no-flow boundary except for the nodes in the area of the pond, which were specified as constant head nodes with a head of zero (which is the same as on the constant head vertical boundaries and the same as the initial condition). The pond was positioned directly above the induced fractures, but was somewhat smaller in size. Three induced fractures at depths of 1.4 m, 1.8 m and 2.2 m were represented in the model with two-dimensional discrete fracture elements, for which a constant transmissivity of 10×10^{-6} m^2/s was assigned. These depths correspond to the depths below the pond of the induced fractures in the field installation. To represent the constant head pumping, a constant head node was specified at the centre of the deepest induced fracture (equivalent to point A on Figure 4.7) for which a head of -0.5 m was specified. A uniform fracture spacing of 0.125 m and hydraulic aperture of 45 μm were used throughout the model domain, which is equivalent to a bulk vertical hydraulic conductivity of 1.2×10^{-6} m/s, similar to that determined through the slug tests

and similar to that determined from steady state conditions during the pumping tests (see Chapter 3). In the simulation, values of 2.5×10^{-10} m/s and 0.25×10^{-3} m^{-1} were used for matrix hydraulic conductivity and matrix specific storage respectively.

The simulation results are illustrated in Figure 4.13, in terms of profiles of head change in the induced fractures, and in terms of the temporal variation in head at five points labelled A, B, C, D and E in Figure 4.13a. Points A-D are located on vertical fractures, and point E is located in the centre of a matrix block adjacent to point C. Points A and B are located midway between the deepest and the middle induced fractures, and points C, D and E are located midway between the middle and the upper induced fractures.

The profile of head change in the deepest induced fracture (Figure 4.13b) indicates that a considerable gradient exists at all times in the plane of the deepest induced fracture, towards the pumping location. In contrast, the change in head throughout the plane of the middle induced fracture (Figure 4.13b) is almost uniform at all times. As a result, the responses at points A and B are quite different, whereas there is practically no difference between the responses at points C and D (Figure 4.13c). It can be concluded that the flow in the vicinity of the pumping location is three-dimensional in nature, but that the middle induced fracture acts to very effectively distribute pressure so that above this plane, flow in the fracture network is essentially one-dimensional (at least in the area beneath the pond). The difference in response between point C and point E indicates that, on the time scale being considered, the pressure in the fractures and in the matrix blocks is not in equilibrium, and thus water is being exchanged between these two portions of the system. At the steady-state condition, there is no difference in head between points C and E.

The results of the simulations described above are for the case of a uniform fracture aperture throughout the model domain. In real systems, fracture apertures will vary, and to

investigate the effects of variable fracture apertures throughout the domain, a simulation was conducted in which 25% of the fractures were assigned an aperture of 75 μm, and the remainder of the fractures were assigned an aperture of 45 μm. The bulk vertical hydraulic conductivity of this arrangement is 2.4×10^{-6} m/s. It was found that the response of this variable aperture model, in terms of the head variation in the middle and upper induced fractures, was equivalent to the response calculated with a constant aperture model for which the vertical bulk hydraulic conductivity was the same (that is, for a model with constant fracture aperture of 57 μm).

FIELD RESULTS FROM CONSTANT HEAD PUMPING TEST

Results from the constant head pumping test in the deepest induced fracture at the field site are illustrated in Figure 4.14. At the commencement of this test, the water level in the casing connected to the deepest induced fracture was reduced by 0.5m over a period of 110 seconds, and was then maintained at this level over the duration of the test. In Figure 4.14, the changes in head as a result of pumping are illustrated at four locations in the middle induced fracture (Transducers I-K and a transducer sealed in the casing IC1-2); at one location in the upper induced fracture (Transducer C); and at five locations midway between the middle and upper induced fractures (Transducers D-H) (see Figure 4.2).

It can be seen that essentially the same response was measured at the four monitoring locations in the middle induced fracture (Figure 4.14a). The slightly different response at Transducer I is most likely due to its location towards the edge of the induced fracture. This uniform response is consistent with the results of the modelling previously discussed, and it appears that the middle induced fracture acts to effectively distribute pressure so that a spatially uniform pressure variation is applied to the base of the column of clay which lies above the middle induced fracture.

A faster response was observed in the upper induced fracture (Transducer C) than in any of the transducers placed midway between the middle and upper induced fractures (Transducers D-H)(see Figure 4.14b), although the upper induced fracture is further from the point at which the perturbation was applied. Since the induced fractures should be well connected to the natural fracture network, it would be expected that, in general, a faster response would be observed in the induced fractures than at other locations where the transducers may be isolated in the clay matrix at some distance from natural fractures. Since the head variation in the middle induced fracture is spatially uniform, the variation in response for Transducers D-H is not due to their position relative to the pumping location. The variation in response could be partly a result of the transducers being located in the clay matrix at varying distance from natural fractures, and partly a result of different properties (hydraulic conductivity and specific storage) for the clay matrix at different locations. After four hours of pumping, pressure disequilibrium between the fractures and matrix at Transducer H is still evident.

INTERPRETATION OF CONSTANT HEAD PUMPING TEST

The observed variability in response between Transducers D-H and the rapid response in Transducer C relative to the other locations could not be reproduced using an equivalent porous medium model, since such models can not simultaneously represent the rapid propagation of pressure through the fractures and the relatively much slower propagation of pressure into the clay matrix. The pumping test was therefore modelled using a discrete fracture model with two orthogonal sets of equally spaced, constant aperture vertical fractures to represent the natural fracture network. Since the head variation in the middle induced fracture is spatially uniform and flow above this level is expected to be essentially one-dimensional, the response of the system above the middle induced fracture can be considered in terms of the variations in head in an isolated block such as that illustrated in

Figure 4.15. The lower boundary of the block is defined as the middle induced fracture, and the applied boundary condition at this boundary is the measured variation in head in the middle induced fracture. The vertical faces of this block are defined by the symmetry boundaries which are located midway between adjacent fractures in each direction, and are thus defined as no-flow boundaries. Simulations with this model geometry were again carried out with the numerical model FRAC3DVS (Therrien et. al., 1995).

Response in Upper Induced Fracture

Simulation results indicated that the response in the upper induced fracture is sensitive to the values of fracture aperture for the vertical fractures (2b) and specific storage for the clay matrix (S_m), but is not sensitive to the spacing of the vertical fractures (2B) or the hydraulic conductivity of the clay matrix (K_m). It has been concluded from laboratory tests and from the results of the slug tests that the specific storage of the clay varies between 0.25×10^{-3} m^{-1} and 2.5×10^{-3} m^{-1}. Consequently, the two extremes of this range were used in the modelling, and for each case, values of fracture aperture were determined to give the best correspondence between the calculated response at point A in the model (see Figure 4.15) and the measured response at Transducer C. A fracture spacing of 0.24m and a matrix hydraulic conductivity of 2.5×10^{-10} m/s were used in the simulations.

The fracture spacing was chosen from a consideration of the results of fracture mapping, which were discussed in Chapter 2. In Chapter 2, a fracture intensity of 8.2 m/m^2 was measured for the fractures beneath the pond. Fracture intensity, I, is defined as the total fracture trace length of vertical fractures per unit area on a horizontal plane. This parameter will control bulk vertical hydraulic conductivity, and since it is closely related to the ratio of fracture surface area to matrix volume, it will exercise an important control on transient fluid exchange between the fractures and the matrix. For the surrogate network of equally spaced orthogonal fractures to have the same value of fracture intensity, a spacing given by:

$$2B = 2/I$$

is required. Thus, a fracture intensity of 8.2 m/m^2 corresponds to a value of 0.24 m for the fracture spacing in the surrogate fracture network chosen.

Calculated responses at point A are illustrated in Figure 4.16 for the two extremes of specific storage and various values of fracture aperture. The measured response at Transducer C is also illustrated. In this figure, the response in the upper induced fracture is plotted as a ratio of the applied lower boundary condition (that is, the response in the middle induced fracture). For a specific storage of 0.25×10^{-3} m^{-1}, the closest match between the calculated response and the measured response is obtained for a fracture aperture of 35 μm (Figure 4.16a), whereas for a specific storage of 2.5×10^{-3} m^{-1}, the closest match is obtained for a fracture aperture of 60 μm (Figure 4.16b).

The response in the upper induced fracture at Transducer C will in fact be influenced by many fractures of different aperture, and thus from the results of the variable aperture modelling investigations described in the last section, these results can be interpreted to indicate that the bulk hydraulic conductivity of the variable aperture fracture network is the same as that of a fracture network with a constant aperture in the range of 35 μm to 60 μm. For the fracture network used in the simulations, bulk vertical hydraulic conductivity is given by:

$$K_{bulk} = 2 \cdot \rho g \cdot (2b)^3 / (12 \cdot 2B \cdot \mu),$$

where, ρ is the density of water, g is gravitational acceleration, 2b is fracture aperture, 2B is the fracture spacing, and μ is the viscosity of water (this equation is an adaptation of the cubic law from Snow, 1969). For a fracture spacing of 0.24m, fracture apertures of 35 μm and 60 μm correspond to bulk vertical hydraulic conductivities of 2.9×10^{-7} m/s and 1.4×10^{-6} m/s respectively. Since the range of values for bulk hydraulic conductivity that was measured from the slug tests and steady state conditions during pumping tests is 9.0×10^{-7} m/s to 5.0×10^{-6} m/s, it would appear that the hydraulic fracture aperture is best represented by a constant value towards the upper end of the 35-60 μm range. The depth interval to which this applies is 1.8 m to 2.2 m below ground surface.

McKay et. al. (1993) calculated fracture apertures for the Laidlaw site from the results of small scale hydraulic conductivity measurements, and concluded that fracture apertures were log normally distributed with a geometric mean of 10 μm. The highest value of fracture aperture reported by McKay et. al. (1993) was 43 μm. It would appear that either the area in which the current experiments were conducted has larger aperture fractures than the area in which McKay et. al. conducted their experiments, or that the small scale measurements are somehow biased towards lower values.

Response at Locations in the Clay Matrix

For locations in the clay matrix, simulation results indicated that the response is sensitive to the values of specific storage and hydraulic conductivity for the clay matrix, and to the spacing of the vertical fractures. It was, however, found to be insensitive to fracture aperture for the vertical fractures.

The exact location of Transducers D-H in relation to fractures is not known, and the values of matrix hydraulic conductivity and specific storage in the vicinity of these point is also not known. Therefore, the approach that was taken was to assess whether the range of responses observed in Transducers D-H could result from the possible variability in matrix diffusivity, and possible variations in the position of transducers relative to fractures.

From laboratory tests and from the results of the slug tests, a range of 0.25×10^{-3} m^{-1} to 2.5×10^{-3} m^{-1} has been established for specific storage of the clay. Burke (1997) examined the results of 55 previously published laboratory scale measurements of hydraulic conductivity for samples of intact clay from the St. Clair clay plain, and found that the 95% confidence interval for hydraulic conductivity was 1×10^{-10} m/s to 5×10^{-10} m/s. Using these ranges of hydraulic conductivity and specific storage, the response of the system was simulated for the two extreme conditions of a combination of high matrix hydraulic conductivity and low specific storage (high matrix diffusivity), and a combination of low matrix hydraulic conductivity and high specific storage (low matrix diffusivity). A constant fracture spacing of 0.24m and a fracture aperture of 60 μm were used in these simulations.

The response in the matrix was considered at four locations, labelled B-E in Figure 4.14. These points are located at an elevation midway between the middle and upper induced fractures. Point E is located in the matrix at the furthest possible distance from the fractures, and Points B-D are equally spaced between the fracture intersection and point E. The

calculated responses at these locations are illustrated in Figure 4.17, in which they are compared to the measured responses at Transducers D-H. It can be seen that the range of measured responses is encompassed by the range of calculated responses, and thus the range of measured values is not unexpected given the variability in clay matrix properties and the possible variation in transducer placement relative to natural fractures. The range of observed responses does not indicate that hydraulic response is controlled by a widely spaced sub-set of the fractures that were observed in the field mapping.

CONCLUSIONS

Transient conditions during short term hydraulic tests in fractured clays can be understood using models which account for the presence of the fractures, and the interaction between the fractures and the clay matrix. Such models can reproduce certain aspects of behaviour, such as the rapid transmission of pressure through fractures and the concurrent slow changes in pressure in the clay matrix, which can not be described using equivalent porous medium models.

The use of induced fractures to conduct pumping tests have made it possible to observe differences in behaviour between the fracture network and the clay matrix during transient hydraulic tests. The results of pumping tests conducted with induced fractures at the Laidlaw site indicates that disequilibrium between fractures and the clay matrix can persist for several hours. Thus, interpretation of scenarios in which hydraulic conditions vary on the time scale of hours or less will require models which account for the interaction between the fractures and the clay.

In this study, a numerical model has been used which allows fractures to be represented as discrete features, and which thus explicitly accounts for interactions between the clay matrix

and the fractures. However, the results of field experiments have been interpreted using a regular geometry for the fracture network, rather than attempting to represent the actual fracture network in the field with the discrete fracture model. This approach has been used to successfully interpret results of slug tests in induced fractures, and a constant head pumping test conducted in an induced fracture. The results of the slug tests indicate that the specific storage of the clay matrix at the Laidlaw site varies locally between 0.25×10^{-3} m^{-1} and 2.5×10^{-3} m^{-1}, and the bulk vertical hydraulic conductivity of the fractured clay is between 1.2×10^{-6} m/s and 5.0×10^{-6} m/s. This range of specific storage is consistent with laboratory-scale measurements, and the range of bulk hydraulic conductivity is consistent with long-term, constant-gradient tests. The results of the pumping test indicates that in the area of the current study, the average fracture aperture at a depth of 2m is in the range of 35 μm to 60 μm, which is larger than the values reported by McKay et. al. (1993) for another location at the Laidlaw site.

REFERENCES

Adams, J.I, Effect of groundwater levels on stress history of the St. Clair clay till deposit: Discussion, *Can. Geotech. J.*, 7, 190-193, 1969.

Adomait, M., Hydraulic responses in fractured clay, M.Sc. project, University of Waterloo, Waterloo, Ontario, Canada, 1991.

Barenblatt, G.I., Iu. P. Zheltov, and N. Kochina, Basic concepts in the theory of seepage of homogeneous liquids in fissured rocks, *J. Appl. Math. Mech.*, 24, 1286-1303, 1960.

Barker, J.A., and J.H. Black, Slug tests in fissured aquifers, *Water Resour. Res.*, 19(6), 1558-1564, 1983.

Bear, J., Modeling flow and contaminant transport in fractured rocks, In: *Flow and contaminant transport in fractured rock*, J. Bear, C-F Tsang, and G. de Marsily, eds. Academic Press, San Diego, 1993.

Beven, K. and P. Germann, Water flow in soil macropores, 2: A combined flow model, *J. Soil Sci.*, 32, 15-29, 1981.

Bradbury, K.R. and M. Muldoon, Hydraulic conductivity determination in unlithified glacial and fluvial materials, *Ground Water and Vadose-Zone Monitoring,* ASTM STP 1053, D.M. Nielson and A.I. Johnston, eds. American Society for Testing and Materials, Philadelphia, 138-151, 1990.

Berkowitz, B., J. Bear and C. Braester, Continuum models for contaminant transport in fractured porous formations, *Water Resour. Res.*, 24(8), 1225-1236, 1988.

Burke, B., Depth of active groundwater flow in the fractured clay of the St. Clair Clay Plain, soutwestern Ontario, M.Sc. Thesis, University of Waterloo, Waterloo, Ontario, Canada, 1997.

Chapman, L.P. and D.F. Putnam, Physiography of southern Ontario, 3rd. ed., Special Vol. 2, Ontario Geological Survey, 1984.

D'Astous, A. Y., W.W. Ruland, J.R.G. Bruce, J.A. Cherry, and R. W. Gillham, Fracture effects in the shallow groundwater zone in weathered Sarnia-area clay, *Can. Geotech. J.*, 26, 43-56, 1988.

Desaulniers, D.E., Groundwater origin, geochemistry and solute transport in three major glacial clay plains of east central North America, Ph.D. thesis, University of Waterloo, Waterloo, Ontario, Canada, 1986.

Duguid, J.O and P.Y.C. Lee, Flow in fractured porous media, *Water Resour. Res.*, 13(3), 558-566, 1977.

Edwards, W.M., R.R. van der Ploeg and W. Ehlers, A numerical study of the effects of non-capillary size pores upon infiltration, *Soil Sci. Soc. Am. J.*, 43, 851-856, 1979.

Einarson, M.D., Enviro-core - A new direct push technology for collecting continuous soil cores, 9th National Outdoor Action Conference, Las Vegas, 1995.

Fitzgerald, W.D., E. Janicki, and D.J. Storrinson, Sarnia-Brights Grove area, southern Ontario, Ontario Geological Survey, Preliminary Map P-2222, 1979.

Gerke, H.H. and M.T. van Genuchten, A dual-porosity model for simulating the preferential movement of water and solutes in structured porous media, *Water Resour. Res.*, 29(2), 305-319, 1993.

Hanna, T.H., Engineering properties of glacial-lake clays near Sarnia, Ontario, *Ontario Hydro Research Quarterly*, 3rd Quarter, 1-12, 1966.

Harris, S. M., Characterization of the hydraulic properties of a fractured clay till, M.Sc. Thesis, University of Waterloo, Waterloo, Ontario, Canada, 1994.

Huyakorn. P.S., B. Lester and C. Faust, Finite element techniques for modeling groundwater flow in fractured aquifers, *Water Resour. Res.*, 19(4), 1019-1035, 1983.

Jones, L., T. Lemar and, C. Tsai, Results of two pumping tests in Wisconsinon Age weathered till in Iowa, *Groundwater*, 30(4), 529-538, 1992.

Klint, K.E.S., Fractures and depositional features of the St. Joseph Till and the upper part of the Black Shale Till at the Laidlaw site, Lambton County, Ontario, Geological Survey of Denmark and Greenland, Report 1996/9, 1996.

McKay, L. D., J.A. Cherry, and R. W. Gillham, Field experiments in a fractured clay till 1. Hydraulic conductivity and fracture aperture, *Water Resour. Res.*, 29(4), 1149-1162, 1993.

McKay, L.D., and J. Fredericia, Distribution, origin, and hydraulic influence of fractures in a clay-rich glacial deposit, *Can. Geotech. J.*, 32, 957-975, 1995.

Murdoch, L., Forms of hydraulic fractures created during a field test in overconsolidated glacial drift, *Quart. J. Eng. Geol.*, 28, 23-35, 1995.

Neuman, S.P. and P.A. Witherspoon, Theory of flow in a confined two aquifer system, *Water Resour. Res.*, 5(4), 803-829, 1969.

Novakowski, K. S., Analysis of pulse interference tests, *Water Resour. Res.*, 25(11), 2377-2387, 1989.

Ogunbadejo, T.A. and R.M. Quigley, Micro-structural and mineralogical influences on the compaction characteristics of weathered clays from Sarnia, Ontario, University of Western Ontario Soil Mechanics Research Report SM-2-73, 1973.

Padusenko, G., The influence of scale on hydraulic conductivity measurements, B.Sc. Thesis, University of Waterloo, Waterloo, Ontario, Canada, 1997.

Ruland, W. W., J.A. Cherry, and S. Feenstra, The depth of fractures and active groundwater flow in a clayey till plain in south-western Ontario, *Groundwater*, 29(3), 405-417, 1991.

Snow, D.T, Anisotropic permeability of fractured media, *Water Resour. Res.*, 5(6), 1273-1289, 1969.

Sudicky, E.A., A.J.A. Unger and S. Lacombe, A noniterative technique for the direct implementation of well bore boundary conditions in three-dimensional heterogeneous formations, *Water Resour. Res.*, 31(2), 411-415, 1995.

Therrien, R., E.A. Sudicky and R.G. McLaren, Users guide for NP - A preprocessor for FRAC3DVS: An efficient simulator for three-dimensional, saturated-unsaturated groundwater flow and chain-decay solute transport in porous or discretely fractured porous formations, University of Waterloo, 1995.

Therrien, R. and E.A. Sudicky, Three-dimensional analysis of variably-saturated flow and solute transport in discretely-fractured porous media, *J. Cont. Hydrology*, 23, 1-44, 1996.

Warren, J.E. and P.J. Root, The behaviour of naturally fractured reservoirs, *Soc. Pet. Eng. J.*, 3, 245-255, 1963.

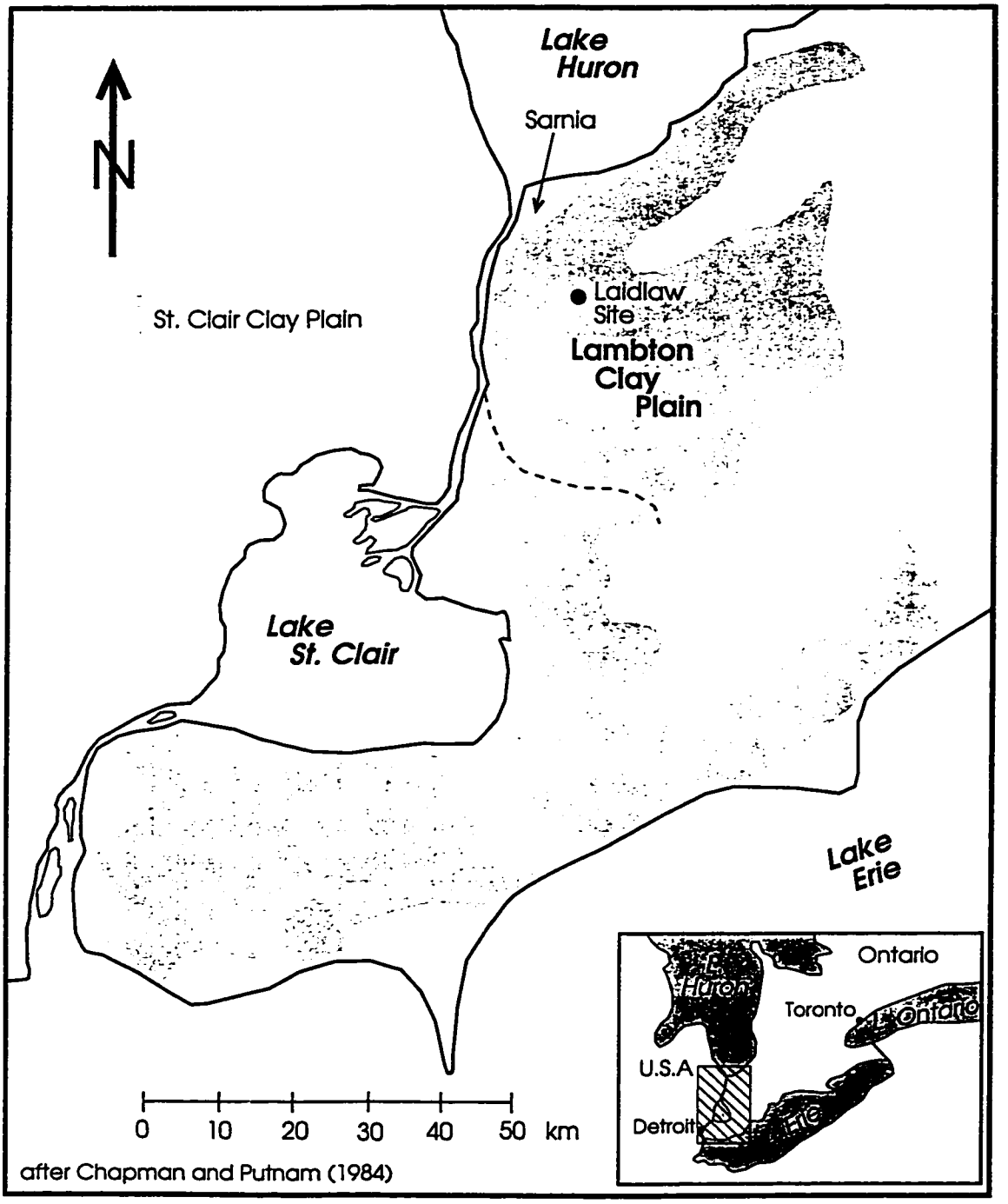

Figure 4.1 - Location of study site

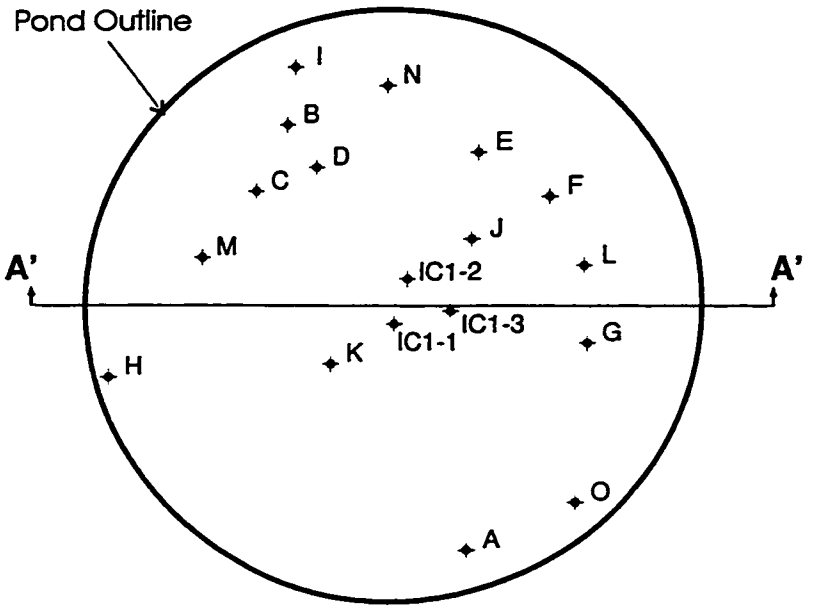

Transducer Location	Depth below pond bottom (m)
A	1.29
B	1.35
C	1.83
D	1.98
E	2.04
F	2.04
G	1.98
H	1.98
I	2.05
J	2.26
K	2.20
L	2.65
M	2.32
N	3.37
O	3.76

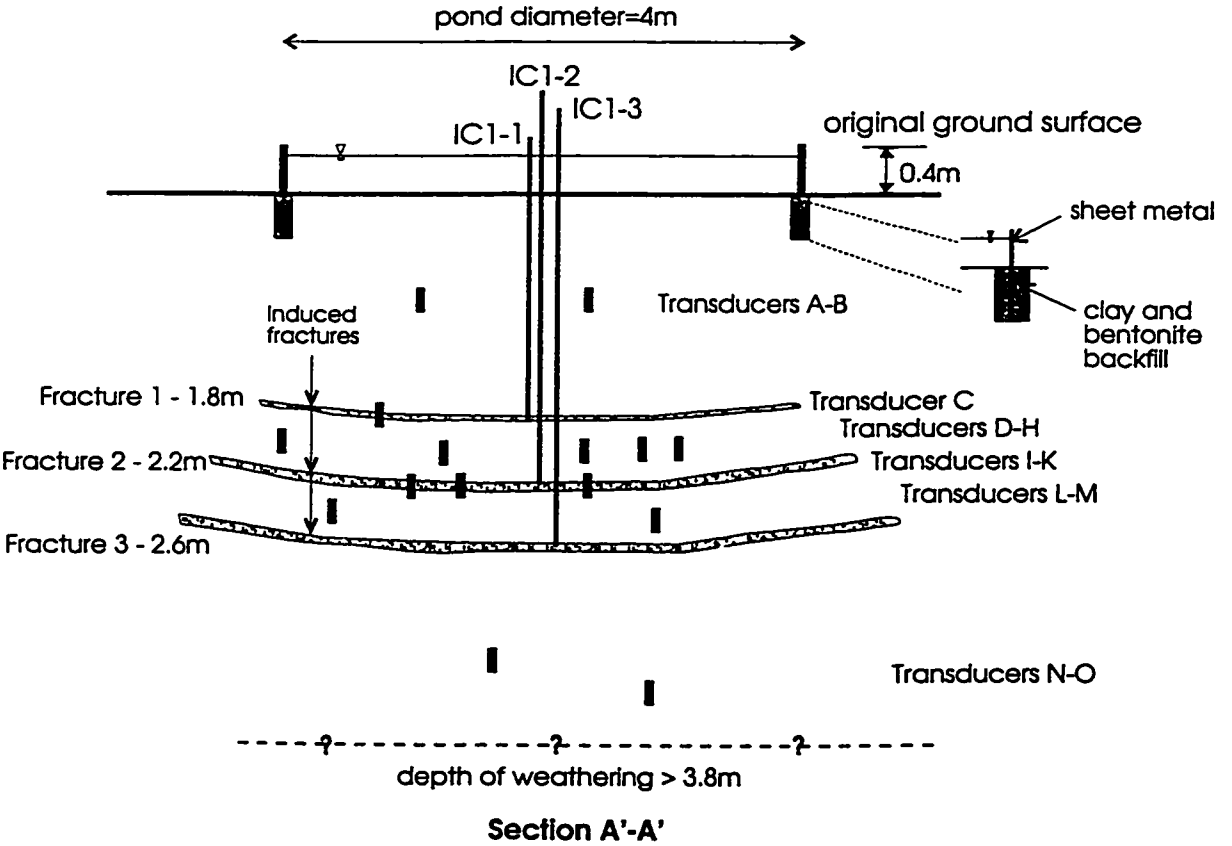

Section A'-A'

Figure 4.2 - Details of experimental setup

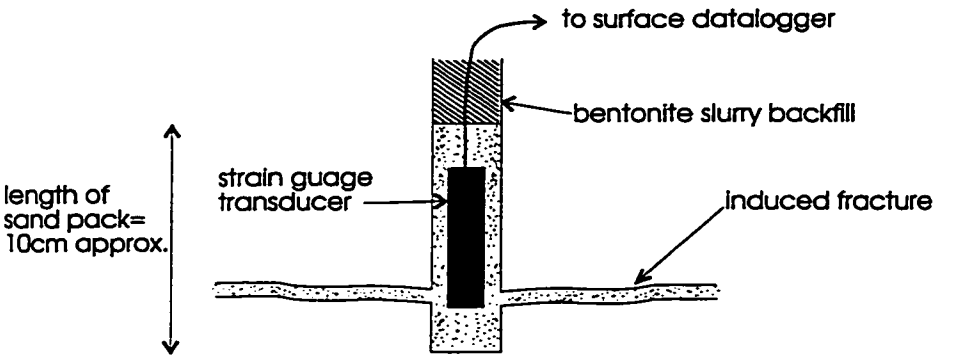

Figure 4.3 - Detail of transducer placement at the level of an induced fracture

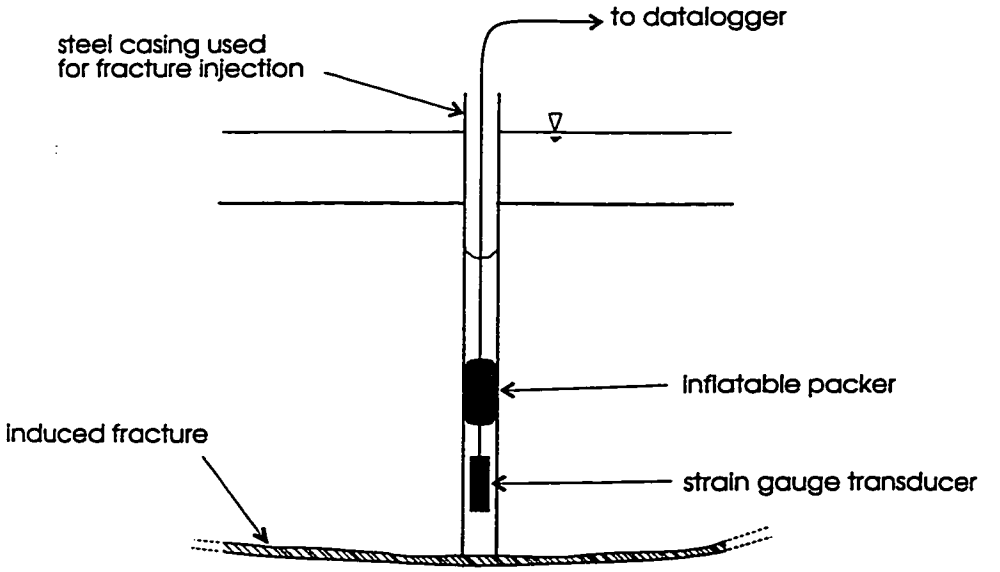

Figure 4.4 - Pressure transducer sealed in casing with inflatable packer

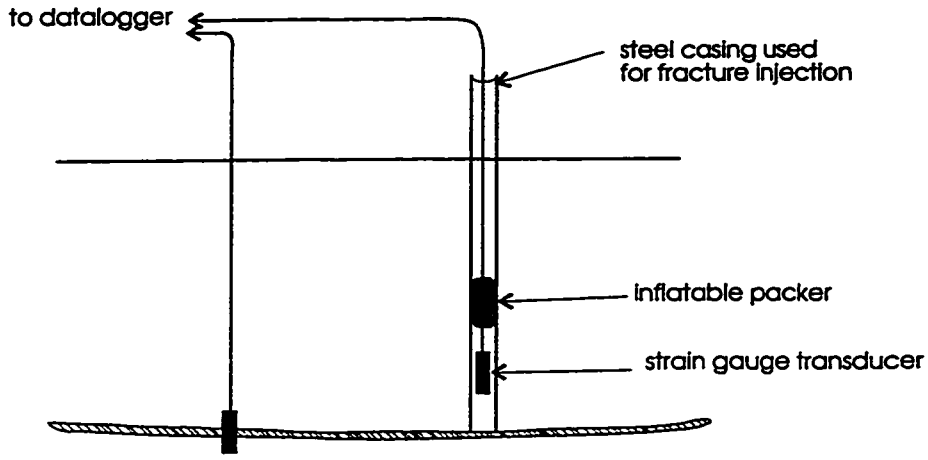

Step 1 - Inflate packer and
fill casing above packer

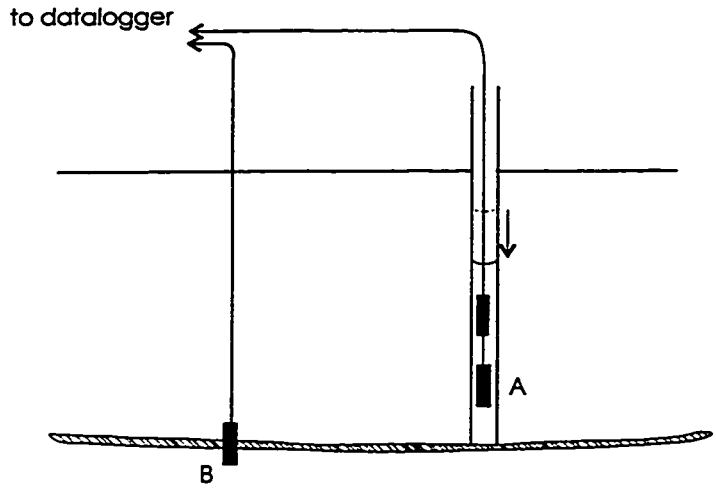

Step 2 - Deflate packer and
monitor pressure change at A and B

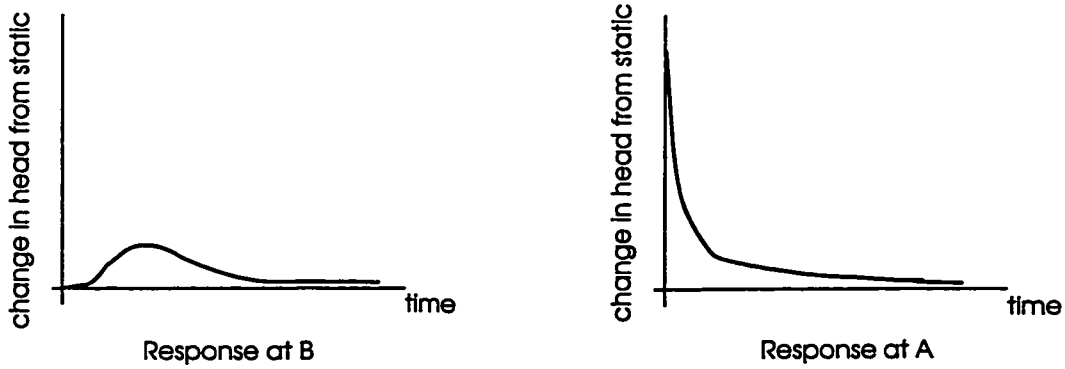

Figure 4.5 - Procedure for performing falling head tests in induced fractures

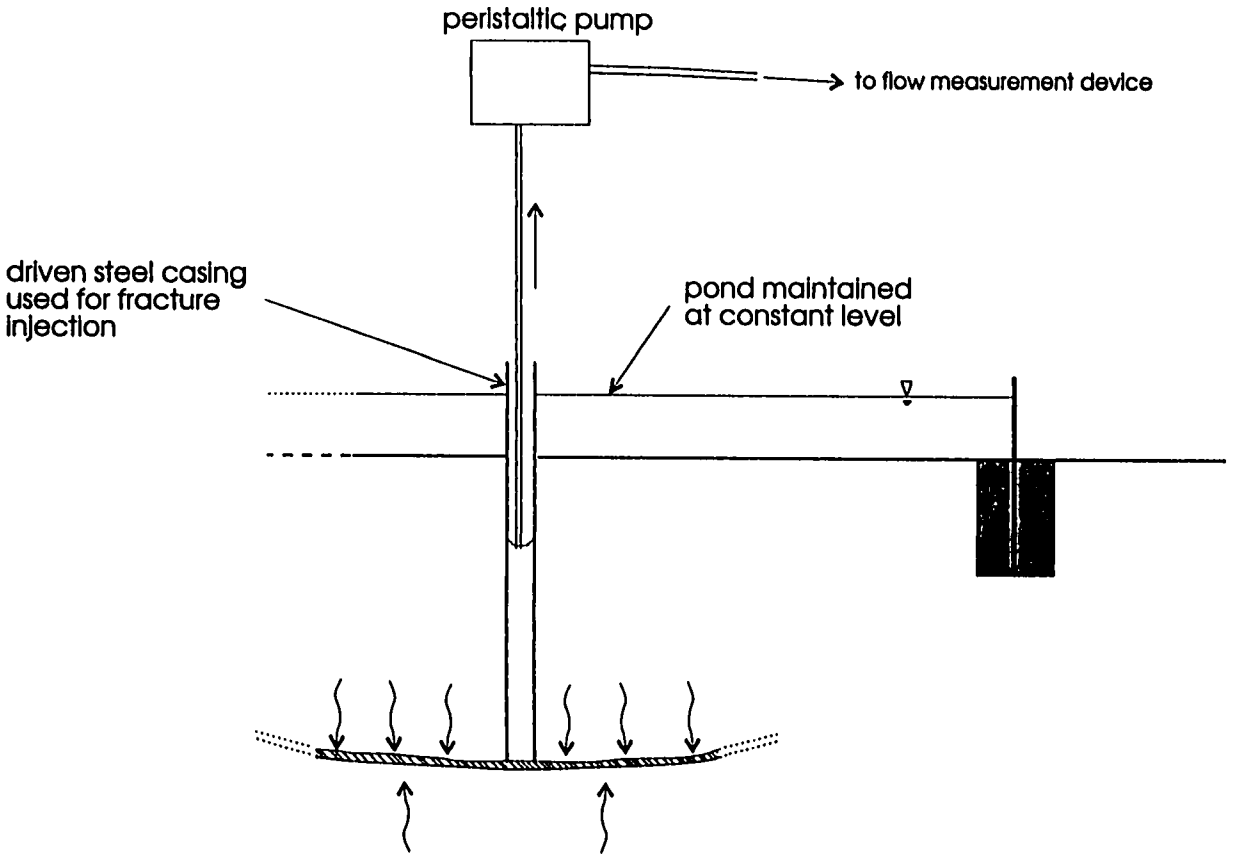

Figure 4.6 - Procedure for conducting constant head pumping tests in induced fractures

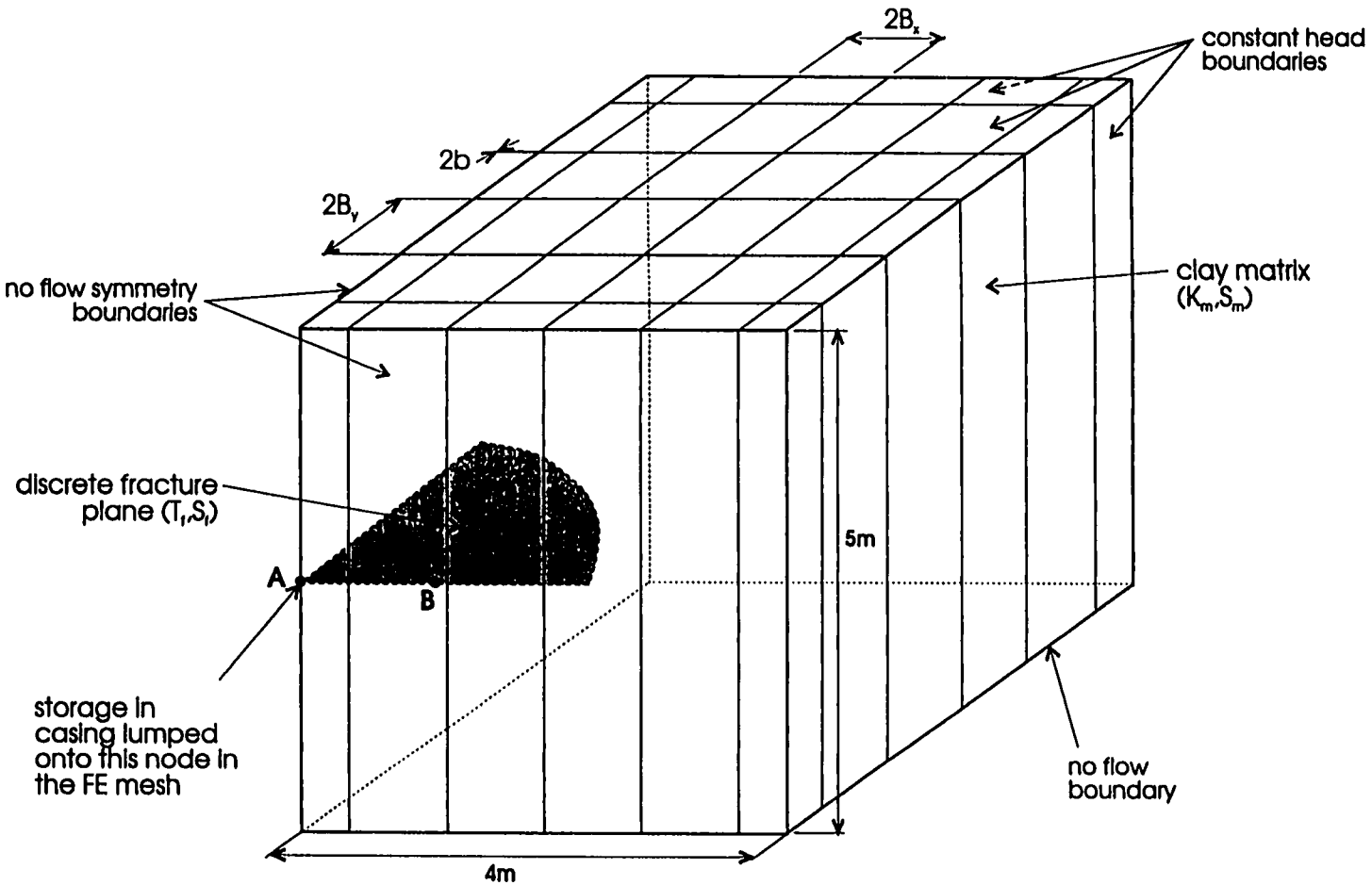

$$\text{bulk vertical hydraulic conductivity} = K_{bulkv} = \left(\frac{1}{2B_x} + \frac{1}{2B_y}\right)\frac{\rho g.(2b)^3}{12.\mu} + K_m$$

(adapted from Snow, 1969)

Figure 4.7 Model geometry and boundary conditions for interpretation of falling head tests

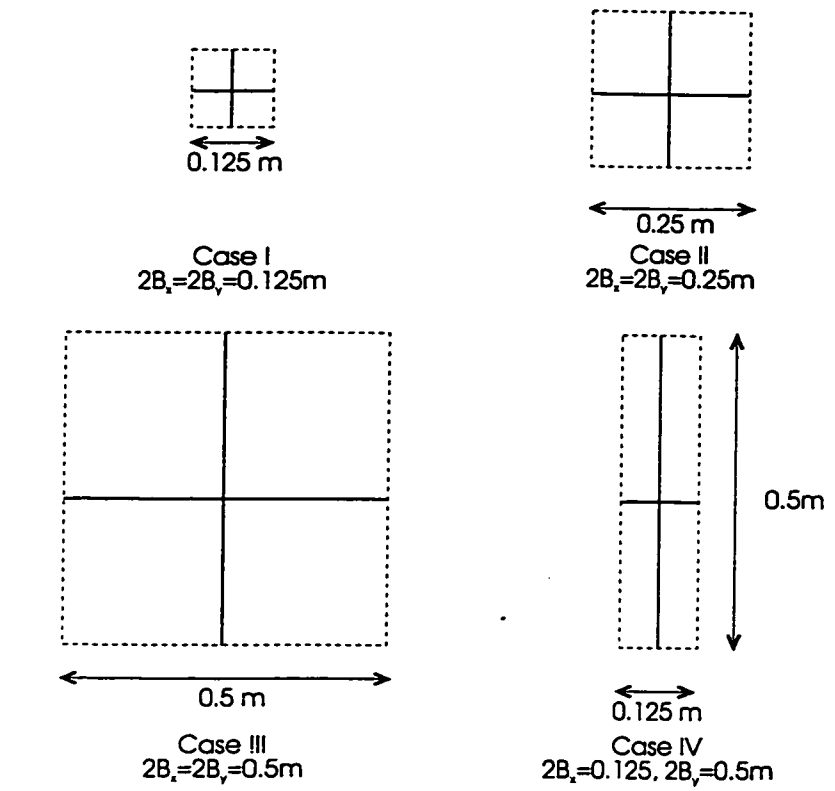

a) Fracture geometries considered

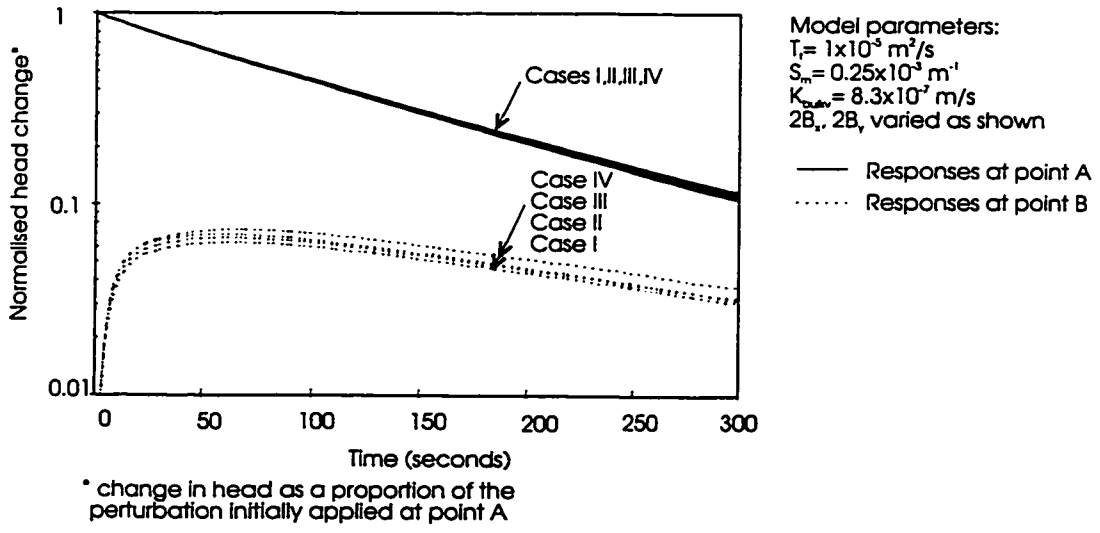

b) Calculated responses for various spacings
(K_{bulk} equal for all cases)

Figure 4.8 - Influence of fracture network geometry on falling head test response

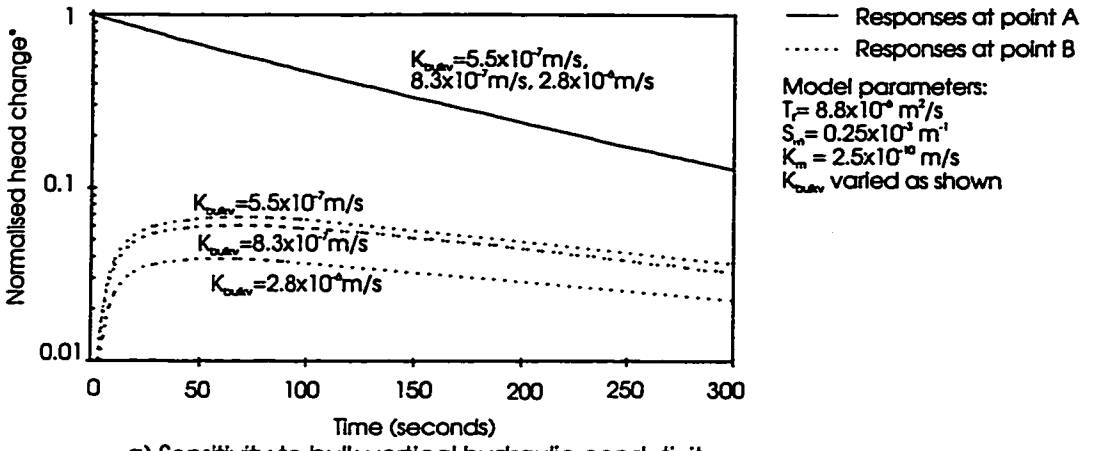

a) Sensitivity to bulk vertical hydraulic condutivity

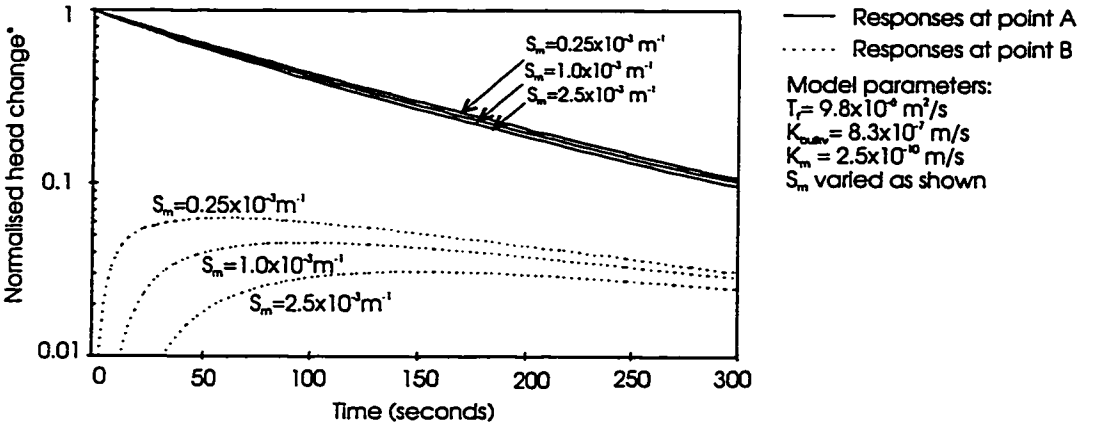

b) Sensitivity to matrix specific storage

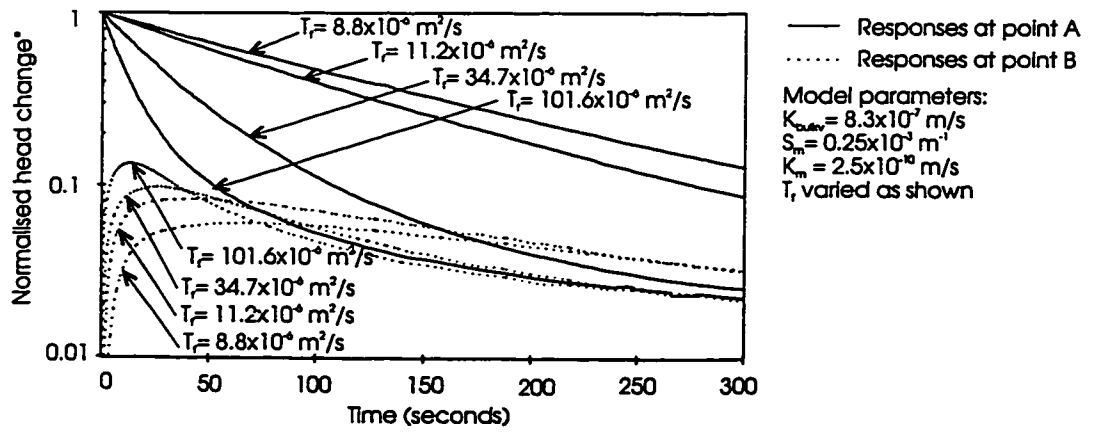

c) Sensitivity to transmissivity of the induced fracture

* change in head as a proportion of the perturbation initially applied at point A

Figure 4.9 - Influence of bulk hydraulic conductivity, specific storage and transmissivity in the induced fracture on falling head test response

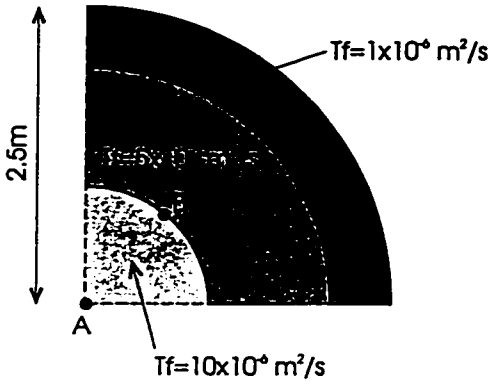

a) Distribution of transmissivity in plane of induced fracture

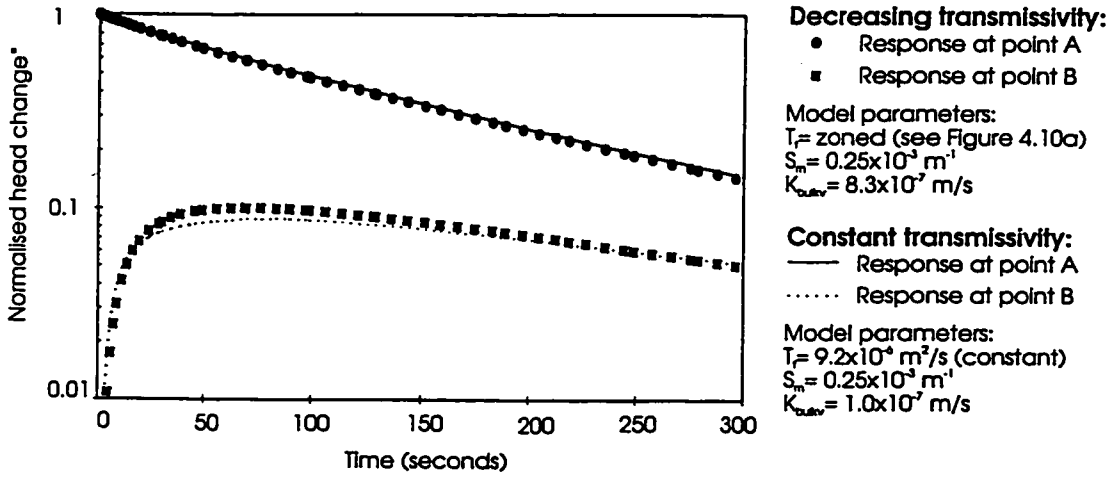

b) Comparison of responses for case of decreasing tranmissivity and case of constant transmissivity

Figure 4.10 - Influence of transmissivity distribution in induced fracture on falling head test response

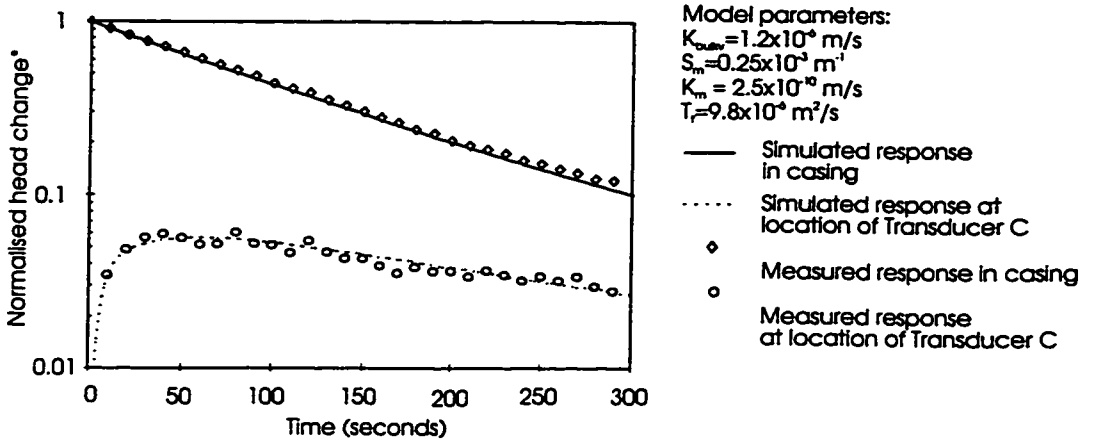

a) Results for slug test in casing IC1-1

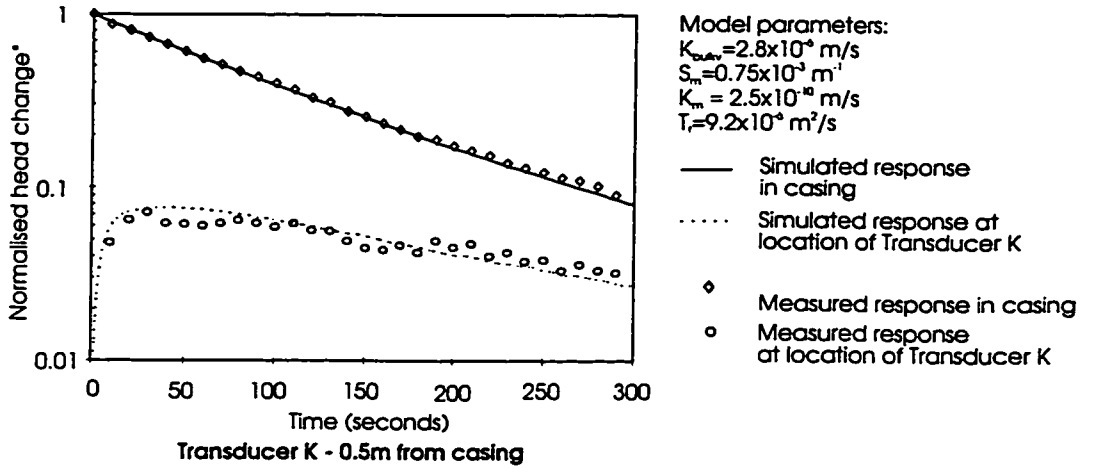

Transducer K - 0.5m from casing

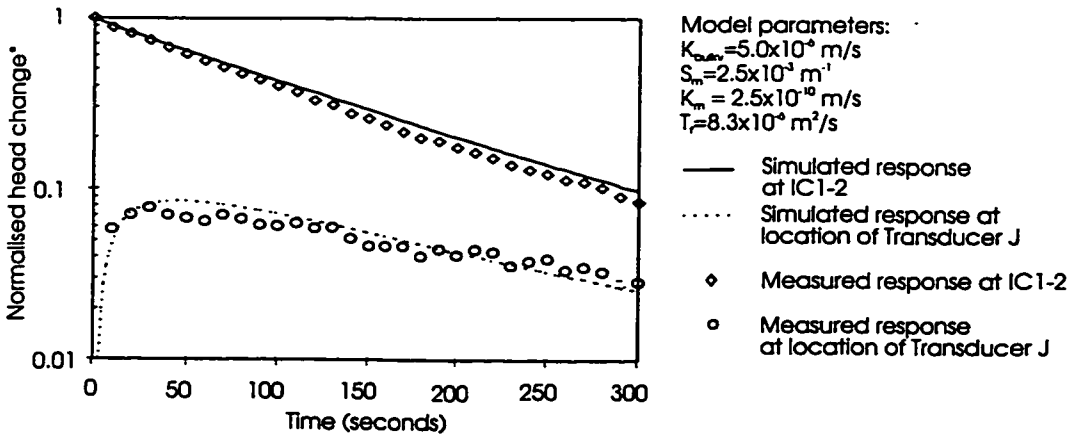

Transducer J - 0.8m from casing

b) Results for slug test in casing IC1-2

* head change as a proportion of the perturbation initially applied in casing

Figure 4.11 - Comparison of simulated and measured responses for falling head tests

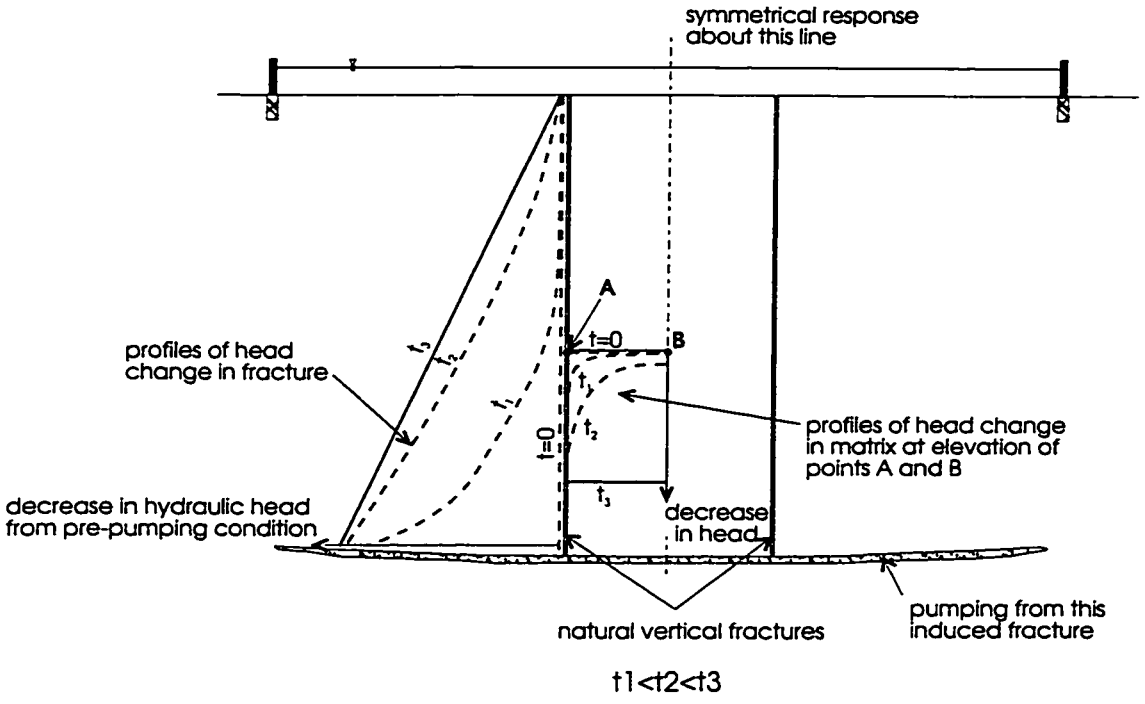

Figure 4.12 - Conceptual model of transient head conditions during constant head pumping tests

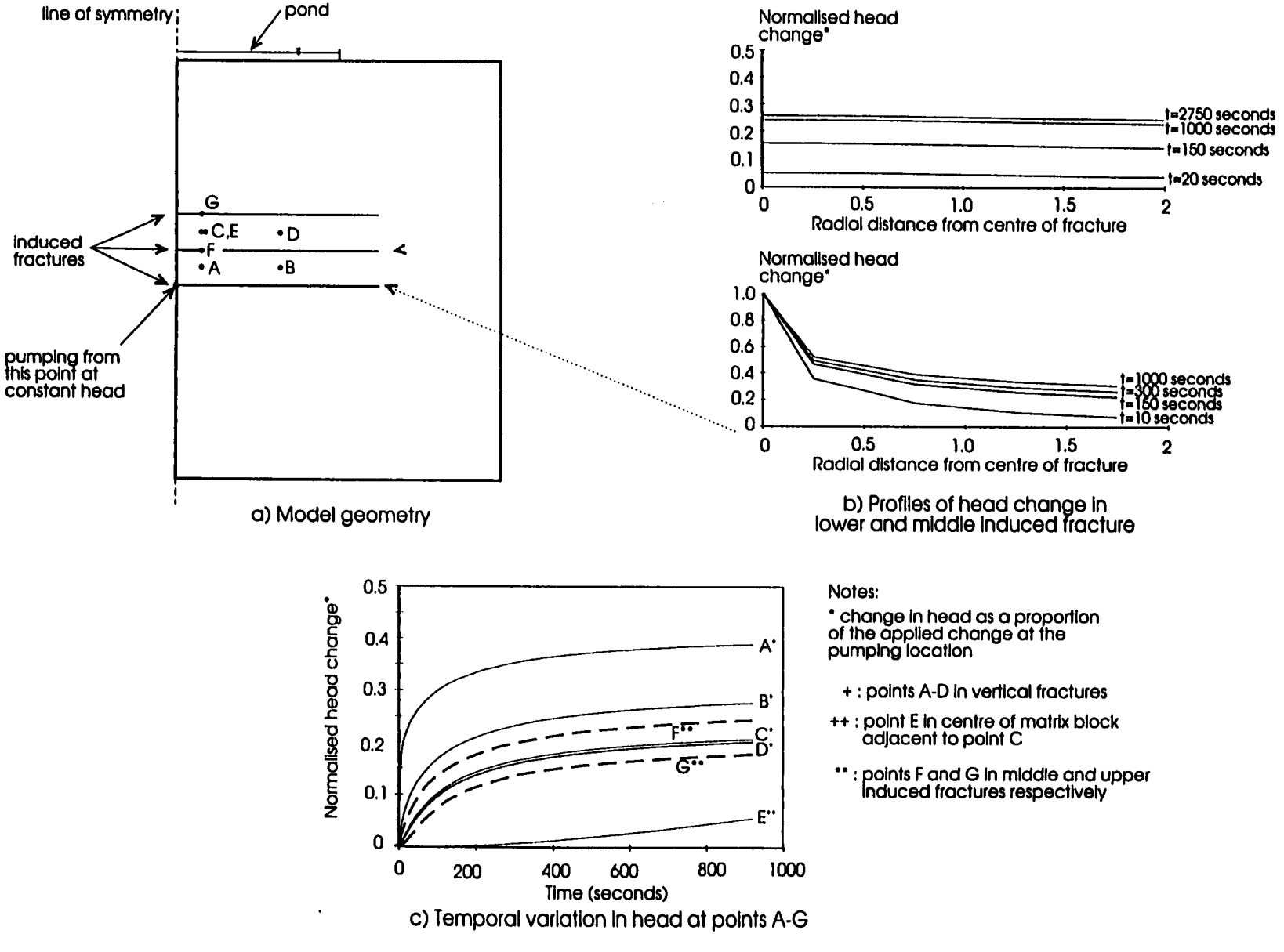

Figure 4.13 - Results of simulated constant head pumping test

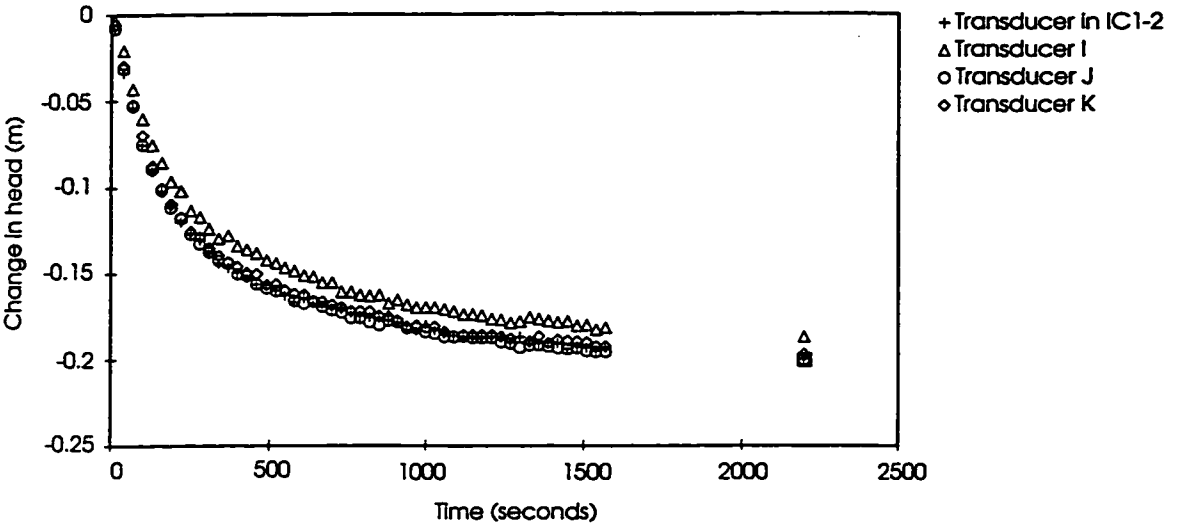

a) Response in middle induced fracture due to pumping in deepest induced fracture

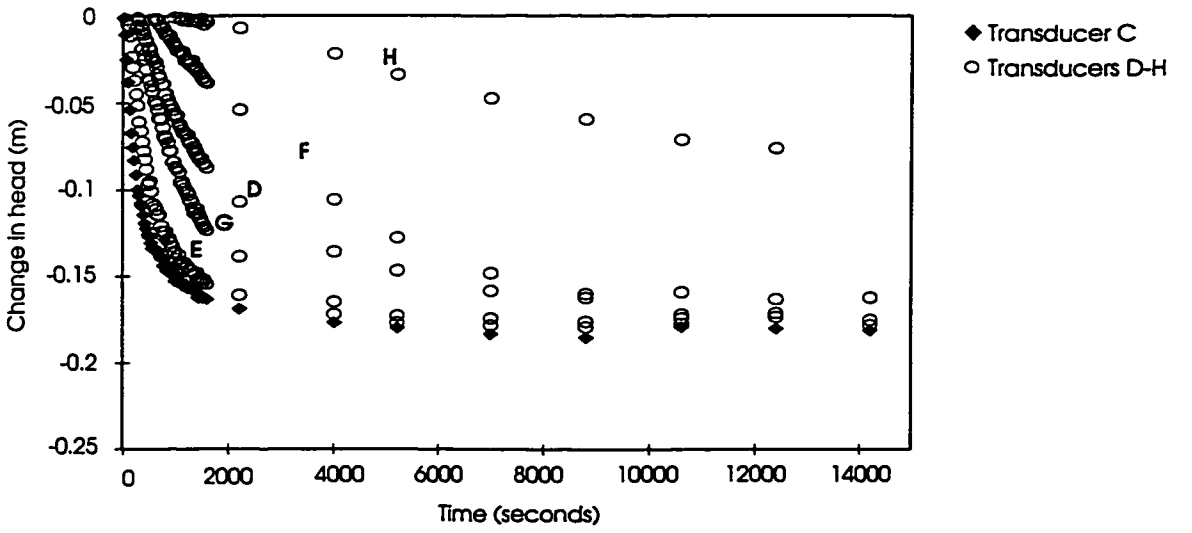

b) Response in upper induced fracture (Transducer C) and at 5 locations midway between middle and upper induced fractures (Transducers D-H)

Figure 4.14 - Results from pumping test in deepest induced fracture

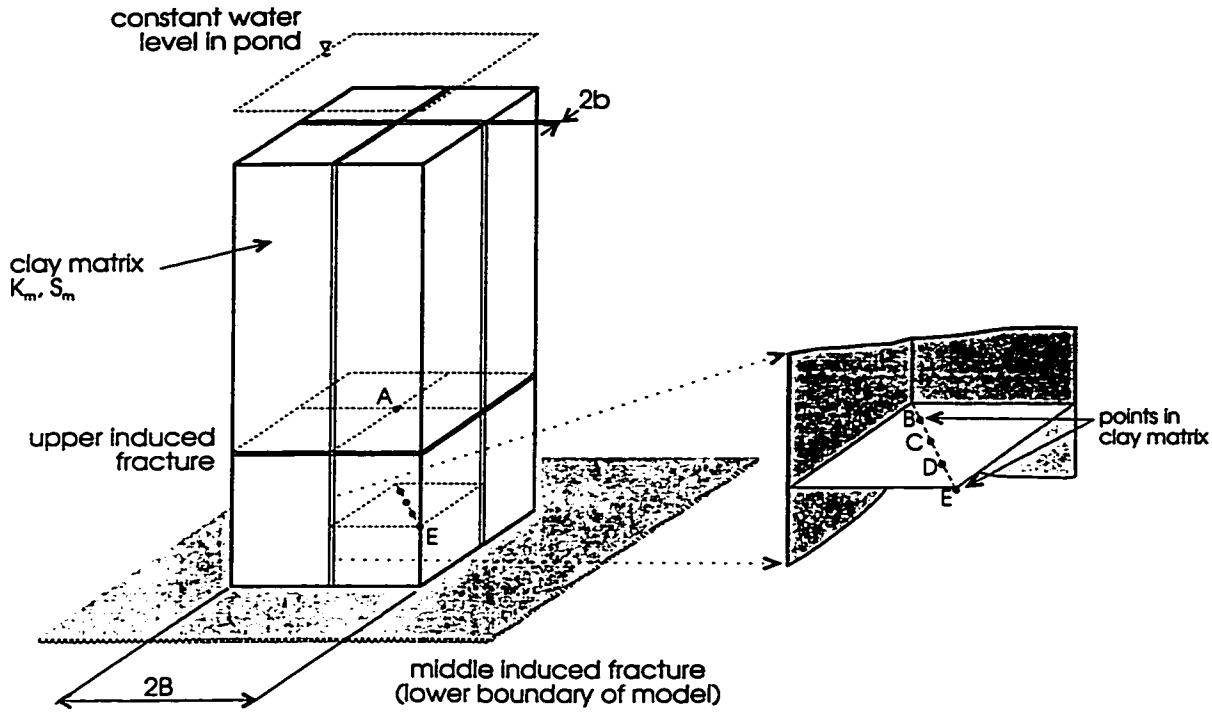

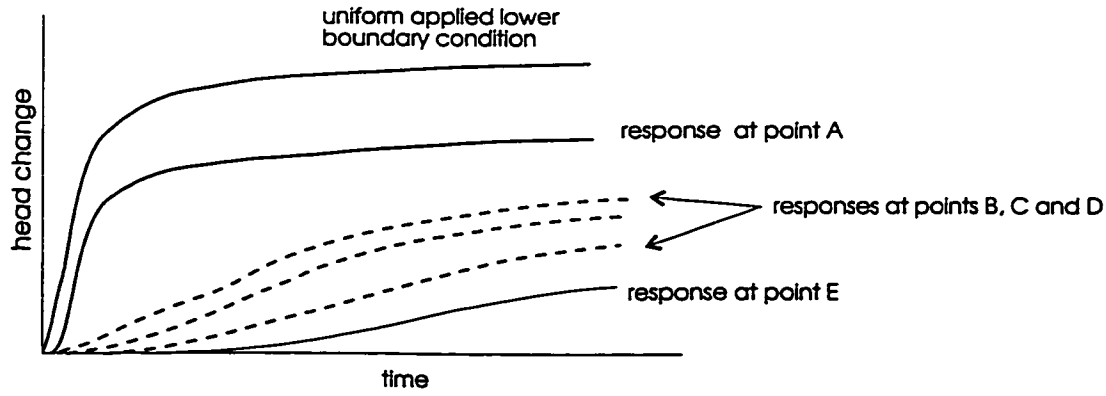

Figure 4.15 - Model geometry and boundary conditions to interpret results of pumping tests for locations above middle induced fracture

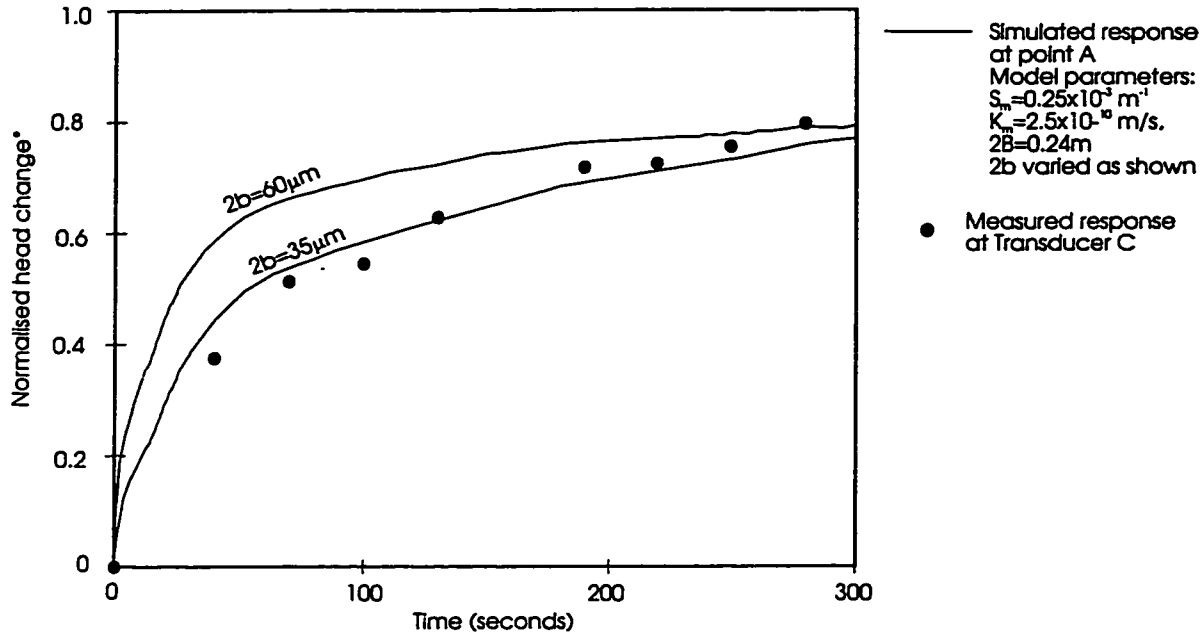

a) Low matrix specific storage

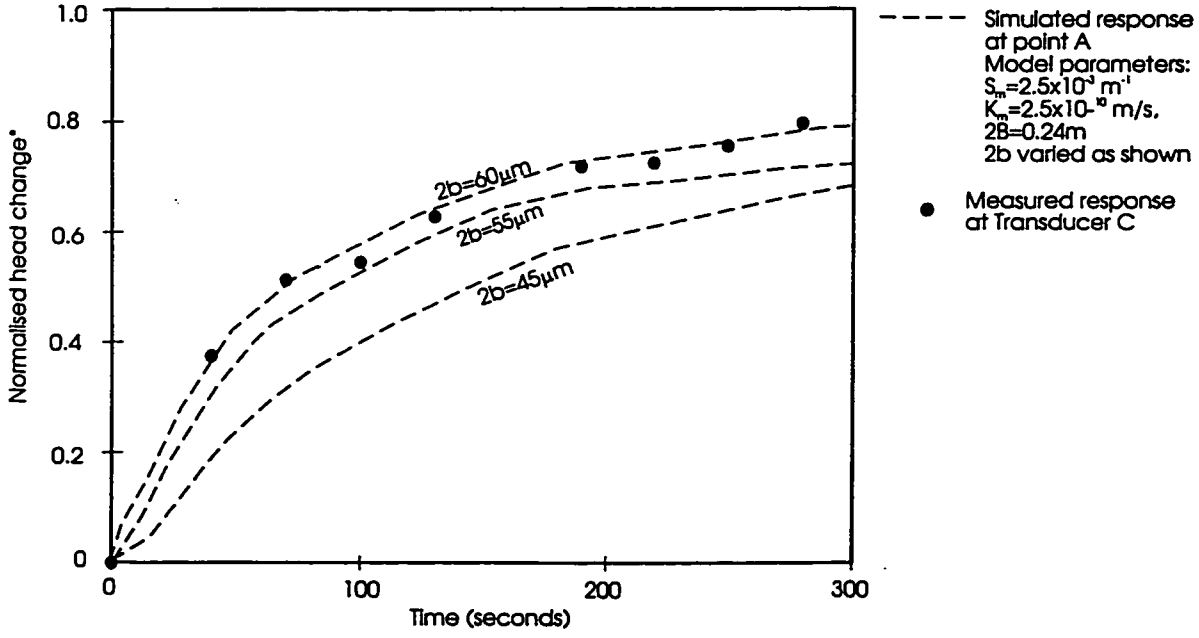

b) High matrix specific storage

* - head change as a proportion of the change applied to the lower boundary

Figure 4.16 - Comparison of simulated and measured responses for constant head pumping tests - upper induced fracture

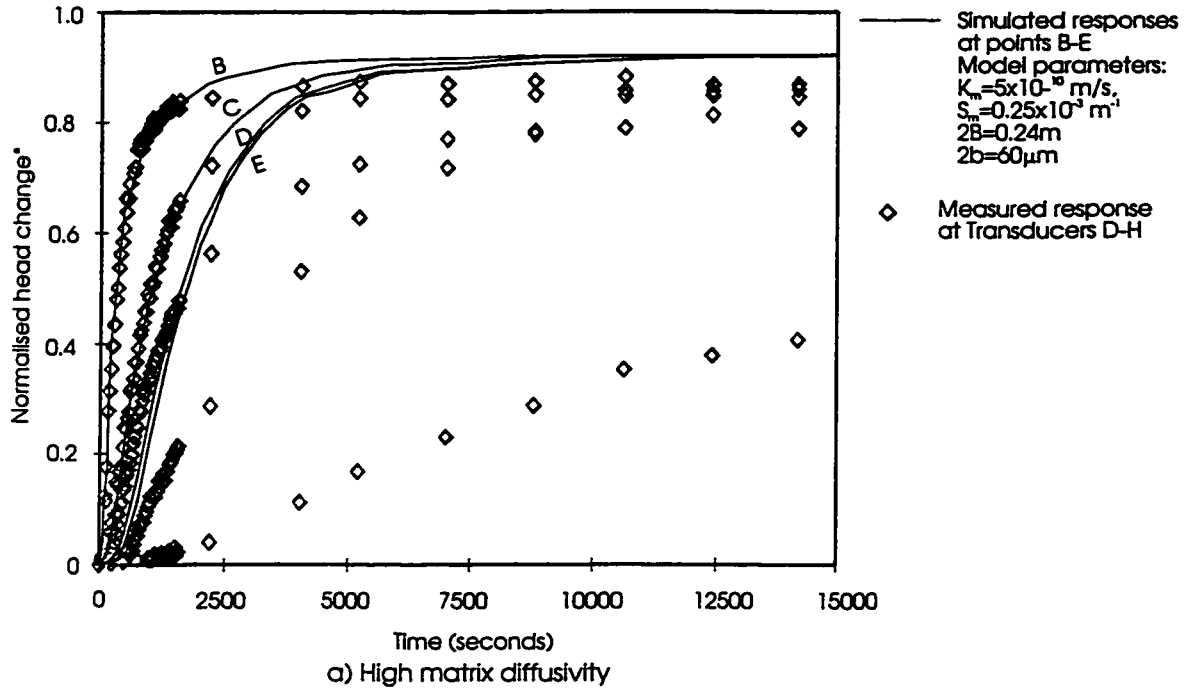

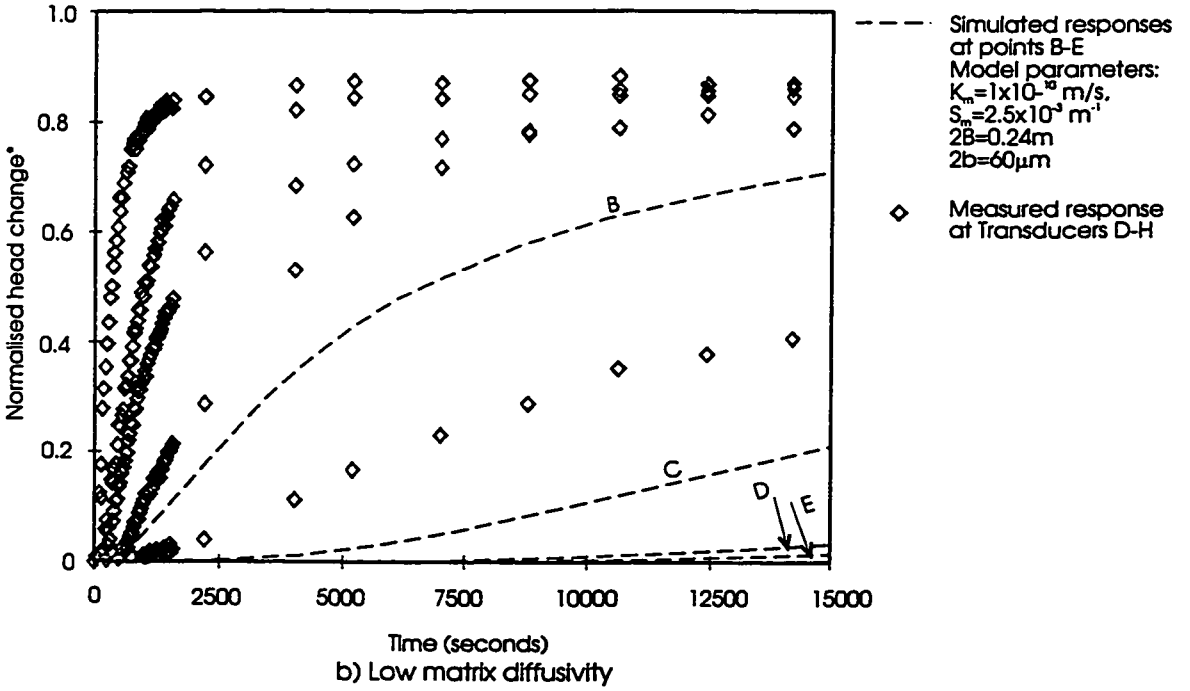

* - head change as a proportion of the change applied to the lower boundary

Figure 4.17 - Comparison of simulated and measured responses for constant head pumping tests - matrix locations

CHAPTER 5

THE INFLUENCE OF MACROPORE GEOMETRY ON TRANSIENT HYDRAULIC RESPONSE AND ON SOLUTE TRANSPORT IN WEATHERED CLAYEY MATERIALS: MODELLING INVESTIGATIONS

INTRODUCTION

Macropore features such as root holes, worm holes and fractures are commonly found in near surface, weathered, clayey deposits (see, for example Bouma et. al., 1977; Beven and Germann, 1982; McKay and Fredericia, 1995). Fractures have also been observed or inferred from hydraulic or solute transport evidence in deeper, unweathered clay deposits at various locations in North America by Keller et. al. (1986), Rudolph et. al. (1991) and Pach (1994). The influence of macropores of all types on hydraulic and solute transport behaviour is widely recognised. Their presence can increase hydraulic conductivity by up to 4 orders of magnitude above the hydraulic conductivity of the clay material itself (Keller et. al., 1986; and McKay et. al., 1993a), and can lead to rapid infiltration of rainfall in unsaturated surface clay (Beven and Germann, 1982). Similarly, their presence can lead to rates of solute migration that are well in excess of the low, diffusion controlled rates that would be expected for intact clay (for example, Wild and Babiker, 1976; and McKay et. al. 1993b).

An important process controlling flow and solute transport in materials which contain discrete high conductivity features and relatively low conductivity blocks of intact material between these features, is the transfer of fluid and/or solute mass between these two components of the system. In general, the macropores represent high conductivity, low storage pathways through which water and solutes can be transmitted, whereas blocks of intact material represent low conductivity regions which have large capacity to store fluid and/or solute. Under transient conditions, where disequilibrium in fluid pressure or solute concentration exists between the macropores and the intact regions, mass is transferred between the two due to the gradient in pressure or chemical potential.

Interaction between macropores and adjacent matrix material in terms of the transfer of solute mass by diffusion is a process that is relatively well understood. It has been discussed

in detail in the literature following the initial discussion of the phenomenon by Foster (1975) and its effects have been observed in various geological settings at various scales (for example, Foster, 1975; McKay et. al. 1993b; Novakowski and Lapcevic, 1994; Hinsby et. al., 1996). The effects of the analogous process of fluid transfer between macropores and less conductive adjacent material due to hydraulic gradients that exist between them under transient hydraulic conditions has not, however, been discussed or interpreted as extensively in the literature, particularly for conditions of saturated flow. In the soil science literature, the problem of infiltration of water into unsaturated soil containing macropores has been investigated in some detail using mathematical models which make allowance for fluid transfer between the macropores and the matrix (Beven and Germann, 1981; Dykhuizen, 1987; and Gerke and van Genuchten, 1993). For unsaturated conditions, the potential for fluid storage in unsaturated matrix blocks is considerably greater than for saturated conditions, and the hydraulic conductivity of the macropores is considerably less than for saturated conditions. It is therefore difficult to use the results of such modelling investigations to understand the effects of macropore/matrix interaction in saturated systems.

Barrenblatt et. al. (1960) and Warren and Root (1963) considered the problem of saturated flow in fractured reservoirs, and assessed the influence of interaction between high conductivity, low storage fractures and low conductivity, high storage matrix blocks on drawdown in a pumping well. However, the formulation used in these studies was based on the assumption of quasi-steady state flow between the fractures and the matrix blocks, and therefore the reported results are not applicable at early times (Gerke and van Genuchten, 1993). Kazemi (1969) describes the development of a model which is similar to the Warren and Root (1963) model, but which allows for unsteady flow in both the fractures and the matrix blocks. He presents model results for systems with relatively incompressible (and therefore low storage) matrix blocks, and concludes that interaction between the fractures and the matrix

blocks can cause effects at a pumping well which can not be reproduced using conventional single continuum flow models.

Mathematical modelling of flow and solute transport in materials which contain discrete high conductivity features and relatively low conductivity blocks of intact material between these features is often based on a dual-porosity formulation (for example, Warren and Root, 1963; Beven and Germann, 1981; Gerke and van Genuchten, 1993). Dual-porosity formulations assume that the macropores and the low conductivity matrix can be represented as two co-existent, interacting continua. Such models are based on governing equations for the macropores and matrix which include an explicit term for the transfer of water between the two continua. The differences between many of the proposed dual-porosity models are primarily associated with the expressions which are used for this term. Many of the models are based on assumptions such as quasi-steady state fluid exchange between the two continua (Warren and Root, 1963), or equal hydraulic head in the two continua (Dykhuizen, 1987), which can be restrictive for problems which involve rapid transient conditions.

The objectives of this chapter are to examine, using a numerical model, the influence of macropore/matrix interactions on the propagation of pressure perturbations for saturated conditions in relatively compressible materials such as clay, and to investigate the effect of various macropore geometries on transient hydraulic response and solute transport in clayey deposits. It might be expected that transient hydraulic response and solute transport behaviour would be affected by the macropore geometry, since the contact area between the clay and the macropores will have a controlling influence on how quickly water and solutes can be exchanged between the two. In the case of planar features such as fractures, the contact area between the macropore and the matrix is relatively large, whereas in the case of linear features such as root holes, the contact area is relatively small. In the numerical model used for the

simulations described in this chapter, macropores are modelled as discrete features embedded in the matrix of lower conductivity, higher storage material, and therefore no explicit transfer term is required, and no restrictions are placed on the time scale of problems that can be considered.

PHYSICAL PROCESSES

Transient hydraulic interaction between macropores and adjacent matrix material is idealised in Figure 5.1, for the case of a fractured aquitard separating two aquifers. It is assumed that the fractures are equally spaced and vertical. An instantaneous and uniform decrease in hydraulic head is imposed in the lower aquifer at t=0, and for the purposes of the illustration, the head in the upper aquifer is assumed to remain unchanged. In Figure 5.1a, profiles of hydraulic head in the fractures and in the matrix are illustrated at various times following the decrease in head in the lower aquifer. Due to the low storage in these elements, hydraulic head in the fractures will approach an almost constant distribution quickly after the application of the perturbation in the lower aquifer, and will then continue to change slowly as water is released to these features from storage in the clay itself. Hydraulic head in the blocks of clay will change more slowly, depending on the relative proximity of the fractures, and on the hydraulic diffusivity of the matrix material (see Figure 5.1b). Immediately following the head decrease in the lower aquifer, the fluid flux from the aquitard to this aquifer will be high, due to the initially steep hydraulic head gradients at the interfaces between the clay and fractures. As the head gradient between the fractures and the clay matrix blocks decreases to zero and the head distribution in the system approaches a steady state, the flux will decrease towards a steady state value that is dictated by the bulk vertical hydraulic conductivity of the fracture/matrix system, and the vertical hydraulic gradient across the aquitard. Conversely, the fluid flux from the upper aquifer to the aquitard will increase from zero, until at steady state it

will equal the fluid flux from the aquitard to the lower aquifer (see Figure 5.1c). These processes and their effects were observed in a field setting and discussed in Chapters 3 and 4.

In addition to interaction between macropores and matrix material at the interface between the two, solute mass and fluid transfer can take place between different macropores, and between different parts of a single, naturally variable macropore. For example, a solute will diffuse between different parts of a single rough-walled fracture in which advective velocities vary, thus retarding the movement of the solute through large aperture regions of the fracture. Similarly, the rapid transmission of pressure through large aperture regions of fractures will be retarded by fluid transfer to or from the surrounding smaller aperture regions. Many models of channelised transport in fractures allow only for variable advective velocities in the plane of the fracture (for example, Tsang and Tsang, 1987; Nordqvist et. al, 1992), and do not take into account interactions in the plane of the fracture due to concentration gradients. However, this process was shown to be important in retarding solute breakthrough in rough-walled fractures by Raven et. al. (1988) and Johns and Roberts (1991). The author is not aware of any studies which have considered the influence of variable fracture aperture on pressure propagation.

The potential for direct interaction between macropores is limited, except, for example, in the case where root holes are located along fracture faces. Several researchers (Bouma and Dekker, 1977; Hendry, 1982; Ruland et. al., 1991; McKay and Fredericia, 1995; Hinsby et. al., 1996) have reported that roots are preferentially located on fracture faces in near-surface weathered deposits. Depending on the root hole diameter and fracture aperture, such cases could be regarded as extreme examples of channelling in the plane of the fracture.

MODELLING APPROACH

All simulations were carried out with the numerical model FRAC3DVS (Therrien et. al., 1995). The features of the model that were used in the current investigation were the solution of the transient groundwater flow equation, and the solution of the advective-dispersive transport equation, for three-dimensional, saturated porous and discretely fractured porous media. The model is formulated such that various solution techniques can be used to solve these equations, however in the current investigation, a finite difference technique was used. A description of the governing equations and numerical formulations used in FRAC3DVS is provided in Therrien and Sudicky (1996).

The influence of macropore geometry on transient hydraulic response and solute transport was considered using the model geometries illustrated in Figure 5.2. Three macropore geometries were considered: linear root holes, planar fractures, and a combination of the two. The models which included a combination of fractures and root holes are intended to represent situations such as those in which root holes are preferentially located on fracture faces, or extreme conditions of fracture channelling due to aperture variation. The vertical model boundaries were specified as zero-gradient boundaries to represent symmetry conditions, and these models therefore simulate representative portions of equally spaced sets of orthogonal fractures, and/or a regular square-grid pattern of root holes, as shown in Figure 5.2d.

The fractures were modelled as discrete parallel plate fracture elements, for which the cubic law (Snow, 1969) was used to determine the fracture conductivity. The root holes were modelled using a column of porous medium elements, for which a value of hydraulic conductivity higher than that of the surrounding material was specified. The option of using one-dimensional well elements (Sudicky et. al., 1995) to model the root holes was investigated,

but since the elements have no dimensions perpendicular to their axis, the important parameter of contact area between the root hole and the surrounding material can not be accounted for. Results obtained using one-dimensional well elements were compared to results obtained using a column of relatively more conductive porous medium, and it was found that the response in the macropore itself was markedly different for the two cases. A much slower response was calculated in the case of finite contact area between the root hole and the surrounding material.

The formulation of FRAC3DVS is fully general and accounts for advection and dispersion in all elements, however, for the properties chosen for the material surrounding the macropores (see below), these processes will only be significant in the macropores themselves. The processes of solute mass transfer between the different macropores, and between the macropores and the surrounding material due to diffusion is accounted for implicitly in the model, without the need for an explicit mass transfer term. Similarly, the process of fluid transfer between the different components of the system due to hydraulic head gradients between them is implicitly accounted for.

To provide a basis for comparison, the spacing and properties of the macropore(s) were chosen in order to give a bulk vertical hydraulic conductivity of $1x10^{-7}$ m/s in all simulations. The relationships used to calculate bulk hydraulic conductivity from the macropore properties are provided in Table 5.1. In Chapter 3, values of bulk vertical hydraulic conductivity in the range $2.5x10^{-8}$ m/s to $2.5x10^{-5}$ m/s were determined from steady state conditions during pumping tests in a weathered clayey glacial deposit in south-west Ontario. The value used in the modelling is therefore towards the lower end of this range. Bulk hydraulic conductivity can be determined independently of a consideration of transient hydraulic conditions or solute transport behaviour, and, therefore, it can be used to constrain models which attempt to match

field observations of hydraulic transients and/or solute transport. In a similar manner, it has been used in this study to constrain the modelling, so that the results presented herein could represent the range of possible behaviour of a number of different deposits, which, on the basis of bulk hydraulic conductivity alone, are equivalent.

In all cases the model geometry was based on the simple geometries illustrated in Figure 5.2, however the dimensions of the model domain were varied. For simulations in which transient hydraulic conditions were examined, the height of the model domain (H) was chosen as 1 m, and various values of macropore spacing (2B) were used (see below). First-type (constant head) boundary conditions were specified on the upper and lower boundaries of the domain. The initial condition for hydraulic head was specified as zero head, and an instantaneous decrease in head of 1 m was applied over the lower boundary at the start of the simulation and then maintained at this value throughout the duration of the simulation. The specified head at the upper boundary was zero head at all times. These conditions are illustrated in Figure 5.3a.

For solute transport simulations, a value of 10 m was chosen for H, and various values of 2B were employed (see below). In all cases, the solute transport simulations were carried out for steady state hydraulic conditions, with a uniform downward gradient of 0.25 between the upper and lower boundaries. A first-type (constant concentration) boundary condition was specified on the upper domain boundary from the start of the simulation and continued throughout the duration of the simulation. The boundary condition for the lower domain boundary was specified as a zero-gradient second-type condition (zero diffusive and/or dispersive flux). The initial condition for concentration in the domain was specified as zero concentration. These conditions are illustrated in Figure 5.3b. The longer domain was employed in the solute transport simulations in order to reduce the influence of the lower

boundary condition on the computed concentrations within the domain. Ideally, a semi-infinite column would be employed so that the lower boundary would exert no influence on concentrations within the domain. However, since concentrations within the domain were solved for numerically, a finite length domain was necessarily employed, and the need to discretise the domain to resolve spatial concentration gradients placed restrictions on the length of column which could be modelled. Since the focus of the current investigation is to examine the influence of different macropore geometries on solute transport, rather than determine temporal or spatial variations of concentration for a particular system, the choices of a finite length domain and second-type boundary condition for the lower domain boundary are not considered to be overly restrictive.

For the majority of the simulations, a macropore spacing (2B) of 0.2 m was used. In Chapter 1, fracture spacing for idealised networks composed of two sets of orthogonal, equally spaced fractures was related to the fracture intensity (fracture trace length per unit area on horizontal exposures) measured in the field for real fracture networks. For the actual and surrogate networks to have the same fracture intensity, a fracture spacing in the surrogate network of:

$$2B = 2/\text{ fracture intensity}$$

is required (see Chapter 1). In Chapter 1, fracture intensities in the range 6.9-8.2 were reported for horizontal surfaces at depths of 0.6-1.5 m in a weathered, clayey glacial deposit in south-west Ontario. This range of fracture intensity corresponds to fracture spacings in the range 0.24-0.29 m. The fracture spacing of 0.2m used in the majority of the simulations therefore represents a slightly more intensely fractured system. For the purposes of comparison, the same spacing was used for root holes. In a limited number of simulations, fracture spacings of up to 0.5m were used, in order to determine whether systems with large

fracture spacings and large fracture apertures (but the same bulk hydraulic conductivity) could be used to represent rapid transport and pressure propagation through root holes.

The fractures were idealised as constant aperture parallel plate fractures. In cases were only fractures were present in the model, the fracture apertures were determined for each value of fracture spacing considered, such that the bulk vertical hydraulic conductivity of the block was 1×10^{-7} m/s. For the range of fracture spacing considered (0.2-0.5 m), fracture apertures in the range 23.1 μm to 31.4 μm result. For the models in which both root holes and fractures were present, fracture apertures of 2 μm, 5 μm and 10 μm were used. McKay et. al. (1993a) provide a review of fracture apertures determined for a number of clayey deposits in North America, and a range of 1 μm to 210 μm is reported. The fracture apertures considered in the simulations therefore fall within the range of values which has been determined for real deposits.

In all cases, the specific storage for the fracture elements was specified as the compressibility of water, which implies that the fractures are not infilled, and that they do not dilate or close with changes in hydraulic head within the range applied. The formulation for solute transport for fractures in FRAC3DVS is for non-infilled fractures, and therefore, by default, the porosity of these features is 1. Various values of longitudinal dispersivity in the range 0.1 m-1.0 m were considered. In all cases, a retardation coefficient of 1 was specified for the fracture elements.

The root hole was idealised as square in cross-section, with dimensions of 1.0 cm x 1.0 cm for all simulations. Beven and Germann (1982) provide a review of observations of root and worm hole macropores, and report diameters up to 50 mm for these features. The hydraulic conductivity of the root hole elements was chosen in order to give the desired bulk

vertical hydraulic conductivity, using the relationships given in Table 5.1. The value used therefore varied, depending on whether fractures were also present for the case being considered. Values of hydraulic conductivity in the range 3.67×10^{-5} m/s to 4.0×10^{-5} m/s were required. The specific storage of the porous medium elements used to represent the root holes was specified as the compressibility of water, which implies that the root holes are entirely water filled (that is, infilling material is not present in the root holes), and that the root holes do not change in size with changes in pressure. For the solute transport simulations, a porosity of 1 (which again implies that the root holes are entirely water filled), a retardation coefficient of 1, and a longitudinal dispersivity of 0.1m were specified for the root hole elements.

A matrix hydraulic conductivity of 1×10^{-10} m/s and a matrix specific storage of 0.25×10^{-3} m^{-1} were used for all simulations. These values are typical for intact clay materials (McKay et. al., 1993a; Keller et. al., 1986). In all simulations, the porosity, tortuosity and retardation coefficient of the matrix material were specified as 0.4, 0.4 and 1.0 respectively. Parker et. al. (1994) provide a summary of previously published porosity measurements for clay from various sites in North America, and report values in the range 0.3 to 0.6. They also provide a summary of values of tortuosity for the same sites, determined from the difference between free solution diffusion coefficients, and laboratory and field measured effective diffusion coefficients for a variety of conservative solutes. Values of tortuosity in the range 0.28 to 0.625 are reported. A free solution diffusion coefficient of 12.5×10^{-10} m^2/s was used in all the analyses, which is approximately the value reported by Parker et. al. (1994) for chloride. The effective diffusion coefficient for the matrix material is therefore 5×10^{-10} m^2/s.

An example of the spatial discretisation which was employed in the horizontal plane is illustrated in Figure 5.4a, which is the discretisation used for models with root holes, and a

macropore spacing of 0.2 m. A very fine discretisation was required in the vicinity of the macropores in order to resolve the very steep hydraulic head and concentration gradients which exist between these features and the matrix material at early times, and in the case of root holes, to define the column of porous medium elements used to represent the root hole. For the example illustrated in Figure 5.4, a total of 39 nodes were used in each of the x and y directions, with a nodal spacing in the vicinity of the macropores of less than 1 mm. In the vertical direction, a uniform nodal spacing of 5 cm was used for all simulations in which transient hydraulic head was considered. The discretisation used in the vertical direction for the solute transport simulations is also illustrated in Figure 5.4.

The various model parameters which were considered, and the ranges of values that were considered are summarised in Table 5.2.

RESULTS AND DISCUSSION

Simulations of Transient Hydraulic Conditions

The response of the system was considered in terms of the change in head as a function of time at two locations, labelled A and B on Figure 5.5. These locations are equally spaced from the upper and lower boundaries, and location A is at the intersection of the fractures and/or in the root hole, whereas location B is in the clay matrix at the furthest possible distance from a macropore.

The temporal variation in hydraulic head at points A and B are illustrated in Figure 5.6, for various root hole and fracture combinations. For each of these cases, Table 5.3 lists the time required for hydraulic head at points A and B to change by 50% of the total change between the initial condition and the final steady state condition (t^H_{50}). It can be seen that for the extreme cases of root holes only or fractures only (Cases I and V in Figure 5.6), the

macropore geometry greatly influences the response at both points A and B. For the same bulk vertical hydraulic conductivity, the value of t^{H}_{50} at point A is approximately 275 times less for the case of a root hole than for the case of two orthogonal fractures. Similarly, the value of t^{H}_{50} at point B is approximately 4.7 times greater for the case of a root hole than for the case of two orthogonal fractures.

In the case of fractures, the contact area between the clay and the fractures is relatively large in relation to the fracture volume, and thus as the head in the fracture decreases, a relatively large volume of water is released from storage in the clay. This tends to slow the response in the fracture itself. In the case of root holes, the contact area is relatively small in relation to the volume of the root hole, and thus a relatively limited volume of water is released from storage in the clay due to a decrease in head in the root hole. The response in the root hole is thus slowed very little from what it would be if the matrix were impermeable.

At locations in the matrix, the response depends to a large extent on the distance to the closest macropore. As a first approximation, the response time at a particular point will increase with the square of the distance to the nearest macropore, based on a consideration of the solutions of the transient flow equation given by Terzaghi (1943) and Theis (1935) for conditions of one-dimensional and radial flow respectively. In the case of models with root holes only, the distance from point B to the root hole is 1.4 times greater than the minimum distance from point B to a fracture, in models which include fractures.

From the results of simulations in which both fractures and a root hole were present (Cases II to IV in Figure 5.6), it can be seen that transfer of fluid from the root hole to relatively small fractures can act to effectively increase the surface area of the root hole, and thus retard the response in the root hole and increase the rate of response in the matrix. Considering Case III in Figure 5.6 and in Table 5.3, it can be seen that although almost 99% of the total flux

passes through the root hole, the presence of two 5 μm fractures increases t^H_{50} at point A by a factor of approximately 20 and decreases t^H_{50} at point B by a factor of approximately 4.1, compared to the case in which no fractures are present. The large influence of even relatively small fractures intersecting the root hole can also be readily seen from a comparison of hydraulic head distributions for the different macropore geometries. Distributions of hydraulic head at t=10000 seconds at the elevation of points A and B are illustrated in Figure 5.7, for Cases I, III and V from Figure 5.6.

The results from models in which both root holes and fractures are present can be used to assess the applicability of parallel plate fracture models for interpreting transient hydraulic data from systems in which flow occurs preferentially through only a small fraction of the fracture area (either through root holes located along the fracture surface or through isolated large aperture regions). In Figure 5.8, the variation in head as a function of time at point A is compared for a series of systems which have fractures only, and a system which has a root hole and 5 μm fractures. In all cases, the bulk hydraulic conductivity is $1x10^{-7}$ m/s. For the systems with fractures only, various combinations of aperture and spacing with this value of bulk hydraulic conductivity were used. It can be seen that models which represent flow through parallel plate fractures only can not be used to reproduce the results obtained for the case in which the majority of the flow takes place through the root hole.

Since macropore geometry exerts such a strong influence on transient hydraulic response, and since simplified models such as parallel plate fracture models appear to be of limited applicability to situations in which flow channelling occurs, direct observations of the macropores and of the preferential flow pathways within the macropores will provide important information that will assist in the interpretation of transient hydraulic phenomena. Direct observations of preferential flow pathways can be made using visible tracers such as dyes (for

example, Bouma et. al., 1977; Chapter 1), or chemical tracers such as solvent DNAPL (O'Hara et. al., 1997).

Simulations of Solute Transport

For the solute transport simulations, the response of the system was considered in terms of the change in concentration as a function of time at three locations, labelled C, D and E on Figure 5.5. Points C and D are located at a distance of 1m from the upper, constant concentration boundary. Point C is at the intersection of the fractures and/or in the root hole, whereas location D is in the clay matrix at the furthest possible distance from a macropore. Point E is located at the intersection of the fractures and/or in the root hole at a distance of 3m from the upper boundary.

The temporal variations in concentration at points C and D are illustrated in Figure 5.9 for various root hole and fracture combinations. For each of these cases, the time required for the concentration at points C and D to reach 50% of the concentration applied at the upper boundary (t^{C}_{50}) is given in Table 5.4. It can be seen that the effects of macropore geometry on solute transport are similar to those observed for hydraulic transients. A considerably faster breakthrough in the macropore and a slower response in the matrix are again observed when the case of root holes only is compared to the case of fractures only (Cases I and IV in Figure 5.9). Similarly, the diffusive mass transfer of solute mass from the root hole to relatively small fractures, and from there into the matrix, can be seen to effectively retard the movement of solute through the root hole (Cases II and III in Figure 5.9)

The dependence of macropore concentrations on the contact area to volume ratio for the macropore, and the variation in response in the matrix as a function of distance from the nearest macropore, is due to the same mechanisms described previously for transient

hydraulic conditions. The process of solute diffusion in the matrix is described by the same equation as that describing fluid flow in the matrix, however the parameters in the equation have different physical meanings and very different magnitudes for the two processes. In the case of the solute transport simulations, a value of $5x10^{-10}$ m^2/s was used for the effective diffusion coefficient in the matrix, whereas a matrix hydraulic diffusivity of $4x10^{-7}$ m^2/s was used in the transient hydraulic simulations. It is primarily due to this difference that the values of t^H_{50} at point B vary from 6320 seconds to 29500 seconds for the transient hydraulic simulations, and the values of t^C_{50} at point D vary from 224 days to 410 days for the solute transport simulations.

Bouma and Woesten (1979) measured the breakthrough of a chloride tracer through laboratory scale soil columns with different macropore structures. They observed extremely rapid breakthrough in saturated columns which contained vertical worm channels, and relatively much slower breakthrough (1-2 orders of magnitude slower) in columns which contained smooth peds but no worm channels. In their analysis, no allowance was made for the effects of matrix diffusion, and it was concluded that the differences in breakthrough indicated a difference in the vertical connectivity between the two types of macropores. However, on the basis of the differences in behaviour illustrated in Figure 5.9 for different macropore structures, the measured differences may have been partly due to differences in the ratio of macropore/matrix contact area to macropore volume.

It was determined in the previous section that for transient hydraulic phenomena, models with fractures only can not be used to reproduce the response obtained from models in which fractures are present, but the majority of the flow takes place through the root hole. This was not, however, found to be the case for solute transport. In Figure 5.10, the calculated responses at points C and E for a system with a root hole and 5 μm fractures is compared to

the responses at these points for a system with the same bulk hydraulic conductivity, but fractures only. Although there are differences, particularly in the shapes of the curves for the response at point C, the match between different simulations which is illustrated in Figure 5.10 would in most instances be regarded as a good match if field data were being compared to model results. The curves illustrated in Figure 5.10 for the model with fractures only were derived for a fracture aperture of 31.4 μm, a fracture spacing of 0.5 m, and a longitudinal dispersivity of 0.8m in the fracture. In this instance, these parameters are simply fitting parameters, which have been used with the parallel plate fracture model to reproduce the response of a system with different geometry. It is significant, however, that the same fitting parameters can be used to match the desired responses at two different points in the system, and that the values are therefore not unique to a particular location in the system. This suggests that if solute breakthrough data at a particular point in a real system can be matched using a parallel plate model, it may be possible to use the model with the fitted parameters to predict the breakthrough at other locations and times, even in cases where there is a strong tendency for flow channelling to occur.

CONCLUSIONS

Numerical simulations have shown that the process of fluid transfer from macropores to the adjacent clay matrix influences the propagation of pressure perturbations in saturated compressible media in much the same manner as the process of matrix diffusion influences the transport of solutes through macropores. They have also shown that fluid and solute mass transfer from a very isolated, highly conductive channel in a fracture to adjacent low aperture regions of the fracture, and from there into the matrix material, can also very effectively retard the movement of solutes and the propagation of pressure perturbations.

Simulations performed with different macropore geometries indicate that the ratio of macropore/matrix contact area to macropore volume exerts an important control on the propagation of pressure perturbations and on the transport of solutes through the macropore network, as a result of the different relative influence of the processes of matrix diffusion (both fluid and solute transfer) for different values of this parameter. In the case of planar features such as fractures, the contact area between the macropore and the adjacent clay is large in relation to the macropore volume, and thus differences in hydraulic head or solute concentration between the macropore and the matrix induce relatively large fluid or solute flux between the two. In the case of linear features such as root holes, the contact area is small in relation to the macropore volume, and thus only limited fluid or solute exchange takes place between the macropore and the matrix as a result of hydraulic head or concentration gradients. The damping of pressure perturbations and the retardation of solute migration as they move through the macropores will both be more pronounced in cases with increased mass transfer to or from the matrix.

It was found that the hydraulic response of systems in which there is a strong tendency for flow channelling could not be adequately approximated using parallel plate fracture models, whereas solute transport in such systems could be adequately described using parallel plate fracture models. This suggests that in some instances, detailed examination of preferential flow paths may be required to interpret transient hydraulic tests.

REFERENCES

Barenblatt, G.I., Iu. P. Zheltov, and N. Kochina, Basic concepts in the theory of seepage of homogeneous liquids in fissured rocks, *J. Appl. Math. Mech.*, 24, 1286-1303, 1960.

Beven, K., and P.Germann, Water flow in soil macropores II. A combined flow model, *J. Soil Sci.*, 32, 15-29, 1981.

Beven, K., and P. Germann, Macropores and water flow in soils, *Water Resour. Res.*, 18(5), 1311-1325, 1982.

Bouma, J., A. Jongerius, O. Boersma, A. Jager and D. Schoonderbeek, The function of different types of macropores during saturated flow through four swelling soil horizons, *Soil Sci. Soc. Am. J.*, 41, 945-950, 1977.

Bouma, J. and L.W. Dekker, A case study on infiltration into dry clay soil 1. Morphological observations, *Geoderma*, 20, 27-40, 1978.

Bouma, J., and J.H.M. Woesten, Flow patterns during extended flow in two, undisturbed swelling clay soils with different macrostructures, *Soil Sci. Soc. Am. J.*, 43, 16-22, 1979.

Dykhuizen, R.C., Transport of solutes through unsaturated fractured media, *Water Res.*, 21(12), 1531-1539, 1987.

Foster, S.S.D., The Chalk groundwater tritium anomaly - a possible explanation, *J. Hydrol.*, 25, 159-165, 1976.

Gerke, H.H. and M.T. van Genuchten, Evaluation of a first-order water transfer term for variably saturated dual-porosity flow models, *Water Resour. Res.*, 29 (4), 1225-1238, 1993.

Hendry, M.J., Hydraulic conductivity of a glacial till in Alberta, *Groundwater*, 20 (2), 162-169, 1982.

Hinsby, K., L.D. McKay, P. Jorgensen, M. Lenczewski and C.P. Gerba, Fracture aperture measurements and migration of solutes, viruses and immiscible creosote in a column of clay-rich till, *Groundwater*, 34(6), 1065-1075, 1996.

Johns, R.A. and P.V. Roberts, A solute transport model for channelized flow in a fracture, *Water Resour. Res.*, 27(8), 1797-1808, 1991.

Kazemi, H., Pressure transient analysis of naturally fractured reservoirs with uniform fracture distribution, *Soc. Petrol. Eng. J.*, 4, 451-462, 1969.

Keller, C.K., G. van der Kamp, and J.A. Cherry, Fracture permeability and groundwater flow in clayey till near Saskatoon, Saskatchewan, *Can. Geotech. J.*, 23, 229-240, 1986.

McKay, L. D., J.A. Cherry, and R. W. Gillham, Field experiments in a fractured clay till 1. Hydraulic conductivity and fracture aperture, *Water Resour. Res.*, 29(4), 1149-1162, 1993a.

McKay, L.D., R.W. Gillham, and J.A. Cherry, Field experiments in a fractured clay till 2. Solute and colloid transport, *Water Resour. Res.*, 29(12), 3879-3890, 1993b.

McKay, L.D., and J. Fredericia, Distribution, origin, and hydraulic influence of fractures in a clay-rich glacial deposit, *Can. Geotech. J.*, 32, 957-975, 1995.

Nordqvist, A.W., Y.W. Tsang, C.F. Tsang, B. Dverstorp, and J. Andersson, A variable aperture fracture network model for flow and transport in fractured rocks, *Water Resour. Res.*, 28(6), 1703-1713, 1992.

Novakowski, K.S. and P. A. Lapcevic, Field measurement of radial solute transport in fractured rock, *Water Resour. Res.*, 30(1), 37-44, 1994.

O'Hara, S.K., B.L. Parker, P.R. Jorgenson and J.A. Cherry, Trichloroethene DNAPL flow and mass distribution in naturally fractured clay: 1. Evidence of aperture variability, Submitted to *Water Resour. Res.*, November 1997.

Parker, B.L., R.W. Gillham, and J.A. Cherry, Diffusive disappearance of immiscible-phase organic liquids in fractured geologic media, *Groundwater*, 32 (5), 805-820, 1994.

Raven, K.G., K.S. Novakowski and P.A. Lapcevic, Interpretation of field tracer tests of a single fracture using a transient solute storage model, *Water Resour. Res.*, 24(12), 2019-2032, 1988.

Rudolph, D.L., J.A. Cherry, and R.N. Farvolden, Groundwater flow and solute transport in fractured lacustrine clay near Mexico City, *Water Resour. Res.*, 27(9), 2187-2201, 1991.

Ruland, W. W., J.A. Cherry, and S. Feenstra, The depth of fractures and active groundwater flow in a clayey till plain in south-western Ontario, *Groundwater*, 29(3), 405-417, 1991.

Terzaghi, K., Theoretical Soil Mechanics, John Wiley and Sons, New York, 1943.

Theis, C.V., The relation between the lowering of the piezometric surface and the rate and duration of discharge of a well using ground-water storage, *Trans. Am. Geophys. Union*, 16, 519-524, 1935.

Therrien, R., E.A. Sudicky and R.G. McLaren, Users guide for NP - A preprocessor for FRAC3DVS: An efficient simulator for three-dimensional, saturated-unsaturated groundwater flow and chain-decay solute transport in porous or discretely fractured porous formations, University of Waterloo, 1995.

Therrien, R. and E.A. Sudicky, Three-dimensional analysis of variably-saturated flow and solute transport in discretely-fractured porous media, *J. Cont. Hydrol.*, 23, 1-44, 1996.

Tsang, Y.W. and C.F. Tsang, Channel model of flow through fractured media, *Water Resour. Res.*, 23(3), 467-479, 1987.

Warrren, J.E. and P.J. Root, The behavior of naturally fractured reservoirs, *Soc. Petrol. Eng. J.*, 3, 245-255, 1963.

Wild, A. and I.A. Babiker, The asymmetric leaching pattern of nitrate and chloride in a loamy sand under field conditions, *J. Soil Sci.*, 27, 460-466, 1976.

Macropore geometry	Expression for calculating bulk vertical hydraulic conductivity (K_{bulkv})
root holes only	$K_{bulkv} = K_r \cdot A_r / (2B)^2 + K_m$
fractures only	$K_{bulkv} = 2 \cdot \rho g \cdot (2b)^3 / (2B \cdot 12 \cdot \mu) + K_m$ *
fractures and root holes	$K_{bulkv} = 2 \cdot \rho g \cdot (2b)^3 / (2B \cdot 12 \cdot \mu) + K_r \cdot A_r / (2B)^2 + K_m$ *

Notes:

1. K_r = hydraulic conductivity of root hole material; A_r = cross-sectional area of root hole; 2B = spacing of macropores; K_m = matrix hydraulic conductivity; ρ = density of water; g = gravitational acceleration; 2b = fracture aperture; μ = viscosity of water.

* adapted from Snow (1969)

Table 5.1 - Relationships between bulk vertical hydraulic conductivity and macropore properties

Component of Model Domain	Hydraulic and solute transport parameters	
matrix	K_m=1x10^{-10} m/s S_m=0.25x10^{-3} m^{-1} α_m=0.1 m	τ_m=0.4 R_m=1.0 n_m=0.4
root hole	A_r=1x10^{-4} m^2 2B=0.2-0.5 m **K_r=3.67-4.0x10^{-5} m/s** S_r=β	α_r=0.1 m R_r=1.0 n_r=0.4
fractures	2B=0.2-0.5 m **2b=2-31.4 mm** S_f=β	**α_f=0.1-1.0 m** R_f=1.0 n_f=1.0

Notes:

1. parameters in bold were varied, other parameters were maintained constant.

2. S_m, S_r, S_f=specific storage of matrix, root hole and fractures respectively; α_m, α_r, α_f=longitudinal dispersivity for matrix, root hole and fractures respectively; R_m, R_r, R_f=retardation coefficient for matrix, root hole and fractures respectively; n_m, n_r, n_f=porosity of matrix, root hole and fractures respectively; τ_m=matrix tortuosity.

3. β= the compressibility of water = 4.74x10^{-10} m^2/N.

4. a free solution diffusion coefficient of 12.5x10^{-10} m^2/s was used in all simulations.

Table 5.2 - Parameters used in modelling

Macropores present	t^{H}_{50} + in macropores (Point A) (seconds)	t^{H}_{50} + in matrix (Point B) (seconds)	Percentage of flux passing through root hole ++
Case I - root hole only	0.55	29500	99.9
Case II - root hole and 2 μm fractures	0.14	14500	99.84
Case III - root hole 5 μm fractures	1.1	7150	98.89
Case IV - root hole 10 μm fractures	8.5	6470	91.81
Case V - 23.1 μm fractures only	15	6320	-

Notes:

1. $K_{bulkv} = 1x10^{-7}$ m/s in all cases.
2. the locations of Point A and Point B are illustrated in Figure 5.5.

\+ t^{H}_{50} = the time required for the hydraulic head change at a point to reach 50% of its final value.

++ percentage of flux passing through the root hole at steady state. Prior to the attainment of steady state conditions, the contribution of the root hole will be greater than this.

Table 5.3 - Influence of macropore geometry on transient hydraulic response

Macropores present	t^{C}_{50} + in macropores (Point C) (days)	t^{C}_{50} + in matrix (Point D) (days)	Percentage of flux passing through root hole ++
Case I - root hole only	1.55	2550	99.9
Case II - root hole and 5μm fractures	3.95	1060	99.89
Case III - root hole and 10μm fractures	37.5	670	91.81
Case IV - 23.1μm fractures only	55.5	650	-

Notes:

1. K_{bulkv} = $1x10^{-7}$ m/s in all cases.
2. the locations of Point C and Point D are illustrated in Figure 5.5.

+ t^{C}_{50} = the time required for the solute concentration at a point to reach 50% of the value at the upper, constant concentration boundary.

++ percentage of flux passing through the root hole at steady state. Prior to the attainment of steady state conditions, the contribution of the root hole will be greater than this.

Table 5.4 - Influence of macropore geometry on solute transport behaviour

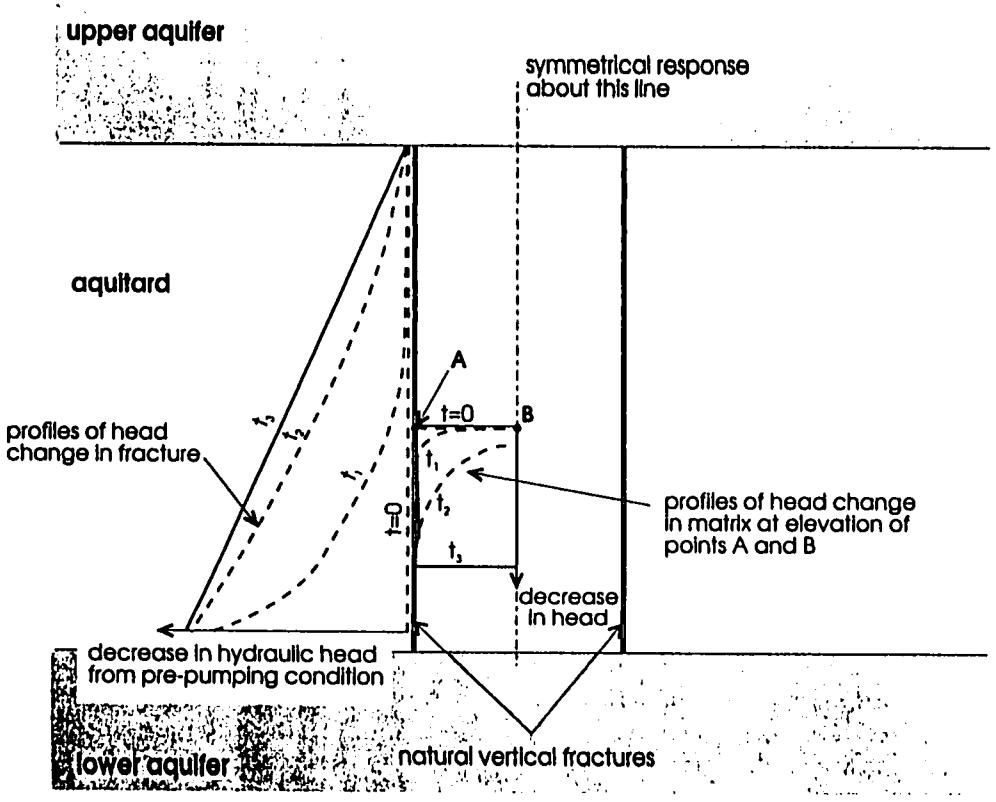

a) Profiles of hydraulic head along vertical fractures and through matrix at various times after head decrease in lower aquifer

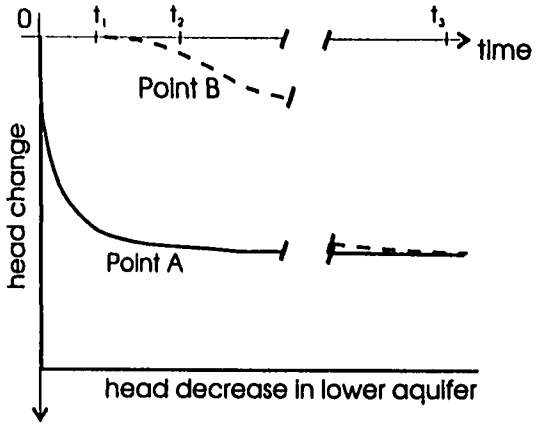

b) Changes in hydraulic head at Points A and B following application of pressure perturbation at surface

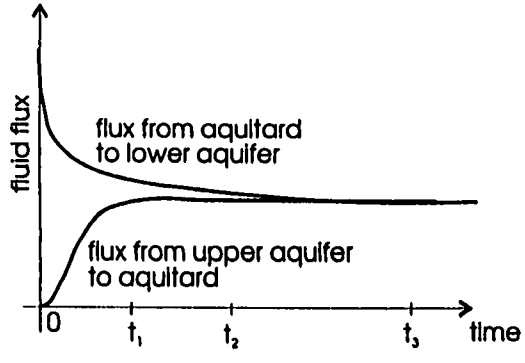

c) Temporal variations in fluid flux at aquifer/ aquitard boundaries

Figure 5.1 - Idealised transient hydraulic behaviour in fractured porous media

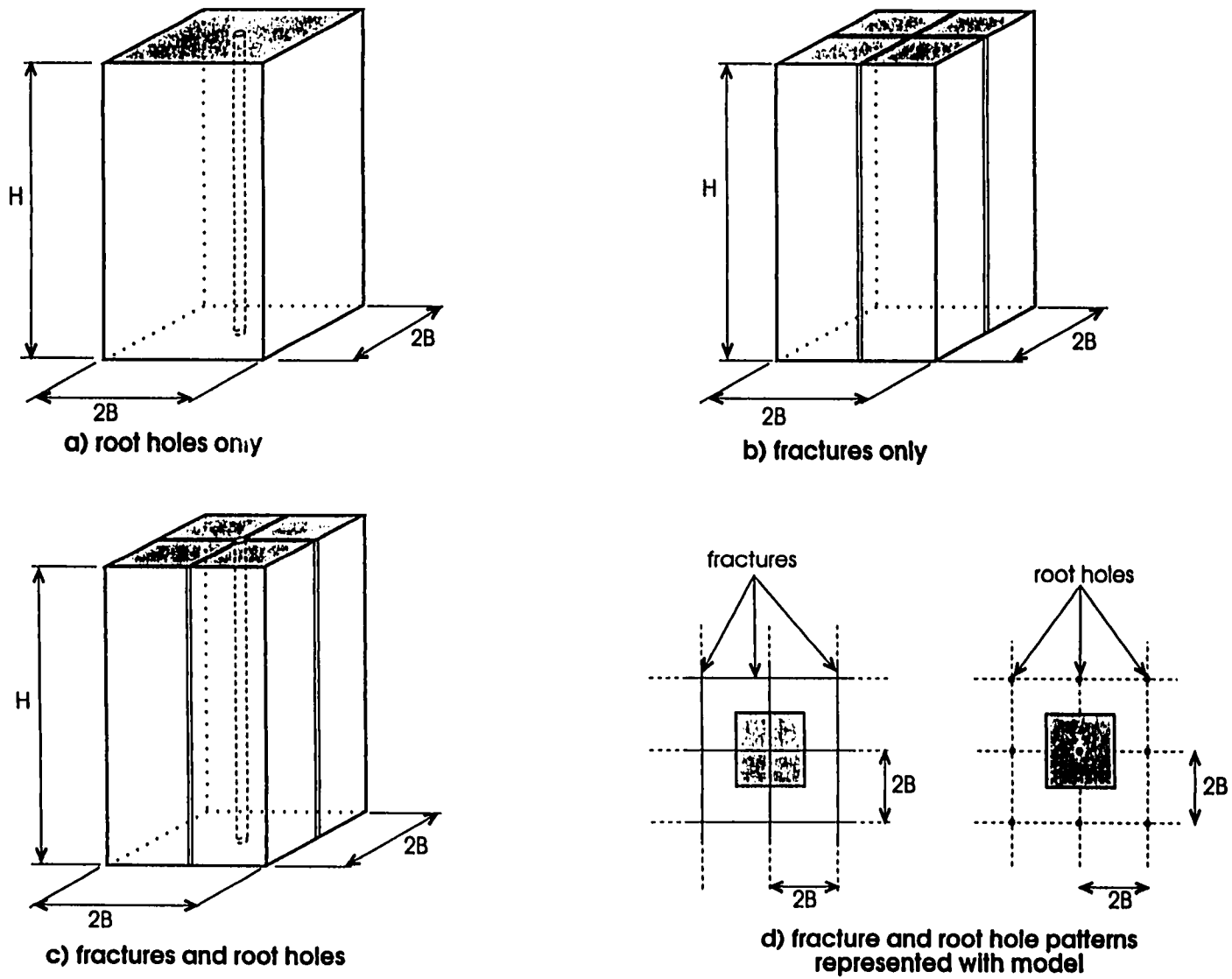

Figure 5.2 - Macropre geometries considered in modelling

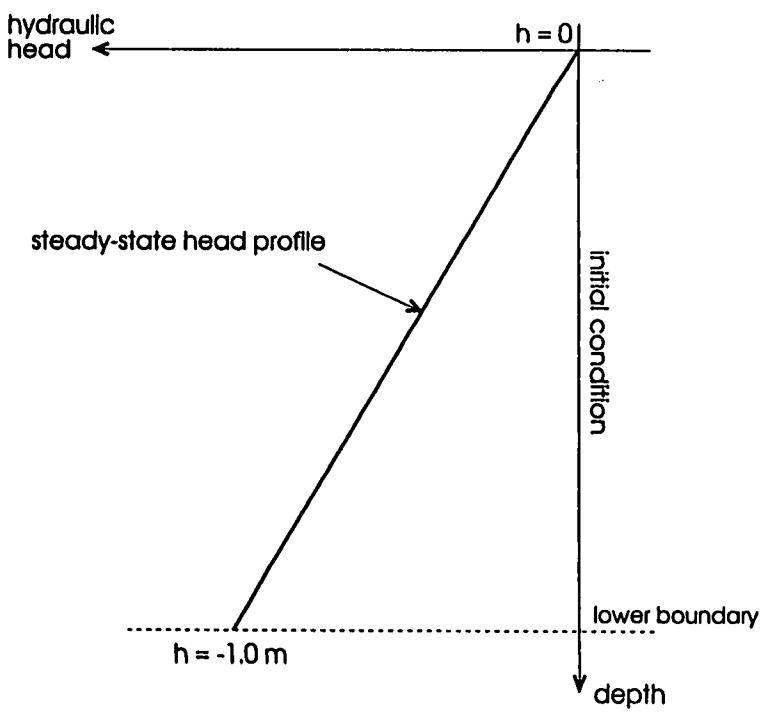

a) simulations of transient hydraulic behaviour

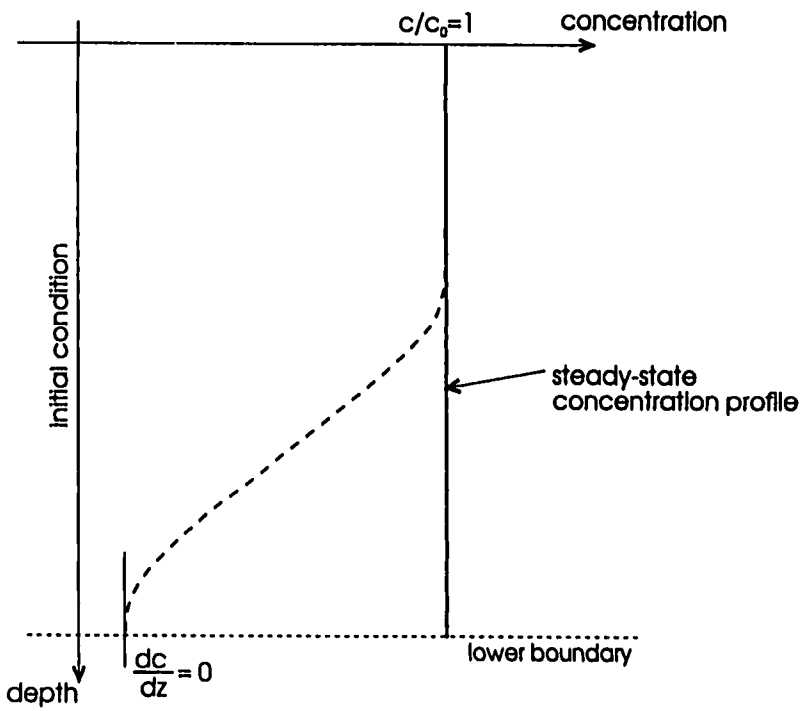

b) solute transport simulations

Figure 5.3 - Initial and boundary conditions for transient hydraulic and solute transport simulations

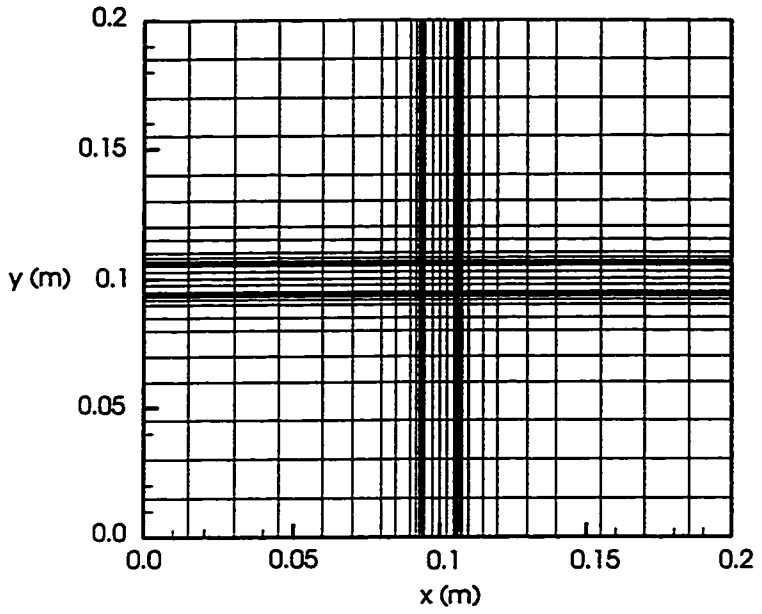

a) discretisation used in horizontal plane

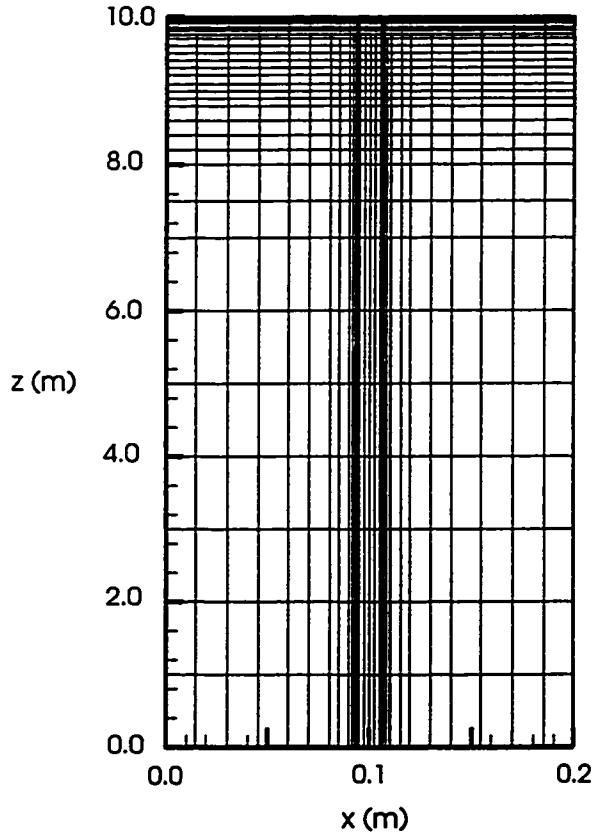

b) discretisation used in vertical plane

Figure 5.4 - Example of spatial discretisation used in numerical model

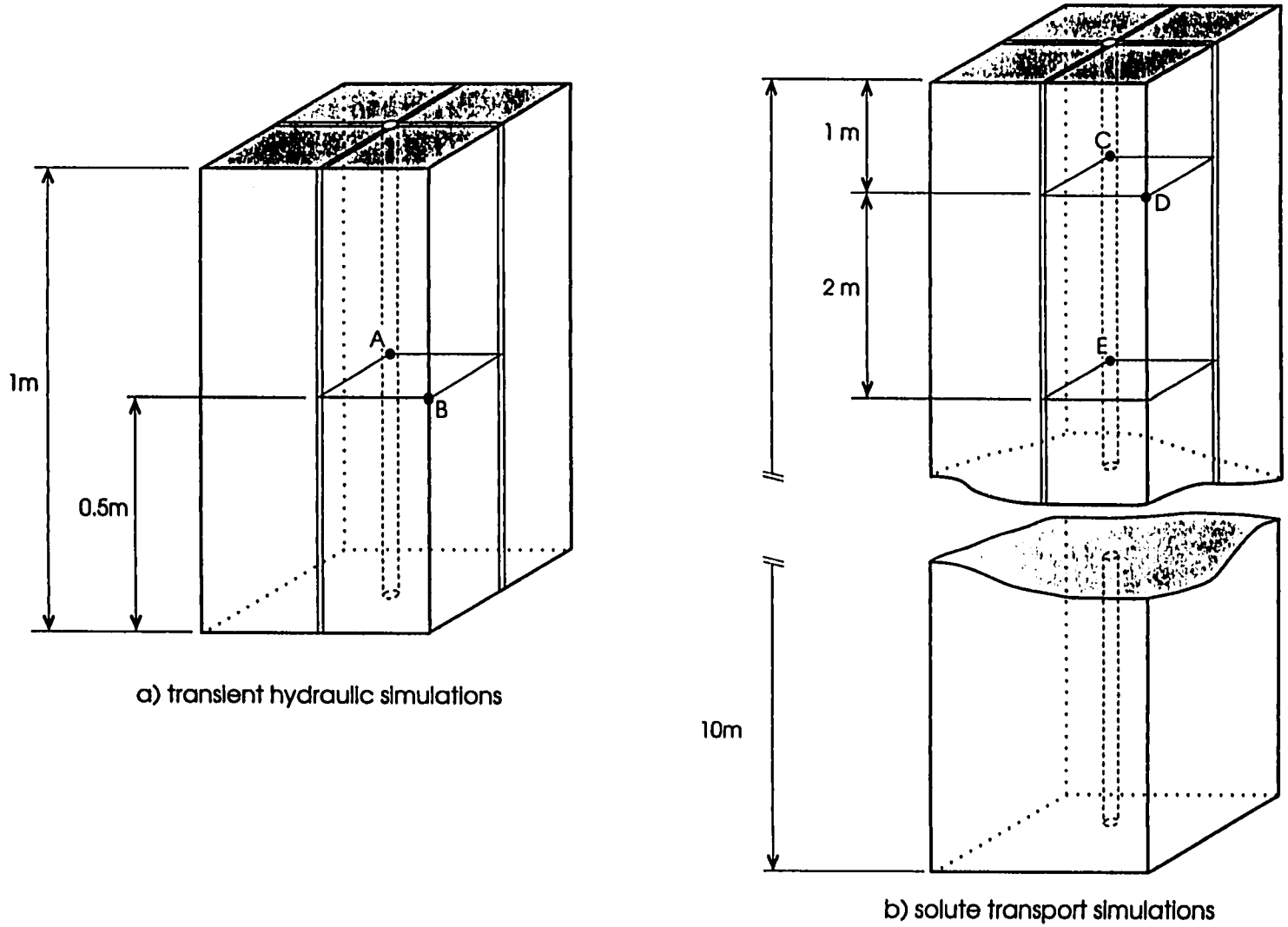

Figure 5.5 - Locations in macropores and in matrix at which hydraulic head and solute concentration variations considered

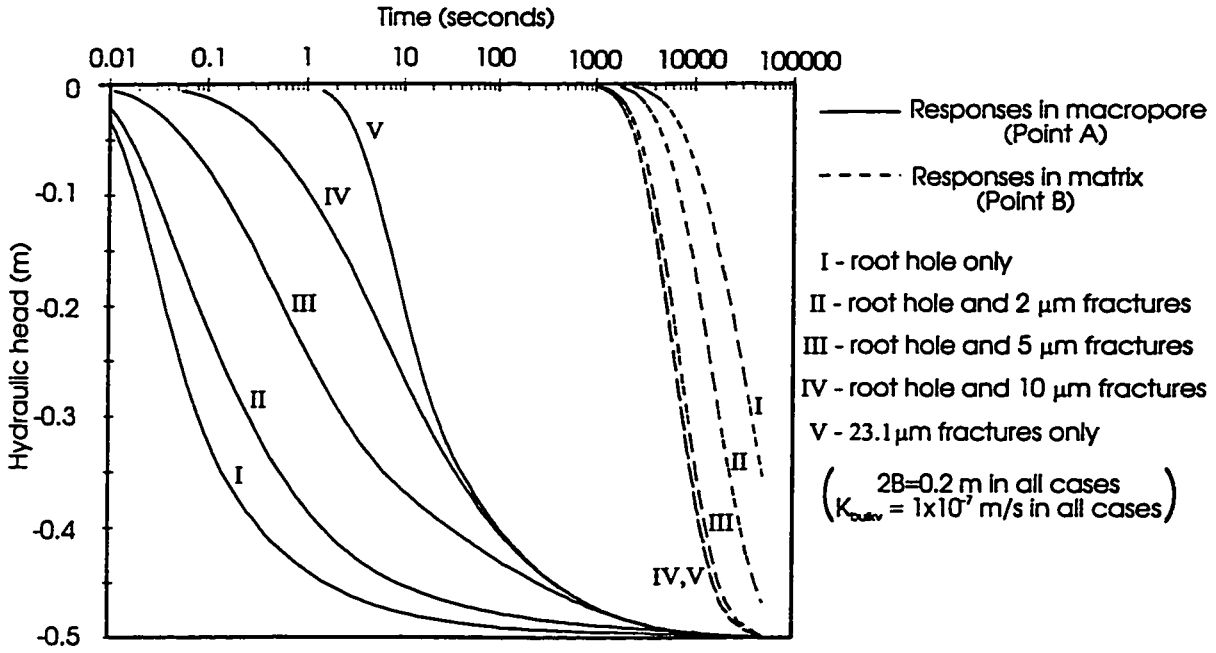

Figure 5.6 - Influence of macropore geometry on hydraulic head at points A and B

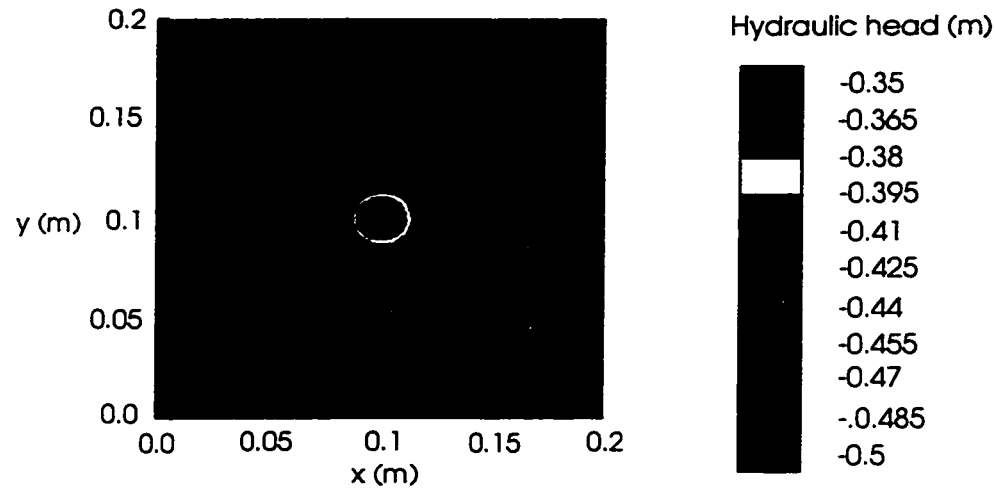

a) Case I - root hole only

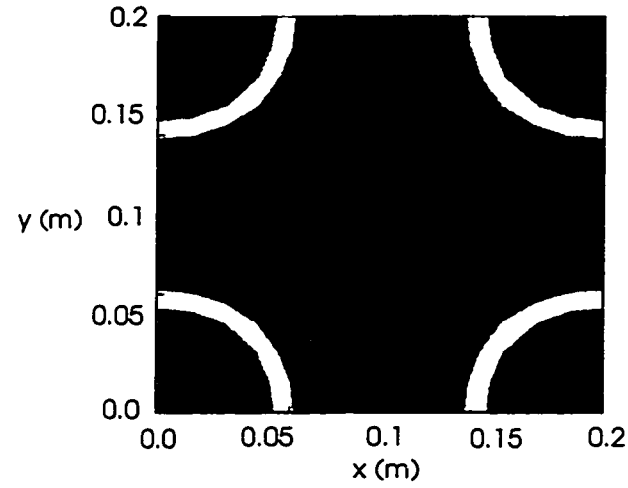

b) Case III - root hole and 5 μm fractures

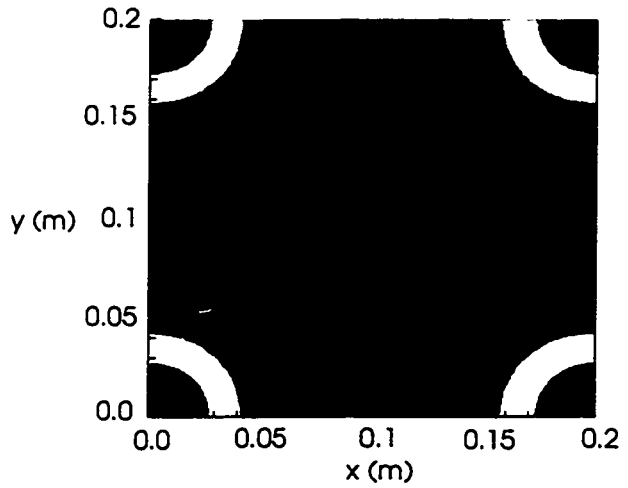

c) Case V - 23.1 μm fractures only

Figure 5.7 - Distributions of hydraulic head at the elevation of points A and B at t=10000 seconds

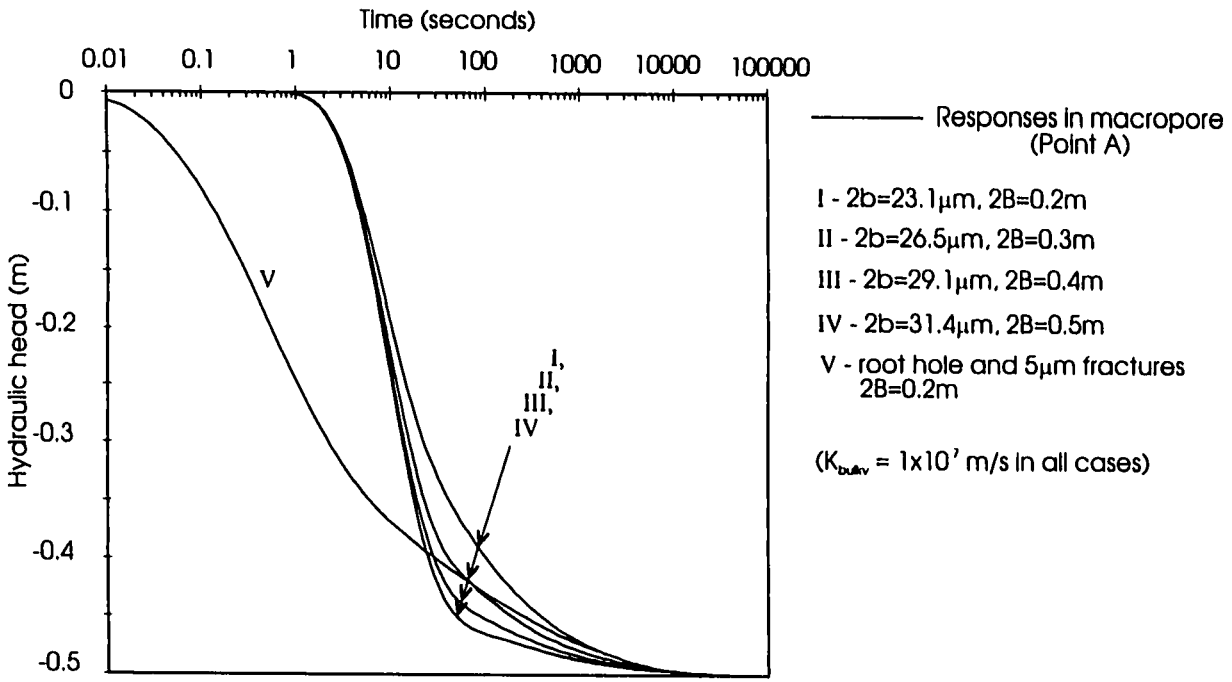

Figure 5.8 - Attempt to match transient hydraulic behaviour of combined fracture and root hole system using system with fractures only

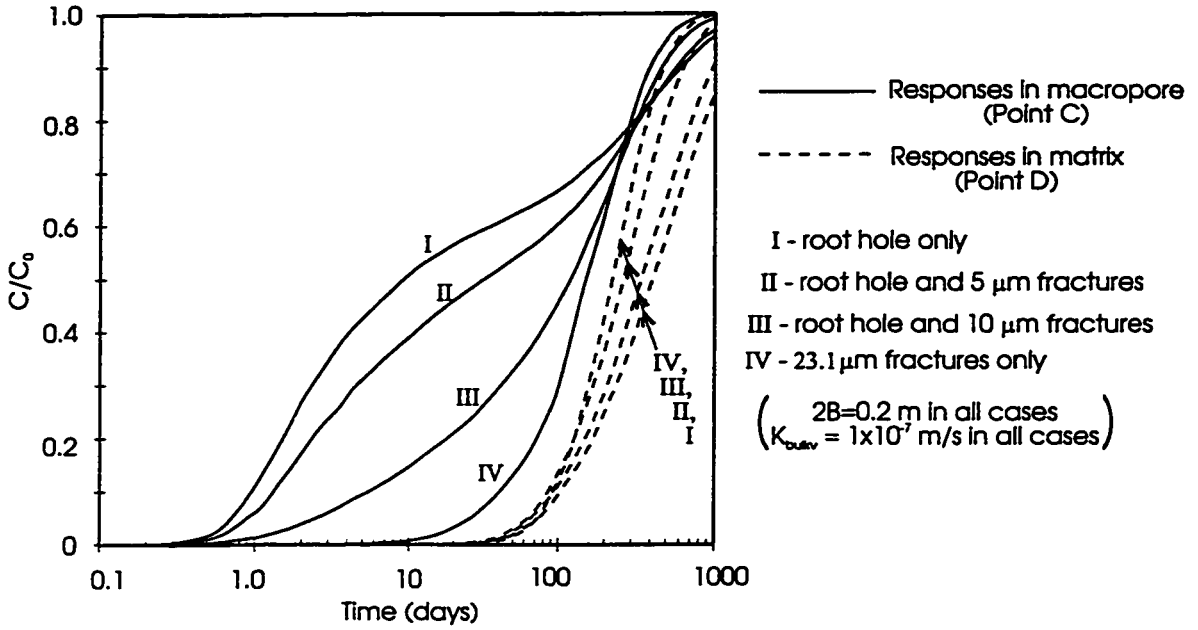

Figure 5.9 - Influence of macropore geometry on solute concentrations at points A and B

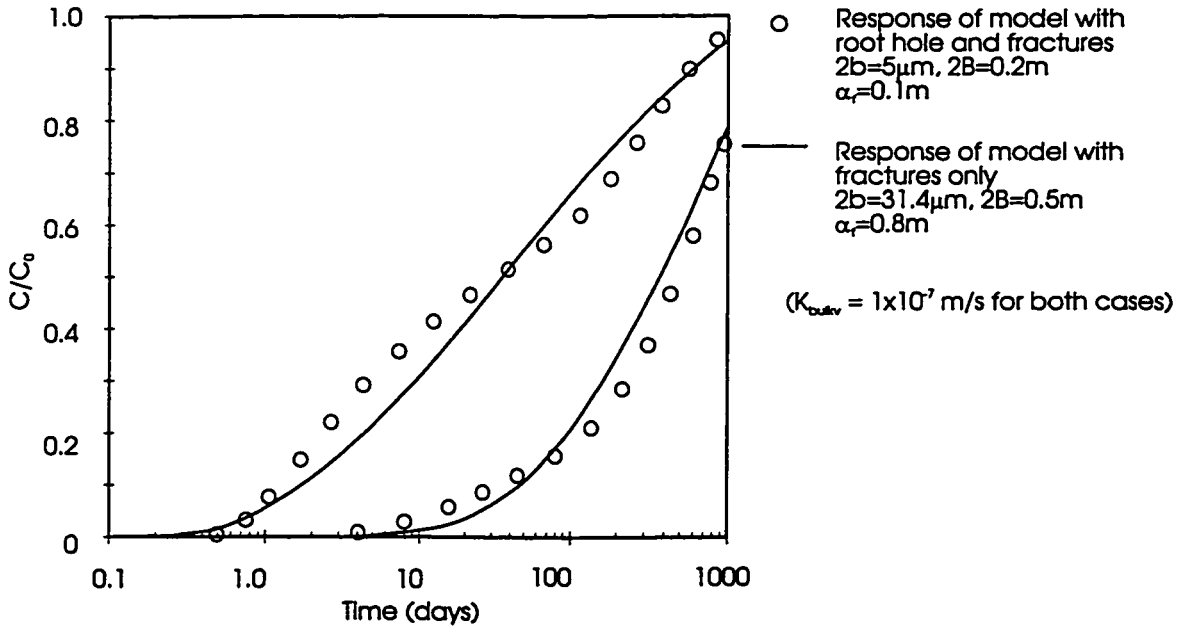

Figure 5.10 - Approximation of solute transport behaviour of combined fracture and root hole system using system with fractures only

CHAPTER 6

SUMMARY OF CONCLUSIONS

Hydraulic testing and mapping of fractures and other macropore features has been carried out in the near-surface, highly fractured and weathered clay at two nearby sites in the St. Clair Clay plain in south-western Ontario. The results of the mapping provide the context and important parameters for the interpretation of the hydraulic tests. In a broader context, the results of the mapping indicate the potential variability in fracture patterns between two nearby sites within the same clay plain. Although surface observations at the sites, which were separated by approximately 1 km, did not reveal any features that suggest they are atypical of the clay plain in general, two very different fracture patterns were observed in the weathered near-surface clay at the two sites considered.

At the first site, the fracture pattern was qualitatively similar to that observed in five previous investigations conducted in the same area. At this site, major fractures (so-called first- and second-order fractures) in the weathered clay are predominantly vertical. The most persistent of these fractures are greater than 1.5 m in length, and tend to cross-cut other less persistent fractures which they intersect. The clay between the first- and second-order fractures is in some areas divided into roughly cubic peds on the order of 1 cm in size by closely spaced vertical and horizontal fractures (so-called third-order fractures). No change in the nature of the fracture pattern was apparent between 0.6 m and 2.5 m below ground surface.

At the second site, major fractures in the upper 1.5 m tend to be randomly oriented and generally less persistent than at the first site, terminating in most cases at their intersection with other fractures rather than cross-cutting them. Randomly oriented third-order fractures dividing the clay into irregular peds with an average maximum dimension of 1.5 cm are present throughout to a depth of 1.5 m. Below 1.5 m, the fracture pattern at the second site is qualitatively similar to that observed at the first site.

Another substantial difference between the two sites is the presence at the second site of primarily vertical cylindrical cavities which were loosely infilled with "plugs" of soft silty clay material. The cavities themselves were up to 5 cm in diameter, although a zone of soft and moist clay of up to 10 cm in diameter was present around most of the cavities. The cavities were observed to be continuous for distances of up to 1m. The origin of the cavities is not known, however it is postulated that they may be abandoned root holes from large trees which were present in the area prior to the commencement of agriculture in the 19th century. They have not been reported in any of the previous investigations that have been conducted at nearby sites.

Mapping of preferential flow paths at the second site was carried out by infiltrating a dye and then mapping its distribution in the subsurface. It was found that the cavities were major conduits for fluid flow, both through the open annulus between the walls of the cavities and the "plugs" of infilling material, and through highly fractured zones immediately surrounding the cavities. Open root holes, often located along fracture faces, were also identified as important conduits for fluid flow. Dye staining did not indicate distributed flow throughout the plane of major fractures in any instances. Although closely spaced, third-order fractures were present throughout in the area of dye infiltration, they were generally only stained in the immediate vicinity of the cavities, which indicates that they are not, in general, highly conductive.

A comparison of fracture mapping on vertical and horizontal faces at the first site indicates that the common practice of determining average fracture spacing from vertical profiles only, and then idealising the fracture network as equally spaced parallel fractures will not in general produce an idealised network which is equivalent to the actual network in terms of important parameters which control flow and transport. Important information, such as the

lateral persistence of fractures, is not obtained from mapping on vertical profiles only, and therefore complimentary mapping on horizontal surfaces is also required.

Hydraulic testing was carried out at the two sites using an experimental arrangement in which a pond was maintained at the surface, overlying several flat-lying sand-filled induced fractures. This arrangement was used to conduct a variety of transient and steady state hydraulic tests, which were monitored using a network of electronic strain gauge pressure transducers. At both sites, the pond and induced fractures were several metres in diameter, and thus influence a relatively large volume of the fractured clay, in proportion to the volume that would be tested with single-well tests.

Steady state conditions during pumping tests in which water was pumped from the induced fractures allowed the calculation of vertical hydraulic conductivity and its variation with depth, and also indirectly allow horizontal hydraulic conductivity to be estimated. At the first site, it was found that vertical hydraulic conductivity does not change with depth in the weathered clay, whereas vertical hydraulic conductivity decreased by an order of magnitude over the depth of the weathered zone at the second site. At the second site, an abrupt decrease in hydraulic conductivity was observed at the interface between the weathered clay and the unweathered clay, which is interpreted to indicate an abrupt decrease in fracture hydraulic aperture. Furthermore, the ratio of bulk horizontal hydraulic conductivity to bulk vertical hydraulic conductivity is much lower at the second site than at the first site. This is interpreted to be a consequence of the dominating influence of the cavities observed at the second site. Although a network of interconnected vertical fractures can impart a relatively large bulk horizontal hydraulic conductivity, the isolated, primarily vertical cavities will do little to enhance horizontal conductivity.

A comparison of the values of hydraulic conductivity measured at different scales at the Laidlaw site indicates that at larger scales, hydraulic conductivity is controlled by the influence of a network of widely spaced, laterally persistent, interconnected fractures which have not been intercepted by the numerous small-scale single well response tests that have previously been carried out at the site.

The use of induced fractures to conduct pumping tests made it possible to observe differences in behaviour between the fracture network and the clay matrix during transient hydraulic tests. The results of pumping tests conducted at the first site indicates that disequilibrium between fractures and the clay matrix can persist for several hours. Thus in general, interpretation of scenarios in which hydraulic conditions vary on the time scale of hours or less will require models which account for the interaction between the fractures and the clay. Such models can reproduce certain aspects of behaviour, such as the rapid transmission of pressure through fractures and the concurrent slow changes in pressure in the clay matrix, which can not be described using equivalent porous medium models.

In this study, a numerical model was used which allows fractures to be represented as discrete features, and which thus explicitly accounts for interactions between the clay matrix and the fractures. Using this approach, the results of falling head tests conducted in the induced fractures were used to obtain values of bulk vertical hydraulic conductivity and specific storage for the clay which are consistent with values measured independently in other tests. The results of the pumping test were also used to derive a range of values for the average fracture aperture for the fractures beneath the pond. The values obtained are larger than those obtained previously at the site.

Numerical simulations were carried out to investigate the influence of macropore geometry on the transfer of fluid and dissolved solutes between highly conductive macropores

and the adjacent low conductivity clay. Simulations performed with different macropore geometries indicate that the ratio of macropore/matrix contact area to macropore volume exerts an important control on the propagation of pressure perturbations and on the transport of solutes through the macropore network. This is a consequence of the different relative influence of the processes of matrix diffusion (both fluid and solute transfer) for different values of this parameter. In the case of planar features such as fractures, the contact area between the macropore and the adjacent clay is large in relation to the macropore volume, and thus differences in hydraulic head or solute concentration between the macropore and the matrix induce relatively large fluid or solute flux between the two. In the case of linear features such as root holes, the contact area is small in relation to the macropore volume, and thus only limited fluid or solute exchange takes place between the macropore and the matrix as a result of hydraulic head or concentration gradients. The damping of pressure perturbations and the retardation of solute migration as they move through the macropores will both be more pronounced in cases with increased mass transfer to or from the matrix.

The simulations also indicated that fluid and solute mass transfer from a very isolated, highly conductive channel in a fracture to adjacent low aperture regions of the fracture, and from there into the matrix material, can also very effectively retard the movement of solutes and the propagation of pressure perturbations. It was found that the hydraulic response of systems in which there is a strong tendency for flow channelling could not be adequately approximated using parallel plate fracture models, whereas solute transport in such systems could be adequately described using parallel plate fracture models. This suggests that in some instances, detailed examination of preferential flow paths may be required to interpret transient hydraulic tests.

APPENDIX A

IMPLEMENTATION OF A ZERO-LENGTH WELL-SCREEN CONDITION IN FRAC3DVS

The partial differential equation describing one-dimensional flow along a well screen is given by Sudicky et. al. (1995) as:

$$\pi r_c^2/L_s \, \partial h_w/\partial t - \pi r_s^2 K_w \, \partial^2 h_w/\partial l^2 \pm q_n|_{r_s} \pm Q \, \delta(l-l') = 0 \qquad (1)$$

where $h_w = h_w(l)$ is the hydraulic head in the well, l is the distance along the well screen, L_s is the total length of the well screen, r_c and r_s are the radii of the well casing and screen respectively, K_w is the hydraulic conductivity of the well, Q is the total pumping rate that is applied at the elevation l' in the well screen, and $\delta(l-l')$ is the Dirac delta function. The first term on the left hand side of (1) represents the storage of water in the well (due to changes in water level in the well), and the second term represents flow of water along the length of the well. Note that storage is uniformly distributed along the length of the well. The third term on the left hand side of (1) represents to the normal component of fluid flux across the well-screen, integrated over the circumference of the screen at $r=r_s$. For a screen length of zero (that is, for a well casing which is open only at its base), and for a well which is not pumped (that is, for Q=0), equation (1) becomes:

$$\pi r_c^2 \partial h_w/\partial t \pm q = 0 \qquad (2)$$

where q=q(t) is rate at which water leaves or enters the well, to or from the surrounding porous medium. Equation (2) is simply a statement of the requirement that the rate of change of volume of water stored in the well is equal to the flow rate between the well and the porous medium. Since the well is of zero length, there are no contributions to be superimposed on the discretised matrix equations representing flow in the porous medium, however (2) imposes a boundary condition on the boundary value problem for which the matrix equations are derived. In the finite element discretisation of the differential equation governing flow in the porous medium, the influence of the well on head in the porous medium can therefore be accounted for in the same manner as point sources and sinks (see, for

example, Huyakorn and Pinder, 1983). However, in this case, the flow rate at the point source/sink is not constant, rather it is a function of head in the well. Assuming continuity of head between the well and the formation, the temporal derivative in (2) can be expressed in terms of differences:

$$\pi r_c^2 (h_i^{k+1}-h_i^k)/\Delta t \pm q = 0 \qquad (3)$$

where i is the finite element node at which the well is placed, and k and k+1 are the old and new time levels respectively.

The implementation of unscreened wells in the code FRAC3DVS (Therrien et. al., 1995) was tested using the finite element mesh illustrated in Figure A.1. The well was placed at the centre of a 1m x 1m x1m block, for which a hydraulic conductivity of $1x10^{-5}$ m/s and a specific storage of $1x10^{-4}$ m^{-1} were specified. The upper and lower boundaries of the model were specified as constant head boundaries with a head of zero, and the lateral boundaries were specified as no-flow boundaries. The initial condition was specified as zero head throughout the domain, except at the node where the well was placed, where an initial head of 1m was specified.

In Figure A.2, the cumulative inflow from the well to the porous medium which was calculated by the model is compared to the cumulative volume change in the well determined from the calculated changes in hydraulic head at the well node. It can be seen that the results are in agreement, and therefore the condition imposed by (3) has been correctly implemented. Although the results are not illustrated, the transient head response in the well was essentially identical to the response calculated for a well placed at the same location but with a screen length of 1cm, using the previously implemented finite length well elements.

REFERENCES

Huyakorn. P.S., and G.F. Pinder, Computational methods in subsurface flow, Academic Press, 1983.

Sudicky, E.A., A.J.A. Unger and S. Lacombe, A noniterative technique for the direct implementation of well bore boundary conditions in three-dimensional heterogeneous formations, *Water Resour. Res.*, 31(2), 411-415, 1995.

Therrien, R., E.A. Sudicky and R.G. McLaren, Users guide for NP - A preprocessor for FRAC3DVS: An efficient simulator for three-dimensional, saturated-unsaturated groundwater flow and chain-decay solute transport in porous or discretely fractured porous formations, University of Waterloo, 1995.

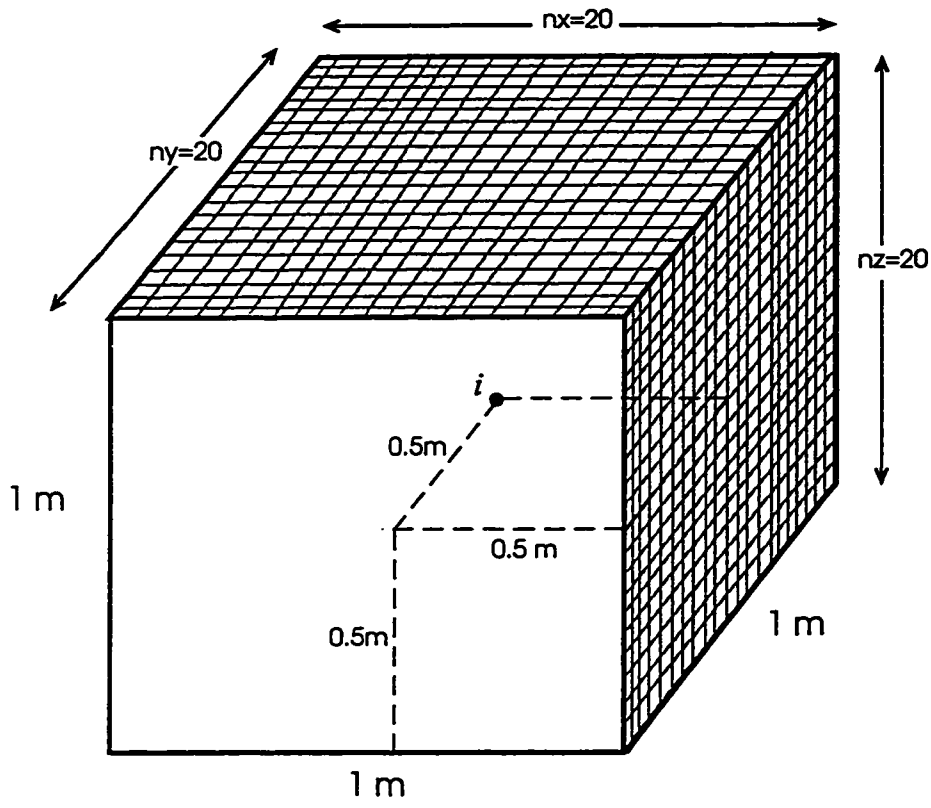

Figure A.1 - Finite element mesh used to test implementation of zero-length well-screen condition

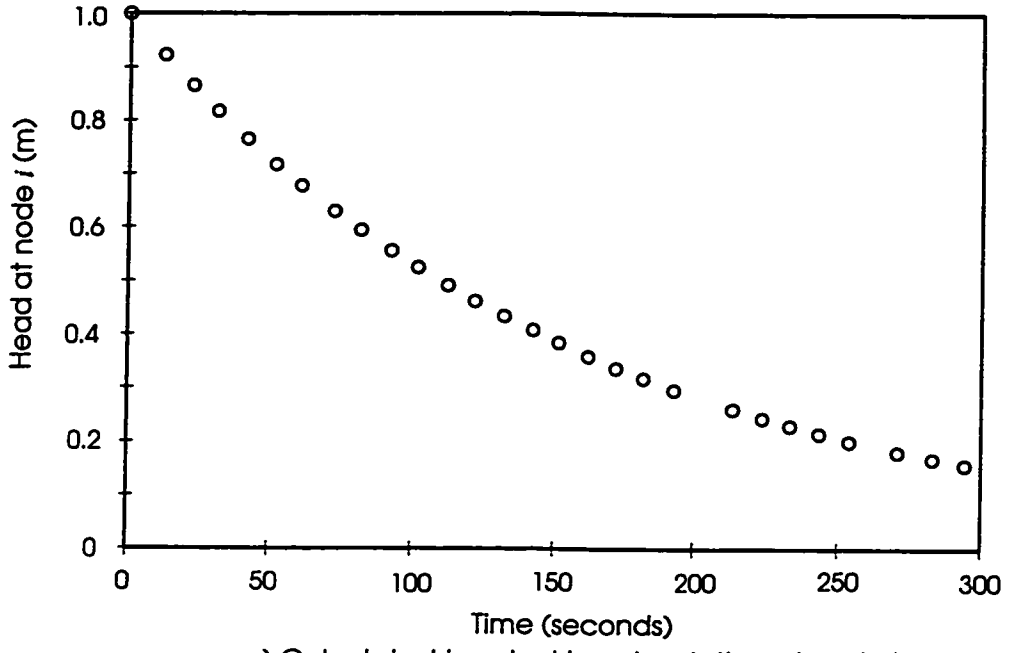

a) Calculated transient head variation at node i

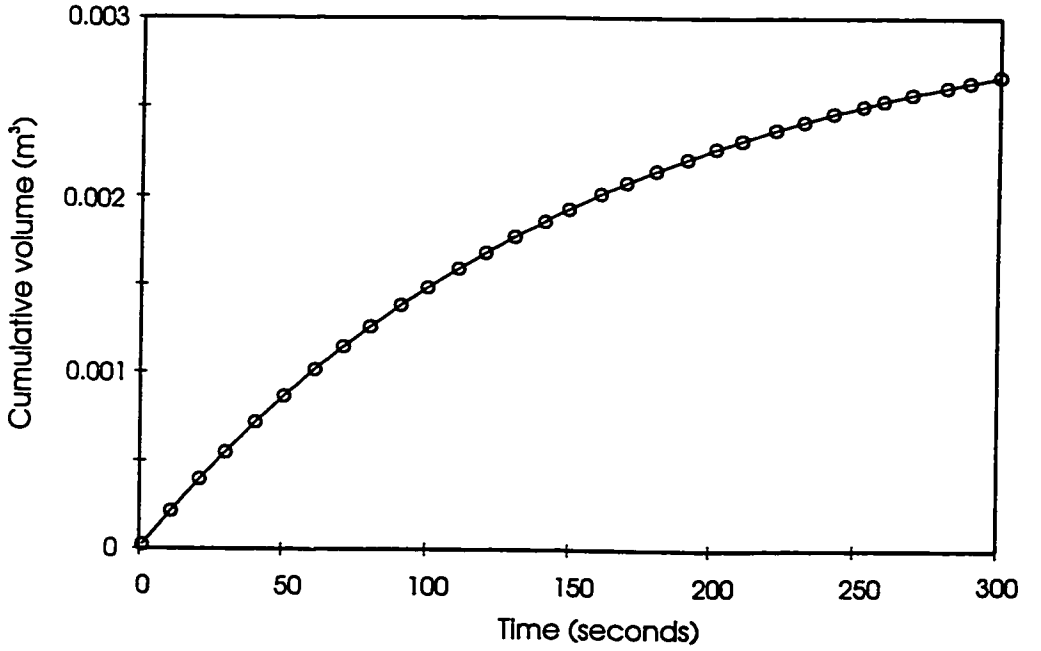

—— cumulative inflow to model domain at node *i*

o cumulative change in volume of water in well

$= \Sigma (h_i^{k+1} - h_i^b) \cdot \Delta t \cdot \pi r_c^2$

b) Comparison of cumulative inflow to model domain and change in volume of water in well

Figure A.2 - Model results for verification of implementation of zero-length well-screen condition

IMAGE EVALUATION TEST TARGET (QA-3)

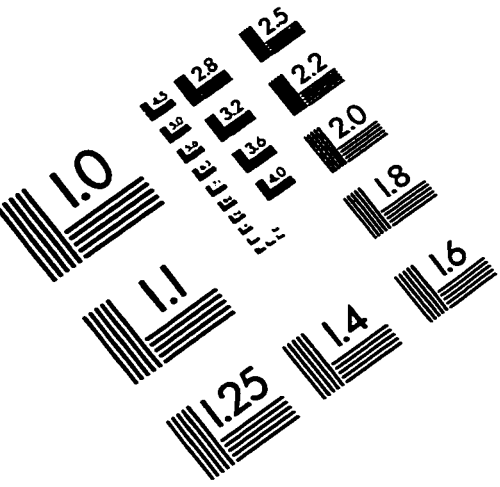

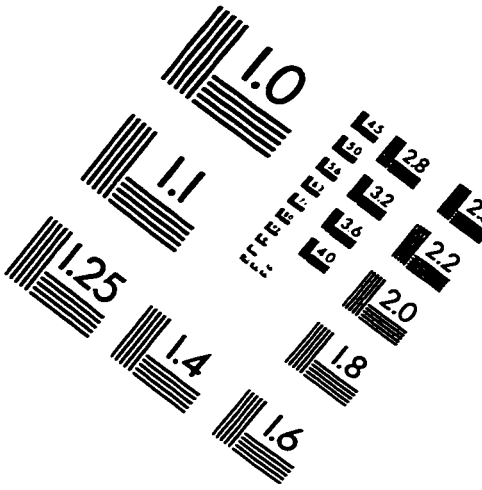

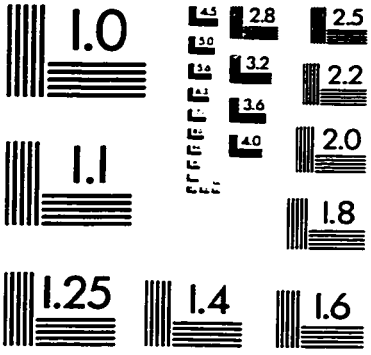

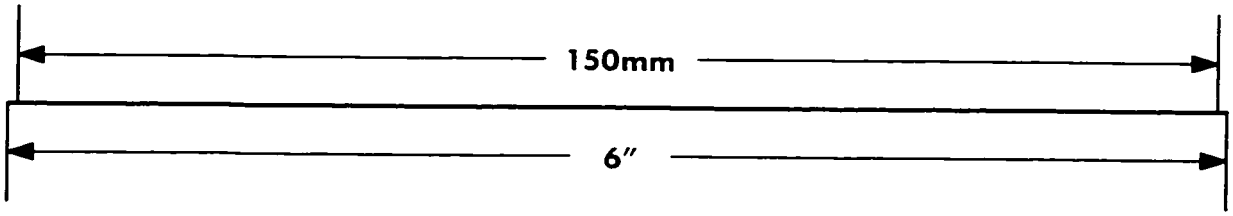

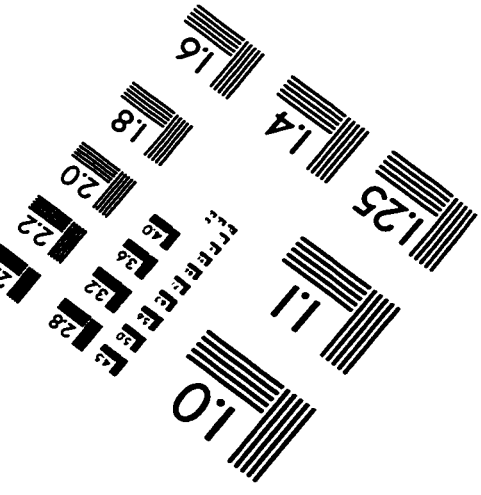

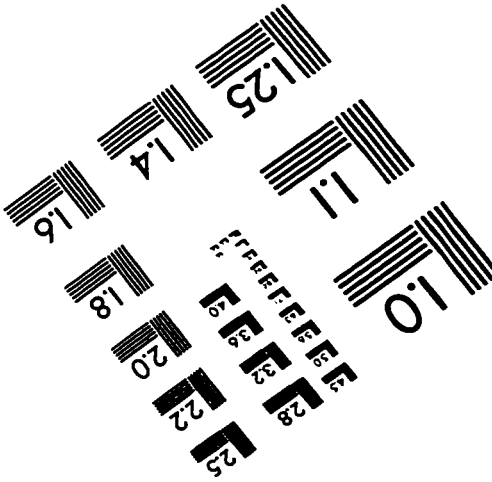

APPLIED IMAGE, Inc
1653 East Main Street
Rochester, NY 14609 USA
Phone: 716/482-0300
Fax: 716/288-5989